Ministry of Higher Education
And Scientific Research
University of Technology
Chemical Engineering Department

THE INFLUENCE OF VARIOUS PARAMETERS ON PITTING CORROSION OF 316L AND 202 STAINLESS STEEL

A Thesis

Submitted to the Department of Chemical Engineering of the University of Technology in a Partial Fulfillment of the Requirements for the Degree of Master of Science in Chemical Engineering

By

Taha Hassan Abood
(B.Sc. in Chemical Engineering 1989)

Supervisor
Dr. Shatha Ahmed Sameh

November (2008)

بسم الله الرحمن الرحيم

(قَالُوا سُبْحَانَكَ لا عِلْمَ لَنَا إِلَّا مَا عَلَّمْتَنَا إِنَّكَ أَنْتَ الْعَلِيمُ الْحَكِيمُ)

صدق الله العظيم

سورة البقرة

الاية (32)

Certification

This is to certify that I have read the thesis titled " ***The Influence of Various Parameters on Pitting Corrosion of 316L and 202 Stainless Steel****" and corrected any grammatical mistakes I found. The thesis is qualified for debate.*

Signature:

Name: Asst.Prof. Eyad Shamseldeen

University of Technology

Date: 8 / 1 / 2008

Certification

*We certify that we have read this thesis as examining committee for the student "*Taha Hassan Abood" *in its contents and that is our opinion, meets the standard of a thesis for the degree of Master of Science in Chemical Engineering.*

Signature:
Name: Dr. Fawziea M. Hussien
Date: / /200
(Member)

Signature:
Name: Asst. Prof. Dr. Najat J. Saleh
Date: / /200
(Member)

Signature:
Name: Asst. Prof. Dr. Shatha A. Sameh
Date: / /200
(Supervisor)

Signature:
Name: Asst. Prof. Dr. Sami I.J.AL-Rubaiey
Date: / /200
(Chairman)

Approved for the University of Technology

Signature:
Name: Dr. Jamal M. Ali
Head of Chemical Engineering Department
Date: / /200

Certification

*I certify that this thesis titled "**The Influence of Various Parameters on Pitting Corrosion of 316L and 202 Stainless Steel**" was prepared under my supervision at the University of Technology, Chemical Engineering Department in a Partial fulfillment of the requirement for the degree of Master of Science in Chemical Engineering.*

Signature:

Supervisor:Dr.ShathaA.Sameh

Date: / / 200

In view of the available recommendations, I forward this thesis for debate by the Examining Committee.

Signature:

Dr. Khalid A. Sukkar

Head of Post-graduate Committee

Departmentof Chemical Engineering

Date: / / 200

TO WHOM I OWE THIS WORK

MY PARENTS

My Brother & Sisters

MY WIFE

MY DAUGHTERS ((SURA & SAMA))

----------TAHA

Acknowledgment

First of all, praise be to God Who offered me patience; power and faith in a way that words can not express.

I wish to express my sincere thanks and deep gratitude to:

My supervisor Dr. Shatha A. Sameh for her valuable guidance continuous encouragement and interest during this work.

Dr. Jamal M. Ali, the Head of Chemical Engineering Department and Dr. Khalid A. Sukkar, the Head of Post- graduate Committee for assistance in providing facilities throughout this work.

Engineer Thamer Y. Ibrahim, the Manager of Al-Basera company for trading.

Engineer Asmaa M. Al-Sadi, the Head of Control Department of the Specialized Institute for Engineering Industries.

Engineer Hazim F. Hassan, (Technical Institute – Al-Anbar).

Finally, I have no words to thank and express my deep gratitude to my parents for their support, my brothers, my wife with my daughter who have suffered so much and my friends for their help.

Taha

Abstract

The present work is aimed to investigate the effect of some variables on the pitting corrosion of two types of stainless steel (316L and 202) and study their electrochemical behavior in NaCl solution using the polarization technique.

The experiments were carried out under static conditions at different temperatures (298,308and318)K and different NaCl concentration solutions (3.5, 2.5 and 1.5)%.

In order to study the effect of velocity on the electrochemical behavior at different rotation speeds (100, 200 and 300) r.p.m., rotating cylinder electrode were used for (3.5 and 2.5)% of NaCl solutions at temperatures (298, 308 and 318)K.

The above experiments were repeated for the two types of SS, i.e,(316L and 202).

The scan rate effect (10,15,30, and 40)mV/min. on the electrochemical behavior of 316L SS at 308K in 3.5% NaCl solution was investigated also.

It was found experimentally that increasing in temperatures and NaCl concentration leads to decrease in the breakdown potential (E_b). For 316L SS, the decreases was from(-80 to -220)mV, while for 202 SS it was from(-120 to -260)mV. Also it is clear that in the present investigation, stagnant solution is the favorite to pitting corrosion.

It can be confirm that at 40 mV/min., the passivation region observed clearly while, this region is difficult observed at another scanning rates (10,15,20,30)mV/min.. This give a good evidence that the passivation region depends on critical scanning rates, therefore the scanning rate must be chosen carefully to obtain a steady state response for passive region dependent on the type of alloys and the electrolyte.

The influence of rotational speed (100-300) r.p.m. on the pitting corrosion of two types of stainless steel, showed the small variation in corrosion current density ($i_{corr.}$). For 316L SS (0.0014-0.0015,0.0018-0.0019)mA/cm^2 at (2.5&3.5)%NaCl solution and 298K, (0.0016-0.0018,0.0018-0.0023)mA/cm^2 at (2.5&3.5)%NaCl solution at 308K, (0.0025-0.0028,0.0028-0.0028)mA/cm^2 at (2.5&3.%)%NaCl solution at 318K while for 202 SS (0.0021-0.002,0.004-0.002)mA/cm^2 at (2.5&3.5)%NaCl solution at 298K, (0.006-0.006,0.005-0.0063)mA/cm^2 at (2.5&3.5)%NaCl solution at 308K, (0.006-0.0068,0.0013-0.005)mA/cm^2 at (2.5&3.5)%NaCl solution at 318K.

It was found that increasing in the NaCl concentration leads to increase the corrosion current density for two types of stainless steel. For 316L SS the increasing was from (0.0012 to 0.0027)mA/cm^2, while for 202 SS, it was from (0.0016 to 0.009)mA/cm^2.

The pitting resistance of 316L SS was higher than that of 202 SS in chloride solutions at the same conditions (E_b for 316L SS higher than of E_b of 202 SS).

CONTENTS

Nomenclature

Symbol	Definition	Units
a , b	Tafel constant in Eq. (1-3)	
A	Surface area of specimen	cm^2
C_b	Bulk concentration of reacting ion	$mol.m^{-3}$
D	Diffusion coefficient of reacting ion	$m^2.s^{-1}$
d	Diameter of specimen	cm
E_i	Electrode potential	mV
E_{eq}	Equilibrium potential	mV
E_{corr}	Corrosion potential	mV
E_b	Breakdown potential	mV
E_p	Pitting potential	mV
E_{pp}	Primary pitting potential	mV
E_r	Repassivation potential	mV
F	Faradays constant = 96487	Coul./eq.
h	Height of cylinder specimen	cm
i	Current density	$A.m^{-2}$
i_a , i_c	Net anodic and cathodic current density respectively	$A.m^{-2}$
i_{app}	Applied current density	$A.m^{-2}$
i_{corr}	Corrosion current density(corrosion rate)	$A.m^{-2}$
i_{lm}	Limiting current density	$A.m^{-2}$
i_0	Exchange current density	$A.\ m^{-2}$
ℓ_e	Resistance path	Ω cm
n,z	Number of electrons transfer	
R	Gas constant =8.314	J/mol.K
R_f	Resistance produced by film or coatings	Ω cm
R_0	Resistance of the electrolyte solution	Ω cm
$R_{solu.}$	The electrical resistance of solution	Ω cm

Symbol	Definition	Units
r_o	Outer radius of cylinder specimen	cm
r_i	Inner radius of cylinder specimen	cm
T	Temperature	^oC, K
v	Linear velocity (ω/2)*d	$m.s^{-1}$

Greek Letters

β_A	Anodic Tafel slope =[3.202RT/ α n F]	mV
β_C	Cathodic Tafel slope =[-3.202RT/(1- α)n F]	mV
σ	Conductivity of the electrolyte solution	$\Omega^{-1}.m^{-1}$
η	Over potential	mV
η_a , η_c	Net anodic and cathodic over potential respectively	mV
η_A	Activation polarization potential	mV
η_C	Concentration polarization potential	mV
η_R	Resistance polarization potential	mV
η_t	Total polarization potential	mV
δ_m	Thickness of the diffusion layer	μm
ω	Rotational speed (**ω=r.p.m.*2π/60)**	
λ	Pit Generation	
α	Constant	

Subscripts

a	Anodic
b	Breakdown
c	Cathodic
corr.	Corrosion
crev.	Crevice
f.	Film
i	Applied
L,lm	Limiting
np	Nucleation potential
o	Equilibrium
sol.	Solution
p.	Pitting
pp.	Primary passive
Prot.	Protection
R	Resistance
red.	Reduction
r,crev.	Crevice repassivation
t	Total

Abbreviations

r.p.m.	Revolution per minute
SHE	Saturated Hydrogen Electrode
RCE	Rotating Cylinder Electrode
SCE	Saturated Calomel Electrode
CPT	Critical Pitting Temperature
PREN	Pitting Resistance Equivalent Number
SS	Stainless Steel

CHAPTER ONE

Introduction

1.1 Introduction

Corrosion engineering is the application of science and art to prevent or control corrosion damage economically and safely. In order to perform his function properly, the corrosion engineer must be well versed in the practices and principles of corrosion; the chemical, metallurgical. physical and mechanical properties of materials; corrosion testing; the nature of corrosive environments; the availability and fabrication of materials; and design. He also must have the usual attributes of the engineer-a sense of human relations, integrity, the ability to think and analyze an awareness of the importance of safety, common sense of organization and of prime importance, a solid feeling for economics. In solving corrosion problems, the corrosion engineer must select the method that will maximize profits [(1)].

The importance of corrosion studies is three folds [(2)]:

The first area of significance is economic including the objective of reducing material losses resulting from the corrosion of piping, tanks, metal components of machines, ships, bridges, marine structures, and so on.

The second area is improved safety of operating equipment which, through corrosion, may fail with catastrophic consequences. Examples are pressure vessels, boilers, metallic containers for toxic materials, turbine blades and rotors, bridges, airplane components, and automotive steering mechanisms. Safety is a prime consideration in the design of equipment for nuclear-power plants and disposal of nuclear wastes.

Third is conservation, applied primarily to metal resources - the world's supply of these is limited, and the wastage of them includes corresponding losses of energy and water reserves associated with the production and fabrication of metal structures.

1.2 Definition of corrosion

Corrosion may be defined in several ways [1,2,3]

1. Destruction or deterioration of a material because of reaction with its environment.
2. Destruction of materials by means other than straight mechanical effect.
3. Extractive metallurgy in reverse.
4. Undesirable interaction of a material with its environment.

1.3 Corrosion of metals and alloys

The corrosion occurs because of the natural tendency for most metals to return to their natural state; e.g., iron in the presence of moist air will revert to its natural state, iron oxide.

Metals can be corroded by the direct reaction of metal to a chemical and electrochemical reaction.The driving force that makes metals corrode is a natural sequence of their temporary existence in the metallic form.

Thermodynamically, corrosion is the ability of the metal to revert to compounds which are more stable, i.e., present in the nature initially [4].

Wagner and Traud in 1938, utilized in the mixed-potential theory, which consists of two simple hypotheses:

1. Any electrochemical reaction can be divided into two or more partial oxidation and reduction reactions.
2. There can be no net accumulation of electric during an electrochemical reaction.

From this it follows that during the corrosion of an electrically isolated metal sample, the total rate of oxidation must equal the total rate of reduction[(1)].

Electrochemical corrosion as shown in Fig.(1.1) is the most important classification of corrosion. Five conditions must exist before electrochemical corrosion can proceed:

1. There must be something that corrodes (the metal anodes).
2. There must be a cathode.
3. There must be a continuous conductive liquid path (electrolyte, usually liquid, condensate, salts, other contaminations).
4. There must be a conductor to carry the flow of electrons from anode to cathode. This conductor is usually in the form of metal-to-metal contact as in bolted or riveted joints**.**
5. The rates of oxidation reaction may equal to the rate of reduction reaction[(1,4)].

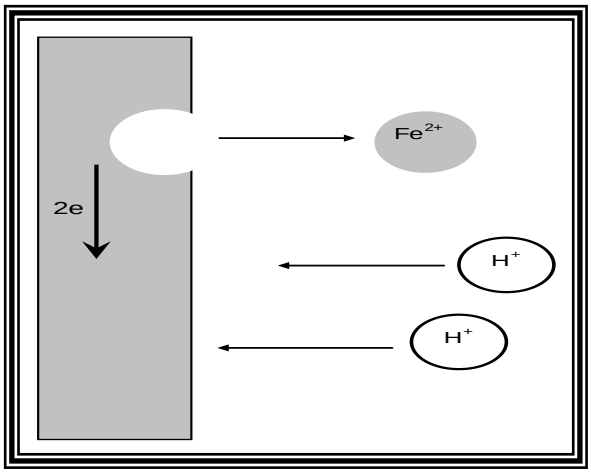

Fig.(1.1): Simple model describing the electrochemical nature of corrosion processes [(5)]

Fig.(1.2) shows the basic of corrosion and the elimination of any one of the five conditions will stop corrosion. An unbroken (perfect) coating on the surface of the metal will prevent the electrolyte from connecting the cathode and anode so the current can not flow. Therefore, no corrosion will occur as long as the coating is unbroken.

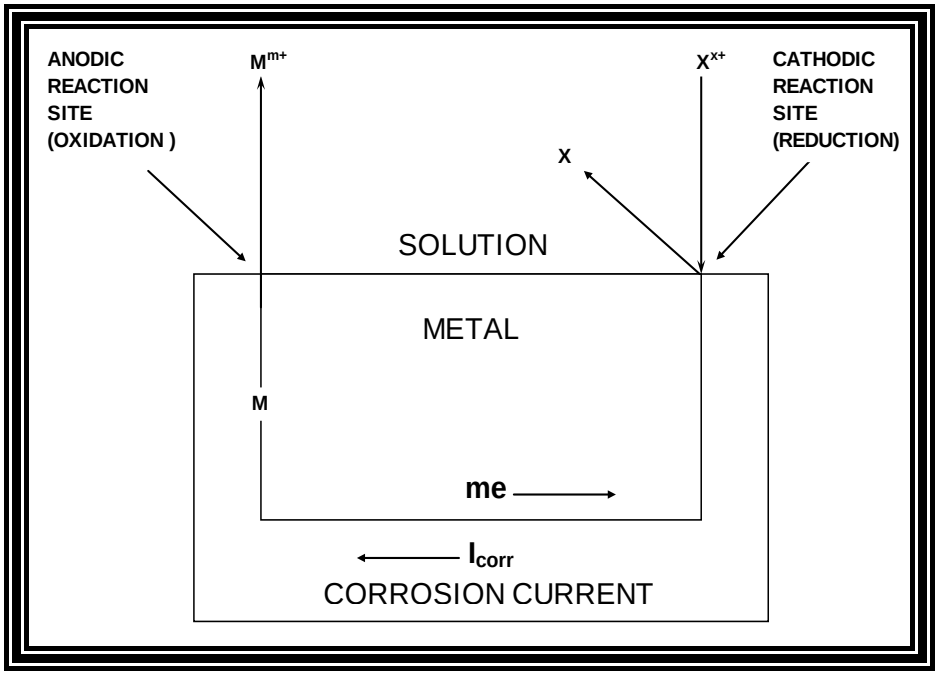

Fig. (1.2): The basic corrosion process [6]

1.4 Classification of corrosion

Corrosion has been classified in many different ways. One method divides corrosion into low-temperature and high temperature corrosion. Another separates corrosion into direct chemical and electrochemical corrosion. The preferred classification here is:

(1) Wet corrosion.

(2) Dry corrosion.

Wet corrosion occurs when a liquid is present. This usually involves aqueous solutions or electrolytes and accounts for the greatest amount of corrosion by far. A common example is corrosion of steel in water or acid liquid.

Dry corrosion occurs in the absence of a liquid phase or above the dew point of the environment. Vapors and gases are usually the corodents. Dry corrosion is most often associated with high temperatures. An example is attack on steel by furnace gases. The presence of even small amounts of moisture could change the corrosion completely. For example, dry chlorine is practically non corrosive to ordinary steel but moist chlorine, or chlorine dissolved in water, is extremely corrosive and attacks most of the common metals and alloys. The

reverse is true for titanium-dry chlorine gas is more corrosive than wet chlorine[1,4] .

1.5 Forms of corrosion

It is convenient to classify corrosion by the forms in which it manifests itself, the basic for classification being the appearance of corroded metal. Each form can be identified by mere visual observation. In most cases the naked eye is sufficient but sometimes magnification is helpful or required. Valuable information for the solution of a corrosion problem can often be obtained through careful observation of the corroded test specimens or failed equipment. Examination before cleaning is particularly desirable [1,4] .

Some of the eight forms of corrosion are unique, but all of them are more or less interrelated. The eight forms are:

1. Uniform (or General) attack.
2. Galvanic (or Two-metal) corrosion.
3. Crevice corrosion.
4. Pitting.
5. Intergranular corrosion.
6. Selective leaching, or parting.
7. Erosion corrosion.
8. Stress corrosion.

1.6 Definition of anode and cathode

Anode is the electrode at which chemical oxidation occurs leading to release of electrons (or + electricity leaves the electrode and enters the electrolyte) [2].

Examples of anodic reactions are:

$$Zn \longrightarrow Zn^{+2} + 2e^{-}$$

$$Al \longrightarrow Al^{+3} + 3e^{-}$$

$$Fe^{+2} \longrightarrow Fe^{+3} + e^{-}$$

These represent oxidation in the chemical sense. Corrosion of metals usually occurs at the anode. The positively charged species are called cations.

Cathode is the electrode at which chemical reduction occurs with consumption of electrons (or + current enters the electrode from the electrolyte) [(2)]. Examples of cathodic reactions are:

$$H^+ + e^- \longrightarrow \tfrac{1}{2} H_2$$

$$Cu^{+2} + 2e^- \longrightarrow Cu$$

$$Fe^{+3} + e^- \longrightarrow Fe^{+2}$$

All of which represent reduction in chemical sense. The negatively charged species are known as anions, e.g. Cl^- , OH^- , and $SO_4^{=}$.

1.7 Polarization

When the metal is not in equilibrium with a solution of its ions, the electrode potential differs from the equilibrium potential by an amount known as the polarization. Other terms having equivalent meaning are over voltage and over potential. The symbol commonly used is (η). Polarization is an extremely important parameter because it allows useful statements to be made about the rates of corrosion process. In practical situations, polarization is sometimes defined as the potential change away from some other arbitrary potential and in mixed potential experiments; this is the free corrosion potential [(7)].

The change in the electrode potential from equilibrium potential depends on the magnitude of the external current and its direction. The direction of potential change always opposes the shift from equilibrium and hence opposes the flow of current, whether the current is impressed externally or is of galvanic origin [(2)].

The potential at which the reaction is occurring changes, when a reaction is forced a way from equilibrium i.e., when one direction of the reaction is favored over the other, the amount by which the potential changes is the over voltage which is defined as [(2,7)]:

$$\eta = E_i - E_{eq} \quad \text{…. (1-1)}$$

where:

η is the over potential,(polarization)

E_{eq} is the equilibrium potential, and

E_i is the polarized (current flowing) potential.

The current applied to cause the departure from equilibrium is the net rate of reaction, thus:

$$i_{app} = \Sigma \vec{i} - \Sigma \overleftarrow{i} \quad \text{…. (1-2)}$$

where: $\vec{i}$, $\overleftarrow{i}$ and i_{app} are the anodic, cathodic and applied current density respectively.

An anodic current density ($i_{app} > 0$) causes a positive anodic over potential and a cathodic current density ($i_{app} < 0$) causes a negative cathodic over potential.

The causes of electrode polarization fall into four different types:

1.7.1 Activation polarization

This polarization refers to an electrochemical process, which is controlled by the reaction sequence at the metal-electrolyte interface **(1)** or stated in another way the reaction at the electrode requires activation energy in order to go. Activation polarization is usually the controlling factor during corrosion in strong acids. This is easily illustrated by considering hydrogen evolution reaction on zinc during corrosion in acid solution. Fig.(1.3) shows some of the possible steps in hydrogen reduction on a zinc surface as:

Activation polarization is a function of the nature and concentration of the species being reduced, surface roughness, composition and temperature. In addition it is sensitive to traces of reducible impurities in the system **(7).** The activation-over potential, and hence the activation energy varies exponentially with the rate of charge transfer per unit area of electrode surface, as defined by Tafel equation **(8):**

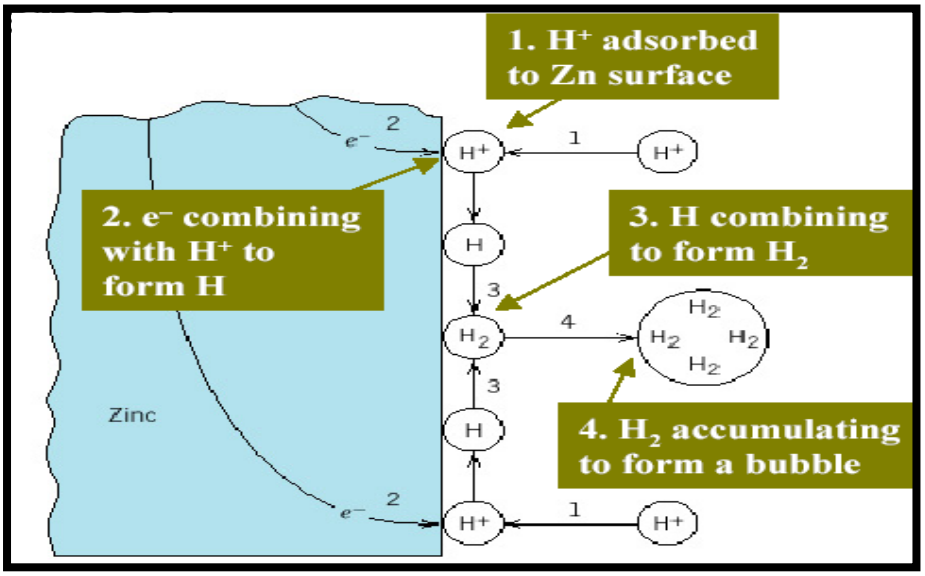

Fig. (1.3) Hydrogen-reduction reaction under activation control [(1)].

$$\eta_A = a \pm b \log i \qquad \text{…. (1-3)}$$

where:

i, is current density,

a&b, are Tafel constants, and

± is anodic or cathodic over potential respectively.

The activation polarization η_A of any kind increases with anodic and cathodic current density according to Tafel equation [(7)]**:**

$$\eta_A = \frac{2.303RT}{\alpha zF}\log\left[\frac{i_a}{i_0}\right] \text{ for anodic reaction} \qquad \text{…. (1-4)}$$

$$\eta_C = -\frac{2.303RT}{(1-\alpha)zF}\log\left[\frac{i_c}{i_0}\right] \text{ for cathodic reaction} \qquad \text{…. (1-5)}$$

These equations may be simplified to:

$$\eta_A = \beta_A \log\left[\frac{i_a}{i_0}\right] \qquad \text{…. (1-6)}$$

$$\eta_C = -\beta_C \log\left[\frac{i_c}{i_0}\right] \qquad \text{.... (1-7)}$$

β_A, β_C, and i_0 are constants of a given metal and environment and are both dependent on temperature. The exchange current density i_0 represents the current

density equivalent to the equal forward and reverse reactions at the electrode at equilibrium. The larger the value of i_0 and the smaller value of β_A and β_C, the smaller is the corresponding over voltage.

1.7.2 Concentration polarization

It refers to electrochemical reaction, which is controlled by a mass transfer process, such that a drop in the concentration of the electrochemically active species on the electrode surface may result in causing a change in potential. The relationship between the reaction rate and concentration polarization is [9]:

$$i = i_{lm}\left[1 - \exp\left(-\frac{zF}{RT}\eta_c\right)\right] \qquad \text{.... (1-8)}$$

Where, i_{lm} is the maximum rate of a possible reaction for a given system, under which all the transferred species to the electrode react very soon.

η_c = concentration polarization

The maximum rate is known as the limiting current and can be defined mathematically by the following equation [1]:

$$i_{lm} = \frac{D\ z\ F\ C_b}{\delta_m} \qquad \text{…. (1-9)}$$

where:

D = diffusion coefficient of reacting ion (m^2/s).

z = number of electrons transfer.

C_b= bulk concentration of reacting ion ($moles/m^3$).

δ_m = thickness of the diffusion layer (m).

eq. (1-8) can be expressed in term of η_c as:

$$\eta_c = -\frac{2.303\ RT}{z \cdot F}\log\left(1 - \frac{i}{i_{lm}}\right) \qquad \text{…. (1-10)}$$

The value of the concentration polarization depends on the concentration, temperature and diffusion boundary layer thickness.

For a particular electrode in any system, the diffusion layer thickness is dependent on the velocity of the solution past the electrode surface.

As the velocity increases, the thickness of this layers decreases and the limiting current increases [10]**.** It has been observed that concentration polarization is the controlling factor during reduction processes where the supply of reducible species is limited as shown in Figs. (1.4and1.5).

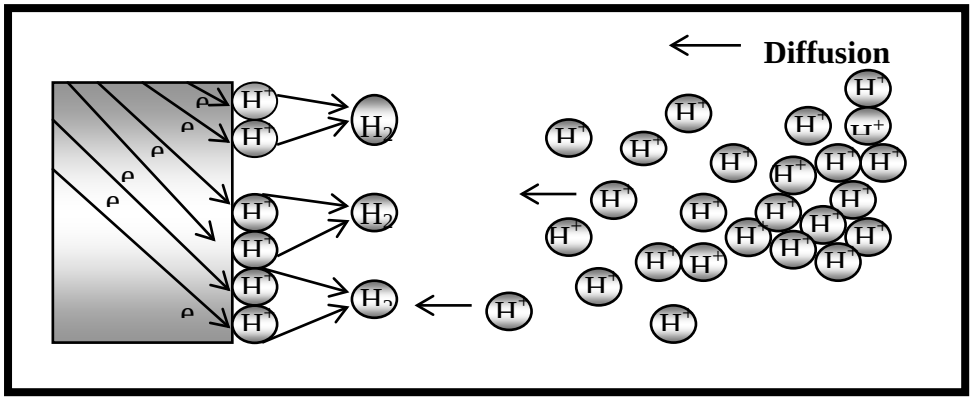

Fig. (1.4) Concentration polarization during hydrogen reduction [1]

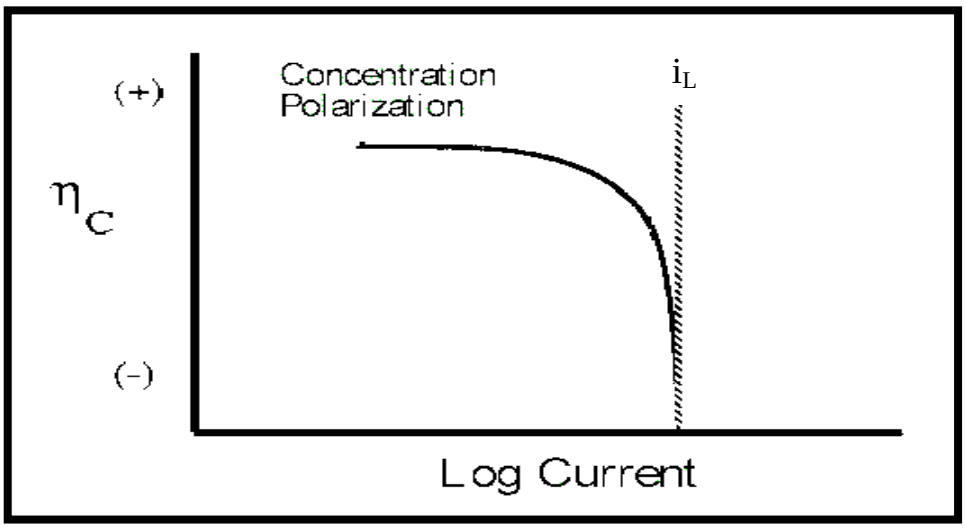

Fig. (1.5) Concentration polarization curve (reduction process) [1,2]

1.7.3 Resistance polarization

It refers to electrochemical reaction, which works under conditions which would result in potential drop through a portion of the electrolyte surrounding the electrode, or through the reaction product. This is usually called the ohmic potential drop, which contributes to polarization as [2]**:**

$$\text{Ohmic potential drop [IR drop)} = IR_0 = \frac{\ell_e I}{\sigma A_e} \qquad \ldots. (1\text{-}11)$$

where:

I, is reaction rate expressed as current density ($i = I/A_e$)($\mu A/cm^2$).

R_0, is resistance of the electrolyte solution(Ωcm).

σ, is conductivity of the electrolyte solution ($\Omega^{-1}cm^{-1}$).

ℓ_e, is resistance path (i.e., separation distance between electrodes) (Ωcm).

A_e, is cross sectional area of electrode (cm^2).

In corrosion the resistance of the metallic path for charge transfer is negligible. Resistance over potential η_R is determined by factors associated with the solution or with the metal surface. Resistance polarization η_R is only important at higher current densities or in higher resistance solution. It may be defined as **[2,10,11]:**

$$\eta_R = I\,(R_{solu.} + R_f) \qquad \text{.... (1-12)}$$

where:

$R_{solu.}$is the electrical resistance which is a function of electrical resistivity (Ω cm) of the solution and the geometry of the corroding system, and R_f is the resistance produced by films or coatings formed on the surface of the sites, which block contact between the metal and the solution, and increase the resistance over potential.

The value of the ohmic potential drop is influenced by the conductivity of the electrolyte; the latter is usually a strong function of temperature and composition. This term of polarization is usually neglected in highly conductive solutions **[7, 9].**

1.7.4 Mixed polarization

Both activation and concentration polarization usually occur at an electrode. At low reaction rates, activation polarization usually controls, while at higher reaction rates, concentration polarization becomes controlling **[2]**. The total

polarization of an electrode is the contribution of activation polarization and concentration polarization [(1)]**:**

$$\eta_t = \eta_A + \eta_C \qquad \ldots. \text{ (1-13)}$$

During reduction process such as hydrogen evolution or oxygen reduction, concentration polarization is important as the reduction rate approaches the limiting diffusion current density. The overall cathodic over potential for activation process is given by [(1)]**:**

$$\eta_{red.} = -\beta_C \log\frac{i}{i_0} - \frac{2.303RT}{nF}\log\left(1-\frac{i}{i_L}\right) \qquad \ldots. \text{ (1-14)}$$

This case is shown in Fig. (1.6).

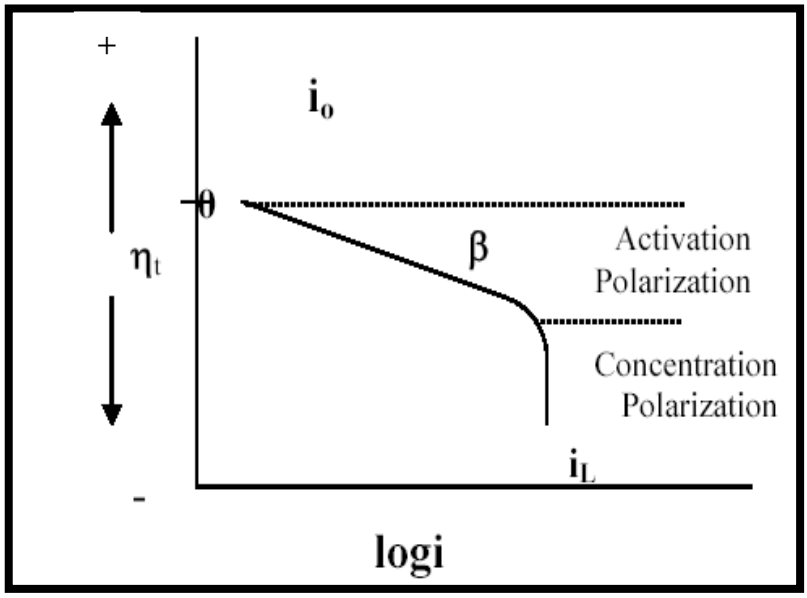

Fig. (1.6) Mixed polarization curve [(1)].

The total polarization at a metal electrode then becomes as the algebraic sum of the three types described above:

$$\eta = \eta_A + \eta_C + \eta_R \qquad \ldots. \text{ (1-15)}$$

1.8 Passivity

Nearly all metals are thermodynamically reactive in most natural environments, e.g. moist air, polluted or hot, and water when it is saline, acid or alkaline. Most metals quickly develop an oxide film when exposed to dry, pure and cool air. This film would soon cease to thicken because it forms a solid

barrier between the metal and oxygen through which metal and oxide ions pass only with difficulty. This is the simplest form of passivity [12].

The study of passivation and passivity is greatly facilitated by observation of the essential anodic process separately, with an external cathode, and in the absence whenever possible of oxidizer capable of giving local cathodic reactions at the nominal anode. By such means the anode electrode potential and current density associated with various passivation phenomena can be readily measured. Therefore passivity is an unusual phenomenon observed during the corrosion of certain metals and alloys [1], It is defined simply as the "loss of chemical reactivity under certain environmental conditions". In the passive state, the corrosion of a metal is very low [13]. It is important to note that during the transition from the active to passive region, a 10^3 to 10^6 reduction in corrosion rate is usually observed [1].

Fig.(1.7) illustrates schematically the typical behavior of an active-passive metal [1,2] .The metal initially demonstrates the typical behavior similar to non-passivating metals. That is, as electrode potential is made more positive, the metal follows Tafel behavior, and dissolution rate increases exponentially. This is active region. At more noble potentials, dissolution rate decreases to a very small value and remains essentially independent of potential over a considerable potential region. This is termed the passive region. Finally, at very noble potentials, dissolution rate again increases with increasing potential in the transpassive region.

One of the important characteristics of active-passive behavior is the position of the maximum anodic current density (i_c) characterized by the primary passive potential E_{pp}. This current is termed the critical anodic current density for passivity i_c which is followed by a passive potential range accompanied by exceedingly small passive current. Fig.(1.7) illustrates the decrease in dissolution rate accompanying the active-to-passive transition. This decrease in dissolution rate just above the primary passive potential is the result of film formation at this point. The transpassive region where dissolution rate again increases with

increasing potential, is apparently due to the destruction of the passive film at very positive potentials.

From the aforementioned points, passivity is defined in two ways which are still in force today [(2)].

1. A metal is passive if it substantially resists corrosion in a given environment resulting from marked anodic polarization.
2. A metal is passive if it substantially resists corrosion in a given environment despite a marked thermodynamic tendency to react.

Wagner[(14)],extended definition (1) by stating that a metal is passive if, on increasing the electrode potential toward more noble values, the rate of anodic dissolution in a given environment under steady-state conditions becomes less than the rate at some less noble potential.

Alternatively, a metal is passive if, on increasing the concentration of an oxidizing agent in an adjacent solution or gas phase, the rate of oxidation, in absence of external current, is less than the rate at some lower concentration of the oxidizing agent. These alternative definitions are equivalent under conditions where the electrochemical theory of corrosion applies.

There are two commonly expressed points of view regarding the nature of the passive film [(2)]. The first holds that the passive film (definition 1 or 2) is always a diffusion-barrier layer of reaction products, for example, metal oxide or other compound which separates metal from its environment and which slows down the rate of reaction. This is sometimes referred to as the oxide-film theory.

The second holds that metals that are passive by definition (1), are covered by a chemisorbed film, for example, of oxygen. Such a layer displaces the normally adsorbed (H_2O) molecules and slows down the rate of anodic dissolution involving hydration of metal ions.

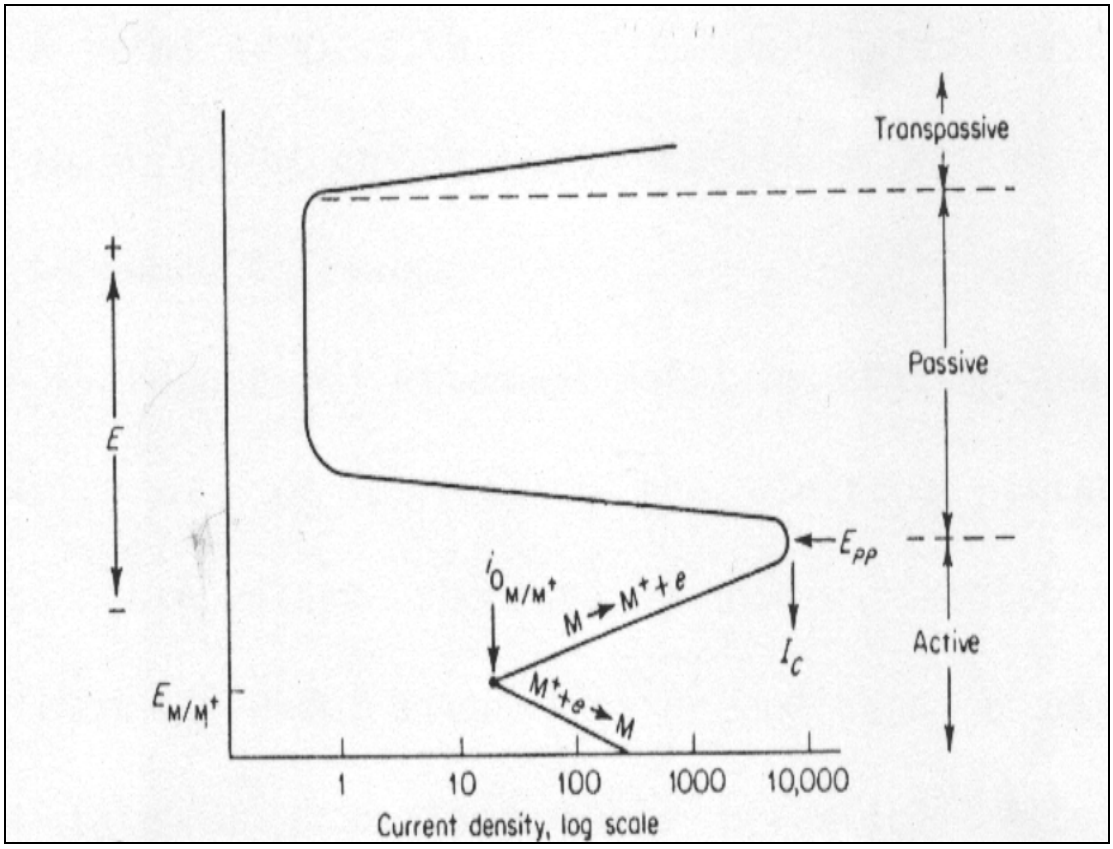

Fig. (1.7) Typical anodic dissolution behavior of an active-passive metal.[1]

Or expressed in another way, adsorbed oxygen decreases the exchange current density (increases anodic over voltage) corresponding to the overall reaction $M \rightleftharpoons M^{z+} + ze^-$. Even less than a monolayer on the surface is observed to have a passivating effect [15,16] , hence it is suggested that the film cannot act primarily as a diffusion-barrier layer. This second point of view is called the adsorption theory of passivity.

Chapter Two

Pitting Corrosion

2.1 Introduction

Pitting corrosion is defined as "localized corrosion of a metal surface, confined to a point or small area, that takes the form of cavities" [(17)]. Pitting is a deleterious form of localized corrosion and it occurs mainly on metal surfaces which owe their corrosion resistance to passivity. The major consequence of pitting is the breakdown of passivity, i.e. pitting, in general, occurs when there is breakdown of surface films when exposed to pitting environment. Pitting corrosion is so complicated in nature because "oxide films formed on different metals vary one from another in electronic conduction, porosity, thickness, and state of hydration" [(18)].

Many engineering alloys, such as stainless steels and aluminum alloys, are useful only because of passive films, which are thin (nanometer-scale) oxide layers that form naturally on the metal surface and greatly reduce the rate of corrosion of the alloys. Such passive films, however, are often susceptible to localized breakdown, resulting in accelerated dissolution of the underlying metal. If the attack initiates on an open surface, it is called pitting corrosion; at an occluded site, it is called crevice corrosion. These closely related forms of localized corrosion can lead to accelerated failure of structural components by perforation or by acting as an initiation site for cracking. Fig.(2.1) shows an example of deep pits on a metal surface [(19)].

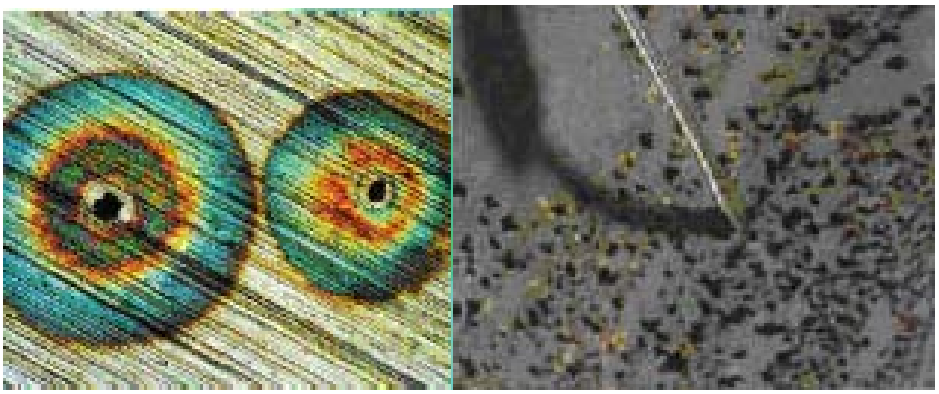

Fig.(2.1) Deep pits in a metal [19,20]

It should be noted that, whereas localized dissolution following breakdown of an otherwise protective passive film is the most common and technologically important type of pitting corrosion, pits can form under other conditions as well. For instance, pitting can occur during active dissolution if certain regions of the sample are more susceptible and dissolve faster than the rest of the surface.

Pitting corrosion is influenced by many different parameters, including the environment, metal composition, potential, temperature, and surface condition. Important environmental parameters include aggressive ion concentration, pH, and inhibitor concentration. Other phenomenological aspects of localized corrosion include the stochastic nature of the processes and the stages of localized attack, including passive film breakdown, metastable attack, stable growth, and perhaps eventual arrest [21,22].

2.2 Phenomenology of pitting corrosion

Classical pitting corrosion caused by passive film breakdown will only occur in the presence of aggressive anionic species, and chloride ions are usually, although not always, the cause. The severity of pitting tends to vary with the logarithm of the bulk chloride concentration [23]. The reason for the aggressiveness of chloride has been pondered for some time, and a number of notions have been put forth. Chloride is an anion of a strong acid, and many metal

cations exhibit considerable solubility in chloride solutions [24]. Chloride is a relatively small anion with a high diffusivity; it interferes with passivation, and it is ubiquitous as a contaminant.

The presence of oxidizing agents in a chloride-containing environment is usually extremely detrimental and will further enhance localized corrosion. Most oxidizing agents enhance the likelihood of pitting corrosion by providing extra cathodic reactants and increasing the local potential. Of course, dissolved oxygen is the most common oxidizing agent. One of the reactions by which oxygen reduction occurs is:

$$O_2 + 2H_2O + 4e^- \longrightarrow 4OH^- \qquad \ldots . (2\text{-}1)$$

$$E_{rev} = 1.23 - 0.059\ PH \quad (\text{ vs.SHE })$$

where SHE is standard hydrogen electrode.

Removal of oxidizing agents, such as removal of dissolved oxygen by deacration, is one powerful approach for reducing susceptibility to localized corrosion. The influence of potential on pitting corrosion is described subsequently.

Pitting is considered to be autocatalytic in nature; once a pit starts to grow, the local conditions are altered such that further pit growth is promoted. The anodic and cathodic electrochemical reactions that comprise corrosion separate spatially during pitting Fig.(2.2). The local pit environment becomes depleted in cathodic reactant (e.g., oxygen), which shifts most of the cathodic reaction (such as is given by eq. (2-1)) to the boldly exposed surface outside of the pit cavity, where this reactant is more plentiful. The pit environment becomes enriched in metal cations as a result of the dissolution process in the pit (written for a generic metallic element, M):

$$M \longrightarrow M^{n+} + ne^- \qquad \ldots . (2\text{-}2)$$

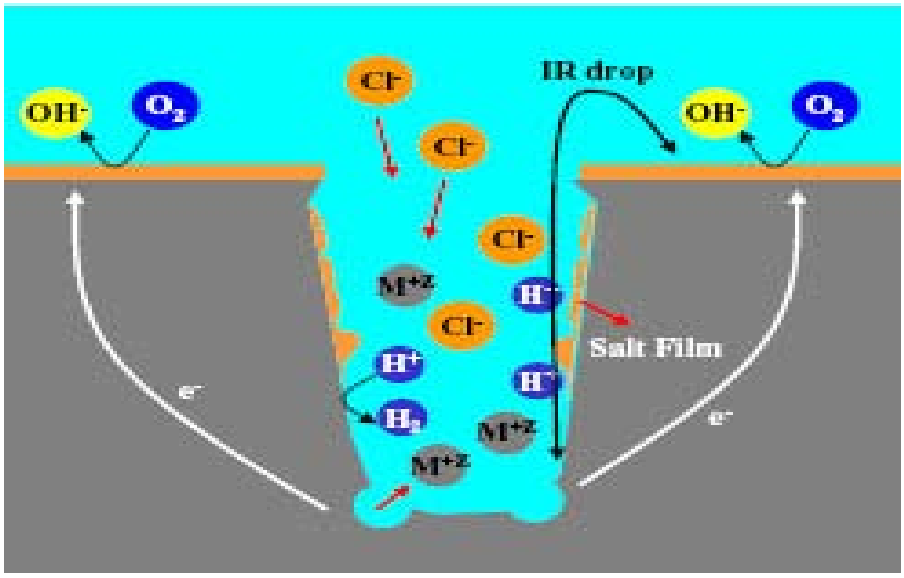

Fig.(2.2) Autocatalytic process occurring in a corrosion pit. The metal ,M, is being pitted by an aerated NaCl solution. Rapid dissolution occurs in the pit, while oxygene reduction takes place on the adjacent metal surfaces [(20)].

The concentration of an anionic species such as chloride must also increase within the pit in order to balance the charge associated with the cation concentration and to maintain charge neutrality. This enrichment of anions occurs by electromigration from the bulk solution in response to the potential gradient that develops as a result of the ohmic potential drop along the current path between the inside of the pit and the cathodic sites on the boldly exposed surface. The final aspect of the local pit environment that must be considered is the pH, which decreases, owing to cation hydrolysis:

$$Me^{2+} + 2H_2O \longrightarrow Me(OH)^{+} + H^{+} + H_2O \longrightarrow Me(OH)_2 + 2H^{+} \quad \ldots. (2\text{-}3)$$

The common cathodic reactions that must accompany the dissolution occurring in the pit, such as the oxygen reduction reaction eq. (2-1), result in a local increase in the pH at the cathodic sites. The acidity developed in the pit is not neutralized by the cathodic reaction because of the special separation of the anodic and cathodic reactions[(24,25)].

In summary, the local pit environment is depleted in the cathodic reactant, such as dissolved oxygen; enriched in metal cation and an anionic species, such

as chloride; and acidified. This acidic chloride environment is aggressive to most metals and tends to prevent repassivation and promote continued propagation of the pit[24,25].

The concentration of various ionic species at the bottom of a model one-dimensional pit geometry was determined as a function of current density based on a material balance that is considered generation of cations by dissolution, outward diffusion, and thermodynamic equilibrium of various reactions such as cation hydrolysis eq.(2-1). It was found that a critical value of the product x • i, where x is pit depth and i is current density, corresponds to a critical pit acidification for sustained pit growth. Current density in a pit is a measure of the corrosion rate within the pit and thus a measure of the pit penetration rate. This x • i value can be used to determine the current density required to initiate or sustain pitting at a defect of a given size.

As the pit current density increases, the ionic concentration in the pit solution increases, often reaching supersaturation conditions. A solid salt film may form on the pit surface, at which point the ionic concentration would drop to the saturation value, which is the value in equilibrium with the salt layer. Under these conditions, the pit growth rate is limited by mass transport out of the pit. Salt films are not required for pit stability (although some have suggested that they are) [26-31], but they enhance stability by providing a buffer of ionic species that can dissolve into the pit to reconcentrate the environment in the event of a catastrophic event, such as the sudden loss of a protective pit cover. Under mass-transport-limited growth, pits will be hemispherical with polished surfaces.

In the absence of a salt film (at lower potentials), pits may be crystallographically etched or irregularly shaped in some other fashion.

2.3 Stages of pitting

Pitting can be considered to consist of various stages: passive film breakdown, metastable pitting, pit growth, and pit stifling or death. Any of these stages may be considered to be the most critical. For instance, once the passive film breaks down and a pit initiates, there is a possibility that a stable pit will grow. On the other hand, pits will not initiate if they cannot grow at least for a short while. The passive state is required for pitting to occur, but some researchers believe that details of the passive film composition and structure play a minor role in the pitting process. This view is supported by the fact that many observations of pitting tendency can be fully accounted for by growth considerations. Furthermore, pit growth is critical in practical applications of failure prediction. Finally, the metastable pitting stage may be thought to be the most important, because only pits that survive this stage become stable growing pits. Metastable pits exist on the edge of stability. Studies of metastable pits can therefore provide insight into fundamental aspects of pitting, because both initiation and stability are key factors in metastable pitting **(19,20)**.

2.3.1 Pit initiation and passive film breakdown

The breakdown of the passive film and the details of pit initiation comprise the least understood aspect of the pitting phenomenon. Breakdown is a rare occurrence that happens extremely rapidly on a very small scale, making direct observation extraordinarily difficult Fig.(2.3). The passive film is often drawn schematically as a simple inert layer covering the underlying metal and blocking access of the environment to the metal. The reality is, of course, much more complicated. Depending on alloy composition, environment, potential, and exposure history, this film can have a range of thickness, structure, composition, and protectiveness. Typical passive films are quite thin and support an extremely high electric field (on the order of 10^6 to 10^7 V/cm). The passage of a finite passive current density is evidence of continual reaction of the metal, to result in

film thickening, dissolution into the environment, or some combination of the two. The view of the passive film as being a dynamic structure, rather than static, is critical to the proposed mechanisms of passive film breakdown and pit initiation.

Theories on passive film breakdown and pit initiation have been categorized into three main steps that focus on passive film penetration, film breaking, or adsorption [32,33]. As with most such situations, different mechanisms or combinations of these mechanisms may be valid for different metal-environment systems. These mechanisms have been considered in terms of pure metal systems. However, pits in real alloys arc most often associated with inclusions or second-phase particles, and these factors must also be taken into consideration.

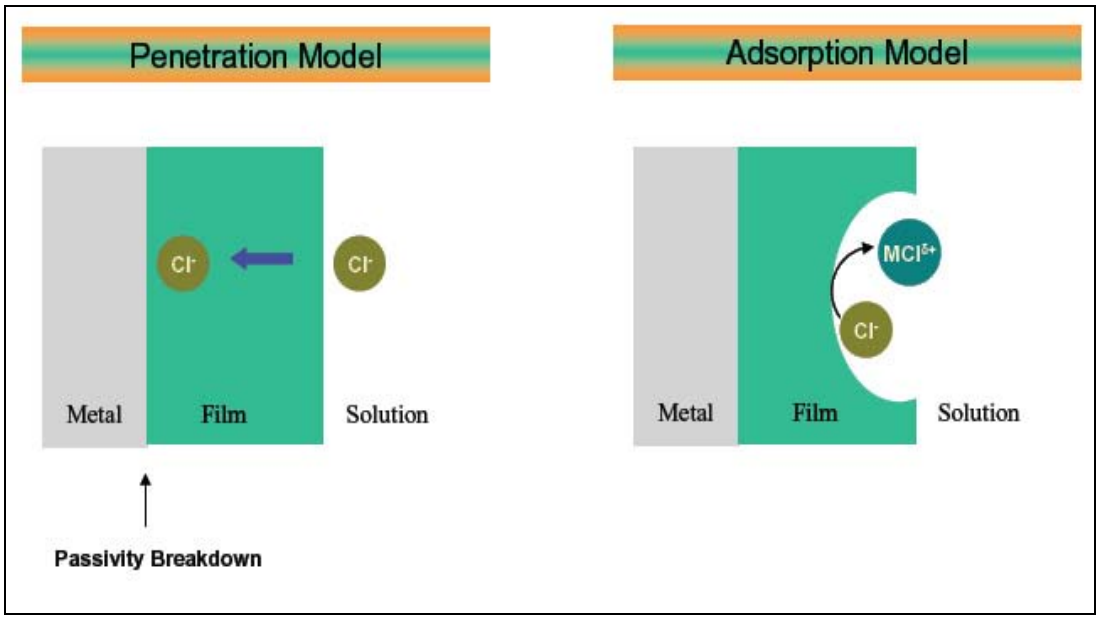

Fig. (2.3) Models on passivity breakdown by Cl^- [20]

2.3.2 Metastable pitting

Metastable pits are pits that initiate and grow for a limited period before repassivating Fig.(2.4). Large pits can stop growing for a variety of reasons, but metastable pits are typically considered to be those of micron size, at most, with a

lifetime on the order of seconds or less. Metastable pits are important to understand because, under certain conditions, they continue to grow to form large pits. Metastable pits can form at potentials far below the pitting potential (which is associated with the initiation of stable pits) and during the induction time before the onset of stable pitting at potentials above the pitting potential. These events are characterized by potential transients in the active direction at open circuit or under an applied anodic current, or anodic current transients under an applied anodic potential. Such transients have been reported in stainless steels [34,35-40] and aluminum [41,42] for many years. Individual metastable pit current transients can be analyzed for pit current density, and stochastic approaches can be applied to groups of metastable pits.

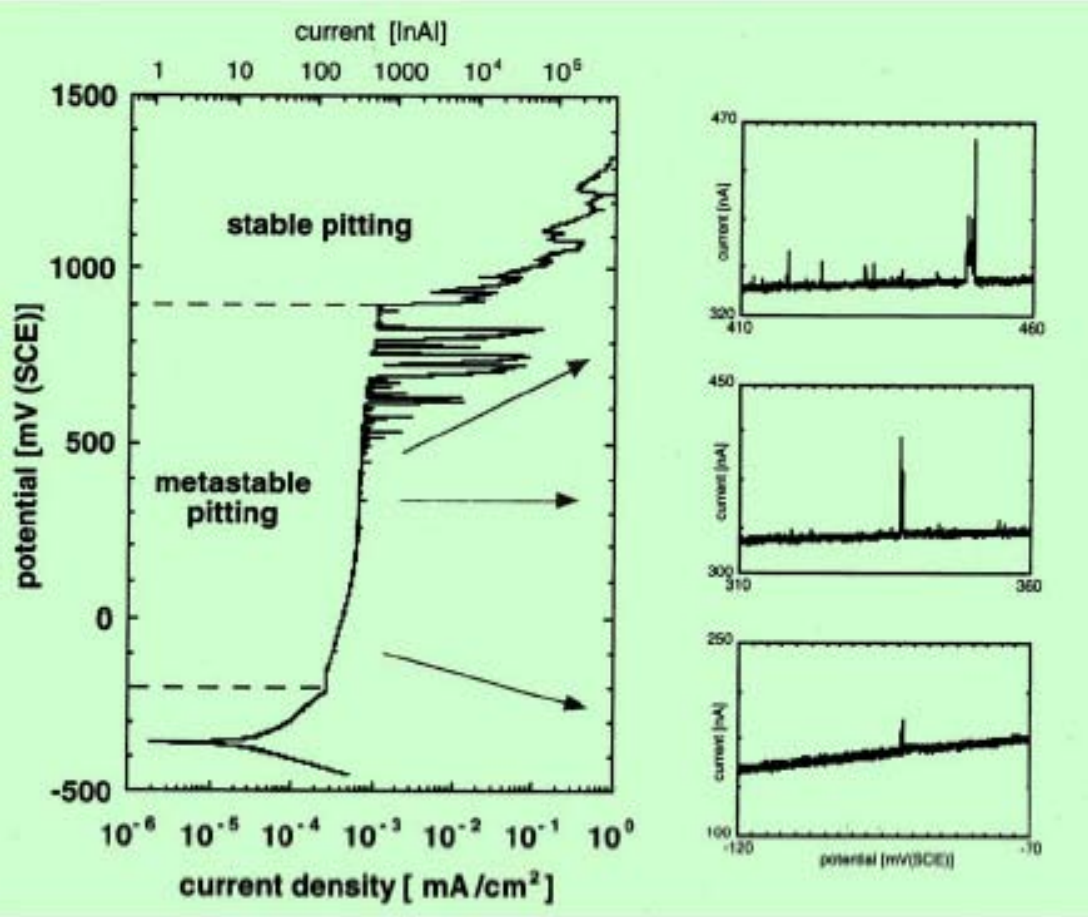

Fig. (2.4) Typical potential current curve of stainless steel in Cl^- showing the different stages of localized corrosion. [20]

It has been argued that when stable pits are small, they behave identically to metastable pits and, in fact, metastable stage and continue to grow, whereas metastable pits repassivate and stop growing, for some reason.

2.3.3 Stable pitting and pit growth

Pits grow at a rate that depends on material composition, pit electrolyte concentration, and pit-bottom potential. The mass-transport characteristics of the pit influence pit growth kinetics through the pit electrolyte concentration. Pit stability depends on the maintenance of pit electrolyte composition and pit-bottom potential that are at least severe enough to prevent repassivation of the dissolving metal surface at the pit bottom.

In order to understand pit growth and stability, it is essential to ascertain the rate-determining factors. Pit growth can be controlled by the same factors that can limit any electrochemical reaction: charge-transfer processes (activation), ohmic effects, mass transport, or some combination of these factors. Pit growth at low potentials below the range of limiting pit current densities is controlled by a combination of ohmic, charge transfer, and concentration overpotential factors. At high potentials, mass transport may be rate controlling. Ultimately, however, mass transport determines the stability of pits even at lower potentials, because the local environment controls passivation. The rate of pit growth decreases with time for pitting controlled by either ohmic or mass-transport effects. The pit growth rate often varies with (t^{-n}) where n is approximately equal to 0.5**(34)**.

Pits often grow with a porous cover. This cover can make visual detection extremely difficult, so that the awareness of the severity of attack is overlooked and the likelihood of catastrophic failure is enhanced. The pit cover might be a thick, precipitated product layer that forms as the concentrated and acidic pit solution meets the bulk environment, which might be neutral or limited in water, as in the case of atmospheric corrosion. Small pits in stainless steels often have a pit cover that is a remnant of the undermined passive film **(34)**.

Larger pits in stainless steel can be covered by a layer with a considerable thickness of metal that is detached from the rest of the metal sample **(43).** These covers make optical detection extremely difficult, because they remain reflective. A short exposure to ultrasonic agitation, however, removes the cover and reveals the whole pit diameter.

Despite the autocatalytic nature of pitting, large pits, which would be considered to be stable by any criterion, can stop growing or die. If the conditions (environment and potential) at the dissolving wall of a pit are not sufficiently aggressive, the pit will repassivate. The potential at the pit bottom is lower than that at the outer surface as a result of the ohmic potential drop associated with current flow out of the pit. As the pit deepens, the ohmic path length and ohmic resistance increase. This tends to cause an increase in the ohmic potential drop, a decrease in the local potential, and a decrease in the pit current density. The environment tends to be acidic and rich in chloride, owing to hydrolysis of the dissolved metal cations and electrolytic migration of chloride into the pit. The high concentration in the pit is depleted by transport out of the pit but is replenished by continued dissolution at the pit bottom, As the pit deepens, the rate of transport out of the pit decreases, so the pit can be stable with a lower anodic current density replenishing the environment. As mentioned previously, the pit current density tends to decrease with time, owing to an increase in the pit depth and ohmic potential drop. Repassivation might occur if a sudden event, such as loss of a pit cover, caused a sudden enhancement of transport and dilution of the pit environment to the extent that the rate of dissolution at the pit bottom would be insufficient to replenish the lost aggressive environment **(19,44).**

2.4 Potential

Electrochemical studies of pitting corrosion have found that characteristic potentials exist. Stable pits form at potentials noble to the pitting potential, E_P, and will grow at potentials noble to the repassivation potential, E_R, which is

lower than E_P. The effect of potential on pitting corrosion and the meaning of these characteristic potentials can best be understood with the schematic polarization curve shown in Fig.(2.5). This figure is a plot of the potential versus the logarithm of the current density. Potential is measured versus a reference electrode, commonly a saturated calomel electrode (SCE), and a potentiostat is used, along with an auxiliary or counter electrode, to make such measurements. As mentioned previously, current density is a measure of the rate of reaction. Common practice for measuring such curves involves potentiodynamic polarization or automatic scanning of the potential from a low value, such as the corrosion potential, to higher values **(45)**.

The schematic polarization curve in Fig.(2.5) shows the case of a spontaneously passive material, meaning that a protective passive film is present on the metal surface at the open circuit or corrosion potential, $E_{corr.}$ During upward scanning, breakdown occurs, and a stable pit starts growing at the pitting potential E_P, where the current increases sharply from the passive current level and, on reversal of the scan direction, repassivates at E_R, where the current drops back to low values representative of passive dissolution. Corrosion experts generally consider that materials exhibiting higher values of E_P and E_R are more resistant to pitting corrosion, and cyclic polarization experiments are commonly used for this purpose. In an oxidizing environment, or for a material that is very susceptible to pitting, the open circuit potential, which is determined by the intersection of the polarization curves associated with the anodic and catbodic partial reactions, will be above E_P, and the material will spontaneously pit at open circuit**.**

A correlation has been found such that metals with low experimentally determined pitting potentials have a higher tendency to form pits naturally at open circuit **(23)**.

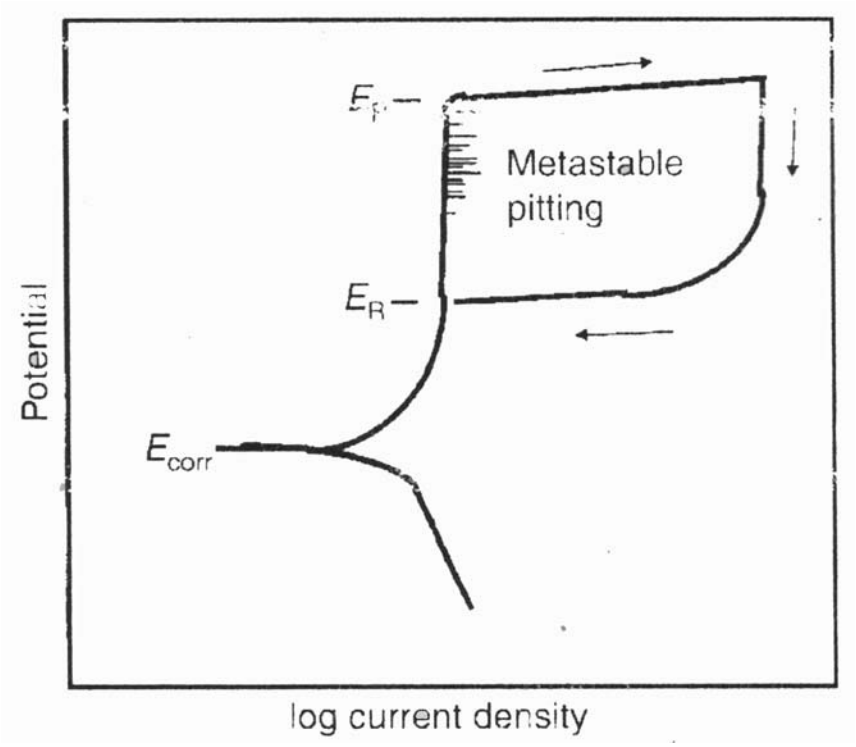

Fig.(2.5) Schematic of a polarizaition curve showing critical potentials and metastable pitting region . E_P, pitting potential; E_R, repassivation potential; E_{corr}.corrosion potential [20,23].

If the $E_{corr.}$ is far below the E_P, then there is a low likelihood that the potential will ever go high enough to approach the E_P and initiate a pit. Therefore , the difference between the E_P and $E_{corr.}$ in a given environment is the margin of safety and is also used as a measure of the susceptibility to localized corrosion [45,46]. Because the repassivation potential E_R is typically lower than E_P, the difference between E_R and $E_{corr.}$ is a more conservative measure of pitting susceptibility. If the corrosion potential is to always remain below the potential at which pits repassivate, then there is a very low likelihood that pitting will occur at all. A final measure of pitting susceptibility is the difference between E_P and E_R, which is related to the extent of hysteresis in a cyclic potentiodynamic polarization curve. Generally, alloys that are susceptible to pitting corrosion exhibit a large hysteresis.

It should be noted that several other names and subscripts have been used to describe these characteristic potentials. For instance, it is common to use the

term breakdown potential (E_b) for the initiation potential, because one is not always sure if the form of localized attack is pitting, crevice corrosion, or intergranular corrosion, or if the current increase is the result of general transpassive dissolution. The pitting potential is sometimes referred to as the pit nucleation potential, E_{np}, and the repassivation potential is sometimes called the protection potential, E_{prot}. If creviced samples are used, the potentials might be referred to as crevice potential, E_{crev}, and crevice repassivation potential, $E_{r,crev}$.

The measures of susceptibility described previously are useful for comparing the vulnerability of various alloys to localized corrosion in a given environment or for comparing the relative aggressiveness of different environments. However, there is abundant experimental evidence suggesting that these interpretations of the characteristic potentials are simplistic and insufficient for the development of a fundamental understanding of the mechanism of pitting corrosion. For instance, the potentiodynamicaliy determined pitting potential of many rnaterials exhibits a wide experimental scatter, of the order of hundreds of millivolts. Furthermore, E_P is, in many cases, a function of experimental parameters, such as potential scan rate. As is described subsequently, so-called metastable pits initiate and grow for a period at potentials well below the pitting potential **(34)**, which provides evidence in contradiction to the definition of the pitting potential as being the potential above which pits initiate. The meaning of the repassivation potential has also been called into question. The E_R of ferritic stainless steel decreases (i.e., moves in the active direction) with increasing values of the current density at which the potential scan direction is reversed **(46,47)**. So, deeper pits apparently repassivate at lower potentials. In contrast, the repassivation potential for pits in aluminum seems to be relatively independent of the extent of prior pit growth for a limited number of experiments **(48)**. A similar lack of dependence of E_R on prior growth has been

found for pits in stainless steel and other corrosion-resistant alloys but only after the passage of large charge densities [49]. Furthermore, pits did not initiate at potentials below this limiting E_R, even after very long times (up to 38 months), which validates the use of the repassivation potential as a design criterion [50].

2.5 Factors influencing pitting

2.5.1 Alloy composition and microstructure

Strong effects act on the tendency for an alloy to pit [22]. Chromium concentration plays the dominant role in conferring passivity to ferrous alloys Fig.(2.6). The pitting potential was correspondingly found to increase dramatically as the chromium content has increased above the critical 13% value needed to create stainless steel [51]. Increasing the concentration of nickel, which stabilizes the austenitic phase, moderately improves the pitting resistance of iron-chromium [51]. Small increases in certain minor alloying elements, such as molybdenum in stainless steels Fig.(2.7), can greatly reduce pitting susceptibility [22]. Molybdenum is particularly effective but only in the presence of chromium. Small amounts of other elements, such as nitrogen and tungsten, also have a strong influence on the pitting resistance of stainless steels [52,53].

Various measures have been developed to describe the beneficial effects of steel composition on resistance to localized corrosion. The pitting resistance equivalent number (PREN) was originally developed as a pitting index for stainless steels [53].

$$PREN = Cr + 3.3Mo + 16N \ (wt\%) \qquad \ldots. \ (2\text{-}4)$$

The multiplier value for nitrogen could be as high as 30. The PREN has been correlated to various other measures of corrosion resistance for stainless steels, such as the critical pitting temperature.

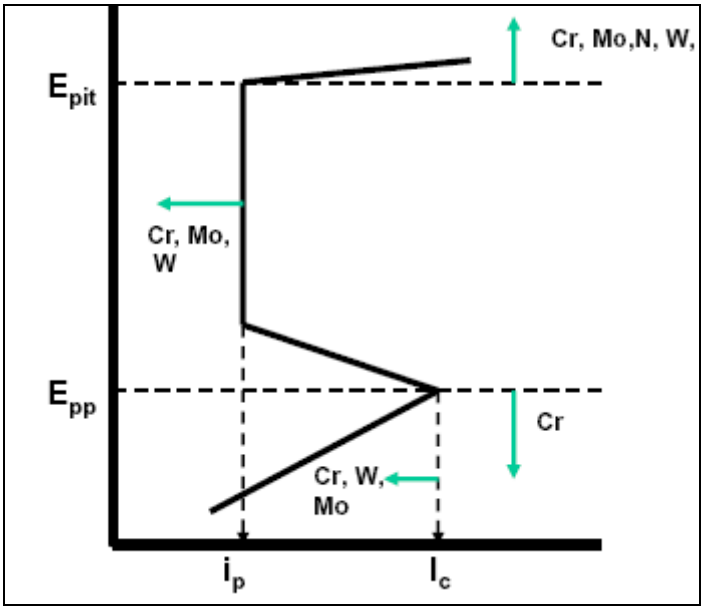

Fig. (2.6) Effect of alloying elements on the resistance to pitting corrosion[20,53]

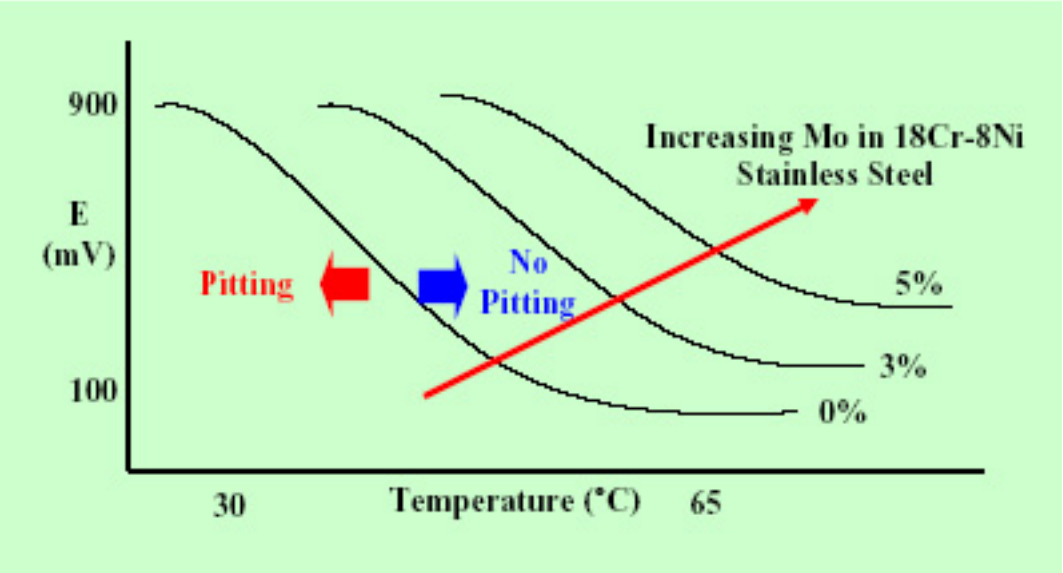

Fig.(2.7) Effect of Mo on pitting resistance of stainless steel [20]

Pits almost always initiate at some chemical or physical heterogeneity at the surface, such as inclusions, second-phase particles, solute-segregated grain boundaries, flaws, mechanical damage, or dislocations [22]. Most engineering alloys have many or all such defects, and pits will tend to form at the most susceptible sites first. Pits in stainless steels are often associated with MnS inclusions, which are found in most commercial steels. The role of MnS inclusions in promoting the breakdown and localized corrosion or stainless steels has been recognized for some

time [54,55,56]. Recent improvements in alloy production have led to steels with lower sulfur content to improve pitting resistance.

2.5.2 Effect of temperature

Temperature is also a critical factor in pitting corrosion, because many materials will not pit at temperature below certain value, which is extremely sharp and reproducible [57-63]. This effect can be seen either by varying the temperature at a range of fixed applied potentials or by varying the potential for a range of constant temperature experiments. Fig. (2.8) is a plot of pitting and repassivation potentials for three different stainless steels in 1 M NaCl as a function of solution temperature [62]. At low temperatures, extremely high breakdown potentials are observed, corresponding to transpassive dissolution, not localized corrosion. Just above the critical pitting temperature (CPT), pitting corrosion occurs at a potential that is far below the transpassive breakdown potential. This value of CPT is independent of environmental parameters and applied potential over a wide range and is a measure of the resistance to stable pit propagation [57]. At higher temperatures, the pitting potential decreases with increasing temperature and chloride concentration. The CPT can be used, similar to pitting potential, as a means for ranking susceptibility to pitting corrosion; the higher the CPT, the more resistant the alloy is to pitting [57]. If crevice corrosion is the primary concern, creviced samples can be used to determine a critical crevice temperature (CCT), which is typically lower than the corresponding CPT, Fig.(2.9). Aluminum alloys do not exhibit a CPT in aqueous chloride solutions at temperatures down to 0 °C (32 °F).

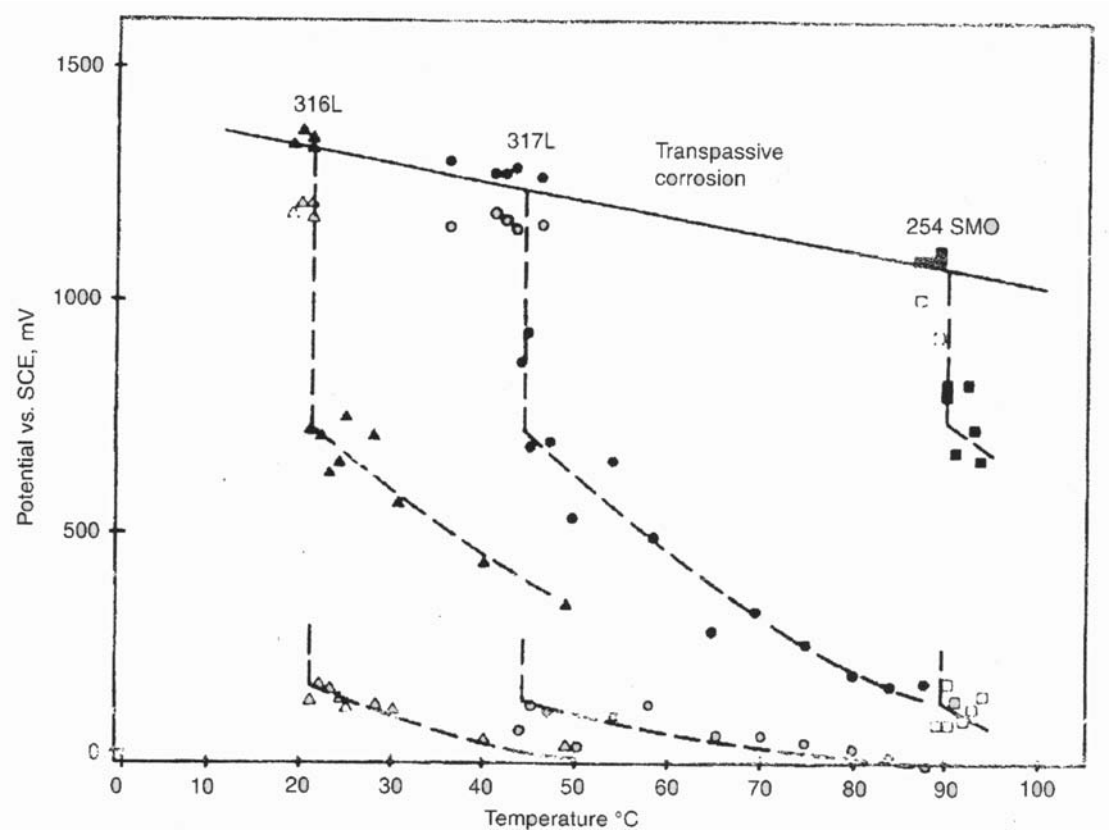

Fig.(2.8) Pitting and repassivation potentials for three different stainless steels in 1 M NaCl as a function of solution temperature [19].

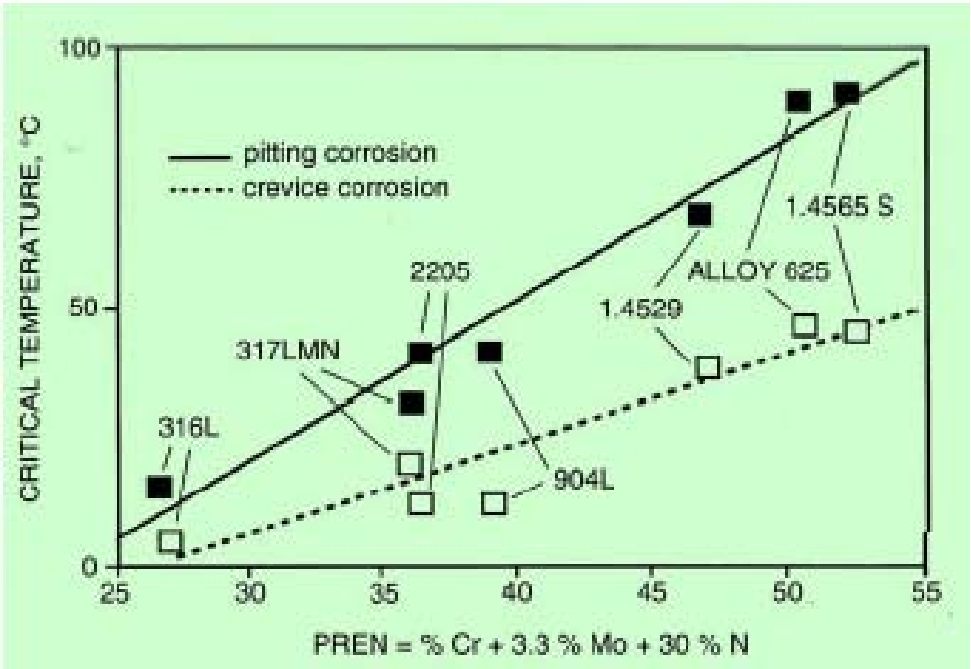

Fig.(2.9) Variation in the critical pitting temperature and critical crevice corrosion temperature.[20]

2.5.3 Effect of pH

The effect of pH on the breakdown potential was not much investigated .It was found with the exclusion of Pourbaixs work [64] that the Eb value is almost constant within a large range of pH values [23,65,66].

Fig.(2.10) shows that iron is thermodynamically immune in neutral and acid solutions (below line **a**) when $Fe^{+2} < 10^{-6}$ M. The metal goes passive on the right of line **d**. Iron does not dissolve at all at pH values between 9 and 13, owing to a passivating film of Fe_3O_4 or Fe_2O_3.

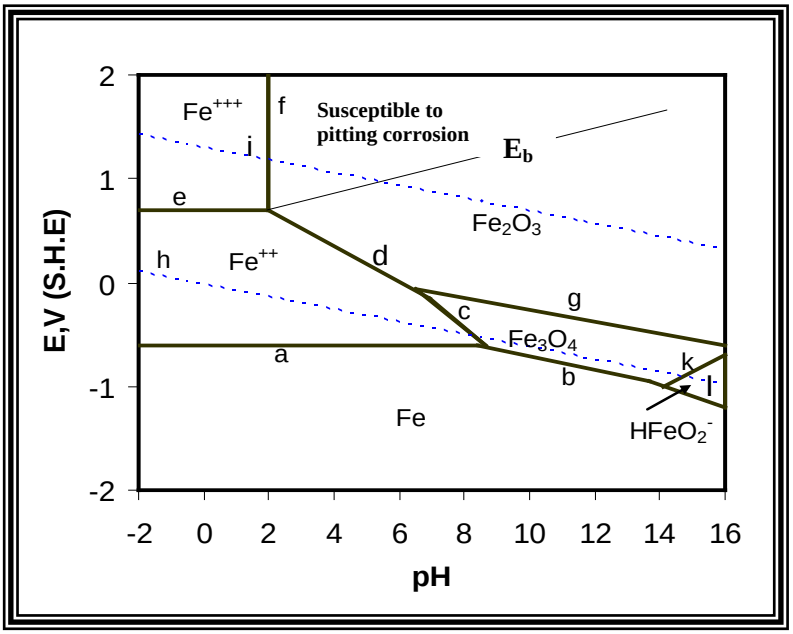

Fig. (2.10): Pourbaix diagram for iron in water (298 K) [67]

2.5.4 Effect of halogen ions

Pitting corrosion can be caused by different halide anions. The type of anion responsible for pitting depends on the type of the metal involved. The most aggresive anions are chlorides which produce pitting in iron, Nickel , Aluminium, Ti, Zr and their alloys[22].

Three main reasons for the specific effect of chloride ion [68] appear to be :

(a) Its ability to increase the activity of hydrogen ion in the pit electrolyte.

(b) Its ability to form salt layer at low pH at the bottom of the pit.

(c) Ability to form complexes with cations and hydroxide.

As the chloride concentration of the solution increases the tendency towards pitting increases for various stainless steels[53], as shown in Fig.(2.11) and eq.(2-5) [69], it is claimed that there is a linear dependence between (E_b) and (Cl^-) for 304 AISI SS.

$$E_b = A \log [Cl^-] + B \quad \ldots. (2\text{-}5)$$

The induction pitting period is also function of Cl^- in the relation:

$$\text{Log } t = C + D \log (Cl^-) \quad \ldots. (2\text{-}6)$$

where A, B, C and D are coefficients depending on temperature

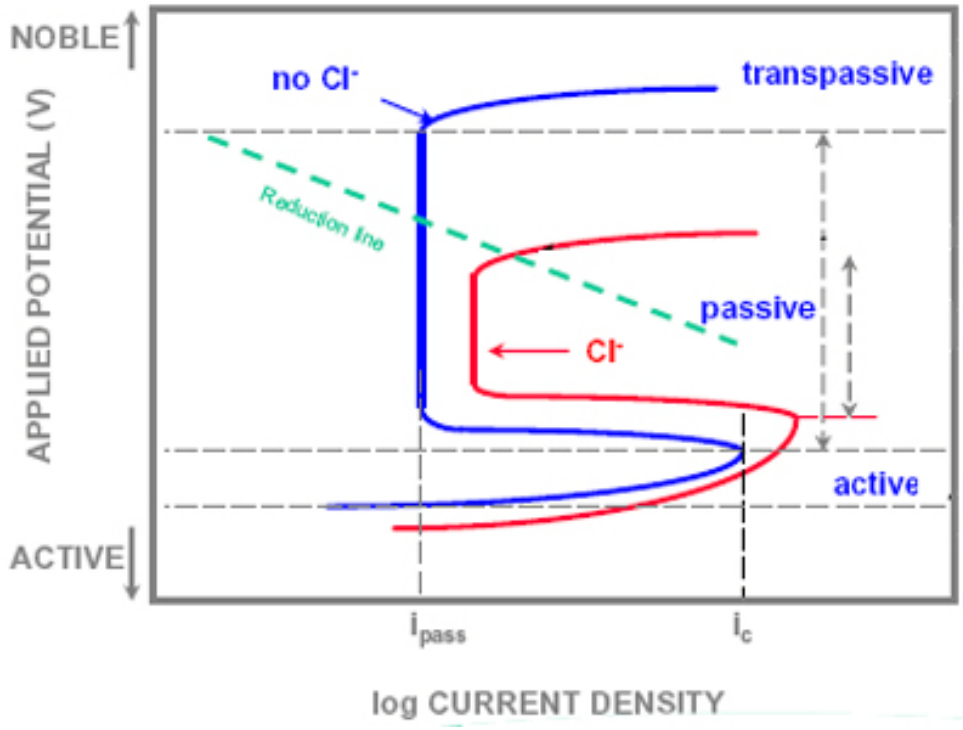

Fig.(2.11) Effect of Cl^- concentration on pitting corrosion [20]

The passivation reaction is totally independent on Cl^- concentration and it is the breakdown of passivity that is directly effected by Cl^- at certain temperature

for AISI 304 and AISI 316 SS. The effect of florid ion action on the metal surface covered with an oxide film can differ from the action of other halogen anion. Thus for different metals the ability to cause pitting normally increases in the following order [(22)].

$$F^- < Cl^- < Br^- < I^-$$

2.5.5 Effect of velocity

The attack on metal immersed in water may vary greatly, depending on the relative velocity between the water and the metal surface. For metals that show passive behavior or form other protective films in water, as most metals do, attack will occur where the changes in water velocity are most pronounced. Water corrosivity can be dramatically increased by dissolved gases, acids, salts, strong bases, entrained abrasives, high temperature, fluctuating pressure, cavitation, or impingement.

Relative difference in velocity between the metal and the aqueous corrosive influence any of the common varieties of iron or steel, including low-carbon or high-carbon steel, low-alloy steel, wrought iron, and cast iron. These corrode in slow-moving freshwater or seawater at almost the same rate, which is about 0.13 mm/year (0.005 in./year). At higher temperatures with equal values of dissolved gas concentration, the rate tends to increase, but remains relatively low. Therefore, steel can be used for boilers in contact with deaerated water. Commercially pure aluminum typically corrodes less in aerated or deaerated fresh water than iron and carbon steels, making it a suitable material for handling distilled water [(1,6,71)].

2.5.5.1 Low-velocity effects

Slow-moving and stagnant waters can prevent, damage, or remove passive films. The low velocity allows loosely adherent solid corrosion products to form on metal surfaces and allows debris to collect, which facilitates further corrosion

damage. In closed systems, if a corrosion inhibitor is used, its effectiveness is often reduced where the water is stagnant or quiet.

In designing for corrosion control, stagnant zones should be eliminated by the following methods:

- Circulation of stagnant liquids or relative movement of metallic surfaces
- Allowing free drainage of water
- Filtering suspended solids
- Providing an N_2 blanket (carbon steels) or free access to O_2 (stainless steels). Weakly passivating metals such as carbon steels are attacked by high O_2, whereas strongly passivating metals such as stainless steels are protected by uniform O_2 distributions.
- Maintaining concentration of dissolved passivating chemicals such as O_2 by infusion or injection **(6,71)**.

2.5.5.2 High-velocity effects

Swift-moving water may carry dissolved metal ions away from corroding areas before the dissolved ions can be precipitated as protective layers. Gritty suspended solids in water scour metal surfaces and continually expose fresh metal to corrosive attack.

In fresh water, as water velocity increases, it is expected that corrosion of steel first increases, then decreases, and then increases again. The latter occurs because erosive action serves to breakdown the passive state.

The corrosion of steel by seawater increases as the water velocity increases. The effect of water velocity at moderate levels is shown in Fig. (2.12), which illustrates that the rate of corrosive attack is a direct function of the velocity until some critical velocity is reached, beyond which there is little further increase in corrosion. At much higher velocities, corrosion rates may be substantially higher.

The effect of changes in water velocity on the corrosion resistance of

stainless steels, copper alloys, and nickel alloys shows much variation from alloy to alloy at intermediate velocities. Type 316 austenitic stainless steel may pit severely in typical seawater especially when stagnant and at velocities of less than 1 or 1.5 m/s (4 or 5 ft/s), but is usually very corrosion resistant at higher velocities.

In seawater at high velocity, metals fall into two distinctly different groups: those that are velocity limited (carbon steels and copper alloys).and those that are not velocity limited (stainless steels and many nickel alloys).

Metals that are not velocity limited are subject to virtually no metal loss from velocity effects or turbulence short of cavitation conditions. The barrier films that form on these metals seem to perform best at high velocities with the full surface exposed and clean. Crevices and under deposit form from low-moving or stagnant seawater because local breakdown of the film and pitting begins **(71-74)**.

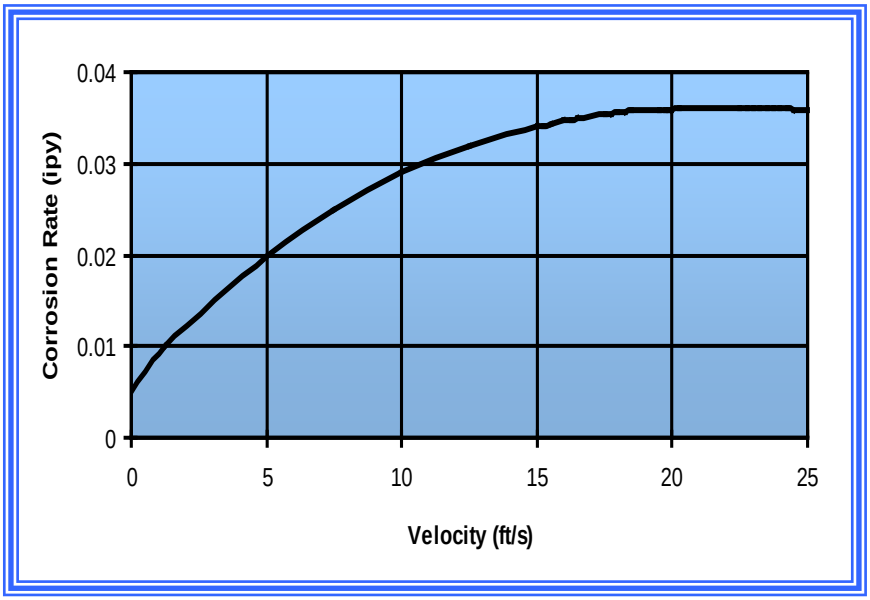

Fig.(2.12) Effect of velocity of sea water at atmospheric temperature on the corrosion rate of steel (71)

2.5.6 Effect of surface condition

The exact condition of a surface can have a large influence on the pitting behavior of a material. In general, samples prepared with a rough surface finish are more susceptible to pitting and exhibit a lower pitting potential. For example, the pitting potential of type 302 stainless steel with a 120-grit finish was shown to be approximately 150 mV lower than that for the same material with a 1200-grit finish over a range of chloride concentrations **(75).** The effect of surface roughness on pitting is related to the stabilization criteria described subsequently. Rougher surfaces have more occluded sites, which can sustain the conditions required for active dissolution at lower current densities and thus lower potentials because of the longer diffusion path length and slower rate of diffusion.

For stainless steels, heat treatment, grinding, and abrasive blasting have been reported to be detrimental to pitting resistance, whereas pickling in HNO_3 + HF scales or passivation in HNO_3 is beneficial **(53).** Heat treatments in air generate a chromium oxide scale and a chromium-depleted region under the scale. The seal is typically removed mechanically, and the chromium-depleted region is removed by pickling **(53).** Other common surface defects include heat tint from welding, embedded iron particles from machining, and MnS inclusions. The detrimental effects of these defects are minimized and the overall-surface condition improved by passivation in nitric acid, which increases the chromium content of the surface oxide film.

The effects of surface condition on localized corrosion are significant enough that care must be taken not to apply experimental data collected on samples with special preparation to a real application without taking the surface condition into account**(76)**.

2.6 Evaluation of pitting damage

Pitting is a localized type of attack, in which the rate of corrosion being greater at some areas than at others. If appreciable attack is confined to a relatively small fixed area of metal, acting as anode, the resultant pits are described as deep. If the area of attack is relatively larger and not so deep, the pits are called shallow[(2)].

Since pitting is a localized form of corrosion, conventional weight loss tests cannot be used for evaluation of pitting damage because metal loss is very small and the instrument does not measured it. The depth of pits are complicated by the, fact that there is a statistical variation in the depths of pits. Note that, the average pit depth is a poor way to estimate pit damage, since it is the deepest pit that causes failure. Therefore a measurement of maximum pit depth in sometime would be reliable way of expressing pitting corrosion.

However, once pitting started, penetration of the metal at an ever increasing rate will take place. In addition, pits tend to undermine or undermine cut the surface as they grow[(1)].

Depth of pitting is sometimes expressed by the term (pitting factor). This is the ratio of deepest metal penetration to average metal penetration as determined by weight loss of the specimen. A pitting factor of unity represents uniform attack as shown in Fig.(2.13).

Iron buried in the soil corrodes with formation of shallow pits, whereas stainless steels immersed in seawater characteristically corrode with formation of deep pits[(2)].

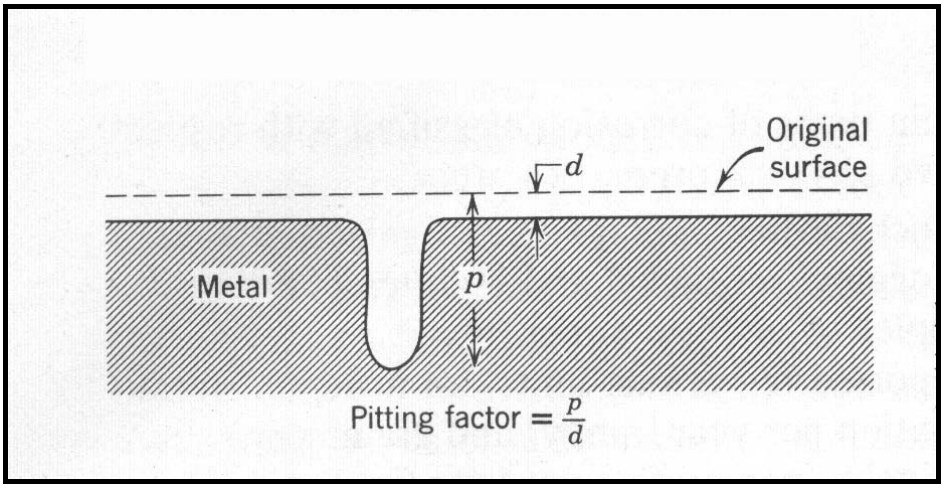

Fig.(2.13) Sketch of deepest pit with relation to average metal penetration and the pitting factor[(2)].

Chapter Three

Stainless Steel

3.1 Stainless steel

For years the food, beverage and pharmaceutical industries have used stainless steels in their process piping system. Most of the time stainless steel components provide satisfactory results. Occasionally a catastrophic failure will occur [77].

Stainless steel is not a single alloy, but a large family of alloys with different properties for each member. There are hundreds of grades and subgrades in the stainless steel family, each designed for a special application. Chromium is the magic element that transforms iron into stainless steel. Stainless steel must contain al least 10.5% chromium to provide adequate resistance to rusting, and the more chromium the alloy contains, the better the corrosion resistance becomes. There is, however an upper limit to the amount of chromium the iron can hold. Therefore additional alloying elements are necessary to develop corrosion resistance to specific medias [1,22,77,78].

Stainless steel is an alloy of iron. According to its definition, stainless steel must contain a minimum of 50% iron. If it contains less iron, the alloy system is named for the next major element. For example, if the iron is replaced with nickel-so that the iron is less than 50%-then it is called a nickel alloy. Chromium imparts a special property to the iron that makes it corrosion resistant. When the chromium is in excess of 10.5%, the corrosion barrier changes from an active film to a passive film .While the active film continues to grow over time in the corroding solution until the base metal is consumed, the

passive film will form and stop growing. This passive layer is extremely thin, in the order of 10 to 100 atoms thick, and is composed mainly of chromium oxide which prevents further diffusion of oxygen into the base metal. But, chromium also is stainless steel Achilles heel, and the chloride ion is stainless steel nemesis. The chloride ion combines with chromium in the passive layer, forming soluble chromium chloride. As the chromium dissolves, free iron is exposed on the surface and reacts with the environment forming rust. Alloying elements like molybdenum will minimize this reaction **(79-81)**.

Other elements, as illustrated in Table (3-1), may be added for special purposes. These purposes include: high temperature oxidation resistance, sulfuric acid resistance, greater ductility, high temperature creep resistance, abrasion resistance, or high strength. Of all these elements, only chromium is required in order for stainless steel to be stainless **(80,81)**.

Table (3-1) Stainless steel alloying element and their purpose (82)

Chromium	Oxidation resistance
Nickel	Austenite former - increases resistance to mineral acids and produces tightly adhering high temperature oxides
Molybdenum	Increases resistance to chlorides
Copper	Provides resistance to sulfuric acid precipitation hardener together with titanium and aluminum
Manganese	Austenite former - combines with sulfur, increases the solubility of nitrogen
Sulfur	Austenite former - improves resistance to chlorides, improves weldability of certain austenitic stainless steels,and improves the machinability of certain austenitic stainless steels
Titanium	Stabilizes carbides to prevent formation of chromium carbide precipitation hardener
Niobium	Carbide stabilizer - precipitation hardener
Aluminum	Deoxidizer - precipitation hardener
Carbon	Carbide former and strengthener

3.2 Classification of stainless steel

There are five classes of stainless steel: austenitic, ferritic, martensitic, duplex, and precipitation hardening. They are named according to how their microstructure resembles a similar microstructure in steel. The properties of these classes differ but are essentially the same within the same class. Table (3-2) lists the metallurgical characteristics of each class of stainless steel [(82)].

Table (3-2) Metallugical characteristics [(82)]

Austenitic	Non-magnetic Non-hardenable by heat treatment Single phase from 0° (K) to melting point crystallographic form - face centered cubic Very easy to weld
Ferritic	Magnetic Non-hardenable by heat treatment crystallographic form - body centered cubic Low carbon grades easy to weld
Duplex	Magnetic Non-hardenable by heat treatment Contains both austenite and ferrite Easy to weld
Martensitic	Magnetic Heat treatable to high hardness levels crystallographic form – distorted tetragonal Hard to impossible to weld
Precipitation hardening	Magnetic Crystallographic form - martensitic with microprecipitates Heat treatable to high strength levels Weldable

3.3 Basic corrosion resistance

Technically, corrosion is the tendency of any metal to return to its most stable thermodynamic state. Namely, that is the state with the most negative free energy of formation. More simply stated, it is a chemical reaction of the metal with the environment to form an oxide, carbonate, sulfate, or other stable compound. In most cases, using a different alloy, material, proper coating, or

impressed current can prevent corrosion problems. When a metal part fans in service, it is essential to determine the cause of the failure so that the replacement part can be manufactured from the proper alloy to prevent future failure. Many times a failed part is replaced with the same alloy. For example, if a piping system is made from type 304L stainless steel and it fails by chloride stress corrosion cracking, replacing with the same alloy will assure failure within the same time frame. If a change of alloy is made, say to a 6%Mo stainless steel such as AL-6XN, the piping may last for the lifetime of the system.**(77-81)**

3.4 Pitting corrosion of stainless steel

Pitting corrosion of stainless steel is a form of galvanic corrosion in which the chromium in the passive layer is dissolved leaving only the corrosion prone iron. The voltage difference between the passive and active layer on an austenitic stainless steel is +0.78 volts. Acid chlorides are the most common cause of pitting in stainless steel. Chlorides react with chromium to form the very soluble chromium chloride ($CrCl_3$). Thus, chromium is removed from the passive layer leaving only the active iron. As the chromium is dissolved, the electrically driven chlorides bore into the stainless steel creating a spherical, smooth wall pit. The residual solution in the pit is ferric chloride ($FeCl_3$), which is very corrosive to stainless steel. This is the reason why ferric chloride is used in so many of the corrosion tests for stainless steel. When molybdenum and/or nitrogen is used as an alloying element in stainless steel, the pitting corrosion resistance improves. In an attempt to quantify the effect of alloying elements, a relationship of the various elements responsible for corrosion resistance was developed. The resulting equation is called the pitting resistance equivalent number, or PREN **(53,83)**. It has a number of different coefficients of which the most commonly used form eq.(2-4).

A PREN of 32 is considered the minimum for seawater pitting resistance.

Three factors influence pitting corrosion: chloride content, pH, and temperature as shown in Fig.(3.1). In general, the higher the temperature and chloride content and the lower the pH, the greater the probability of pitting. For a given chloride content, a higher temperature and lower pH encourage pitting. Conversely, a lower temperature and a higher pH reduce pitting. The worst conditions occur with acid chlorides, and less dangerous conditions occur with alkaline or high pH chlorides. Pitting can occur rapidly once it starts**.**[78,82]

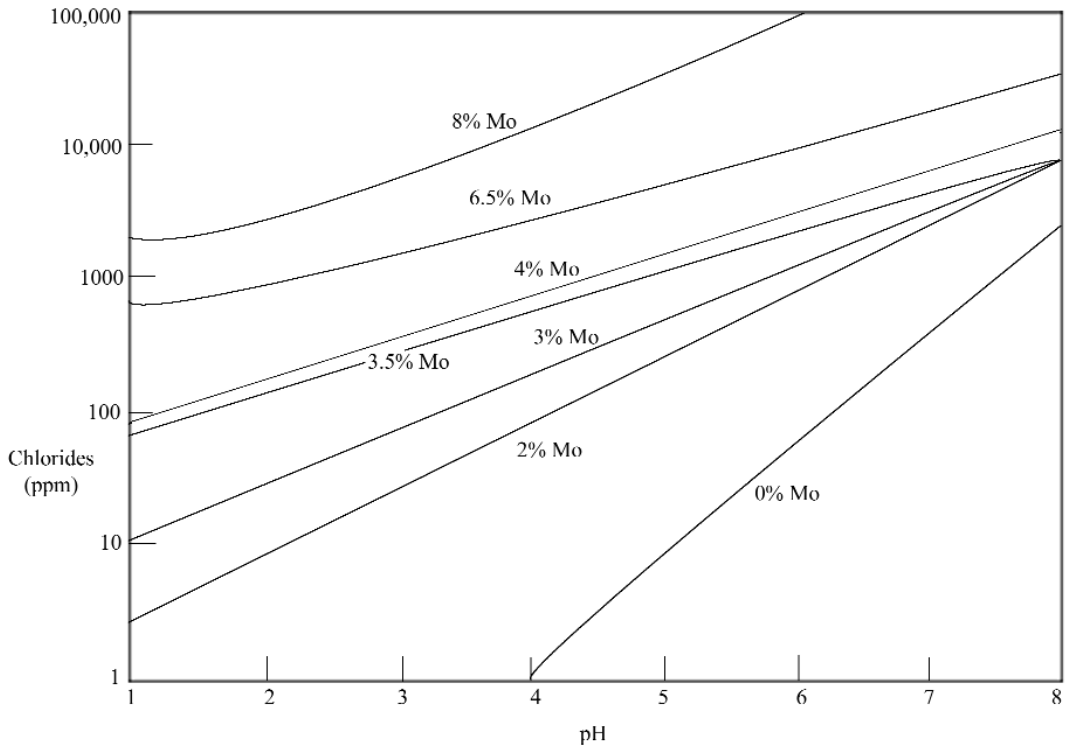

Fig.(3.1): Pitting corrosion relationship as a function of chloride content, pH and molybdenum content of austenitic chromium alloys. At temperature range, (150-180) F (65-80) ºC, pitting is not a problem below the line, but may be severe above the line [81]

For example, under the right conditions of chloride content, pH and temperature, a type 304 tube with a .035" (0.89mm) wall thickness will pit through in less than 8 hours. Increasing the molybdenum in the alloy produces greater resistance to pitting. Therefore high molybdenum – high chromium alloys generally provide the best pitting resistance.

3.5 Literature review

Salh **(84),** studied the pitting corrosion of Carbon Steel in Sodium Molybdate Solution, and found that the Sodium molybdate was a good (corrosion and pitting) inhibitor in solutions of moderate and low concentrations of chloride and the corrosion potentials shifted to more positive value in the presence of molybdate. He also found that the increasing the speed of rotation leads to a noble shifts, i.e. more positive, of the breakdown potential.

Malik et. al **(85)**,investigated the pitting behavior of type 316L SS in Arabian Gulf Sea Water, and found that the maximum pit depth of 316L stainless steel in Arabian gulf chlorinated sea water and the influence of exposure area on corrosion rate of 316L stainless steel can be expressed by the following equations:

$$D = 0.0082 * A^{(0.512)}$$

$$CR = 0.008 * A^{(0.089)}$$

where : D: maximum pit depth(mm), A: exposed area(cm^2)

They also found that the maximum pit depth of 316L stainless steel in gulf sea water can be expressed by the following equation:

$$D = 0.022 * t^{(0.136)}$$

where: (t) is the exposure time (month).

They conclude that the pitting potential varies for the same material under identical conditions depending upon the technique which has been used and decrease with increase in temperature, but corrosion rate and pitting tendency will increase.

Malik, et.al also studied the effect of scan rate on pitting corrosion of 316L SS, they suggest that the scan rate will not be affected by minor variations in the experimental procedure, and will let the film thickening to occur, therefore, the slow rate is the best while using of the potentiodynarnic pitting test

to study the localized corrosion.

Moreno, et.al[(86)] investigated using the potentiodynamic polarization to assess pitting of stainless steel by sulfate- reducing bacteria and found Biogenic sulfides in laboratory media enhance passivity breakdown of different SS in the presence of chloride anions. However, sulfide concentrations higher than 10^{-2} M are needed to induce pitting in SS surface. At lower sulfide concentrations, passive behavior of SS remains undisturbed, as was found for chloride solutions.

Smialowska [(87)] studied the effect of alloying elements on passivity and breakdown of passivity of Fe- and Ni- based alloys and found that the penetration of chloride ions to the metal is not the rate determining step in pitting corrosion. The rate determining step for stable pit growth is the establishment of solution composition within the preexisting defect at the metal/film interface that allows an active dissolution of the metal and she suggested the metastable pits are formed when the alloy/ metal dissolution rate within the pits is too low to sustain a sufficiently low pH. Therefore, repassivation occurs.

Dawood [(88)] studied the pitting corrosion of duplex stainless steel and found that the duplex stainless steel SAP 2205 was found to have superior pitting corrosion resistance in chloride solution at room temperature, far noble over that of 316L SS. Pitting resistance of alloy SAP 2205 decreases sharply as the temperature increases above room temperature .Duplex stainless steel SAP 2205 loses much of its pitting corrosion resistance, when annealed at temperatures above 1373K up to 1573K. The addition of 0.05 & 0.01N of fluorides to 0.5N NaCl solution decreases the pitting corrosion resistance of the SAP 2205 alloy, but further addition (0.15N) causes no decrease in the pitting resistance.

Park, et.al [(89)] ,studied the effect of bicarbonate ion additives on pitting

corrosion of type 316L SS in aqueous 0.5 M sodium chloride solution using potentiodynamic polarization, the abrading electrode technique, alternating current (AC) impedance spectroscopy combined with x-ray photoelectron spectroscopy (XPS), and scanning electron microscopy (SEM). Addition of HCO_3^- ions to NaCl solutions extended the passive potential region in width and, at the same time, raised the pitting potential in value on the potentiodynamic polarization curve. Potentiostatic current transients obtained from the moment just after interrupting the abrading action showed the repassivation rate of propagating pits increased and that the pit growth rate decreased with increasing HCO_3^- ion concentration. Over the whole applied potential, the oxide film resistance was higher in the presence of HCO_3^- ions. The pit number density decreased with increasing HCO_3^- ion concentration. Moreover, addition of HCO_3^- ions to NaCl solutions retarded lateral pit growth, while promoting downward pit growth from the surface.

Kolman, et.al **(90)** investigated the Corrosion of 304 SS exposed to nitric acid - chloride environments and found that some solution chemistries promoted active corrosion upon immersion. Corrosion in these solutions was observed to be autocatalytic, with the corrosion rate increasing exponentially with time and potential. Increasing NaCl was deleterious to the corrosion resistance of 304 SS at all temperatures examined, from room temperature to boiling. Increasing NaCl concentrations promoted active dissolution upon initial immersion, a larger anodic overpotential required for passivation, pitting, longer active corrosion periods, larger anodic charge densities preceding passivation, and larger corrosion current and peak current densities. During active corrosion, increasing HNO_3 concentration increased anodic charge density, corrosion current density, and peak current density. The time required for spontaneous passivation was a maximum at intermediate HNO_3 concentrations. Susceptibility to pitting was the highest at intermediate HNO_3

concentrations; the pit initiation and repassivation, potentials decreased with increasing HNO_3 until pitting susceptibility was entirely eliminated. Passive current densities were not affected by NaCl or HNO_3 concentration. Increasing solution temperatures increased the susceptibility to both pitting and active dissolution. Higher temperatures resulted in increased corrosion current densities and peak current densities as well as lower pit initiation and repassivation potentials. Increasing temperature increased anodic kinetics more rapidly than cathodic kinetics.

Newman,**(91)**pointed out that the quality of the passive film mainly affects the nucleation frequency of pits and has little or no bearing on the effects of environmental or metallurgical variables: T, Cl^-, Br^-, H_2S: Mo, N,.... ,and found that the anodic kinetics of the metal in the already-developed microenvironment of a pit can account for the effects of a large number of variables in pitting corrosion. Specifically, above the critical pitting temperature (CPT). The CPT itself is associated with the inability of the metal to maintain active dissolution because passivation intervenes, even in the most aggressive possible microenvironment.

Yashiro, et.al **(92)** investigated the effect of nitrogen alloying on the pitting of type 310 stainless steel and found that the pitting is suppressed by nitrogen addition to stainless steel remarkably when temperature is lower than the critical value and also found that the addition of nitrogen is effective to increase the critical pitting temperature. Nitrogen in a metal matrix and nitrate ion in a solution have a common feature in terms of potential dependency of pitting inhibition. Finally alloying stainless steels with nitrogen does not give a remarkable effect to enhance the pitting resistance under every condition as is the case at high temperature but the weak point of nitrogen could be made up for by additional alloying with molybdenum.

Neusa, et.al **(93)**investigated the correlation between corrosion potential

and pitting potential for AISI 304L &304LL austenitic stainless steel in 3.5% NaCl aqueous solution in which the Ni content of 304LL steel is considerably in excess of the maximum value specified for AISI 304L & the C,P,S,Si,Mn and N contents in 304LL steel are lower than in 304L steel and the second"L" is used to indicate this condition. and found the corrosion potential E_{corr} of 304L and 304LL stainless steels in 3.5%Nacl aerated solution, as well as its standard deviation, are strongly affected by the type of surface finish. A linear correlation between the pitting potential E_p and the corrosion potential E_{corr} was observed for four of the five surface finishes tested. The difference between these potentials is considerably larger than that anticipated by the above linear correlation. The above correlations imply that the E_{corr} value can also be used to evaluate the resistance of a given stainless steel to pitting corrosion.

Martin, et.al **(94)** studied the effect of fluoride ions on the anodic behavior of mill annealed and aged alloy 22 and found Alloy 22 is highly resistant to localized corrosion in saturated NaF solutions at 90°C .Neither pits nor crevices were found after anodic polarizations reached currents up to 1-10 mA.cm-2. The lower the solutions pH the higher the passive and transpassive current densities.

Jacek, et.al **(95)** studied the effect of sequence of sol-gel multilayer coatings deposition on corrosion behavior of stainless steel 316L and found that the addition of nanosilica and the cation surfactant DoDAB has a favourable effect on the protective properties of the sol-gel coatings on stainless steel substrates of the type 316L. It is also the sequence of deposition at the layers that contribute to the protective properties of the coatings obtained.

Kear, et.al **(96)** investigated the electrochemical study of UNS S32550 super duplex SS corrosion in turbulent seawater using the rotating cylinder electrode ,and found that the UNS S32550 alloy exhibited excellent passivation and re-passivation characteristics in the filtered seawater at turbulent flow velocities of up to 1.5 m s^{-1}. In this relatively short-term exposure study, the

material exhibited a high corrosion resistance to the filtered seawater when in both the freshly polished and pre-reduced states. A passive film formed on the pre-reduced surface over the corrosion potential equilibration period with comparatively low electronic resistance. Both cathodic and anodic polarization close to the corrosion potential behaved independently of reactant/product mass-transfer rates. Thus, the corrosion rate of UNS S32550 is predicted to have little dependence on fluid velocity via a mass-transfer-facilitated, flow-induced corrosion mechanism.

Zhenqiang, et.al **(97),** investigated that surfactants as green inhibitors for pitting corrosion of stainless steels, and found that the sodium dodecylsulfate (SDS) and some other surfactants have shown to be promising inhibitors for the pitting corrosion of stainless steels and aluminum alloys in chloride media. It was shown that calcium ion increased the pitting inhibition efficiency of SDS. The efficiency increase was attributed to the increased SDS adsorption in the presence of calcium.

Gaben, et.al **(98),** studied the influence of the chemical composition and electronic structure of passive films grown on 316L SS on their transient electrochemical behavior and found that the ageing of a passive film by a dc or ac passivation treatment involves important modifications of its chemical and electronic structure, leading to an improvement in its pitting resistance. It appears probable that the electronic properties control the shape of the coupling current, and could consequently have a strong influence on the metastable to stable pitting transition.

Guo, et.al **(99),** studied the effect of environmental factors on the corrosion of 2024T3 Aluminium, and found that the pitting occurs after the six day alternate immersion test and the statistical maximum corrosion depth and among the four factors representing oceanic atmosphere environment, concentration of CI^- and SO_4^{2-} and temperature have great effect on the

corrosion of 2024T3 aluminum alloy while humidity contributes less to it. With the relative humidity increasing from 55% to 95%, the maximum corrosion depth decrease slightly.

Carranza, et.al **(100)**, studied the corrosion behavior of Alloy 22 in chloride solutions containing organic acids and found that the corrosion rates of Alloy 22 after 24hr. of immersion in 1M NaCl solutions with the addition of oxalic acid in concentrations ranging from 0.1M to 0.001M were higher than those obtained for pure 1M NaCl solutions at the same pH, while the addition of the same concentrations of acetic acid produced no corrosion rate increase. Higher passive current densities were found during cyclic potendtiodynamic polarization of Alloy 22 in solutions containing oxalic acid compared to 1M NaCl solutions at the same pH values .The transpassivity potential was dependent on solution pH.

Refaey, et.al**(101)** investigated corrosion and inhibition of 316L SS in neutral medium by 2-Mercaptobenzimidazole (MBI),and found that the MBI compound has proven to be efficient inhibitor for general and pitting corrosion of 316L SS in NaCl solution. The inhibition efficiency of MBI inhibitor increases with increasing of the inhibitor concentration, but decreases with the increasing of temperature. The increase of MBI concentration increases the breakdown potential towards the positive direction .The inhibition of 316L SS in NaCl solution at different temperatures found to obey the Langmuir adsorption isotherm.

James, **(102),** investigated stainless steel process equipment and chloride – induced failure, and found the chloride-induced SS is a readily avoided problem. By appropriate modification of the use of cleaning chemicals, corrosion problems can usually be eliminated. If this can not be achieved , then many specially alloys exist that can provide long –term service in chloride-rich environments.

Lameche, et.al **(103),** studied the effect of temperature on the pitting of three stainless steels. (High-cost duplex:22%Cr-6%Ni-3%Mo), (Modified: 13%Cr-5%Ni-0.7%Mo), and (Conventional cheap 13%Cr- 0.08%Ni) in chloride containing solutions and found that the influence of the temperature was highlighted, in the case of stainless steels .With the cyclic polarisation technique, it was possible to measure E_b and E_{rep}, this technique provideS information about pitting corrosion and passivation, the higher the value of E_b, the more resistant the alloy is to pitting corrosion, increasing the temperature causes the surface films to become less stable, and reduces the values of potential of pitting E_b. The (PREN) value is a function of temperature though the presence of significant chloride content is also important. Chromium and molybdenum enhance the stability of passive films. The duplex stainless steels with 22%Cr-5%Ni-3%Mo showed pitting corrosion resistance higher than, the conventional 13%Cr and modified 13%Cr stainless steels since it contains alloy elements like molybdenum and the nickel which ensures the passivity and resistance to chloride.

Yahia, et.al **(104),** studied the influence of cold work by traction on the resistance of 304L stainless steel to pitting in 30 g/1 of NaCl and found that the hardness of the 304L steel increases with the increasing of the elongation rate, the presence of inclusion of MnS is a site favourable to a pit, the noblest corrosion potential corresponds to the weakest elongation rate .The more hardness increases the corrosion potential corrosion increases in absolute value.

Troels,et.al **(105),** investigated that unusual corrosion failures of stainless steel in low chloride waters and found that the presented examples demonstrate that in few cases fresh water can be corrosive to conventional stainless steels like AISI 304 and AISI 316 although full resistance was expected from the combination of temperature, corrosion potential and chloride concentration. The observed corrosion was always associated with formation of voluminous

tubercles that sometimes contained bacteria producing aggressive components, such as sulphide or thiosulphate. When combined with the slight ennoblement from the biofilm formation on free surfaces, pitting or crevice corrosion was enabled. Based on experience from a research program on manganese bacteria we doubt the possibility of correlating the corrosion risk with bacterial analysis of water samples, although it is clear that stagnant water containing nutrients for any type of growth should be avoided. In our view a more beneficial approach is to ensure a high degree of cleanliness and manufacturing quality during installation, and follow this by thorough flushing of the stainless steel system before use.

3.6 The aim and the scope of present work

From the study and the analysis of theoretical part of this dissertation and literature review, it can be found that, the study of the parameters effected on the pitting corrosion vary in their results.

Some investigators found that the temperature has no effected on (E_b) value, while others reported that temperature has a great effect on (Eb), whearse, some authors indicated that (E_b) remains constant at a range of temperature.

Also the effect of scanning rates had been varied according to the studies and researchers. Some researchers observed(E_b) values goes to more noble as the scanning rate increase and they found a straight line dependence between the scanning rate and (E_b). Other researchers found that (E_b) independent on the scanning rate but the applied scanning rate fills within the straight line of the relationship between (E_b) and scanning rate.

However, some studies admitted that the low scanning rate gives more noble of (E_b) value than those obtained at higher scanning rates. Other reported

that applied scanning rates should not be to high or low to give more noble (E_b) value than the actual.

The effects of the concentration and the velocity of the solution on pitting corrosion are complex and depends on the characteristics of the metal and the environment to which it is exposed, for example, when agitation or solution velocity are increased, there are some effect on the pitting corrosion according to some studies, while the others had shown no effect of theses parameters on the pitting formation. Others admitted that these parameters effected generally when an oxidizers are present(although in very small amounts).

Some metals and alloys owe their pitting resistance in certain mediums to the formation of massive bulk protective films on their surface. When these metals and alloys are exposed extremely high velocities, mechanical damage or removal these films can occurs, resultant in accelerated on pitting corrosion. Therefore, the effects of the concentration and the velocity of the solution vary with types of metals and concentration of the solution.

From above explanation, the aim and scope of the present work include to study:

1. The influences of temperatures of the NaCl solution on the electrochemical behavior of two types of stainless steel(316L&202).
2. The influences of scanning rates(10,15,30,40)mV/min. on the electrochemical behavior of 316L stainless steel at 308K in 3.5%NaCl solution.
3. The influences of the concentration of NaCl solution on the electrochemical behavior of two types of stainless steel (316L&202).
4. The influences of the velocity (speed of rotation cylindrical elyctrode) on the electrochemical of two types of stainless steel(316L&202).

In this study the range of temperatures which had selected are (298,308 and 318)K, concentration of NaCl solution(2.5&3.5)wt% and the velocity (100,200and300)r.p.m., these conditions are taken place as dynamic, while at static condition, temperatures(298,308and318)K and (1.5,2.5and3.5)wt%NaCl solution at scanning rate 20mV/min..

The (316L&202) stainless steel, where selected in this work because there widely used in industry.

CHAPTER FOUR

EXPERIMENTAL WORK

4.1 Introduction

The present work is aimed to investigate the effect of some variables on the pitting corrosion of two types of stainless steel (316L and 202) and study their electrochemical behavior in NaCl solution using the polarization technique.

The experiments were carried out under static conditions at different temperatures (298,308and318)K and different NaCl concentration solutions(3.5, 2.5 and 1.5)%.

In order to study the effect of velocity on the electrochemical behavior at different rotation speeds (100, 200 and 300) r.p.m using rotating cylinder electrode were studied for (3.5 and 2.5)% of NaCl solutions at temperatures (298, 308 and 318) K.

The above experiments were repeated for the two types of SS, i.e,(316L and 202).

The scan rate effect of (10, 15, 30, and 40)mV/min. on the electrochemical behavior of 316L SS at 308K in 3.5% NaCl solution was investigated also.

4.2 Experimental apparatus

The experimental apparatus used in this work is shown in Fig. (4.1). It consists mainly of:

- Potentiostat (Wenking LT. 87)
- Polarization cell
- Rotating cylinder electrode assembly

- Digital multimeters
- Constant temperature bath (Memert P21S6)
- Car jack

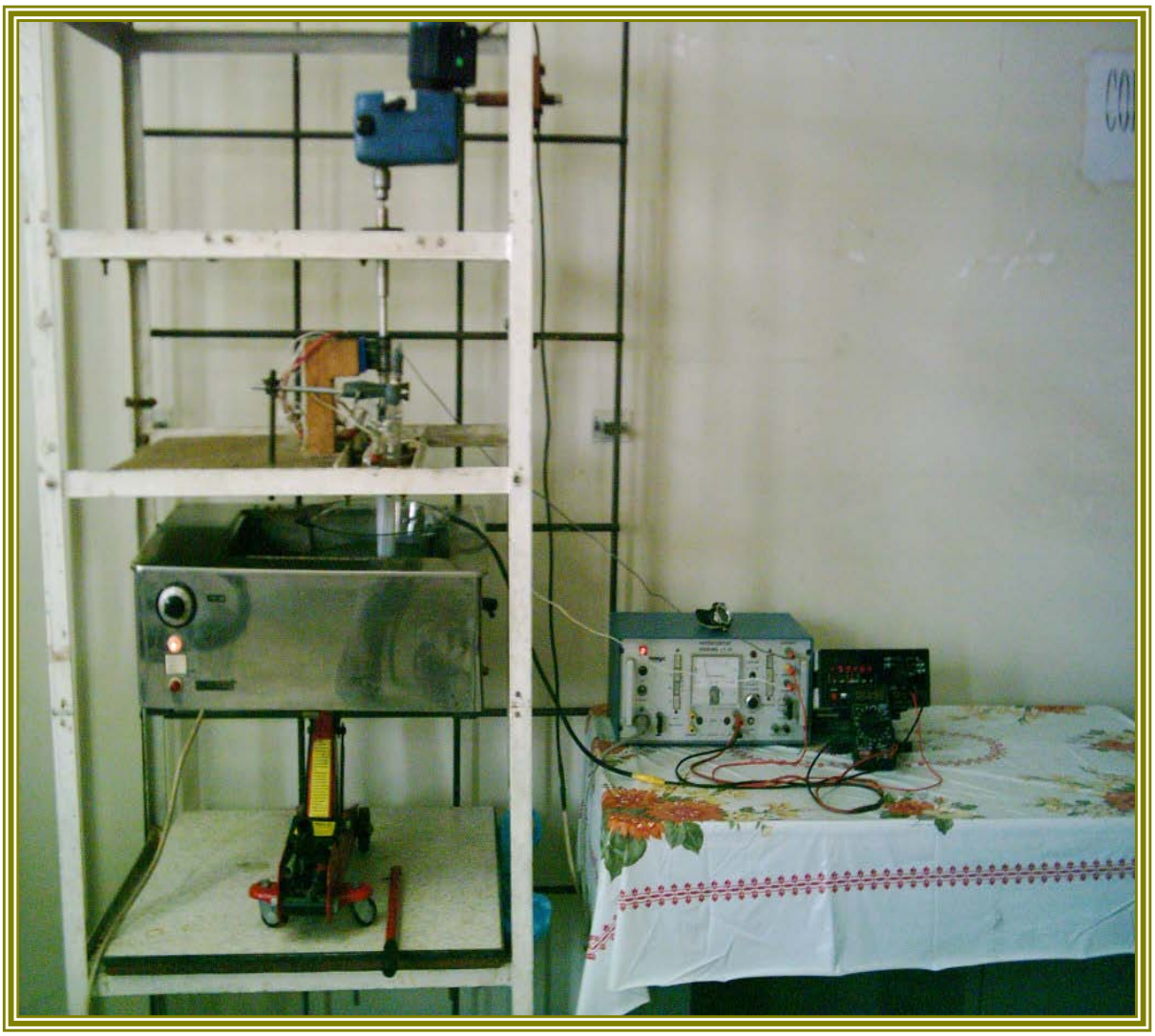

Fig.(4.1): The apparatus

4.2.1 The rotating cylinder, electrode assembly

The rotating electrode assembly used in this work consists of the following items as shown in Fig. (4.2):

1. The rotating cylinder electrode shaft.
2. A driving shaft, bearing unit and slip-ring (together described later as the electrode mounting); and

3. A driving unit (motor and speed controller).

The description and design of each part of the rotating electrode assembly is shown below:

4.2.1.1 The rotating cylinder electrode

Rotating cylinder electrodes have become more widely used. This method has well established flow patterns and to determine the hydrodynamics parameters (wall shear stress and mass transfer coefficient and Reynolds number) are well established. This method is carried out only at atmospheric pressure **(106)**.

4.2.1.1.1 The working electrode (rotating cylinder)

The rotating cylinder comprises a stainless steel cylinder; see Fig. (4.3), which has the following dimensions:

r_o = 15 mm

r_i = 8 mm

h = 20 mm

The spectrographic analysis of the two types of stainless steel is given in Table (4.1).

Table (4.1): Spectrographic composition of two types of stainless steel (wt%)

Metal Composition	C	Cr	Ni	Mo	Si	Mn	P	S	Cu	Nb	Ti	V	Fe
Standard 316L	0.1max	16-18	10-14	2-3									
316 L	<.03	16.7	10.2	2	.405	1.67	<.025	.0295	.378	.072	<.03	.134	67.5
Standard 202	.15max	17-19	4-6			7.5-10							
202	<.025	17.3	4.1	.131	.375	7.61	.128	.0194	1.45	-	-	.0344	68.43

The chemical analysis was performed by Specialized Institute for Engineering Industries.

The inside surface of each specimen was provided with a screw thread to facilitate its attachment to, and removal from, the electrode shaft at the beginning and end of each experiment.

4.2.1.1.2 The electrode shaft

The electrode shaft has the following features.

1. The lower part of the electrode shaft has means to facilitate the attachment and removal of the specimen;
2. A provision for electrical connection to the working electrode (the specimen), and,
3. A provision for mounting the electrode shaft on the driving shaft.

The details of the electrode shaft design for RCE are shown in Fig. (4.3).

4.2.1.2 The electrode mounting

The electrode mounting comprises a driving shaft, bearing units and a slip-ring unit as shown in Fig. (4.2).

4.2.1.2.1 The driving shaft

A stainless steel shaft, which consists of three parts, was used to connect the driving motor and the rotating electrode. The lower part (20mm diam. × 100 mm long) was screw threaded in order to facilitate the mounting of the rotating electrode onto the shaft. The middle part (12.5mm× 150 mm long) was used to secure the slip-ring mount onto the driving shaft. The upper part (20 mm dia. × 170 mm long) was used to connect the driving shaft to the driving motor.

A hole of 12 mm diameter was drilled in the lower part of the shaft at a distance of 90 mm from the top to the rotating electrode. This hole was made to facilitate the passage of wire from the working electrode upward through the lower bearing unit.

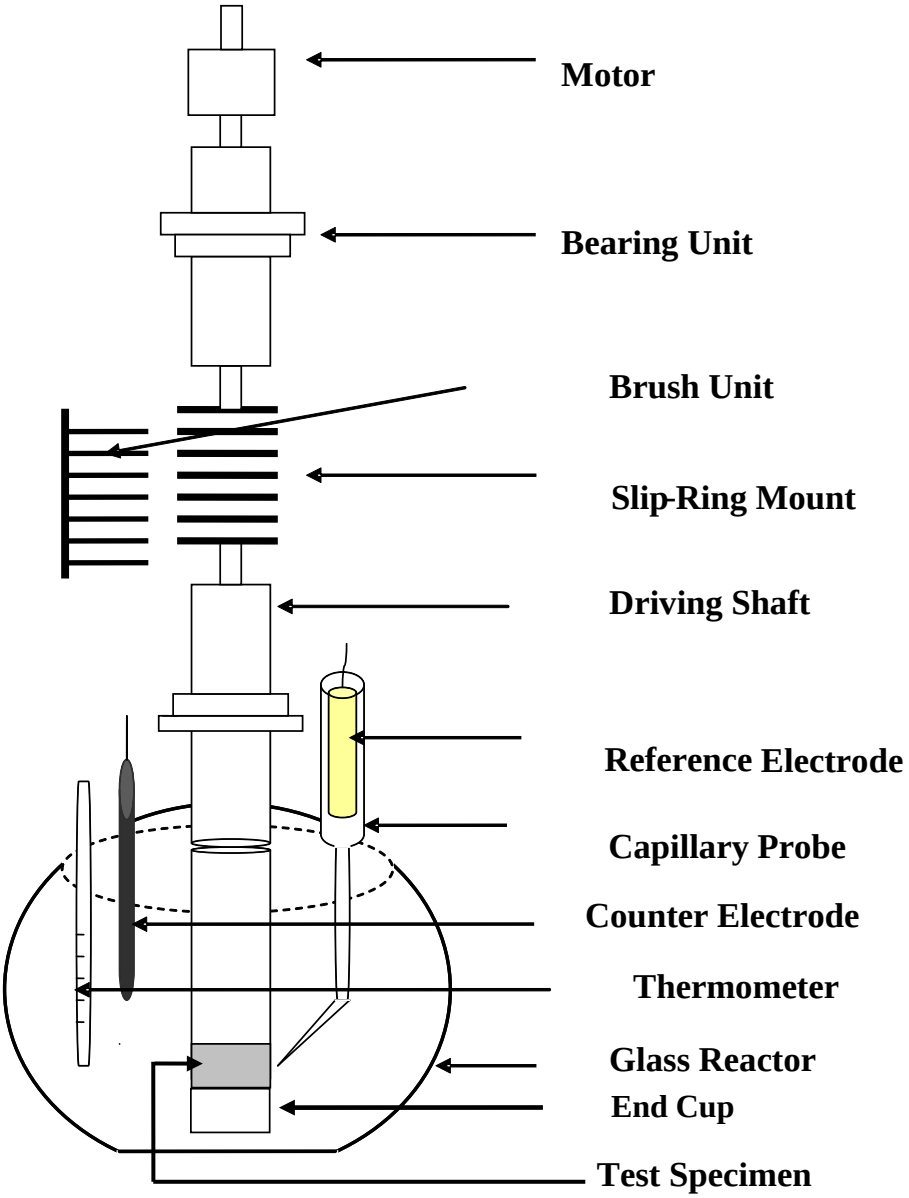

Fig.(4.2): The rotating cylinder electrode assembly in polarization cell

4.2.1.2.2 The bearing unit

In order to reduce eccentricity to the minimum two (20mm) bore diameter self lube flange bearing units were mounted onto the driving shaft at a distance of 30mm and 340mm from its top.

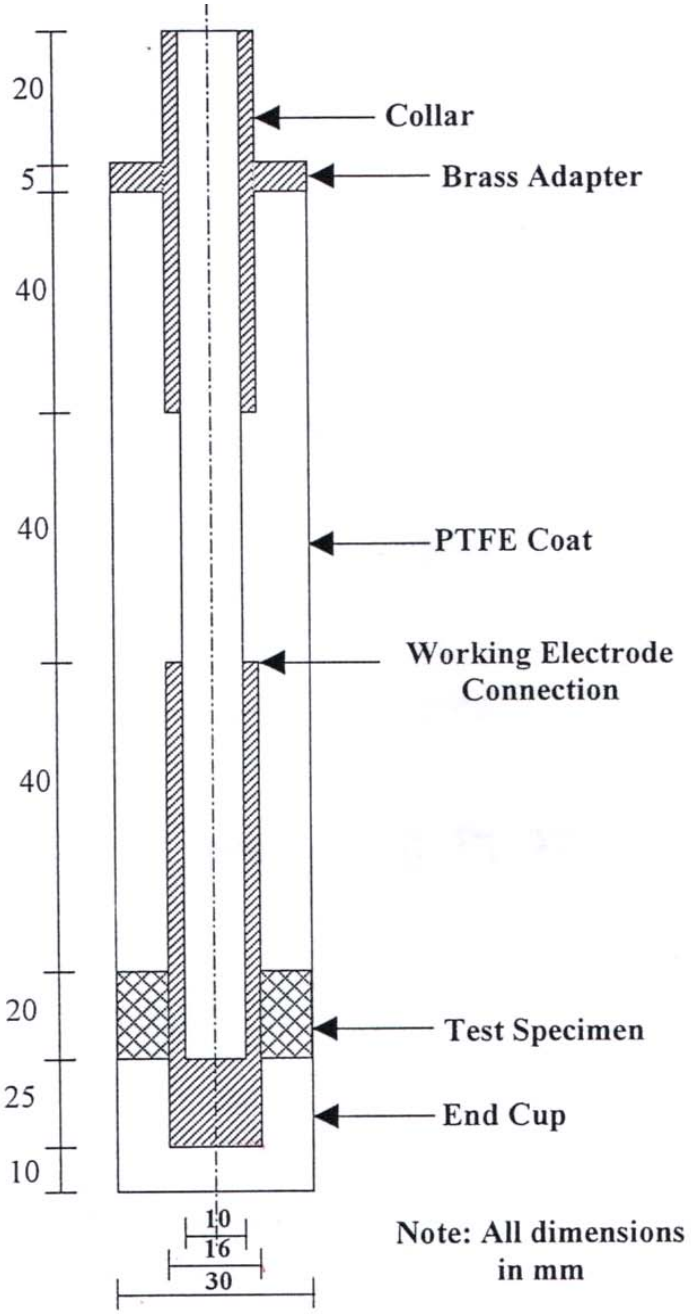

Fig.(4.3): Rotating cylinder electrode

4.2.1.2.3 The slip-ring unit

Electrical contact between the rotating electrode, on the side and the potentiostat on the other side was made by a 12.5mm bore diameter cylindrical types slip-ring unit (D.J. Mouldings Ltd.)

The unit consists of a 12 silver slip-ring mount and a matching silver graphite tipped brush unit.

The working electrode was contacted to the slip-ring and electrically insulated wire. A similar arrangement was made at the brush unit.

4.2.1.3 The driving unit

The driving unit comprises:

1. 1/8 h.p motor with a maximum speed of 2000 r.p.m.
2. A speed controller with a selector switch of two stages.

The first stage is up to 200 r.p.m. and the second stage from 200 to 2000 r.p.m.

The motor is fixed to the main supporting framework using a special arrangement to prevent vibration as shown in Figs (4.1) and (4.2).

When the RCE assembly was finally completed in the arrangement shown in Fig.(4.1) and, it was kept undisturbed throughout the whole experimental programmed except for the removal of the cylinder section itself. This helped to prevent misalignment and hence reduce eccentricity to the minimum.

4.2.2 The polarization cell

The polarization cell, see Fig.(4.2), consists of a cylindrical glass reaction vessel, lugging capillary probe, reference electrode, counter electrode, the working electrode and a thermometer.

The glass reaction vessel (230mm diameter × 160mm high) has a capacity of 3 liters.

A capillary connection to the reference electrode (saturated calomel electrode, SCE) was used with its tip acting as the lugging probe. The tip was adjusted at a distance of 1-2 mm from the working electrode surface **(107)**.

All the potential values were measured with a reference to saturated calomel electrode (SCE).

Graphite counter electrode was used and fitted to the cell via rubber bung.

4.2.3 Experimental solution

Distilled water was used to prepare solutions. Sodium chloride (NaCl) was used with different concentrations (3.5, 2.5 and 1.5) wt%. Solutions were prepared over-night.

4.3 Metal specimens

Two types of stainless steel (316L and 202) specimens were 2 cm long, 3 cm outside diameter and 1.6 cm inside diameter. The inside cylindrical surface was tapped leaving only the outside cylindrical surface exposed to test solution. The specimens were cleaned carefully and degreased by acetone.

4.4 Experimental procedure

4.4.1 Experimental program

The experiments were carried out to determine the polarization curves (cathodic and anodic) in (3.5, 2.5)% NaCl solutions.

Potentiostaic experiments were carried out at constant temperatures (298, 308, 318) K with controlled conditions of speed, i.e.,(0, 100, 200, and300) r.p.m. for RCE. A single experiment involved electrochemical polarization for each type of stainless steel electrode, from – 500mV and scanned potentiostatically in the noble (positive) direction until +500mV, with scan rate of 20mV/min..

For 1.5% NaCl solutions, potentiostatic experiments were carried out at temperatures (298,308,318)K with static conditions, i.e., (0 r.p.m.)for two types of stainless steel.

For 3.5% NaCl solutions, potentiostatic experiments were carried out at constant temperatures (308)K with static conditions, i.e., (0 r.p.m). with different scan rate (10, 15, 30, 40) mV/min. for 316L stainless steel only.

4.4.2 Electrode surface preparation

Prior to every experiment, each type of stainless steel electrode surface was a braded on successive grades of silicon carbide from 400,500 and 1200 to grit under running tap water to avoid heating due to friction. It was then washed with running tap water followed with distilled water, rinsed with acetone and dried with clean tissue paper. It was, then, kept in a desiccator over a silica gel **(108)**.

4.4.3 Electrochemical polarization

The polarization cell was filled with (2.5) liter of the required test solution, and then placed inside a constant temperature water bath supplied with a thermostat to keep the temperature constant within (±1°C) until the solution reached the preset temperature. After that, the water bath was raised up using a car jack, until the RCE was introduced into the solution.

The lugging probe was kept at a distance of 1-2mm from the specimen surface. The working, counter and reference electrodes were connected to a potentiostat (Wenking LT. 87). Immediately, the stainless steel electrode was electrochemically polarized to – 500mV. The RCE was set in motion at the required r.p.m. by manually adjusting the speed controller and scanned potentiostatically in the noble (positive) direction until breakdown was reached, at a rate of 20mV/min..

Potential and current were checked and read off digital multimeters (DT-830B Fuke and Solartron-7050 Schlumberger respectively). Each test was made twice, and if reproducibility was in doubt a third test was carried out.

Chapter Five

Results and Discussion

5.1 Introduction

The present work aims to study the influence of temperature (298,308,318)K, concentration of NaCl solution (3.5,2.5 and 1.5) wt% and the speed of rotation of the Rotating Cylinder Electrode (RCE) (0,100,200 and 300) r.p.m. on the corrosion of two types of stainless steel (316L and 202). The potentiostatic method used from negative potential in cathodic region (-0.5V) until breakdown potential is reached with scan rate of 20 (mV/min.) was applied for static and dynamic conditions.

The influence of scan rate (10,15,20,30 and 40) (mV/min.) on the breakdown potential have been studied at (308) K for 316L in 3.5% NaCl solutions at static condition.

The results will split into two categories (316L and 202) SS. Each one will be grouped into two main parts the first under static conditions, and the second under dynamic conditions.

5.2 Stainless steel type 316L

5.2.1 Static conditions

Potentiodynamic method which involve a continuous change of potential at constant rate of (2mV/sec) and recording the corresponding current density {i.e, i=f(E)} is used to determined the E_b to confirmed the results in potentiostatic method which had be shown in Figs.(5.1-5.3).

Fig.(5.0),shows the electrochemical method used to determine (E_b). (E_b), in this figure represents the point sudden increase in current density occurs

while pitting corrosion (E_p) represents the point at which the current density retained to the passive region when reversing the potential after pit initiation i.e, repassivation of pits occurs. The value of current density at which the potential reversed is used to be taken as(i_p), which is required for pits initiation . These results have good agreement with work of [119].

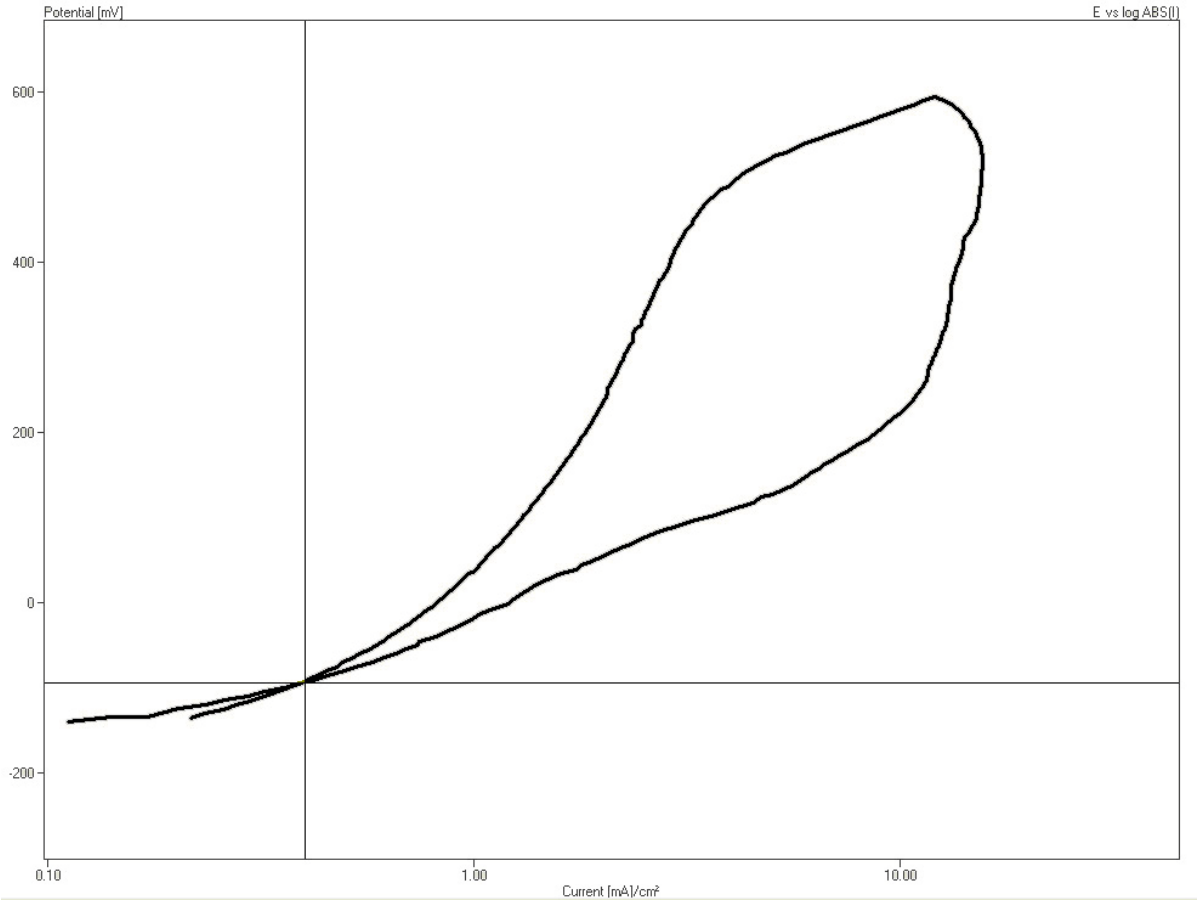

Fig.(5.0) Repassivation of a potentiodynamic of 316L at static condition in 3.5%NaCl solution by using scanning rate 2mV/sec. at room temperature.

The first set of these results are presented in Figs.(5.1-5.3),which show the influence of temperatures (298,308 and 318)K on the corrosion behavior of 316L SS in the solutions containing (3.5,2.5 and 1.5)wt% of NaCl respectively.

5.2.1.1 Effect of temperature

Figs.(5.1-5.3), show the effect of temperatures on the electrochemical behavior of 316L SS in (3.5,2.5 and 1.5)% of NaCl solutions. They indicate that

increasing in temperatures leads to decreases in passive region of the metal and shift the E_b to more negative direction. The main characteristics of the results from these figures are shown in Tables (5.1-5.3) respectively.

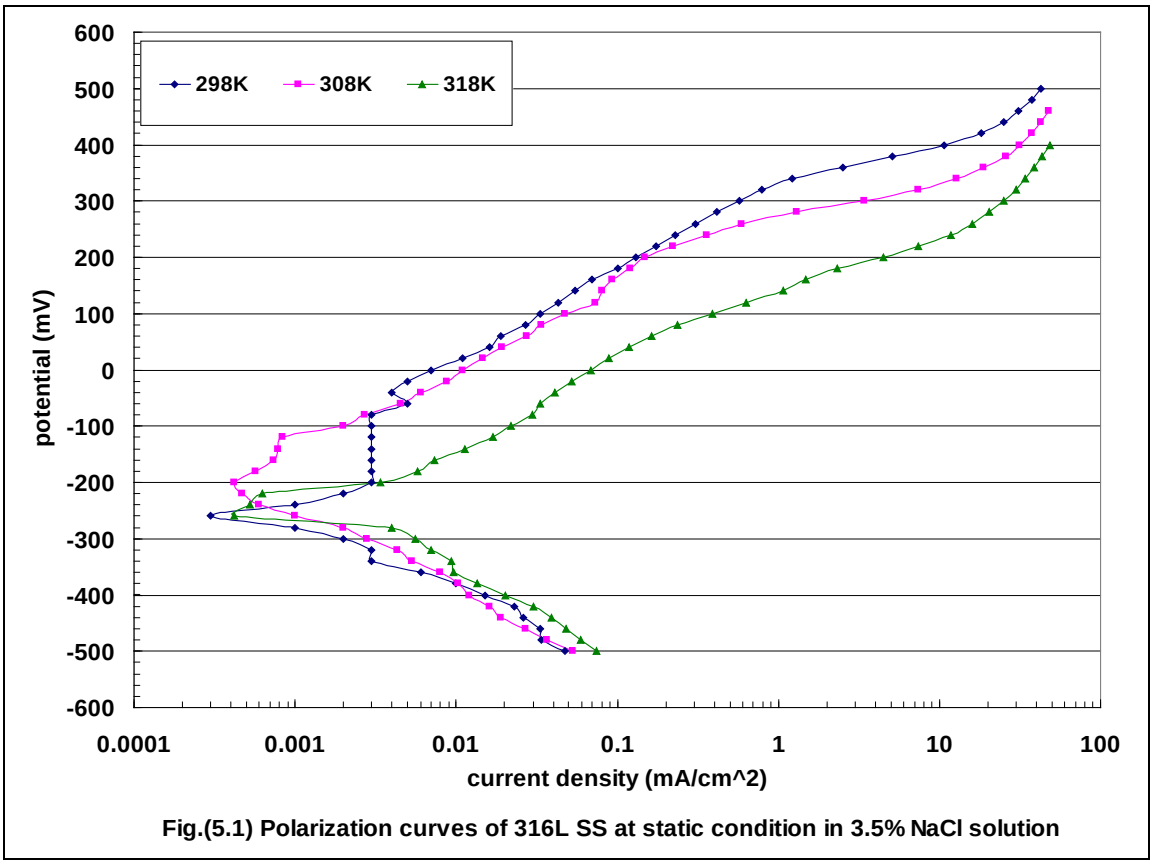

Fig.(5.1) Polarization curves of 316L SS at static condition in 3.5% NaCl solution

Table (5.1) The effect of temperatures (K) on the corrosion potential (mV), primary passive potential (mV),breakdown potential (mV) and corrosion current density (mA/cm^2) of 316L SS at static condition in 3.5%NaCl solution

Temp. K	$E_{corr.}$ (mV)	$E_{pp.}$ (mV)	E_b (mV)	$i_{corr.}$ (mA/cm^2)
298	-260	-200	-80	0.0015
308	-200	-180	-120	0.0016
318	-260	-240	-220	0.0027

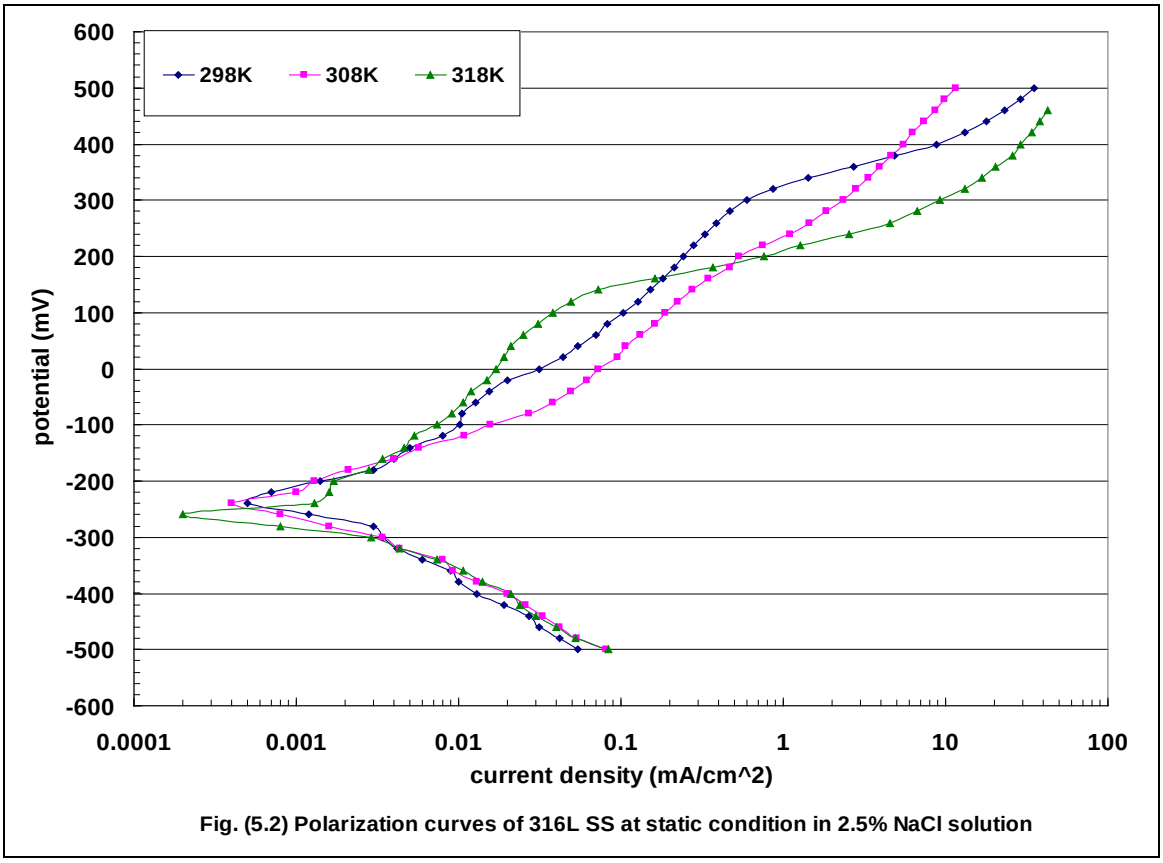

Fig. (5.2) Polarization curves of 316L SS at static condition in 2.5% NaCl solution

Table (5.2) The effect of temperatures (K) on the corrosion potential (mV), primary passive potential (mV),breakdown potential (mV) and corrosion current density (mA/cm^2) of 316L SS at static condition in 2.5%NaCl solution.

Temp. K	$E_{corr.}$ (mV)	$E_{pp.}$ (mV)	E_b (mV)	$i_{corr.}$ (mA/cm^2)
298	-240	-100	-80	0.0014
308	-240	-200	-140	0.0016
318	-260	-260	-200	0.0025

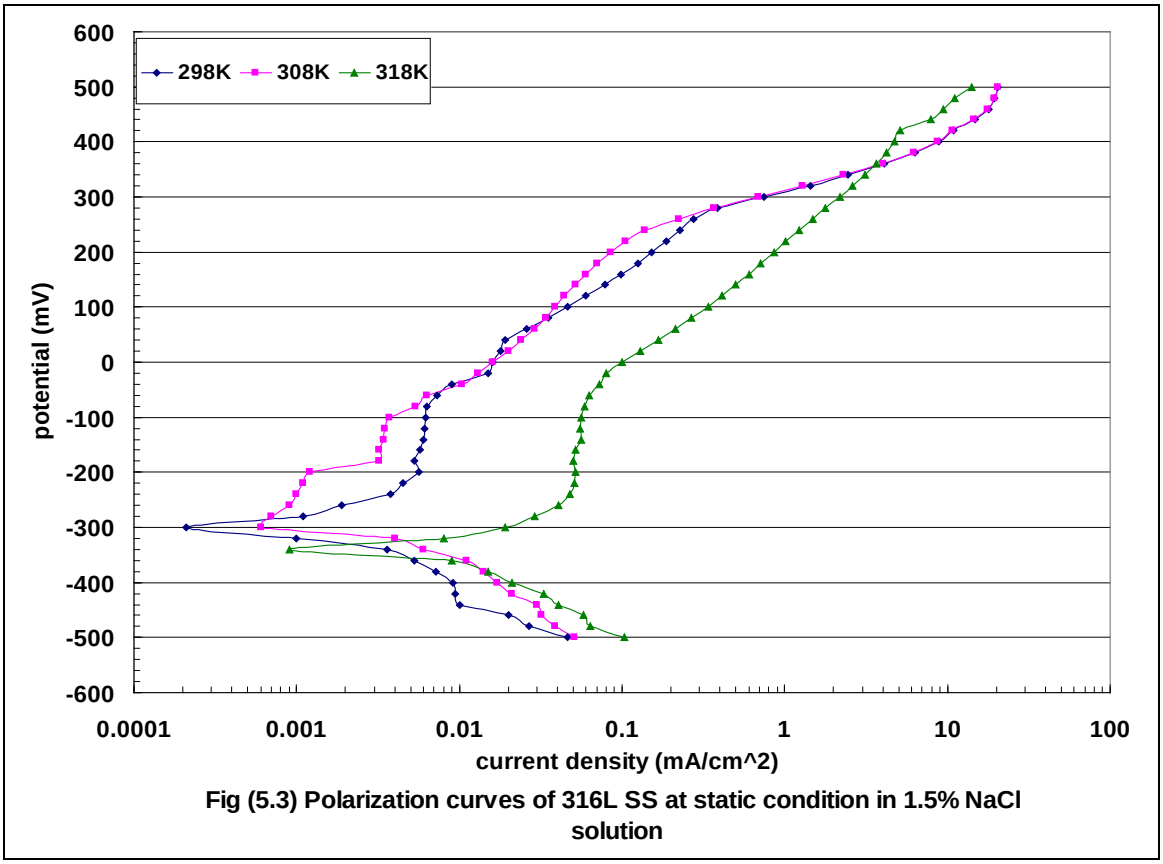

Fig (5.3) Polarization curves of 316L SS at static condition in 1.5% NaCl solution

Table (5.3) The effect of temperatures (K) on the corrosion potential (mV), primary passive potential (mV),breakdown potential (mV) and corrosion current density (mA/cm^2) of 316L SS at static condition in 1.5%NaCl solution

Temp. K	$E_{corr.}$ (mV)	$E_{pp.}$ (mV)	E_b (mV)	$i_{corr.}$ (mA/cm^2)
298	-300	-200	-80	0.0012
308	-300	-180	-100	0.0013
318	-340	-240	-80	0.0016

Table (5.4) and Fig.(5.4), show the effect and the relationship between the breakdown potential (E_b) of 316L SS and the temperatures at various concentrations (3.5,2.5 and 1.5)wt% of NaCl solutions. From this figure, it can be seen that , as the temperature of the solution increases the breakdown potential decreases, i.e, shift of breakdown potential to more active direction, this indicates that the pitting resistance of 316L SS decreases with increasing temperatures.

Simalowska[22] reported that the effect of temperature on decreasing E_b value is a specialty of alloys, that are highly resistant to pitting corrosion at room temperature.

Table (5.4) Effect of temperatures & concentration of NaCl solutions on the breakdown potential of 316L SS

Temperature (K)	1.5wt%NaCl	2.5wt% NaCl	3.5wt% NaCl
	E_b (mV)	E_b (mV)	E_b (mV)
298	-80	-80	-80
308	-100	-140	-120
318	-80	-200	-220

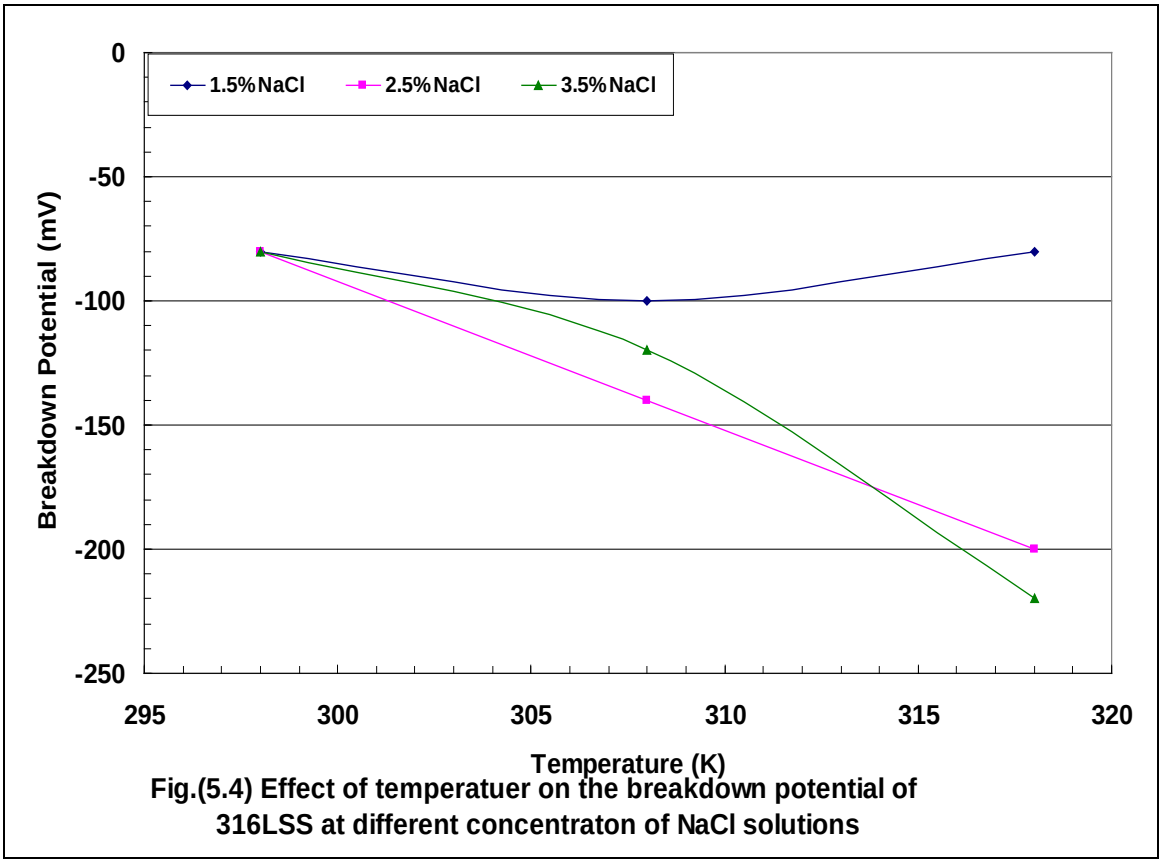

Fig.(5.4) Effect of temperatuer on the breakdown potential of 316LSS at different concentraton of NaCl solutions

Most of the chemical and electrochemical reactions proceed more rapidly at higher temperature [22]. Therefore the rate of pitting would increase as the temperature increases, as shown in Fig.(5.5). Processes accompanying pitting are active dissolution of metal or alloy, growth of the oxide film, dissolution of the oxide film, diffusion of various species through the oxide film into and out

of the pit and formation of salt layer on the bottom of the pit. Rate of the above reactions increases with temperature. So as the diffusion of chloride ion through the passive film increases, the pitting susceptibility of the alloy increases.

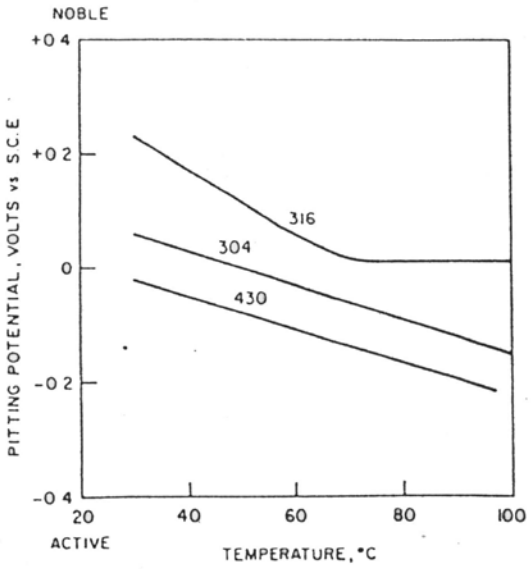

Fig (5.5) Effect of temperature on the pitting potential of various ss in 3% NaCl solution [22]

Similar results on the effect of temperatures to that of the present study was noticed by Leckie et.al[23], on austenitic 18:8 SS in 0.1M NaCl. They found that at 0°C (E_b) had a value above (0.9V) (noble), but it decreases to (-0.35V) at 25°C. They attributed this high shift to the active direction when the temperature increases, due to the high chemical affinity of this SS for water at temperatures around room temperature. So it is difficult for Cl^- to displace both water and oxygen adsorbed causing this noble potential at this temperature (room temperature and below), At higher temperatures the ability of Cl^- to displace water and oxygen adsorbed becomes effective. This is in agreement with many workers [22, 85, 88].

Table (5.5), shows the values of corrosion current densities at different temperatures and NaCl concentration. This table indicates that at constant concentration, the corrosion current density increases as the temperatures increases. However at constant temperature, the corrosion current density

increases as the concentration of NaCl increases.

Table (5.5) Effect of temperatures & concentration of NaCl solutions on the corrosion current density

Temperature (K)	1.5wt%NaCl	2.5wt% NaCl	3.5wt% NaCl
	$i_{corr.}$ (mA/cm^2)	$i_{corr.}$ (mA/cm^2)	$i_{corr.}$ (mA/cm^2)
298	0.0012	0.0014	0.0015
308	0.0013	0.0016	0.0016
318	0.0016	0.0025	0.0027

Fig.(5.6), shows the variation in ($i_{corr.}$) with temperature at different NaCl concentrations.

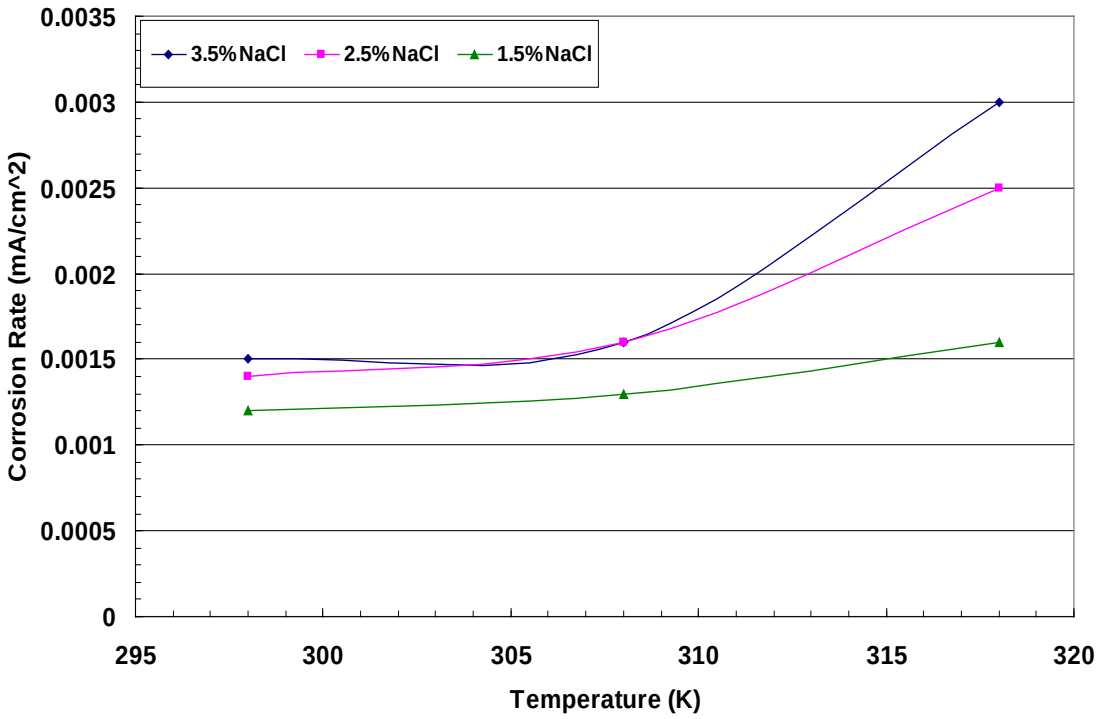

Fig.(5.6) Effect of tempretauers of solutions on the corrosion rate of 316LSS at different concentration of NaCl solutions

The kinetics of chemical and electrochemical reactions are usually affected by the variations in temperature. According to Arrhenius equation the majority of the reactions proceed more rapidly at higher temperatures.

The relationship of logarithm of corrosion rate with the reciprocal of absolute temperature, i.e. Arrhenius plot is shown in Fig.(5.7). It is a linear

relationship.

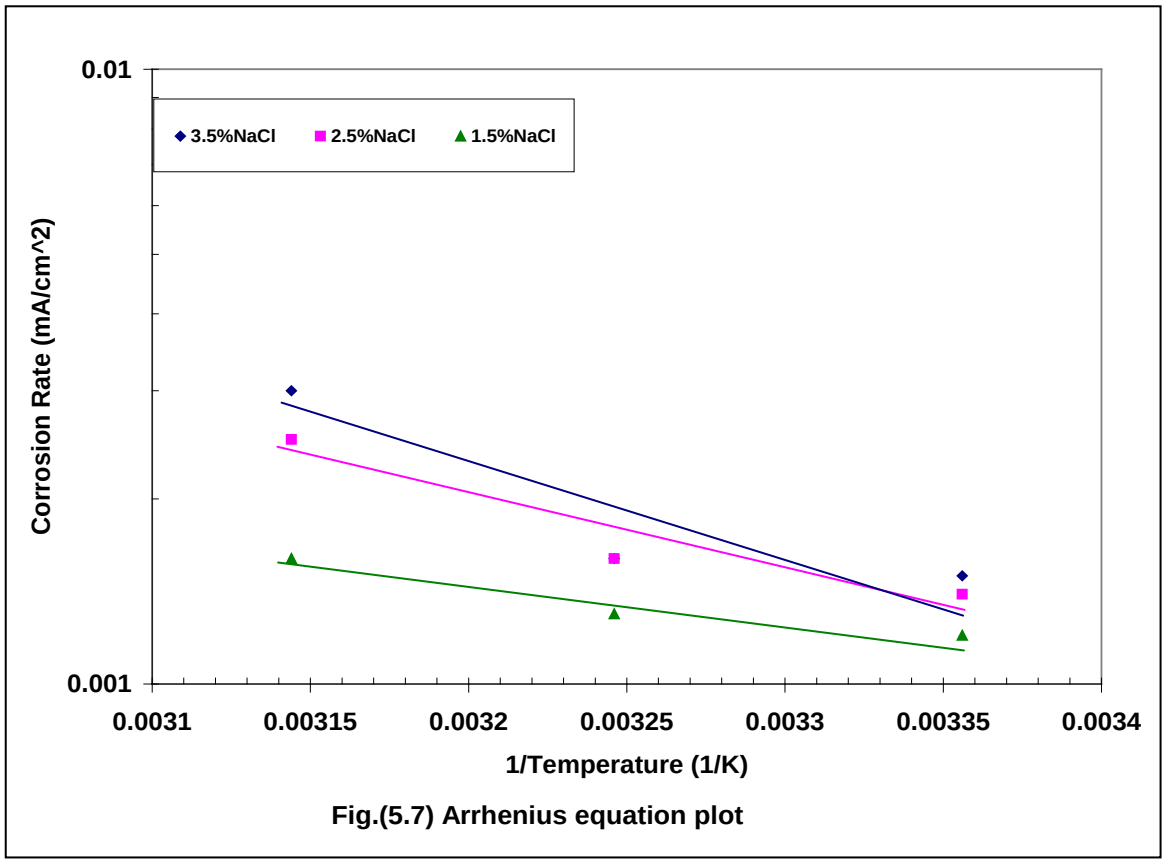

Fig.(5.7) Arrhenius equation plot

5.2.1.2 Effect of NaCl concentration

Fig.(5.8), shows the effect of Cl^- ions concentration on the breakdown potential. This figure shows that the breakdown potential E_b shifts to more negative values as the Cl^- concentration increases at 308K and 318K , while it remains constant at room temperature.

Efird [(109)] et.al claimed that the passivation reaction is totally independent of (Cl^-) concentration and it is the breakdown of passivity that is directly affected by (Cl^-) at certain temperature for AISI 304 and 316 SS. Fig.(5.9) ,shows the effect of (Cl^-) concentration on pitting potential of different austenitic SS.

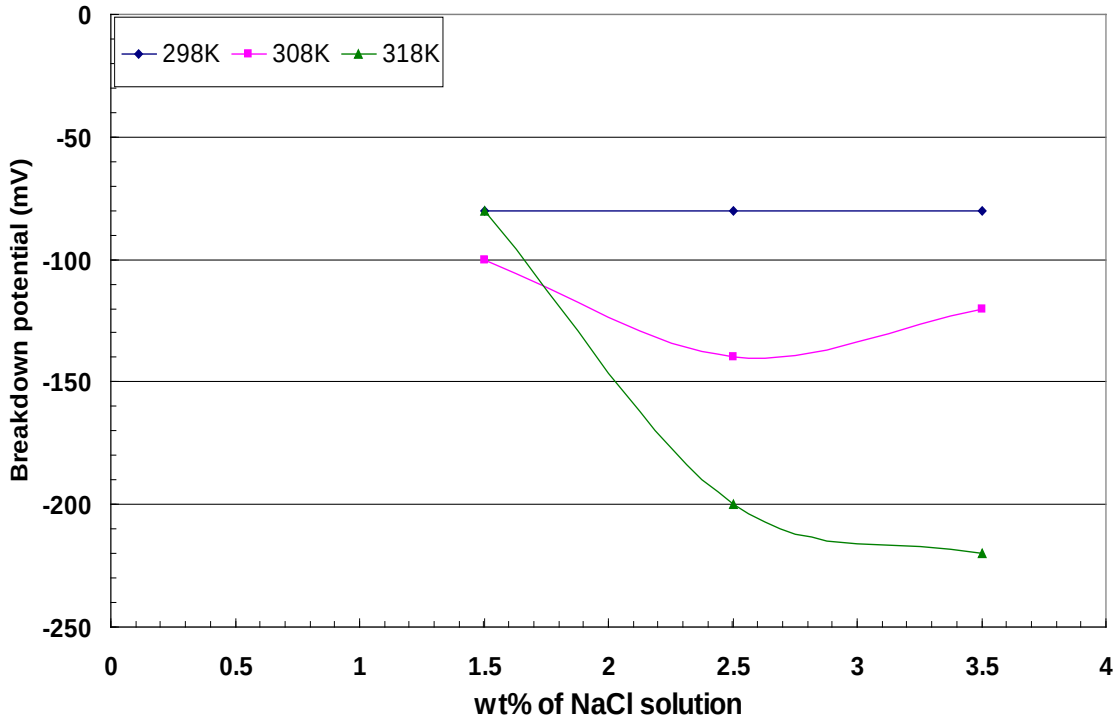

Fig.(5.8) Effect of the concentration of NaCl solutiuons on the breakdown potential of 316L SS at different temperatures

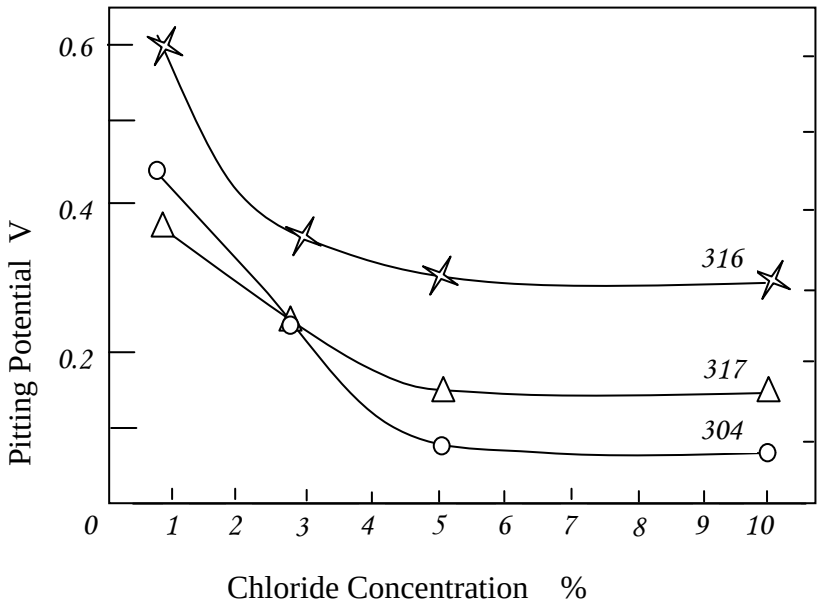

Fig.(5.9) Effect of (Cl^-) concentration on pitting potential of different austenitic ss[110]

Generally, the anodic process associated with metal passivation is strongly affected by the presence of halide ions in the electrolyte. At higher concentration of halide ions, the passive film susceptible to pitting suffers local damage, while low concentration causes an increase of the anodic current in the passive region **(22)**. The true situation may be related to high affinity of the metals for O_2 making it difficult for Cl^- to displace O_2 in the passive films and the presence of (NaCl) enhanced metal electrodissolution at higher chloride concentrations **(2)**.

Fig.(5.10), shows the relationship between the corrosion rate with the concentration of NaCl solutions. It indicates that at constant temperature, the corrosion rate increases as the concentration of Cl^- increases. Once a pit initiates, a passive - active cell is set up of large potential difference. The resultant high current density accompanies a high corrosion rate of anode (pit) and at the same time, polarizes the surface immediately surrounding the pit to a values below the critical potential. Through flow of current, chloride ions transfer into the pit forming concentrated solutions of Fe^{+2}, Ni^{+2}, Cr^{+3} chlorides, which by hydrolysis account for an acid solution. The high Cl^- concentration and low pH ensure that the pit surface remain active **(2)**.

Moreover increasing the Cl^- leads to increase the conductivity of the solution and as a result the corrosion current density will increase also.

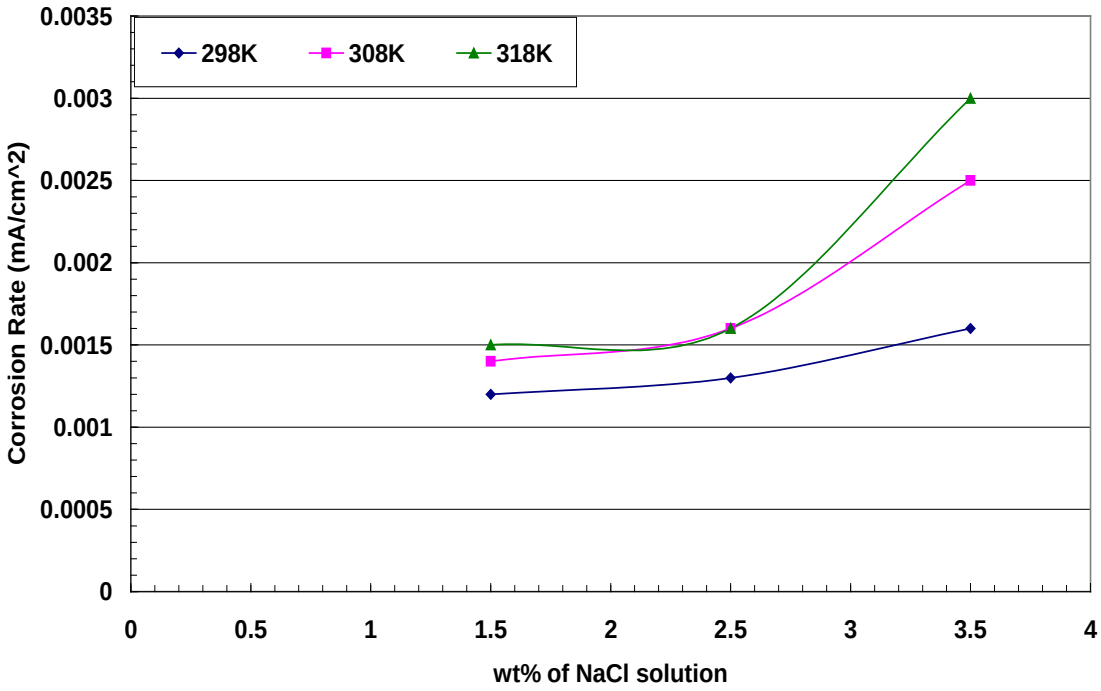

Fig. (5.10) Effect of the concentration of NaCl on the corrosion rate of 316L SS at different temperatuers

5.2.2 Dynamic conditions

The second set of the experimental results are presented in Figs.(5.11-5.16), which show the influence of the speed of Rotating Cylinder Electrode (RCE)(0,100,200 and 300) r.p.m at temperatures (298,308 and 318)K on the corrosion behavior of 316L SS in solutions of (3.5 & 2.5)wt% of NaCl respectively.

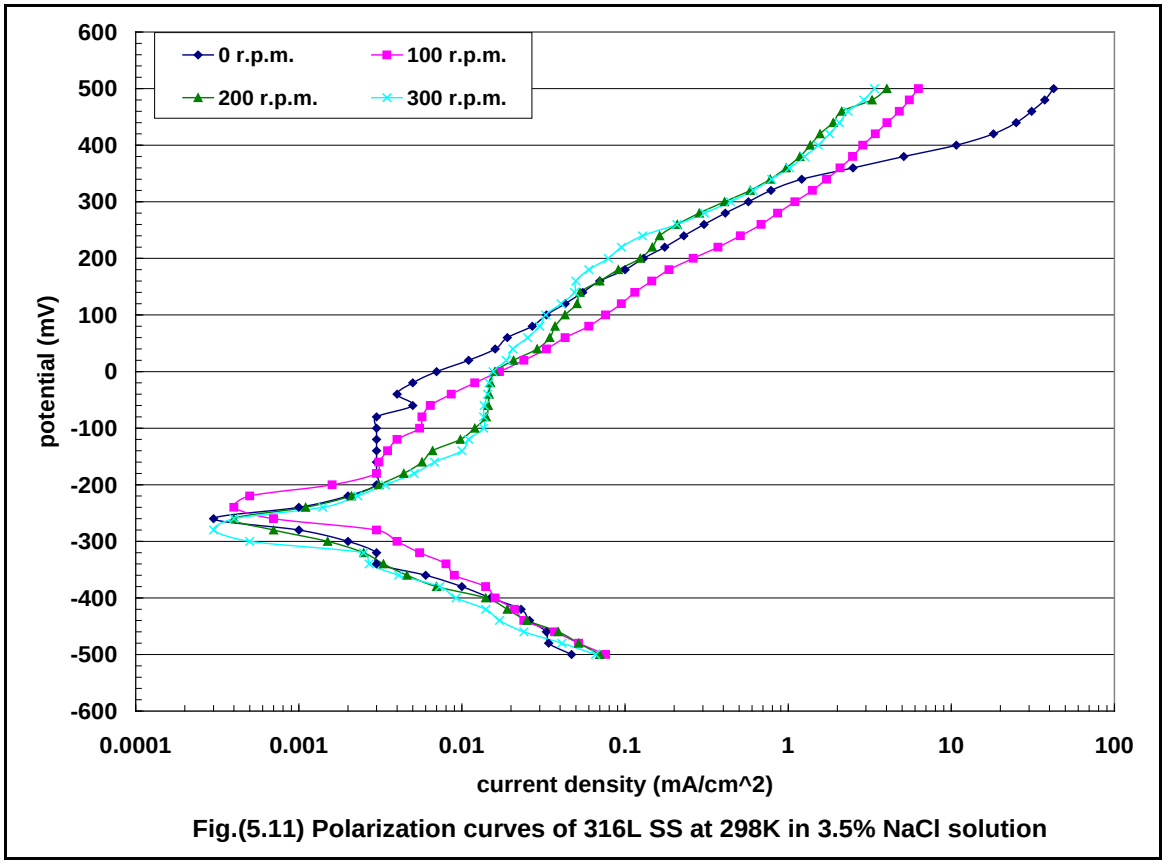

Fig.(5.11) Polarization curves of 316L SS at 298K in 3.5% NaCl solution

Tabel (5.6) The effect of rotational speed (r.p.m) on the corrosion potential (mV) ,primary passive potential (mV),breakdown potential (mV) and corrosion current density (mA/cm^2) of 316L SS at 298K in 3.5% NaCl solution.

Rotation r.p.m.	(ω) = r.p.m.*2π/60	v = (ω/2)*d (m/s)	$E_{corr.}$ (mV)	$E_{pp.}$ (mV)	E_b (mV)	$i_{corr.}$ (mA/cm^2)
0	0	0	-260	-200	-80	0.0015
100	10.49	0.315	-240	-180	-60	0.0018
200	20.98	0.629	-260	-80	0	0.0018
300	31.47	0.944	-280	-100	0	0.0019

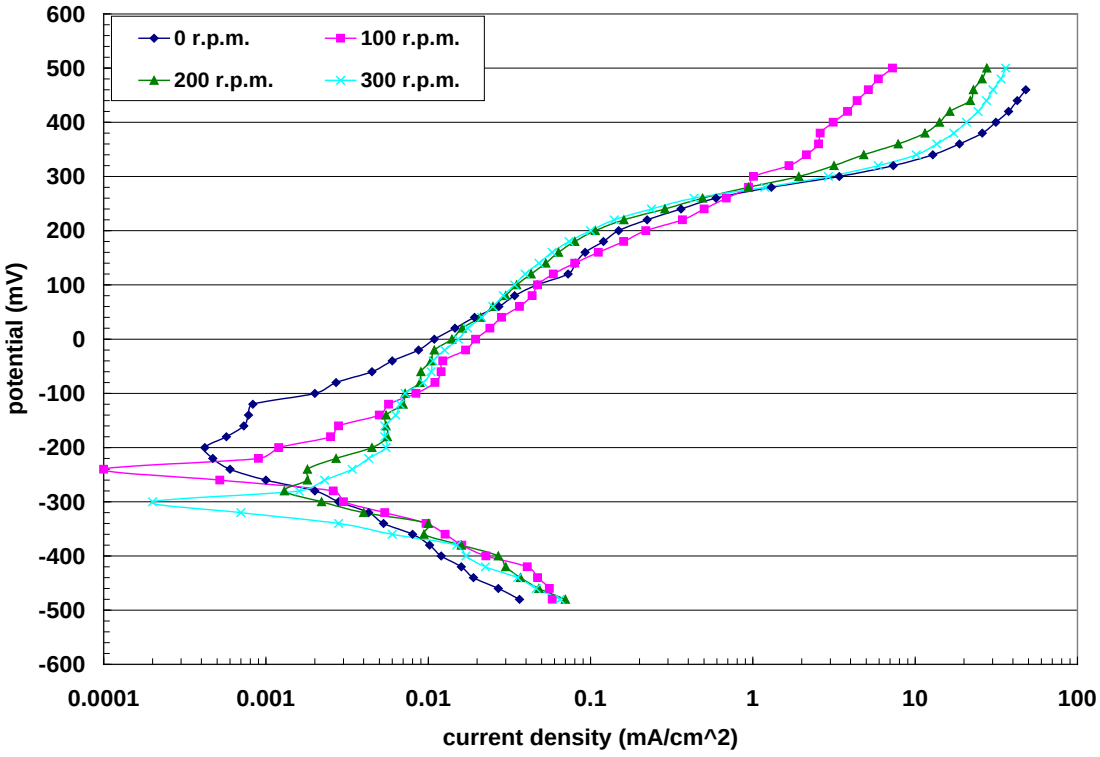

Fig.(5.12) Polarization curves of 316L SS at 308K in 3.5% NaCl solution

Tabel (5.7) The effect of rotational speed (r.p.m) on the corrosion potential (mV) ,primary passive potential (mV),breakdown potential (mV) and corrosion current density (mA/cm^2) of 316L SS at 308K in 3.5%NaCl solution.

Rotation r.p.m.	(ω) = r.p.m.*2π/60	v = (ω/2)*d (m/s)	$E_{corr.}$ (mV)	$E_{pp.}$ (mV)	E_b (mV)	$i_{corr.}$ (mA/cm^2)
0	0	0	-200	-160	-120	0.0016
100	10.49	0.315	-240	-100	-40	0.0018
200	20.98	0.629	-280	-180	-20	0.0023
300	31.47	0.944	-300	-200	-40	0.0023

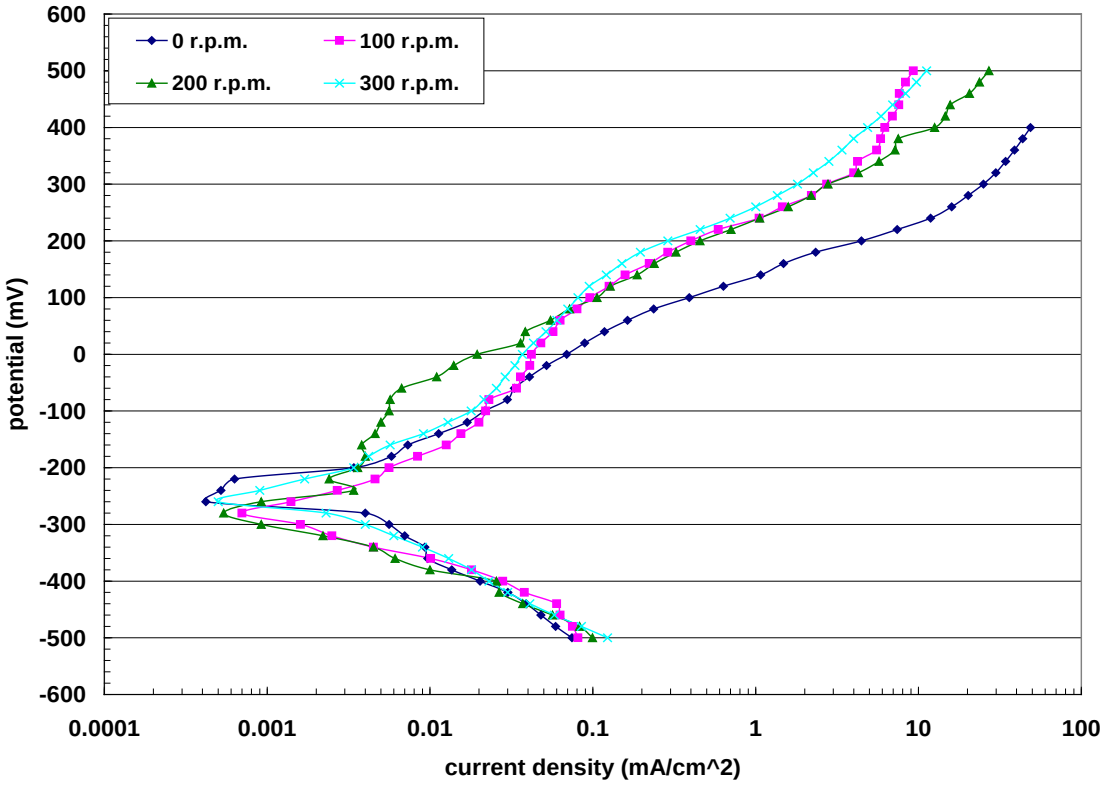

Fig.(5.13) Polarization curves of 316L SS at 318K in 3.5% NaCl solution

Tabel (5.8) The effect of rotational speed (r.p.m) on the corrosion potential (mV) ,primary passive potential (mV),breakdown potential (mV) and corrosion current density (mA/cm^2) of 316L SS at 318K in 3.5%NaCl solution.

Rotation r.p.m.	(ω) = r.p.m.*2π/60	v = (ω/2)*d (m/s)	$E_{corr.}$ (mV)	$E_{pp.}$ (mV)	E_b (mV)	$i_{corr.}$ (mA/cm^2)
0	0	0	-260	-240	-220	0.0027
100	10.49	0.315	-280	-120	0	0.0028
200	20.98	0.629	-280	-240	-60	0.0028
300	31.47	0.944	-260	-100	120	0.0028

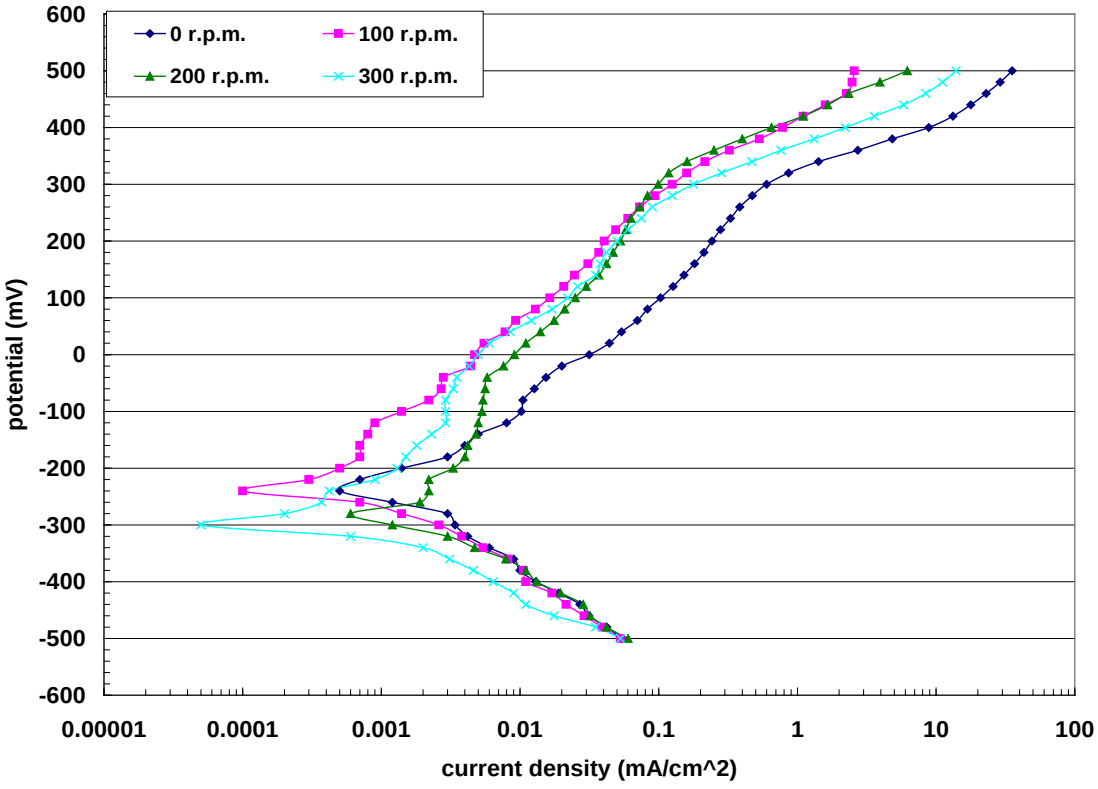

Fig.(5.14) Polarization curves of 316L SS at 298K in 2.5% NaCl solution

Tabel (5.9) The effect of rotational speed (r.p.m) on the corrosion potential(mV) ,primary passive potential (mV),breakdown potential (mV) and corrosion current density (mA/cm^2) of 316L SS at 298K in 2.5%NaCl solution.

Rotation r.p.m.	(ω) = r.p.m.*2π/60	v = (ω/ 2)*d (m/s)	$E_{corr.}$ (mV)	$E_{pp.}$ (mV)	E_b (mV)	$i_{corr.}$ (mA/cm^2)
0	0	0	-240	-100	-20	0.0014
100	10.49	0.315	-240	-180	-120	0.0014
200	20.98	0.629	-280	-200	-40	0.0015
300	31.47	0.944	-300	-120	-80	0.0015

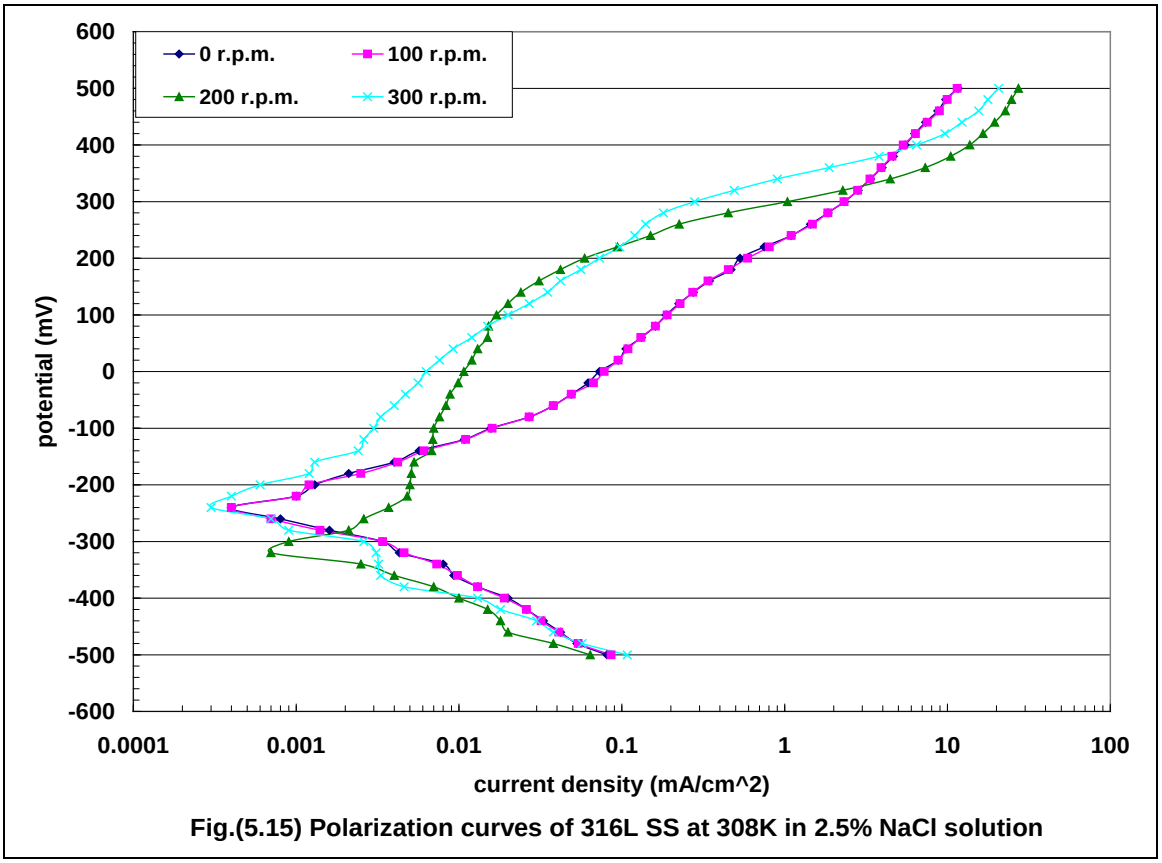

Fig.(5.15) Polarization curves of 316L SS at 308K in 2.5% NaCl solution

Tabel (5.10) The effect of rotational speed (r.p.m) on the corrosion potential (mV),primary passive potential (mV),breakdown potential (mV) and corrosion current density (mA/cm^2) of 316L SS at 308K in 2.5%NaCl solution.

Rotation r.p.m.	(ω) = r.p.m.*2π/60	v = (ω/ 2)*d (m/s)	$E_{corr.}$ (mV)	$E_{pp.}$ (mV)	E_b (mV)	$i_{corr.}$ (mA/cm^2)
0	0	0	-240	-220	-200	0.0016
100	10.49	0.315	-240	-220	-200	0.0016
200	20.98	0.629	-320	-220	120	0.0018
300	31.47	0.944	-240	-140	280	0.0018

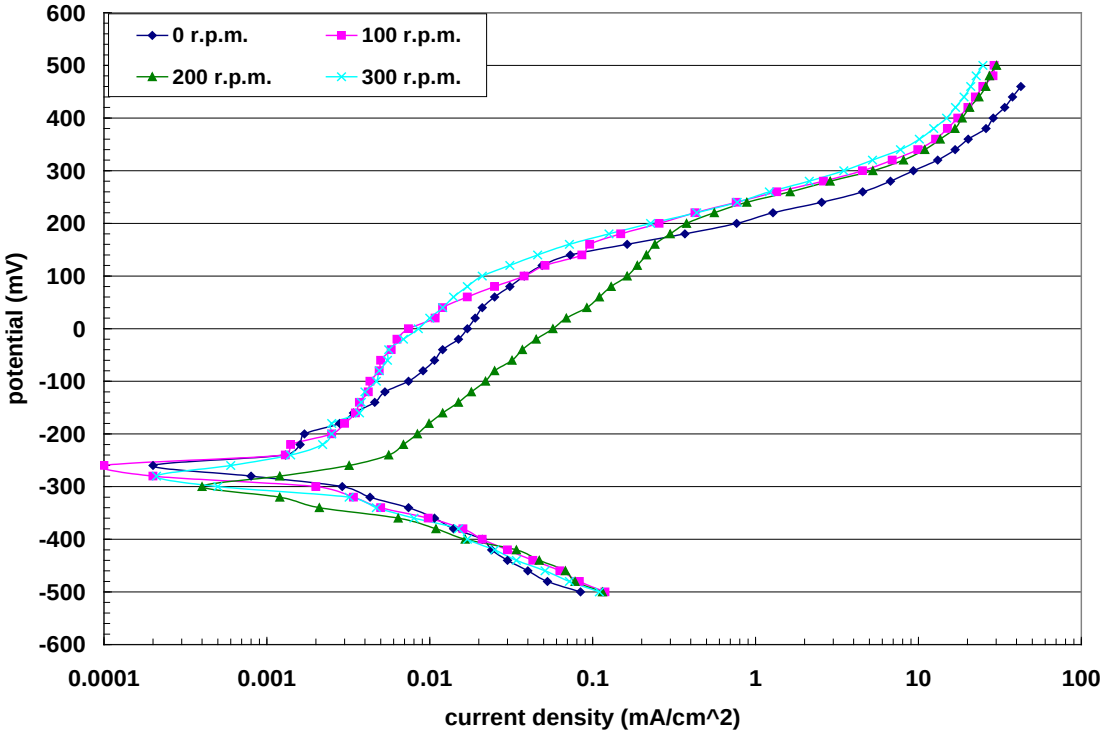

Fig. (5.16) Polarization curves of 316L SS at 318K in 2.5% NaCl solution

Tabel (5.11) The effect of rotational speed (r.p.m)on the corrosion potential (mV),primary passive potential (mV),breakdown potential (mV) and corrosion current density (mA/cm^2) of 316L SS at 318K in 2.5%NaCl solution.

Rotation r.p.m.	(ω) = r.p.m.*2π/60	v = (ω/ 2)*d (m/s)	$E_{corr.}$ (mV)	$E_{pp.}$ (mV)	E_b (mV)	$i_{corr.}$ (mA/cm^2)
0	0	0	-260	-200	120	0.0025
100	10.49	0.315	-260	-200	0	0.0025
200	20.98	0.629	-300	-240	200	0.0026
300	31.47	0.944	-280	-220	100	0.0028

5.2.2.1 Effect of temperature

Figs.(5.11-5.16), show the polarization curves of 316L SS using RCE at (0,100,200 and 300) r.p.m at temperatures (298, 308 and 318)K in (3.5 & 2.5)wt% of NaCl solutions and Tables (5.6-5.11), represent the main characteristics of the results obtained from these figures.

Table(5.6), shows that the velocity of the solution has complex effect on the electrochemical behavior of 316L SS at temperature(298)K. This can be explain by the results of (E_b) at(200&300)r.p.m.. The value of (E_b) goes to more noble direction respect to(0,100)r.p.m. and the (E_b) becomes independent on the velocity of the solution above 200 r.p.m., therefore the (E_b) takes a constant value. This influences observed also on ($i_{corr.}$) at different velocities, ($i_{corr.}$)takes roughly constant values(0.0018-0.0019)mA/cm^2.

Tables (5.12 & 5.13), indicate the effect of temperatures on the breakdown potential (E_b) of 316L SS with various speeds of rotation in (3.5 & 2.5)% NaCl solutions. These tables show that there is no clear effect of rotational speed on E_b. At (0 & 200) r.p.m and 3.5% NaCl solution, E_b decreases as the temperature increase. But this behavior is not concerned with other speed and with 2.5% NaCl solution.

Table (5.12) The effect of temperatures on the breakdown potential of 316L SS with various speed rotation in 3.5% NaCl solutions

Rotation r.p.m	E_b (mV) 298 K	E_b (mV) 308 K	E_b (mV) 318 K
0	-80	-120	-220
100	-60	-40	0
200	0	-20	-60
300	0	-40	120

Table (5.13) The effect of temperatures on the breakdown potential of 316L SS with various speed rotation in 2.5% NaCl solutions

Rotation r.p.m	E_b (mV) 298 K	E_b (mV) 308 K	E_b (mV) 318 K
0	-20	-200	120
100	-120	-200	0
200	-40	120	200
300	-80	280	100

Tables (5.14 & 5.15), show the effect of temperatures on the corrosion rate at various speeds of rotation in (3.5 & 2.5)wt% NaCl solutions respectively. From these tables it can be seen that the corrosion rate ($i_{corr.}$) increases when the temperatures increases as shown in Figs.(5.17 & 5.18). Moreover, at constant temperature, the corrosion rate increases with increasing rotational speed.

Table (5.14) Effect of temperature on the corrosion rate of 316L SS at different rotational speed in 3.5wt% NaCl solutions

Rotation r.p.m	298 K	308 K	318 K
	$i_{corr.}$ (mA/cm^2)	$i_{corr.}$ (mA/cm^2)	$i_{corr.}$ (mA/cm^2)
0	0.0015	0.0016	0.0027
100	0.0018	0.0018	0.0028
200	0.0018	0.0023	0.0028
300	0.0019	0.0023	0.0028

Table (5.15) Effect of temperature on the corrosion rate of 316L SS at different rotational speed in 2.5wt% NaCl solutions

Rotation r.p.m	298 K	308K	318 K
	$i_{corr.}$ (mA/cm^2)	$i_{corr.}$ (mA/cm^2)	$i_{corr.}$ (mA/cm^2)
0	0.0014	0.0016	0.0025
100	0.0014	0.0016	0.0025
200	0.0015	0.0018	0.0026
300	0.0015	0.0018	0.0028

The effect of temperature changes on corrosion rate in water is more complex than the simple chemical principle that an increase in temperature increases the reaction rate. An increase in temperature of a corroding system has four main effects [(111)]:

1. The rate of chemical reaction is increased.
2. The solubility of some of the reaction products may change resulting in different corrosion reaction products.
3. The solubility of gases in solution is decreased.
4. Viscosity is decreased, and any thermal differences will results in increased circulation.

In general, as temperature rises, diffusion increases, and both overvoltage

and viscosity decrease. Increased diffusion enables more dissolved oxygen to reach a cathodic surface, thereby depolarizing the corrosion cell. Overvoltage decreases causing depolarization by hydrogen evolution. A decrease in viscosity aids both depolarization mechanisms because it favors solution of atmospheric oxygen and enhances hydrogen evolution [(112)]. This in agreement with the results of Mahato [(113)], who presented fundamental hydrodynamic concepts as applied to corrosion in pipes by many investigators. They indicated that the flow speed of water, degree of turbulence, geometry of system and other physical properties have a direct influence on the movement of dissolved oxygen and ions through the fluid, these factors in turn exert effects on the formation of corrosion products, on depolarization and thus on the corrosion reaction itself.

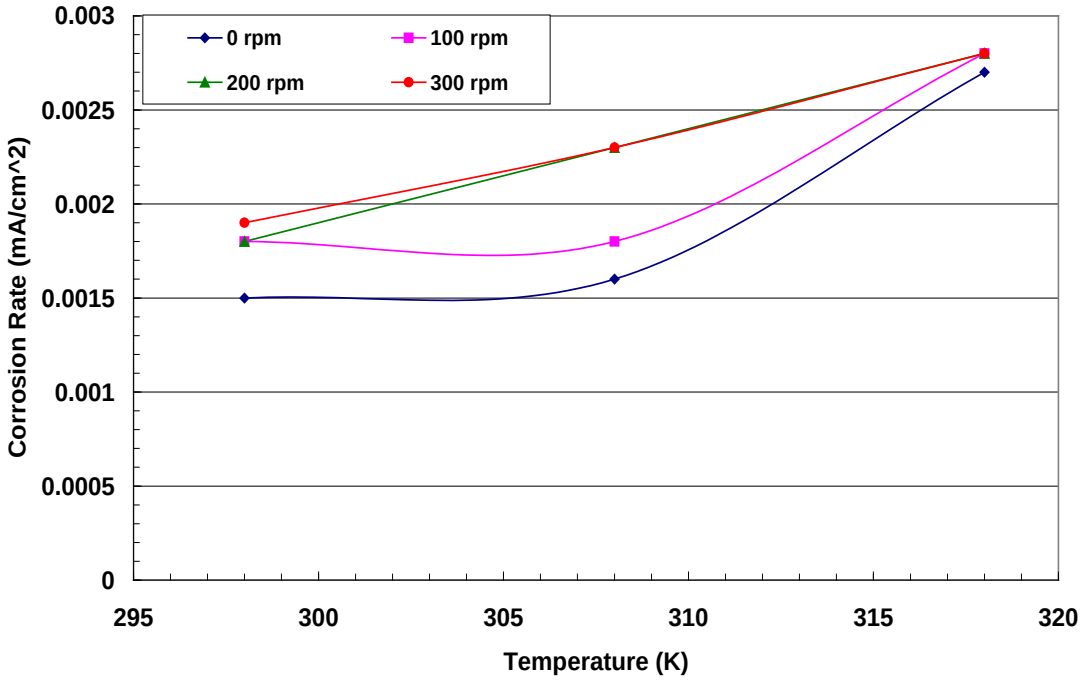

Fig.(5.17) Effect of temperatures on the corrosion rate of 316L SS at different speed of rotation in 3.5wt% of NaCl solutions

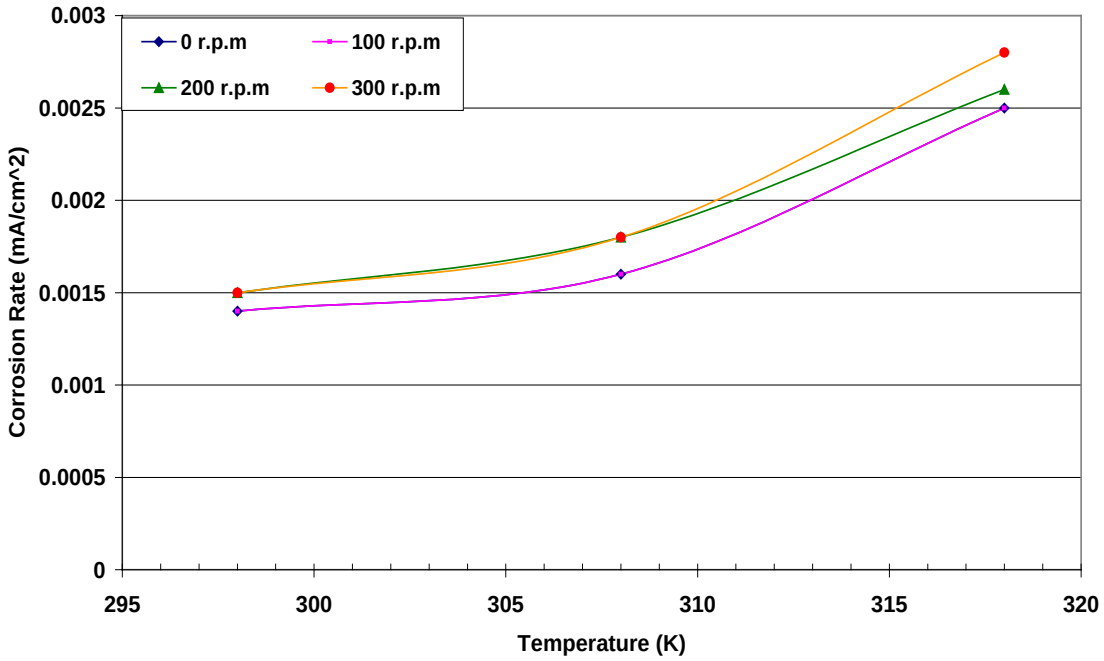

Fig. (5.18) Effect of temperatures on the corrosion rate of 316LSS at different speed of rotation in 2.5 wt% of NaCl solutions

5.2.2.2 Effect of NaCl concentration

Tables (5.16-5.18), show the effect of NaCl concentration on the corrosion current density of 316L SS at various temperatures and rotational speed .These tables show that at low velocity there are small effect of the concentration on the ($i_{corr.}$) values, at (0,100)r.p.m. the ($i_{corr.}$) is equal to(0.0014)mA/cm^2 at 2.5% NaCl and 298K. At 0 r.p.m. in (2.5&3.5)%NaCl , the ($i_{corr.}$) is equal to(0.0016)mA/cm^2, while at temperature 308K with 100 r.p.m. and (2.5&3.5)% NaCl, ($i_{corr.}$) is equal to (0.0016,0.0018)mA/cm^2 respectively. At higher temperature (318)K with(0,100)r.p.m. and (2.5)%NaCl ($i_{corr.}$) is equal to(0.0025)mA/cm^2 while at 3.5% NaCl with (0,100)r.p.m., ($i_{corr.}$) is equal to(0.0027,0.0028)mA/cm^2 respectively. From these results can be concluded that the temperatures had small effects on the ($i_{corr.}$).

From these tables, show at constant speed the corrosion current density increases with increasing the concentration of NaCl, this is due to the electrical

conductivity of Cl^- ions. As the concentration increases, the number of ions in the solution increases, this leads to an increase in the conductivity of the solution. This is in agreement with results of many workers [2,85].

Table (5.16) Effect of NaCl % solution on the corrosion rate of 316L SS at 298 K in different rotation speed

NaCl wt%	0 r.p.m	100 r.p.m	200 r.p.m	300 r.p.m
	$i_{corr.}$ (mA/cm^2)	$i_{corr.}$ (mA/cm^2)	$i_{corr.}$ (mA/cm^2)	$i_{corr.}$ (mA/cm^2)
2.5	0.0014	0.0014	0.0015	0.0015
3.5	0.0015	0.0018	0.0018	0.0019

Table (5.17) Effect of NaCl % solution on the corrosion rate of 316L SS at 308K in different rotation speed

NaCl wt%	0 r.p.m	100 r.p.m	200 r.p.m	300 r.p.m
	$i_{corr.}$ (mA/cm^2)	$i_{corr.}$ (mA/cm^2)	$i_{corr.}$ (mA/cm^2)	$i_{corr.}$ (mA/cm^2)
2.5	0.0016	0.0016	0.0018	0.0018
3.5	0.0016	0.0018	0.0023	0.0023

Table (5.18) Effect of NaCl % solution on the corrosion rate of 316L SS at 318 K in different rotation speed

NaCl wt%	0 r.p.m	100 r.p.m	200 r.p.m	300 r.p.m
	$i_{corr.}$ (mA/cm^2)	$i_{corr.}$ (mA/cm^2)	$i_{corr.}$ (mA/cm^2)	$i_{corr.}$ (mA/cm^2)
2.5	0.0025	0.0025	0.0026	0.0028
3.5	0.0027	0.0028	0.0028	0.0028

5.2.2.3 Effect of velocity

Figs.(5.19 and 5.20), show the effect of velocity on the corrosion rate of 316L SS at different temperatures in (3.5 and 2.5)wt% of NaCl solutions respectively. It can be seen that the corrosion current density (corrosion rate) is almost constant or in other word it increases slightly as the velocity increases. The effect of changes in water velocity on the corrosion resistance of stainless steel shows much variation. In stagnant sea water and at velocities less than 1 or 1.5 m/s, type 316L SS may pit severely. But it is very corrosion resistant at higher velocities. This is in agreement with the results of Malik [85] as mentioned in section (2.5.5.2).

The influence of rotation on the pitting corrosion of metals is not much

investigated. It was found from a technical note [114], that the breakdown potentials of type 304 SS in 3.5% NaCl are not affected by rotation.

In general, increasing the solution velocity steps up corrosion rate especially if NaCl is present, because chlorides tend to destroy the protective film [115].This is in agreement with [71] as mentioned in section (2.5.6.2).

Movement tends to keep all the surface in contact with aerated solution and uniformly passive.

Figs.(5.21-5.26),show the surface after potentiostatic polarization of 316L in the solution containing (3.5and2.5)% NaCl at different temperatures (298,308and 318)K with various rotational speed (0,100,200 and 300)r.p.m respectively.

Fig.(5.27), shows the surface after potentiostatic polarization of 316L in the solution containing 1.5% NaCl with different temperatures and at static condition.

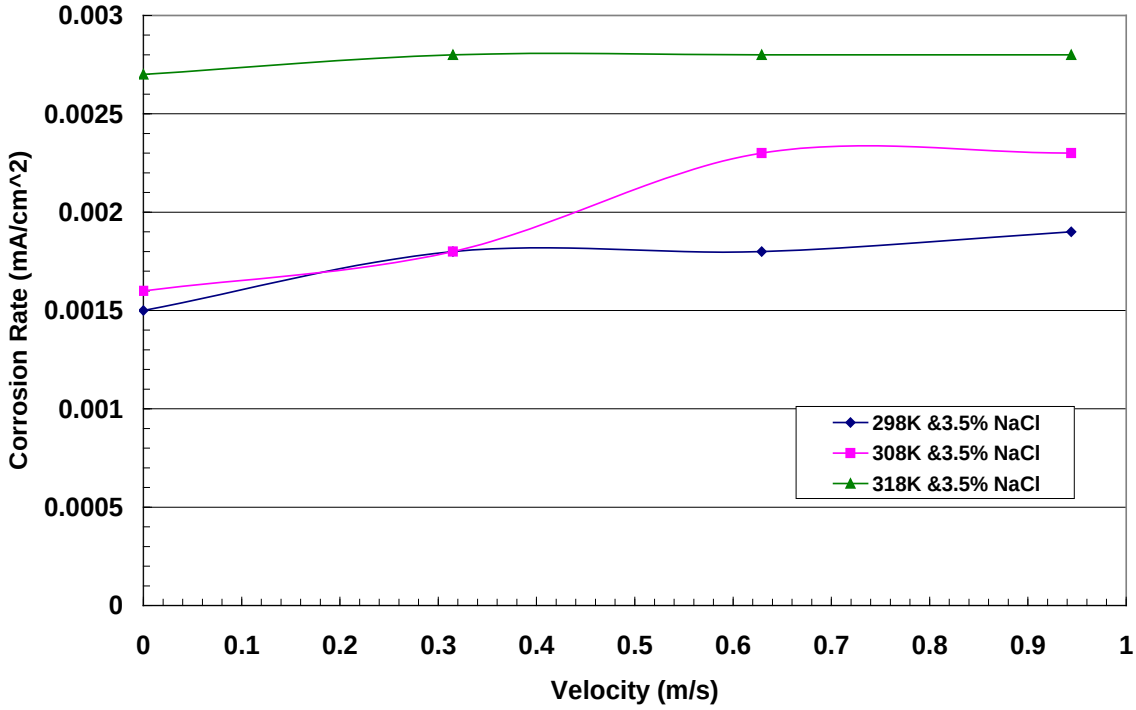

Fig.(5.19) Effect of the velocity on the corrosion rate of 316L at different temperatures of 3.5wt% of NaCl solutions

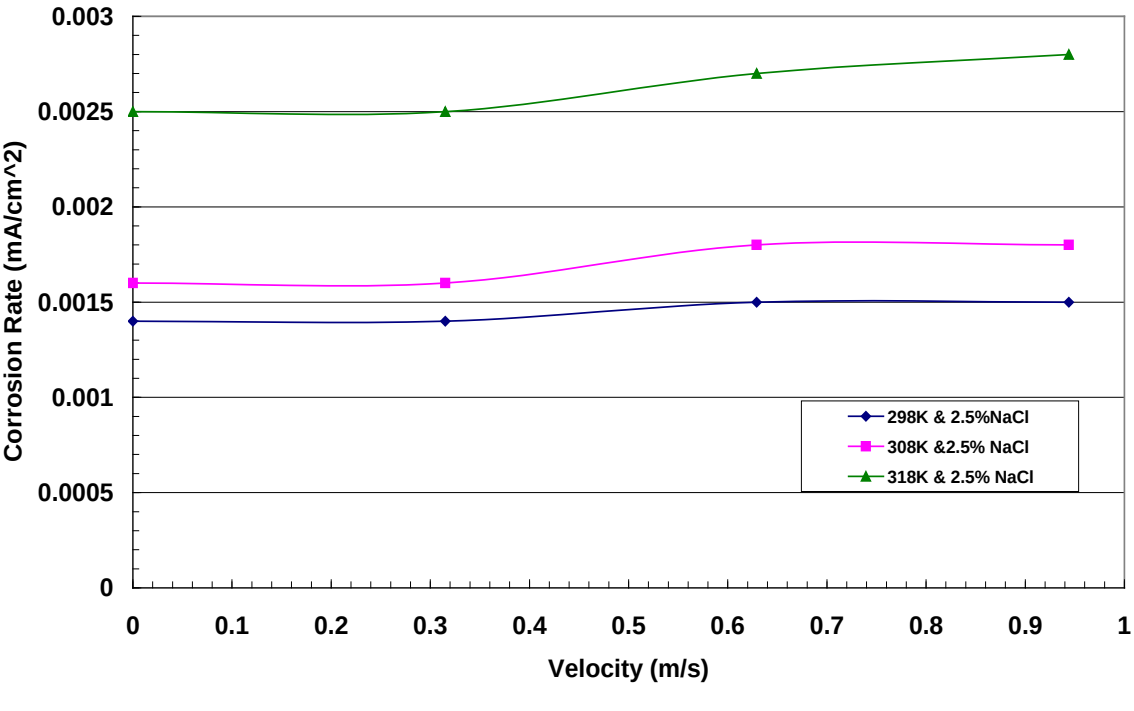

Fig. (5.20) Effect of velocity on the corrosion rate of 316L SS at different temperatures in 2.5wt% of NaCl solutions

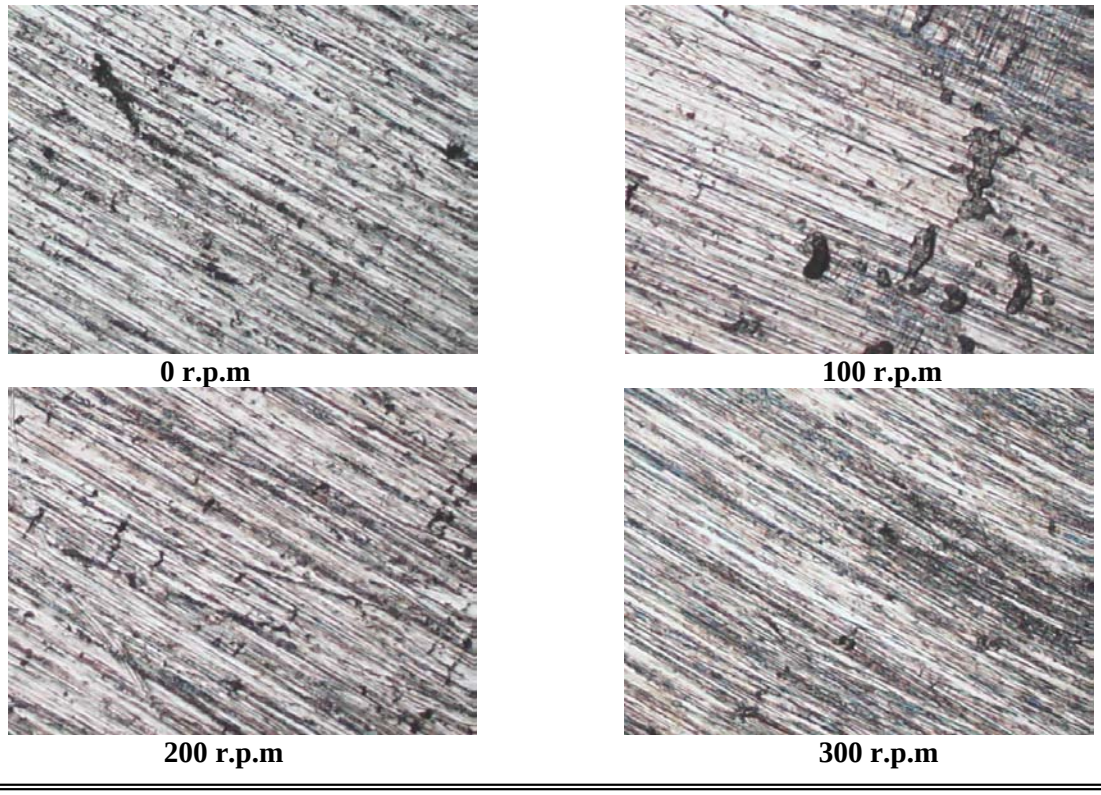

Fig.(5.21)316L SS after potentiostatic polarization in 3.5% NaCl solutions at 298K(270X)

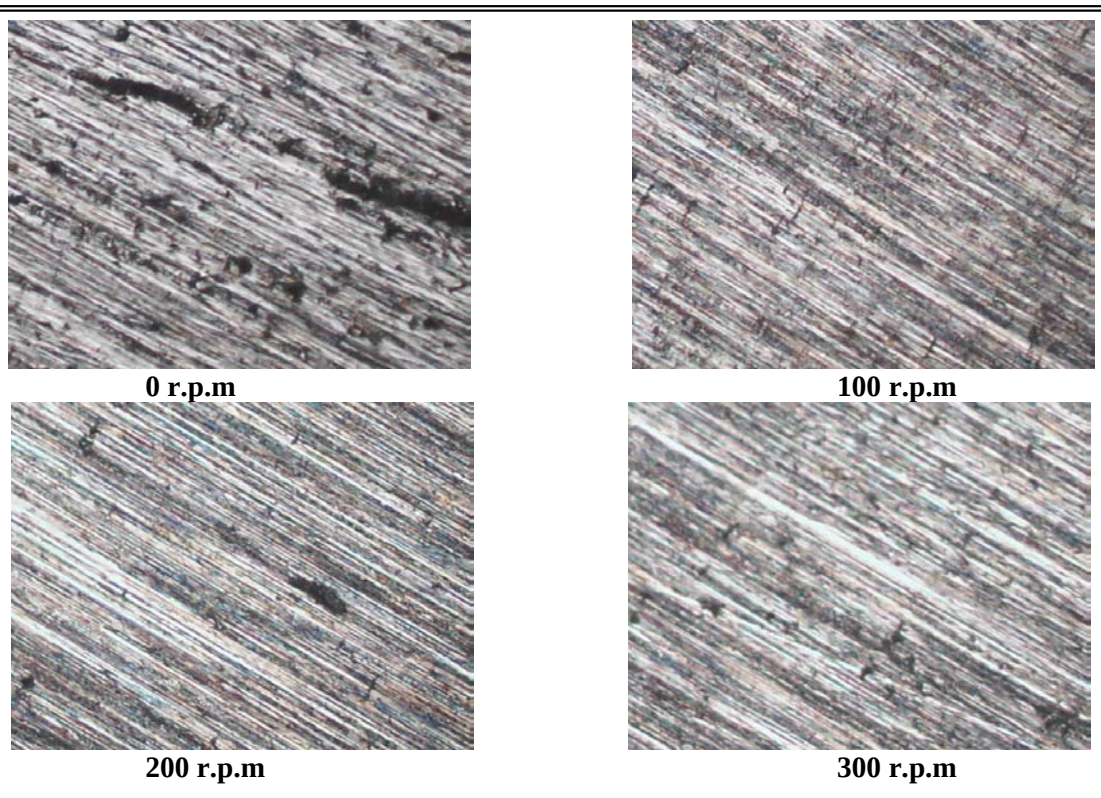

Fig.(5.22)316L SS after potentiostatic polarization in 3.5% NaCl solutions at 308K(270X)

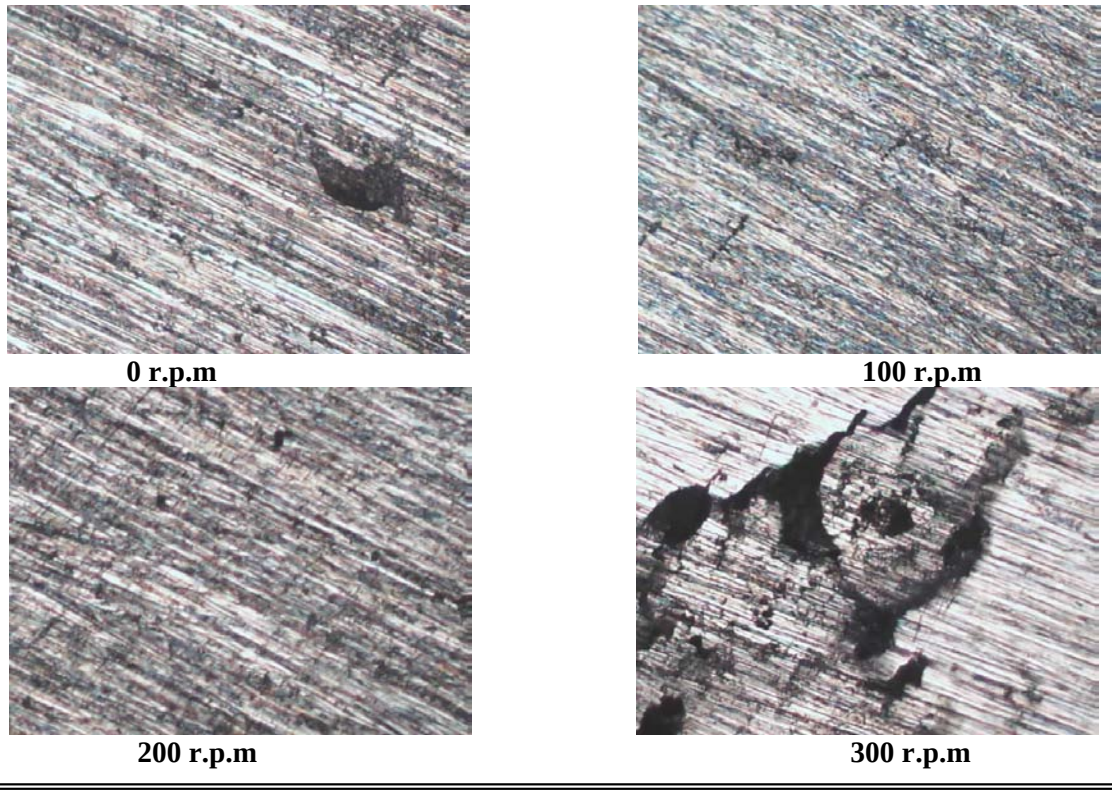

Fig.(5.23)316L SS after potentiostatic polarization in 3.5% NaCl solutions at 318K(270X)

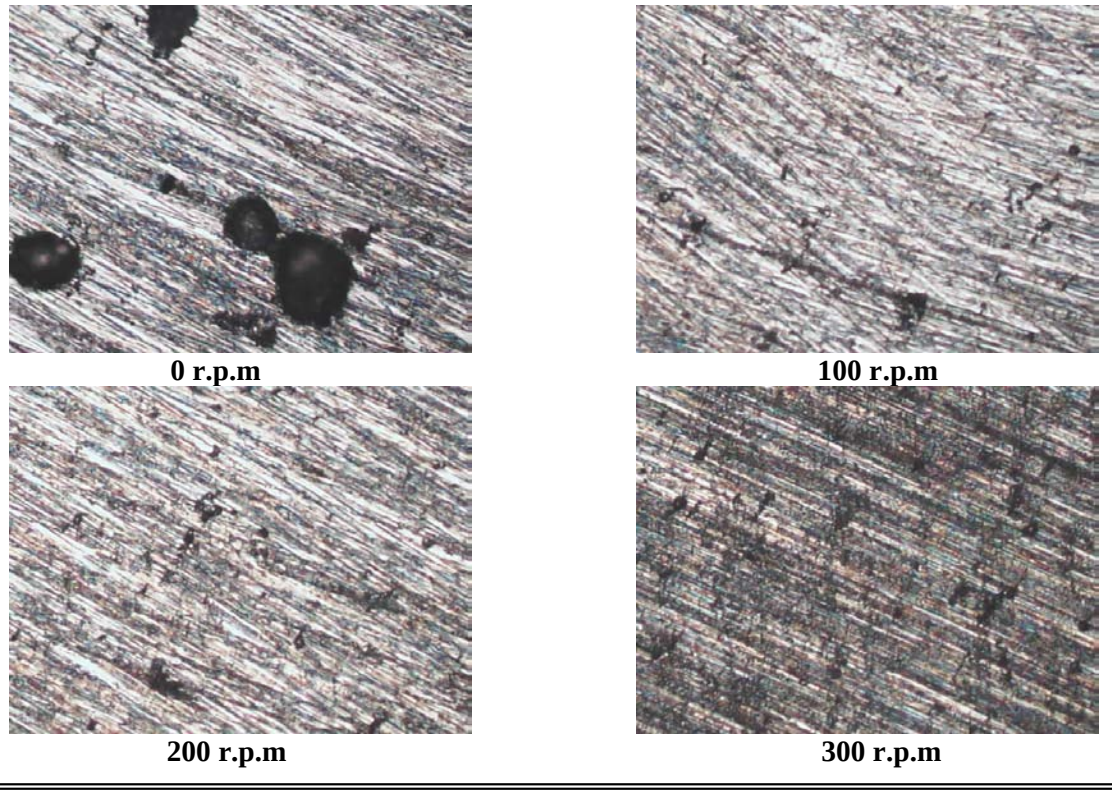

Fig.(5.24)316L SS after potentiostatic polarization in 2.5% NaCl solutions at 298K(270X)

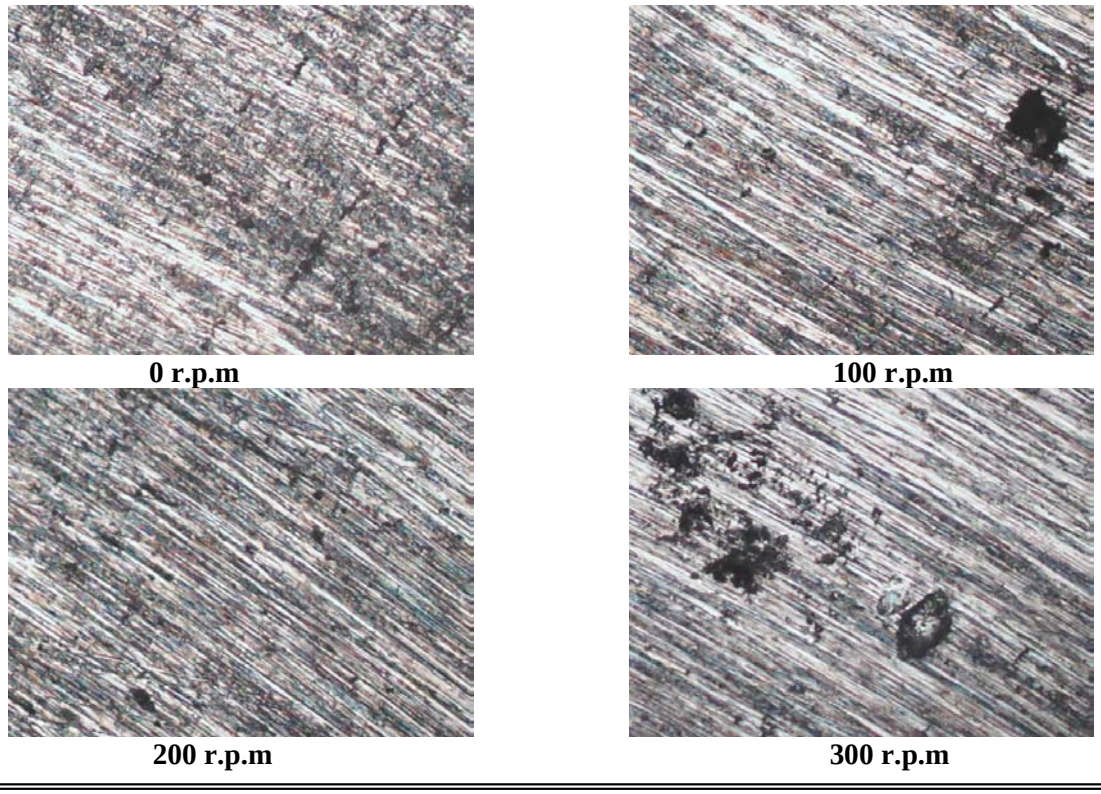

Fig.(5.25)316L SS after potentiostatic polarization in 2.5% NaCl solutions at 308K(270X)

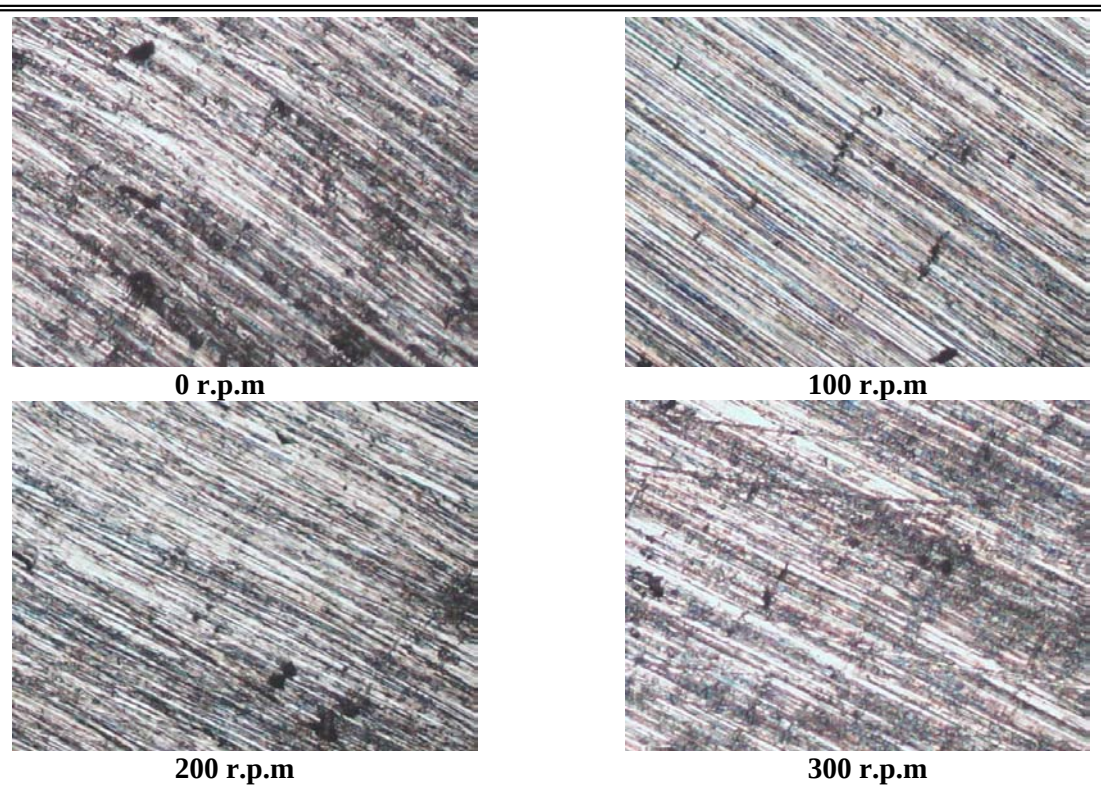

Fig.(5.26)316L SS after potentiostatic polarization in 2.5% NaCl solutions at 318K(270X)

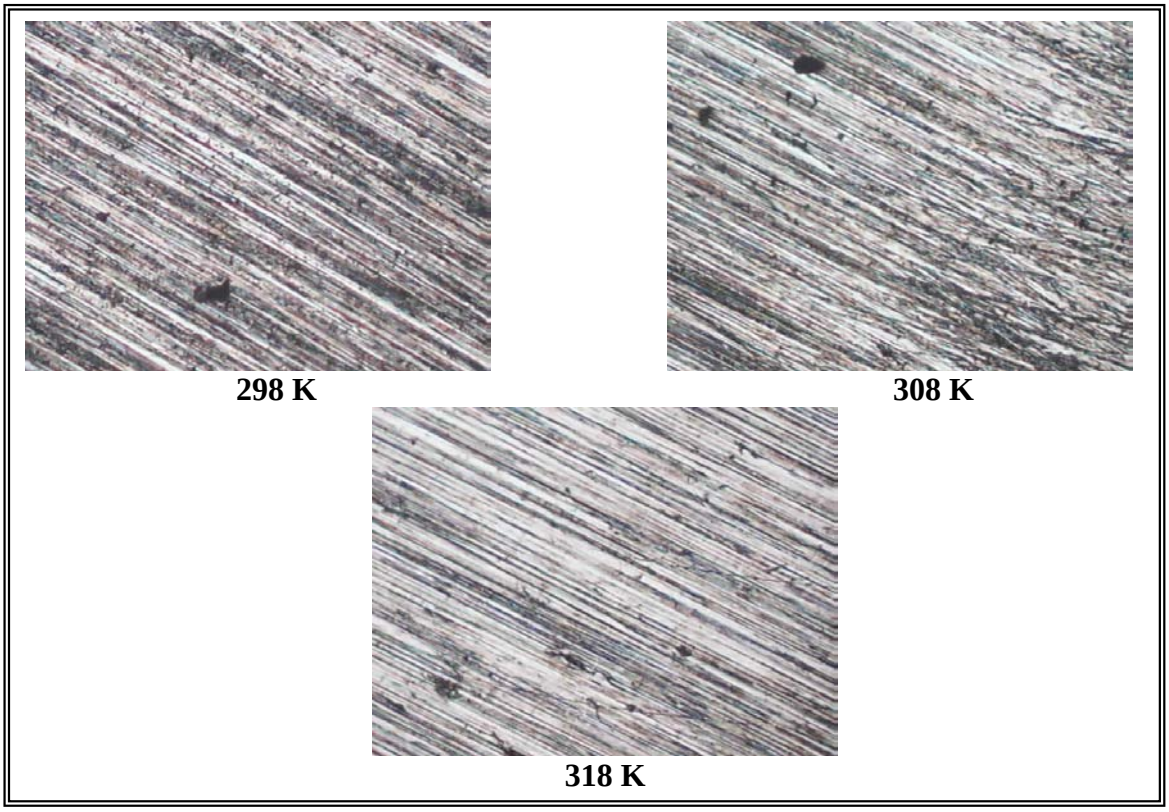

Fig. (5.27) 316L SS after potentiostatic polarization in 1.5% NaCl solutions at static condition (270 X)

5.2.2.4 Effect of scan rate

The effect of scan rate on the electrochemical behavior of 316L SS at 308K in 3.5wt% of NaCl solutions is shown in Fig.(5.28). It can be seen that the characteristic of pitting corrosion (E_b) depends on the scanning rate as shown in Fig.(5.29).This results is in agreement with that of Malik [(85)].

As polarization resistance increases, then the necessary scan rate to obtain a steady state response is decreased. Systems with high values of polarization response (i.e. highly passive) or systems with large values of interfacial capacitance (i.e. highly active) are generally most sensitive to scan rate [(116,117)].Schwenk [(118)], explained that, as the potential increases the induction time for pitting initiation decreases. Thus, when the scan rate increases a rapid increase in the current density at potential corresponds to the short induction time.

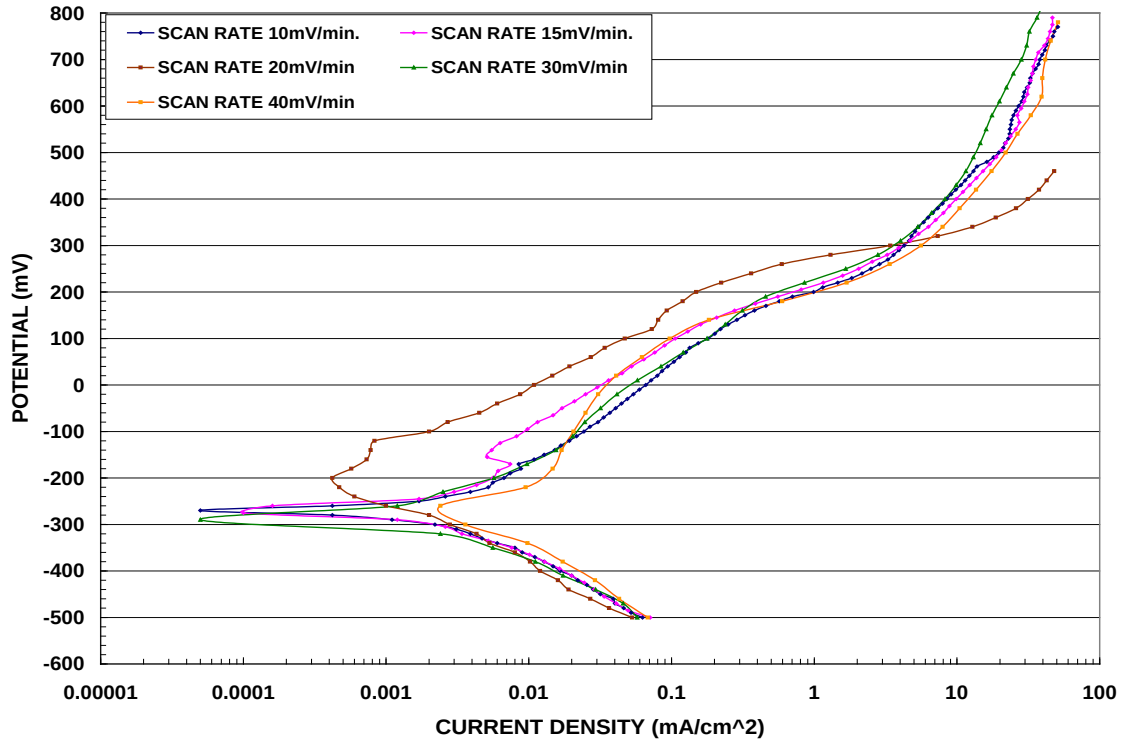

Fig.(5.28) Polarization curves of 316L SS at 308K in 3.5% NaCl solution

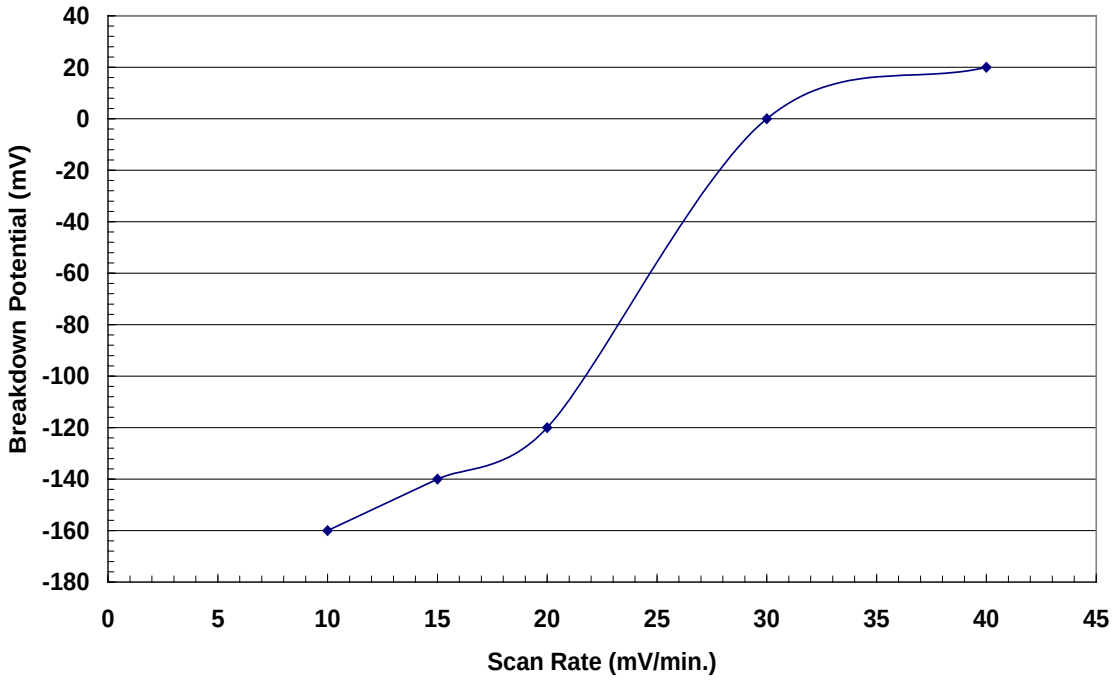

Fig.(5.29) Effect of scan rate on the breackdown potential of 316L SS at 308K in 3.5% NaCl solutions

From Fig.(5.28), it can be confirm that at 40 mV/min., the passivation region observed clearly while, this region is difficult observed at another

scanning rates(10,15,20,30)mV/min.. This give a good evidence that the passivation region depends on critical scanning rates, therefore the scanning must be chosen carefully. These results also confirmed by many other authors[119,120].

Fig.(5.30), shows the surface after potentiostatic polarization of 316L in 3.5% NaCl solution at 308K with different scan rates (10,15,20,30 and 40)mV/min.

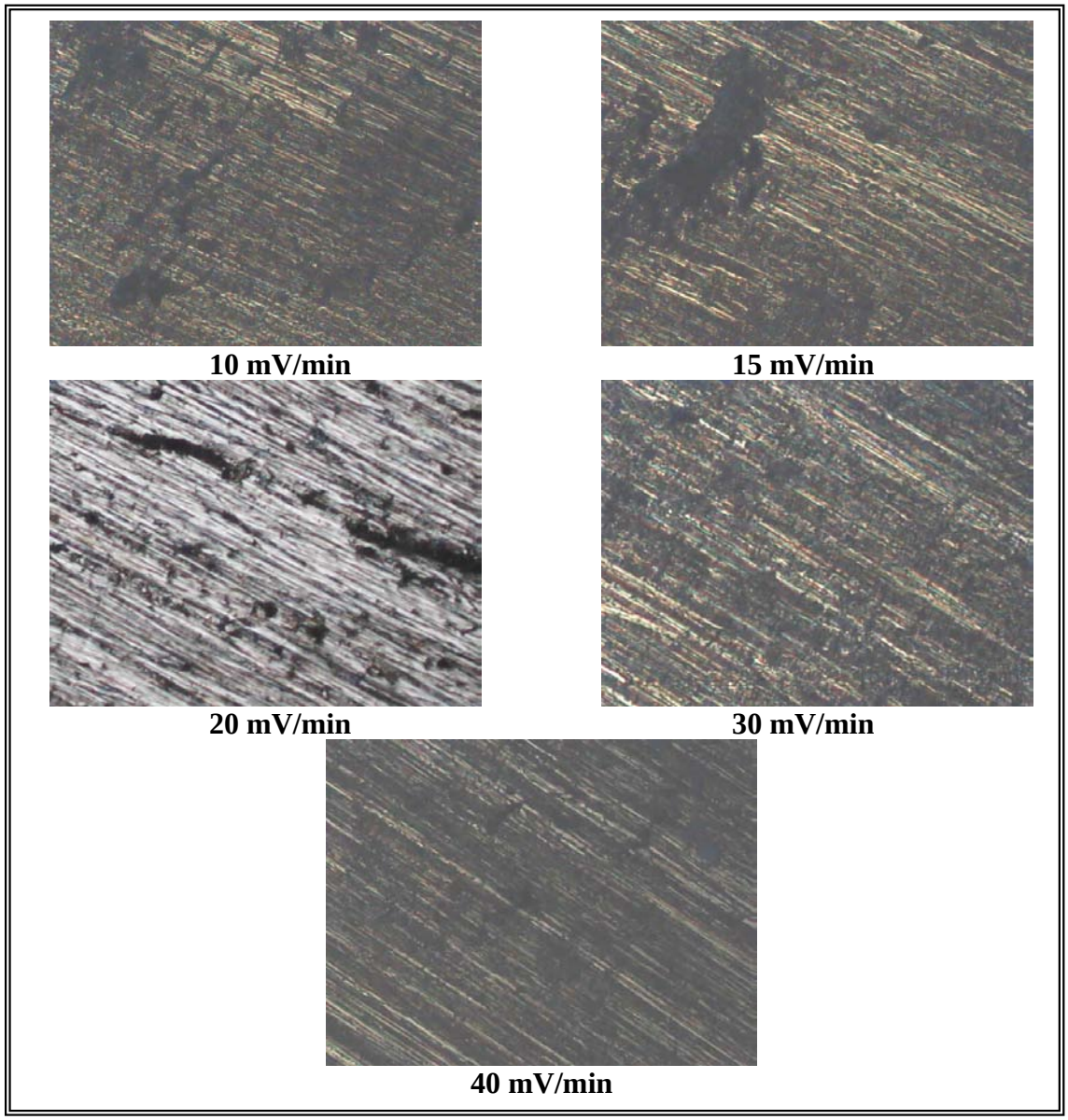

Fig. (5.30) 316L SS after potentiostatic polarization in 3.5% NaCl solutions at 308K (270 X)

5.3 Stainless steel type 202

5.3.1 Static conditions

The first set of the experimental results are presented in Figs.(5.31-5.33), which show the influence of temperatures of(298,308 and 318)K on the corrosion behavior of 202 SS in the solutions of (3.5,2.5 and 1.5)wt% of NaCl.

5.3.1.1 Effect of temperature

Figs.(5.31-5.33), show the effect of temperatures of(298,308 and 318)K on the electrochemical behavior of 202 SS at static condition in (3.5,2.5 and 1.5)wt% of NaCl solutions. The main characteristics of these results are shown in Tables (5.19-5.21). From Table (5.19), it can be seen that there is no clear effect of temperature at (308&318)K on the ($E_{corr.}$) in 3.5% NaCl ($E_{corr.}$=-360mV), while these temperatures(308&318)K have a small effect on the E_b(-200&-220)mV respectively. And from Table(5.20), the effect of temperatures as the Nacl concentration decreases had no clearly effect on the ($E_{corr.}$&E_b) at 318K ($E_{corr.}$=-340, E_b=-220)mV. At 1.5%NaCl, the effect of temperatures on the (E_b) as shown in Table(5.21) will be clear at different temperatures (298,308and318)K, (E_b) have(-180,-120and -140)mV respectively.

The effect of temperature on the breakdown potential at different NaCl solution was shown in Table (5.22) and is plotted in Fig.(5.34). It can be seen that at constant temperature the breakdown potential decreases as the concentration of NaCl increases while at constant concentration the breakdown potential almost increases with increasing temperatures. This is in agreement with that of many workers **(22,85,88)** and are discussed before in section (5.2.1.1).

Moreover the breakdown potential values of 202 SS are less than that obtained for 316L SS at the same conditions. This is a specialty of alloys as mentioned before **(22)**.

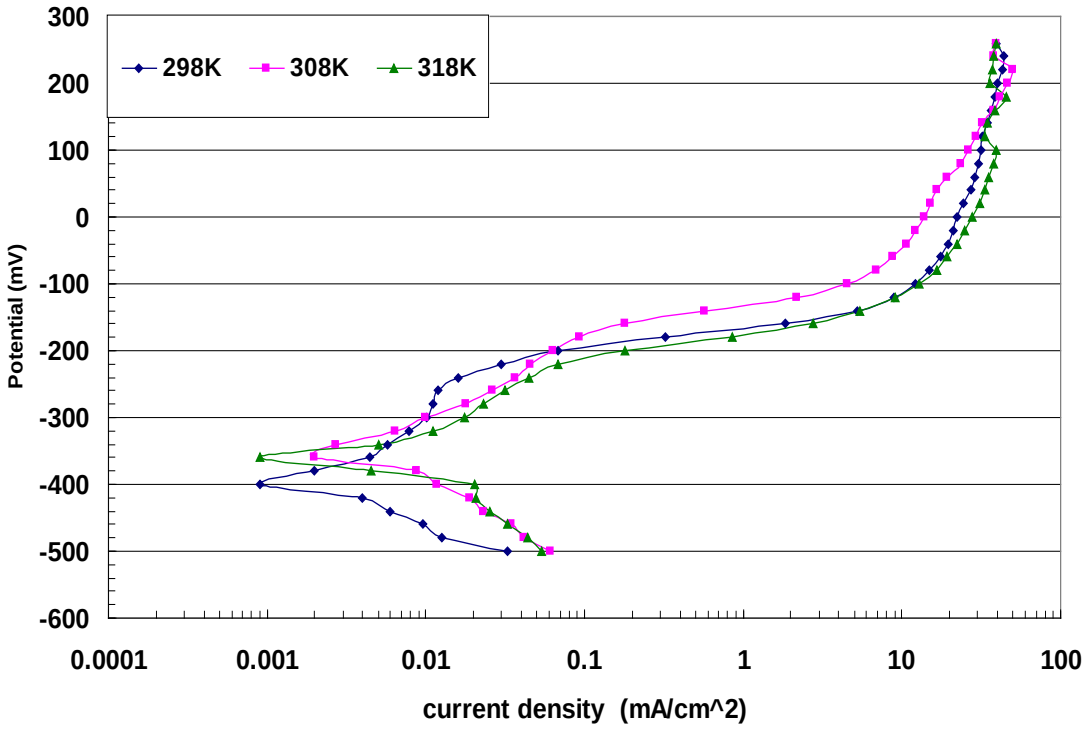

Fig.(5.31) Polarization curves of 202 SS at static condition in 3.5%NaCl solution

Table (5.19) The effect of temperatures (K) on the corrosion potential (mV), primary passive potential (mV),breakdown potential (mV) and corrosion current density (mA/cm^2)) of 202SS at static condition in 3.5%NaCl solution.

Temp. K	$E_{corr.}$ (mV)	$E_{pp.}$ (mV)	E_b (mV)	$i_{corr.}$ (mA/cm^2)
298	-400	-360	-260	0.002
308	-360	-300	-200	0.0059
318	-360	-300	-220	0.009

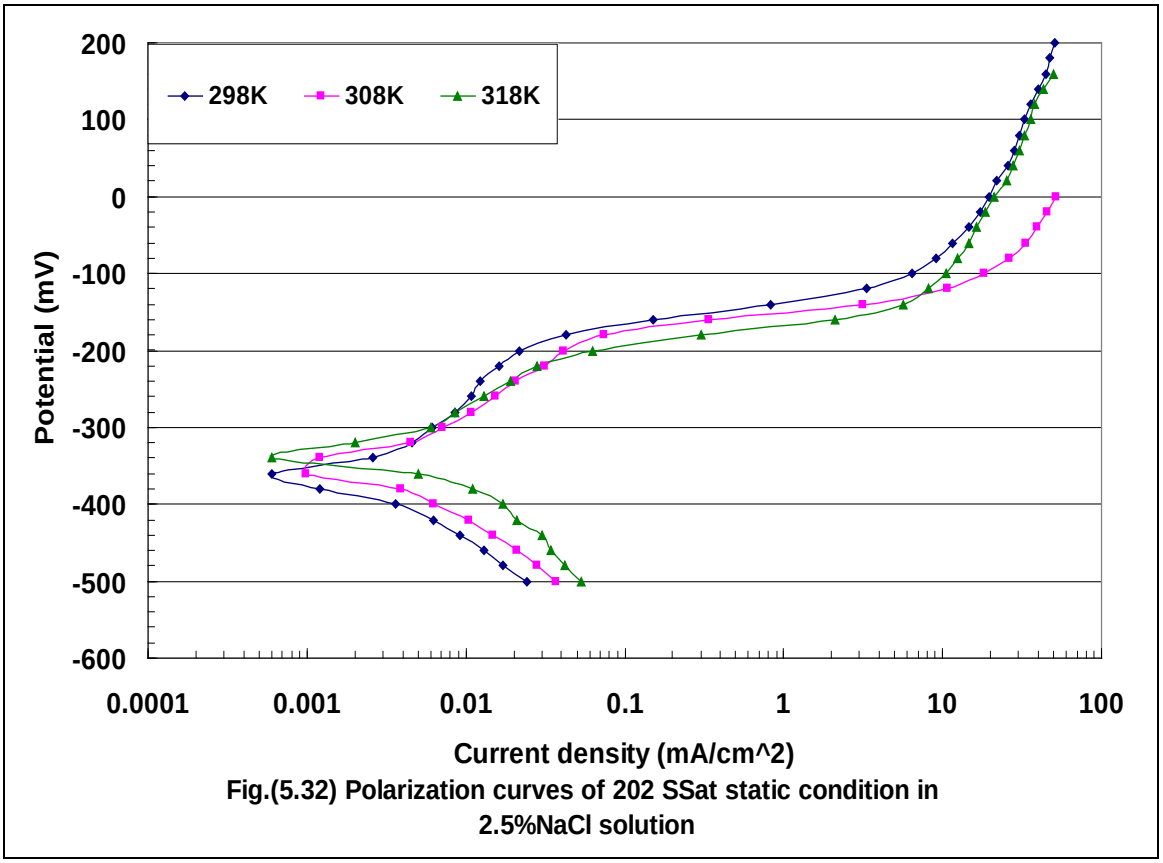

Fig.(5.32) Polarization curves of 202 SSat static condition in 2.5%NaCl solution

Table (5.20) The effect of temperatures (K) on the corrosion potential (mV), primary passive potential (mV),breakdown potential (mV) and corrosion current density (mA/cm^2)) of 202SS at static condition in 2.5%NaCl solution

Temp. K	$E_{corr.}$ (mV)	$E_{pp.}$ (mV)	E_b (mV)	$i_{corr.}$ (mA/cm^2)
298	-360	-300	-200	0.0017
308	-360	-300	-200	0.003
318	-340	-300	-220	0.007

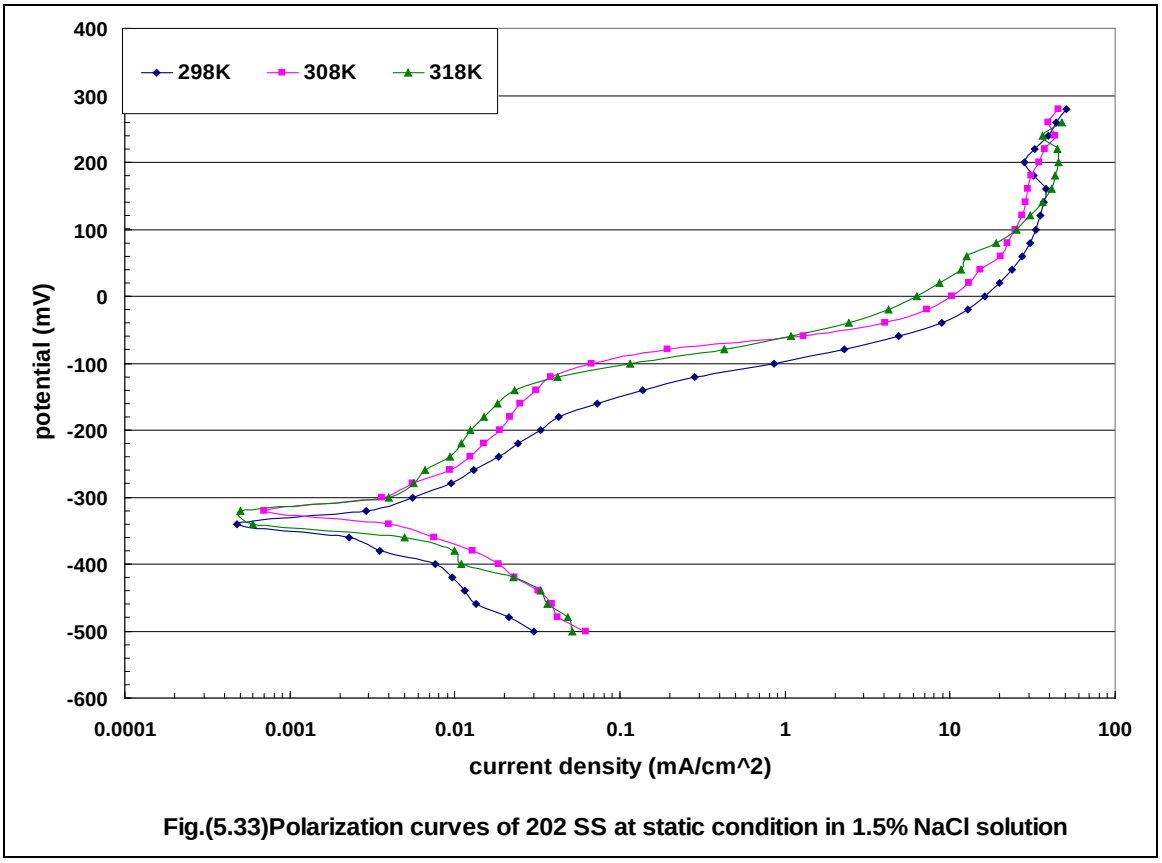

Fig.(5.33)Polarization curves of 202 SS at static condition in 1.5% NaCl solution

Table (5.21) The effect of temperatures (K) on the corrosion potential (mV), primary passive potential (mV),breakdown potential (mV) and corrosion current density (mA/cm^2)) of 202SS at static condition in 1.5%NaCl solution

Temp. K	$E_{corr.}$ (mV)	$E_{pp.}$ (mV)	E_b (mV)	$i_{corr.}$ (mA/cm^2)
298	-340	-300	-180	0.0016
308	-320	-260	-120	0.0028
318	-320	-300	-140	0.005

Table (5.22) Effect of temperatures & concentration of NaCl solutions on the breakdown potential of 202 SS

Temperature (K)	1.5wt%NaCl	2.5wt% NaCl	3.5wt% NaCl
	E_b (mV)	E_b (mV)	E_b (mV)
298	-180	-200	-260
308	-120	-200	-200
318	-140	-220	-220

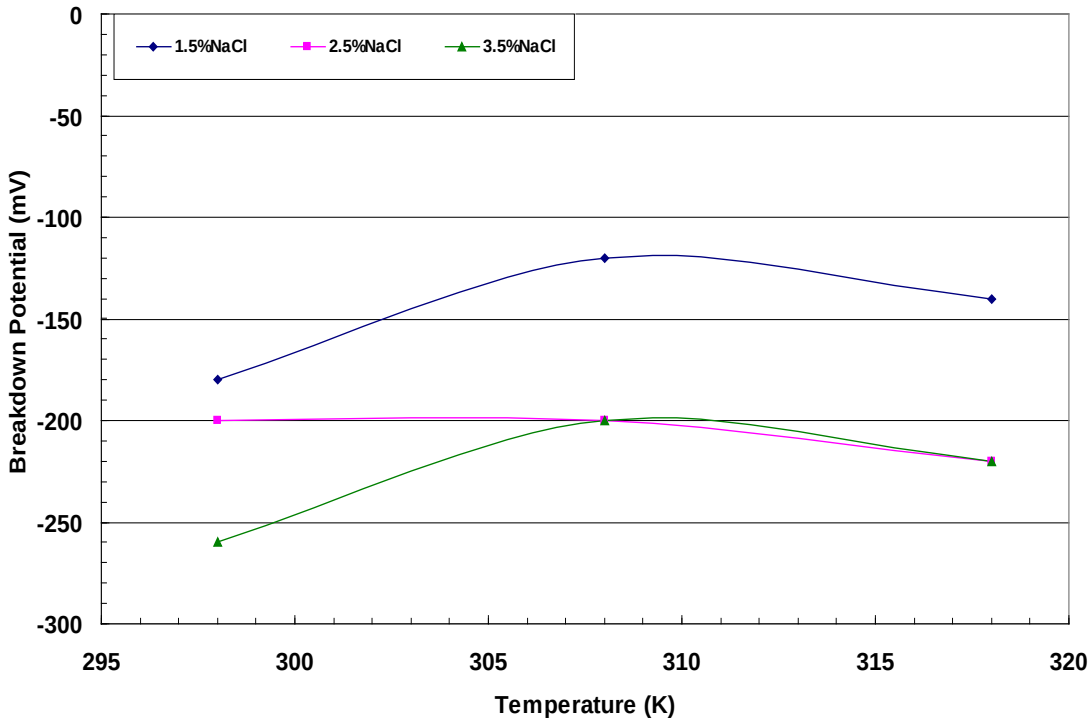

Fig.(5.34) Effect of temperatures on the breakdown potential of 202 at different concentrations of NaCl solutions

Table (5.23), shows the values of corrosion current densities at different temperatures and NaCl solutions. This table indicates that at constant concentration, the corrosion current density increases as the temperatures increases. However at constant temperature, the corrosion current density increases as the concentration of NaCl increases as shown in Fig.(5.35).

Moreover the value of the corrosion current densities of 202 SS are higher than that of 316L SS at the same conditions. This indicates that 316L SS has higher resistance to corrosion than 202 SS at these conditions. This may be

discussed later in section (5.4)

Table (5.23) Effect of temperatures & concentration of NaCl solution on the corrosion rate of 202 SS

Temperature (K)	1.5wt%NaCl	2.5wt% NaCl	3.5wt% NaCl
	$i_{corr.}$ (mA/cm^2)	$i_{corr.}$ (mA/cm^2)	$i_{corr.}$ (mA/cm^2)
298	0.0016	0.0017	0.002
308	0.0028	0.003	0.0059
318	0.005	0.007	0.009

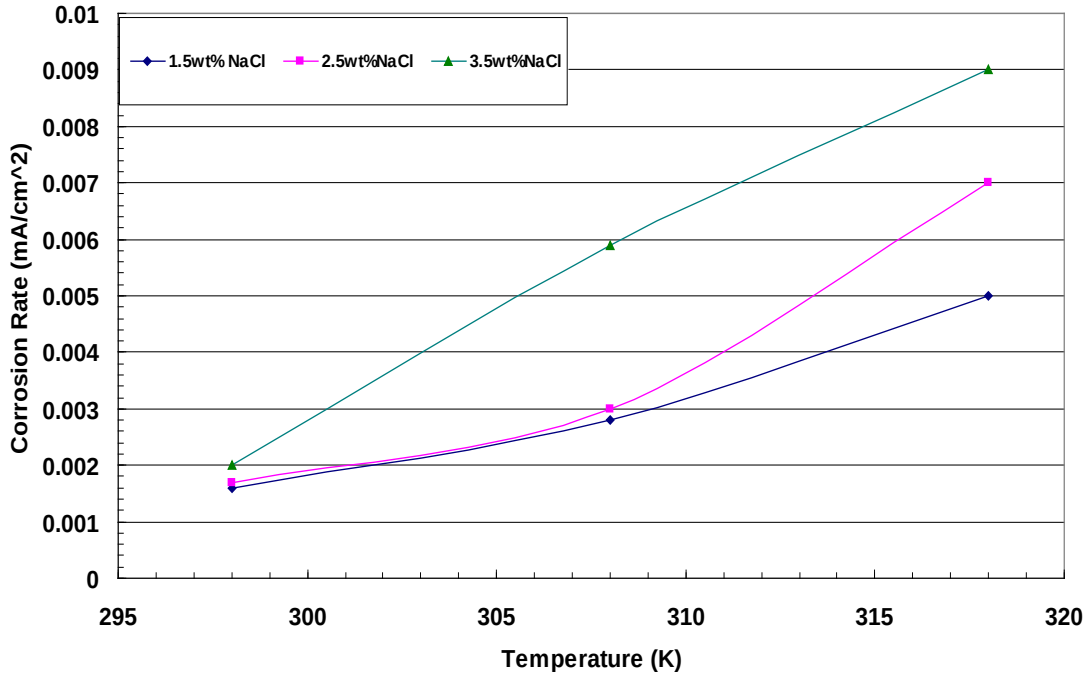

Fig.(5.35) Effect of the temperature on the current density of 202 SS at different concentrations of NaCl solutions

The relationship of logarithm of corrosion rate with the reciprocal of absolute temperature i.e, Arrhenius plot shown in Fig.(5.36) is linear. These results are in agreement with those of Malik [(85)].

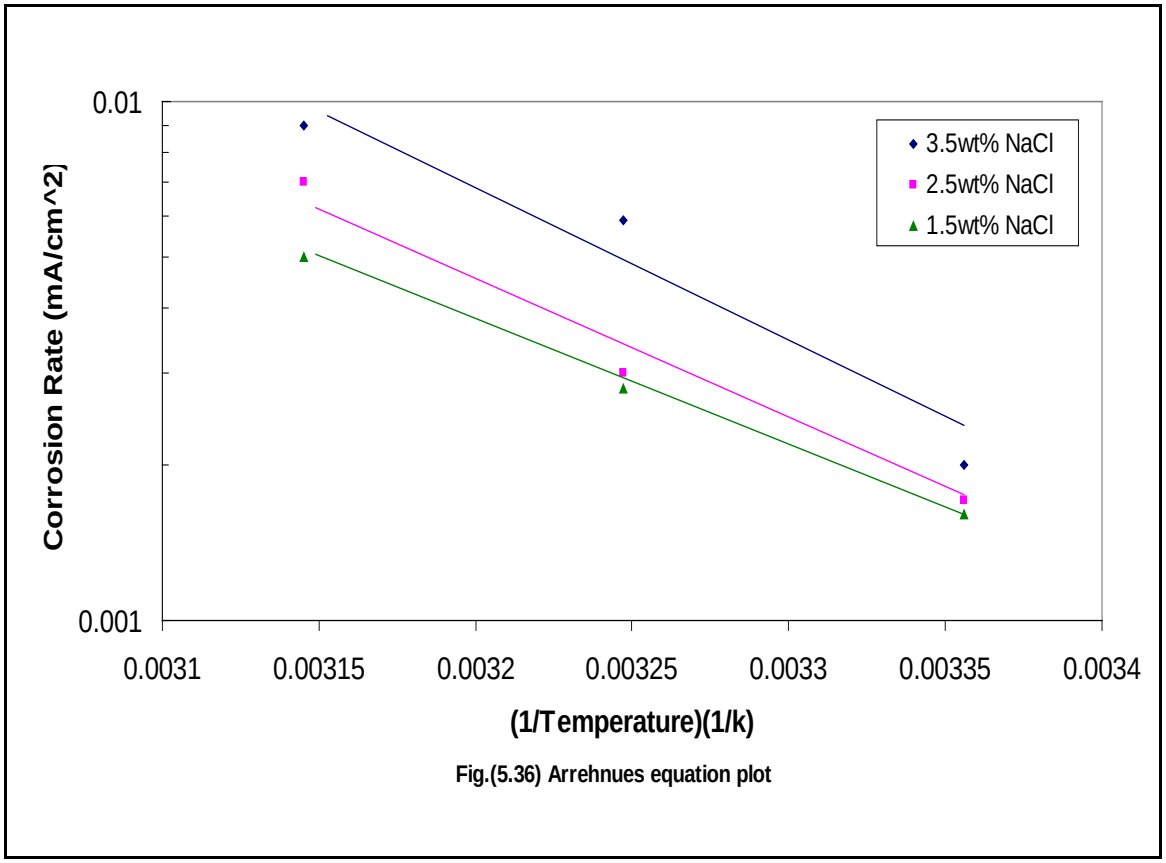

Fig.(5.36) Arrehnues equation plot

5.3.1.2 Effect of NaCl concentration

Fig. (5.37), shows the effect of the concentration of NaCl solution on the breakdown potential of 202 SS at different temperatures. It can be seen that at constant temperature the breakdown potential decreases as the concentration of NaCl solutions increases. i.e E_b shifts to the active direction. These results are in agreement with the workers **(20, 85, 88)**.

Fig.(5.38), shows the effect of NaCl concentration on the corrosion rate of 202 SS at different temperatures. It indicates that at constant temperature, the corrosion rate increases as the concentration of NaCl increases. These results are similar to that of 316L SS and the reasons for these results which were obtained are discussed and mentioned before in section (5.2.1.2).

Moreover the corrosion rate of 202 SS is higher than that of 316L SS. This may be discussed later in section (5.4).

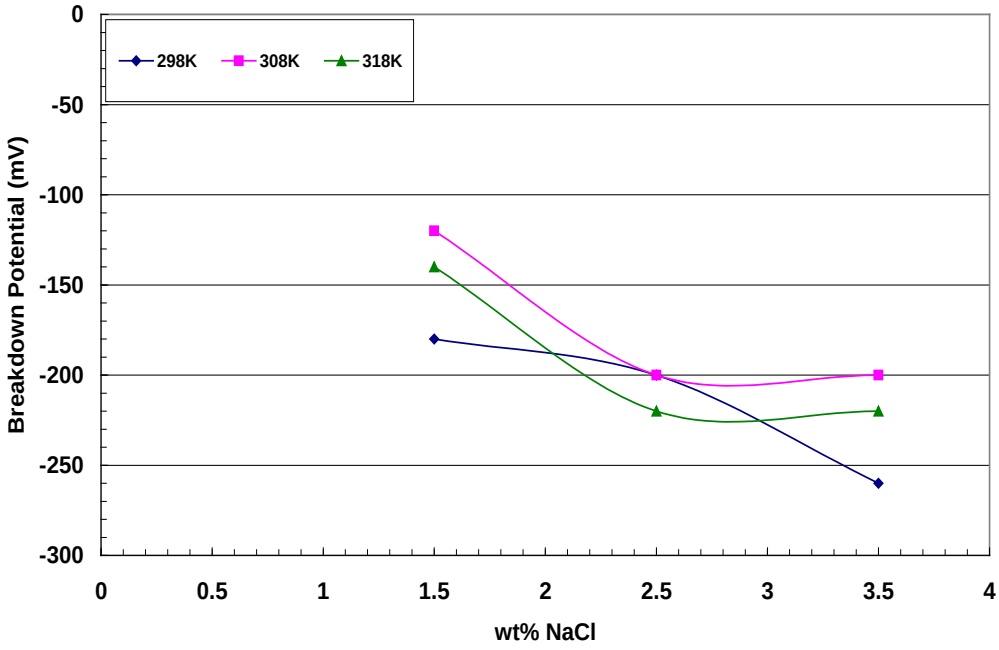

Fig.(5.37)Effect of NaCl concentration on the breakdown potential of 202 SS at different temperatures.

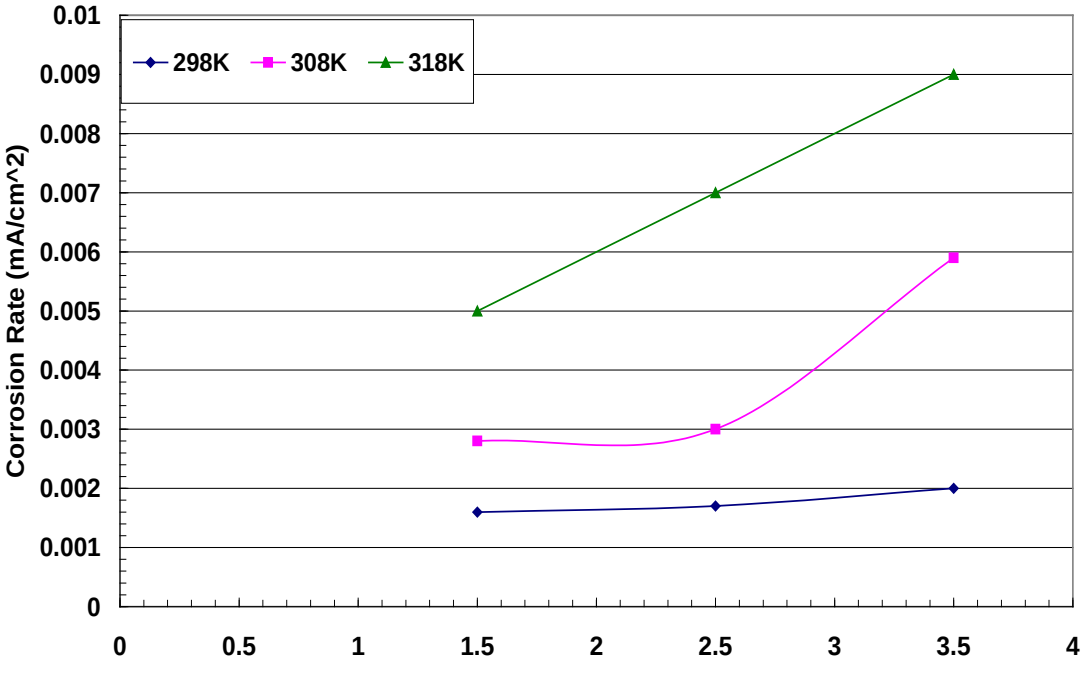

Fig.(5.38) Effect of NaCl concentration on the current density of 202 SS at different temperatures

5.3.2 Dynamic conditions

The second set of the experimental results are presented in Figs.(5.39-5.44), which show the influence of the speed of Rotating Cylinder Electrode at various temperatures and NaCl concentrations on the corrosion behavior of 202 SS in solutions.

5.3.2.1 Effect of temperature

Figs.(5.39 - 5.44), show the effect of the speed of RCE (0,100,200 and 300)r.p.m at temperatures (298,308 and 318)K in (3.5 & 2.5)wt% of NaCl solutions on the corrosion rates and breakdown potential of 202 SS.

Tables (5.24 - 5.29), represent the main characteristics of the results obtained from Figs.(5.39- 5.44).

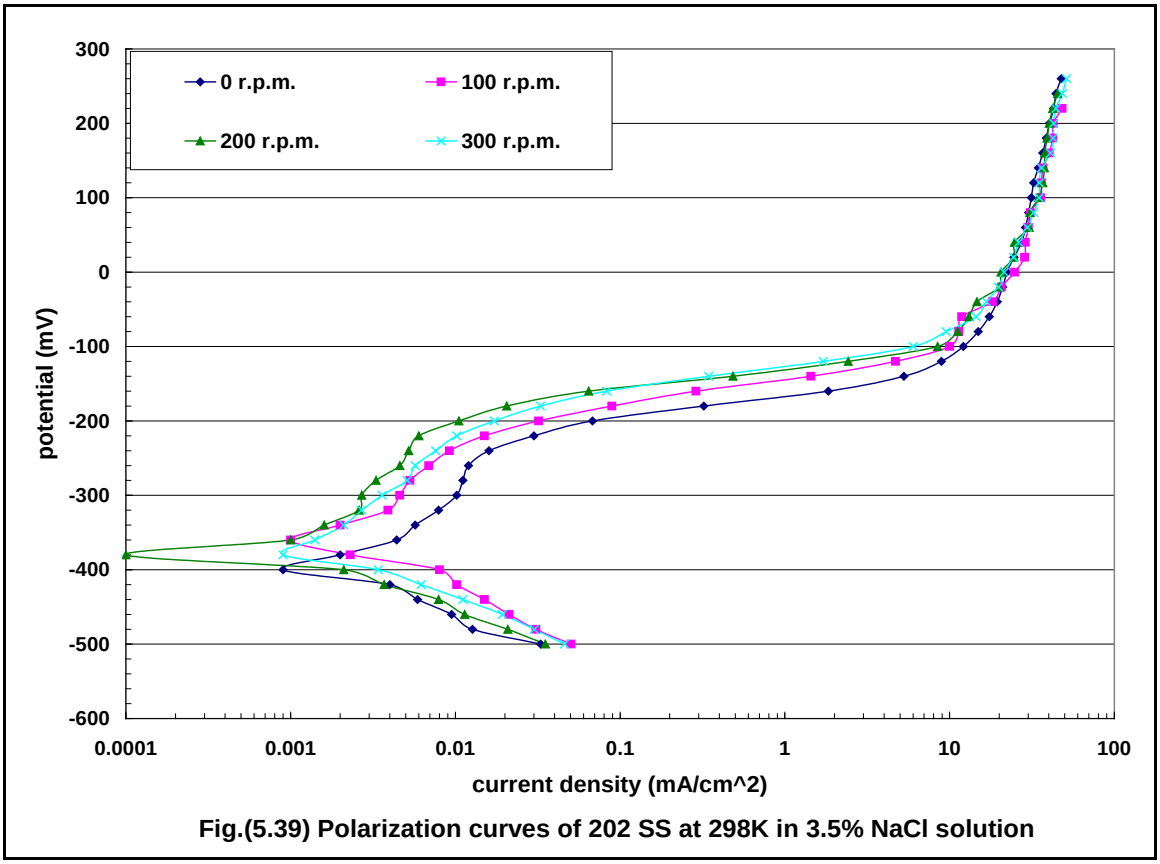

Fig.(5.39) Polarization curves of 202 SS at 298K in 3.5% NaCl solution

Table (5.24) The effect of rotational speed (r.p.m) on the corrosion potential (mV),primary passive potential (mV),breakdown potential (mV) and corrosion current density (mA/cm^2) of 202 SS at 298K in 3.5%NaCl solution.

Rotation r.p.m.	(ω) = r.p.m.*2π/60	v=(ω/2)*d (m/s)	$E_{corr.}$ (mV)	$E_{pp.}$ (mV)	E_b (mV)	$i_{corr.}$ (mA/cm^2)
0	0	0	-400	-360	-260	0.002
100	10.49	0.315	-360	-320	-240	0.004
200	20.98	0.629	-380	-300	-220	0.0018
300	31.47	0.944	-380	-280	-220	0.002

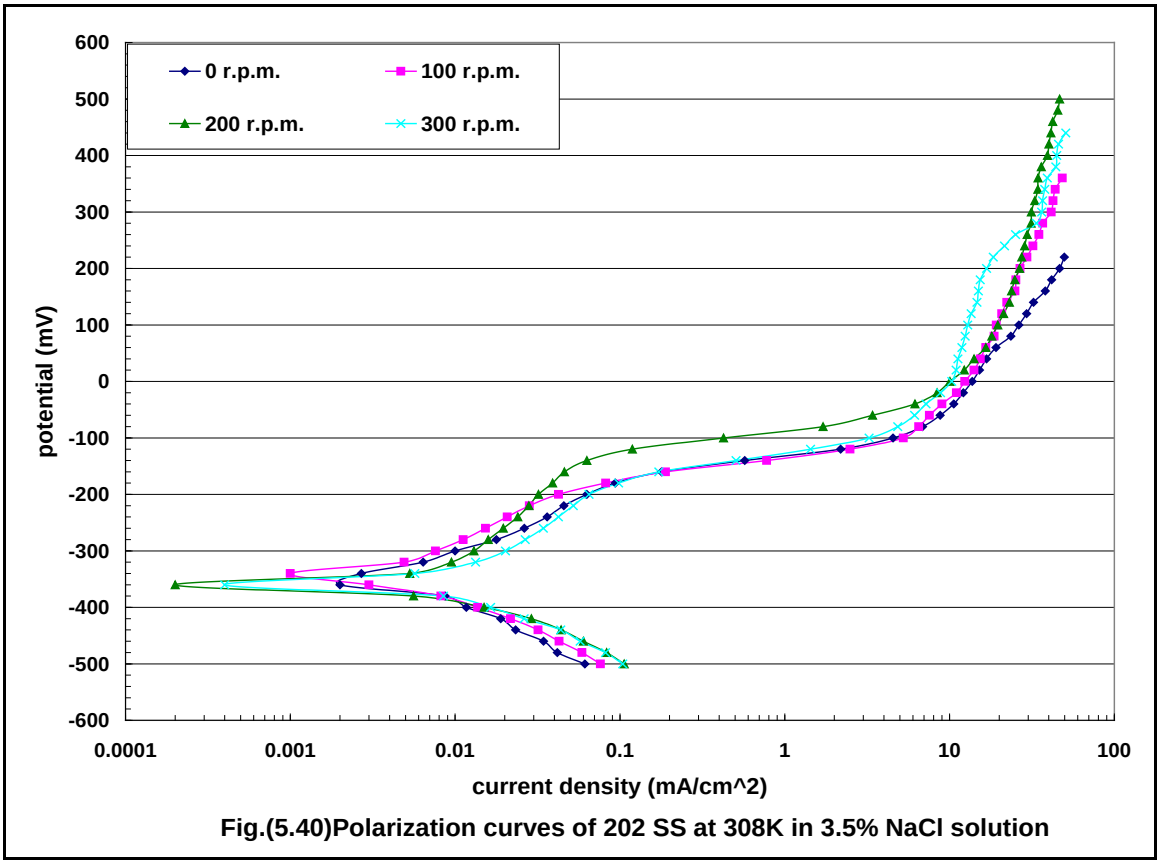

Fig.(5.40)Polarization curves of 202 SS at 308K in 3.5% NaCl solution

Table (5.25) The effect of rotational speed (r.p.m) on the corrosion potential (mV),primary passive potential (mV),breakdown potential (mV) and corrosion current density (mA/cm^2) of 202 SS at 308K in 3.5%NaCl solution.

Rotation r.p.m.	(ω) = r.p.m.*2π/60	v=(ω/2)*d (m/s)	$E_{corr.}$ (mV)	$E_{pp.}$ (mV)	E_b (mV)	$i_{corr.}$ (mA/cm^2)
0	0	0	-360	-300	-180	0.0059
100	10.49	0.315	-340	-300	-200	0.005
200	20.98	0.629	-360	-300	-160	0.0056
300	31.47	0.944	-360	-300	-200	0.0063

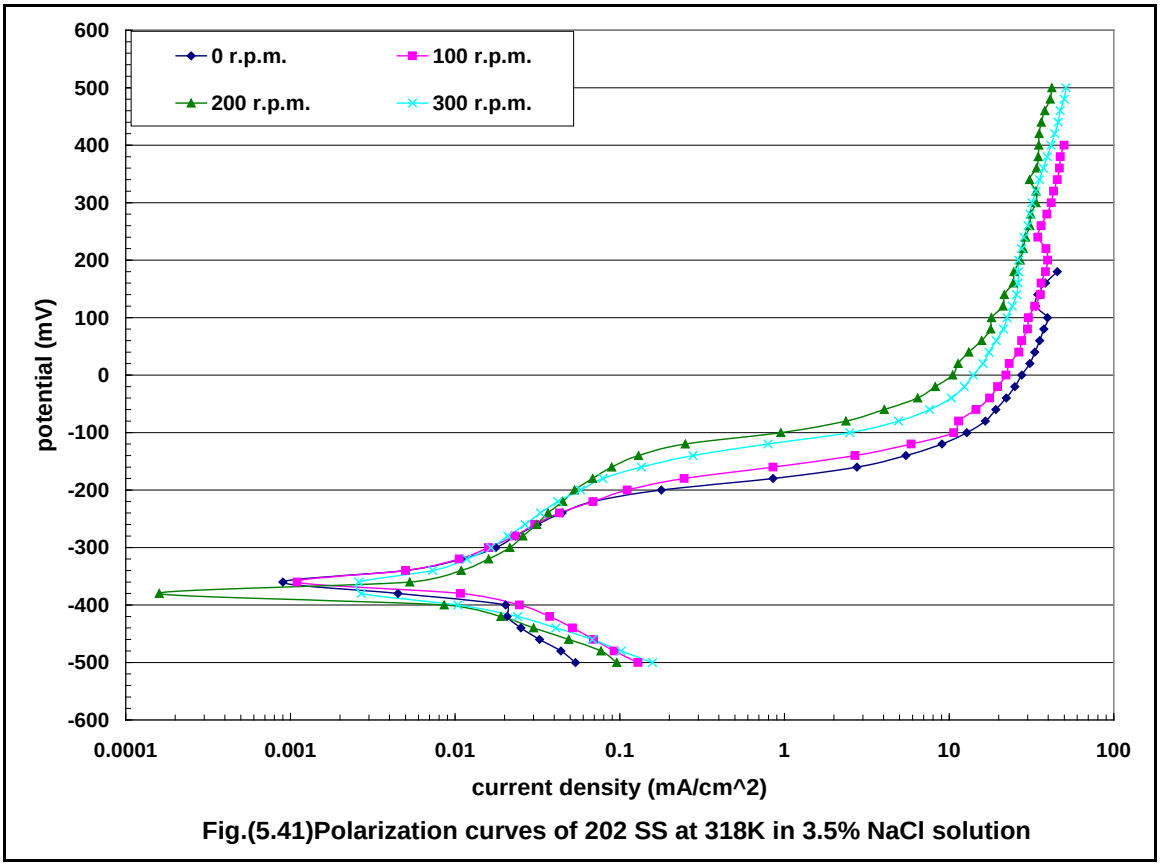

Fig.(5.41)Polarization curves of 202 SS at 318K in 3.5% NaCl solution

Table (5.26) The effect of rotational speed (r.p.m) on the corrosion potential (mV),primary passive potential (mV),breakdown potential (mV) and corrosion current density (mA/cm^2) of 202 SS at 318K in 3.5%NaCl solution.

Rotation r.p.m.	(ω) = r.p.m.*2π/60	v=(ω/2)*d (m/s)	$E_{corr.}$ (mV)	$E_{pp.}$ (mV)	E_b (mV)	$i_{corr.}$ (mA/cm^2)
0	0	0	-360	-320	-220	0.009
100	10.49	0.315	-360	-320	-200	0.013
200	20.98	0.629	-380	-320	-140	0.006
300	31.47	0.944	-360	-340	-160	0.005

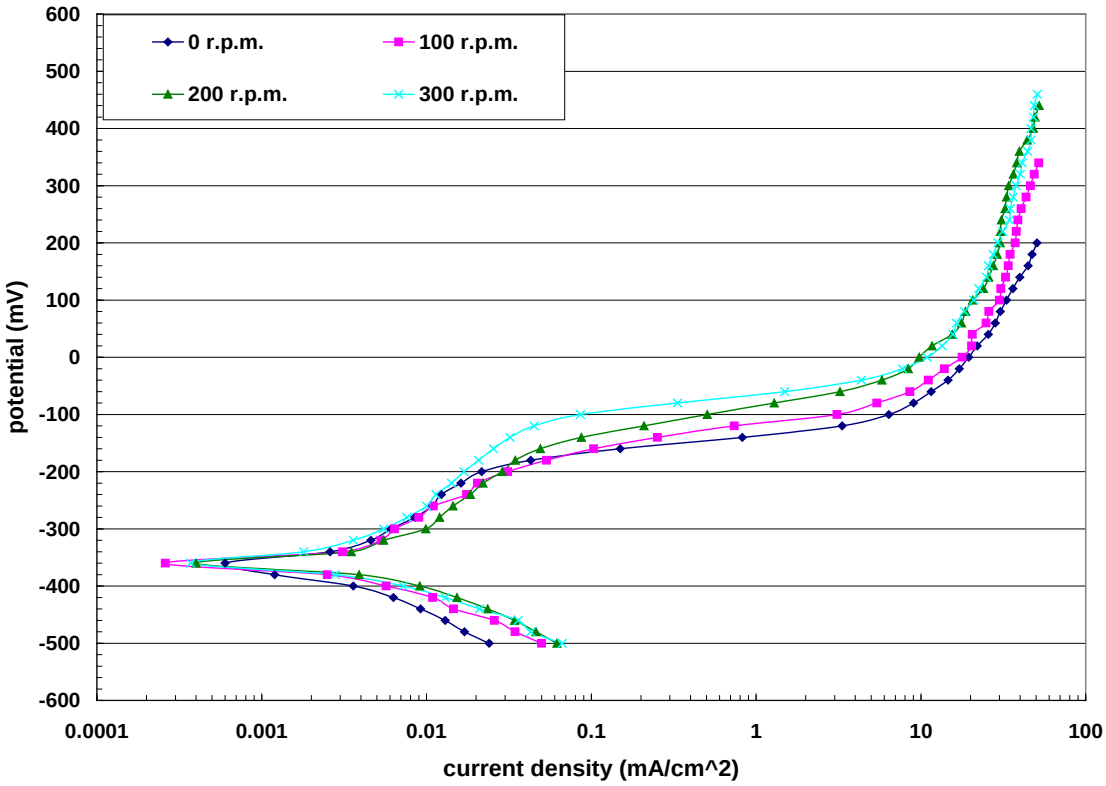

Fig. (5.42)Polarization curves of 202 SS at 298K in 2.5% NaCl solution

Table (5.27) The effect of rotational speed (r.p.m) on the corrosion potential (mV),primary passive potential (mV),breakdown potential (mV) and corrosion current density (mA/cm^2) of 202 SS at 298K in 2.5%NaCl solution.

Rotation r.p.m.	(ω) = r.p.m.*2π/60	v=(ω/2)*d (m/s)	$E_{corr.}$ (mV)	$E_{pp.}$ (mV)	E_b (mV)	$i_{corr.}$ (mA/cm^2)
0	0	0	-360	-320	-200	0.0017
100	10.49	0.315	-360	-320	-200	0.0021
200	20.98	0.629	-360	-300	-180	0.0022
300	31.47	0.944	-360	-300	-120	0.002

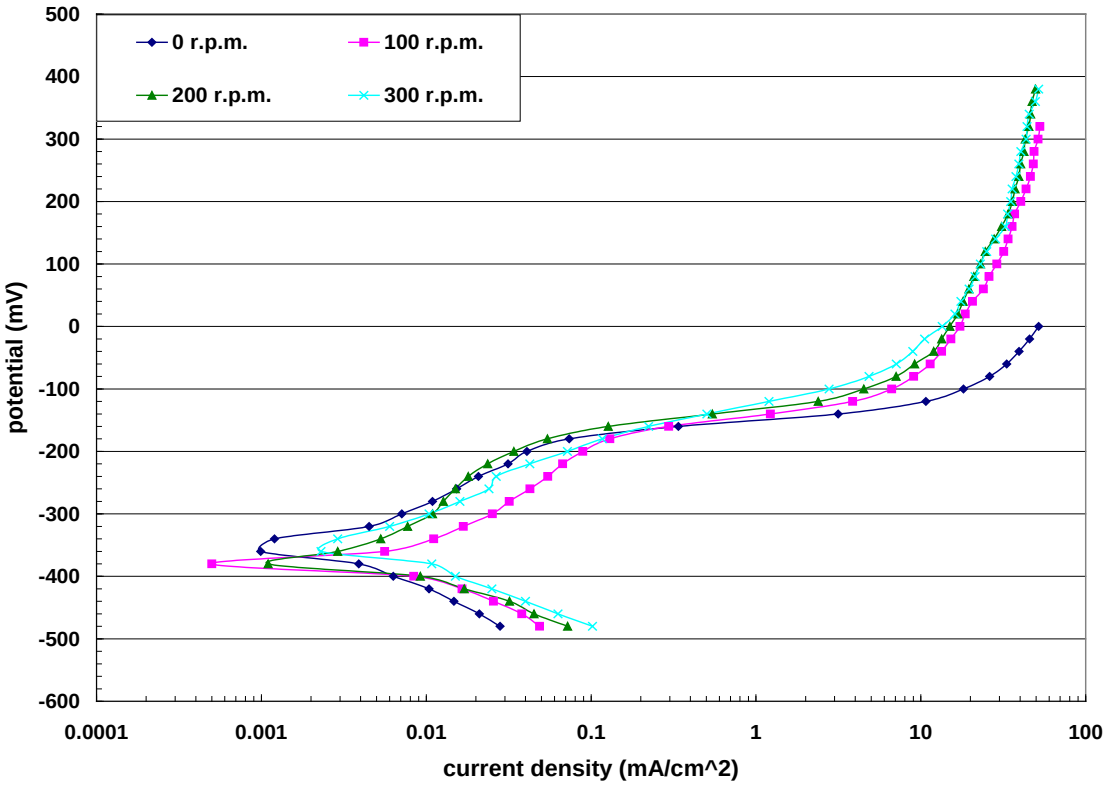

Fig. (5.43)Polarization curves of 202 SS at 308K in 2.5% NaCl solution

Table (5.28) The effect of rotational speed (r.p.m) on the corrosion potential (mV),primary passive potential (mV),breakdown potential (mV) and corrosion current density (mA/cm^2) of 202 SS at 308K in 2.5%NaCl solution.

Rotation r.p.m.	(ω) = r.p.m.*2π/60	v=(ω/2)*d (m/s)	$E_{corr.}$ (mV)	$E_{pp.}$ (mV)	E_b (mV)	$i_{corr.}$ (mA/cm^2)
0	0	0	-360	-320	-200	0.003
100	10.49	0.315	-380	-340	-180	0.006
200	20.98	0.629	-380	-340	-180	0.006
300	31.47	0.944	-360	-340	-180	0.006

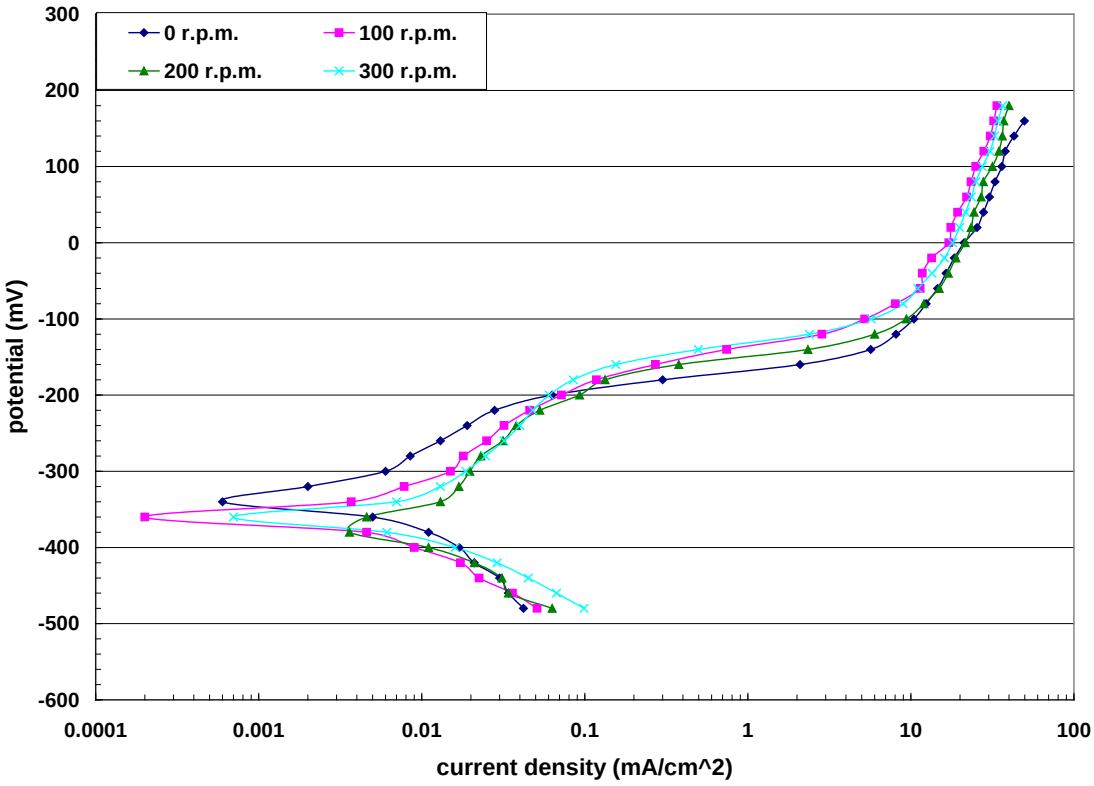

Fig.(5.44) Polarization curves of 202 SS at 318K in 2.5% NaCl solution

Table (5.29) The effect of rotational speed (r.p.m) on the corrosion potential (mV),primary passive potential (mV),breakdown potential (mV) and corrosion current density (mA/cm^2) of 202 SS at 318K in 2.5%NaCl solution.

Rotation r.p.m.	(ω) = r.p.m.*2π/60	v=(ω/2)*d (m/s)	$E_{corr.}$ (mV)	$E_{pp.}$ (mV)	E_b (mV)	$i_{corr.}$ (mA/cm^2)
0	0	0	-340	-300	-220	0.007
100	10.49	0.315	-360	-300	-200	0.006
200	20.98	0.629	-380	-340	-220	0.007
300	31.47	0.944	-360	-320	-180	0.0068

Tables (5.30and5.31), show the effect of temperatures on the breakdown potential of 202 SS with various speeds of rotation in (3.5% and2.5%) of NaCl solutions. These tables show that there is no clear effect of temperatures on the breakdown potential. This is in agreement with those many workers **(113,114,115)** as mentioned and discussed before (see section 5.2.2.1).

Table (5.30) The effect of temperatures on the breakdown potential of 202 SS with various speeds rotation in 3.5% NaCl solutions

Rotation r.p.m	E_b (mV)	E_b (mV)	E_b (mV)
	298 K	308 K	318 K
0	-260	-180	-220
100	-240	-200	-200
200	-220	-160	-140
300	-220	-200	-160

Table (5.31) The effect of temperatures on the breakdown potential of 202 SS with various speeds rotation in 2.5% NaCl solutions

Rotation r.p.m	E_b (mV)	E_b (mV)	E_b (mV)
	298 K	308 K	318 K
0	-200	-200	-220
100	-200	-180	-200
200	-180	-180	-220
300	-120	-180	-180

Tables (5.32 and 5.33), show the effect of temperatures on the corrosion rate at various speeds of rotation in (3.5%and2.5%) of NaCl solutions respectively .From these tables it can be seen that the corrosion rate ($i_{corr.}$) increases when the temperature increases as shown in Figs.(5.45 and 5.46).

Table (5.32) Effect of temperature on the corrosion rate of 202 SS at different velocities in 3.5wt% NaCl solutions

Rotation r.p.m.	298 K	308 K	318 K
	i_{corr}. (mA/cm^2)	i_{corr}. (mA/cm^2)	i_{corr}. (mA/cm^2)
0	0.002	0.0059	0.009
100	0.004	0.005	0.013
200	0.0018	0.0056	0.006
300	0.002	0.0063	0.005

Table (5.33) Effect of temperature on the corrosion rate of 202 SS at different velocities in 2.5wt% NaCl solutions

Rotation r.p.m	298 K	308 K	318 K
	i_{corr}. (mA/cm^2)	i_{corr}. (mA/cm^2)	i_{corr}. (mA/cm^2)
0	0.0017	0.003	0.007
100	0.0021	0.006	0.006
200	0.0022	0.006	0.007
300	0.002	0.006	0.0068

Moreover the corrosion current densities of 202 SS are higher than that obtained for 316L SS under the same conditions. This is discussed later in section (5.4).

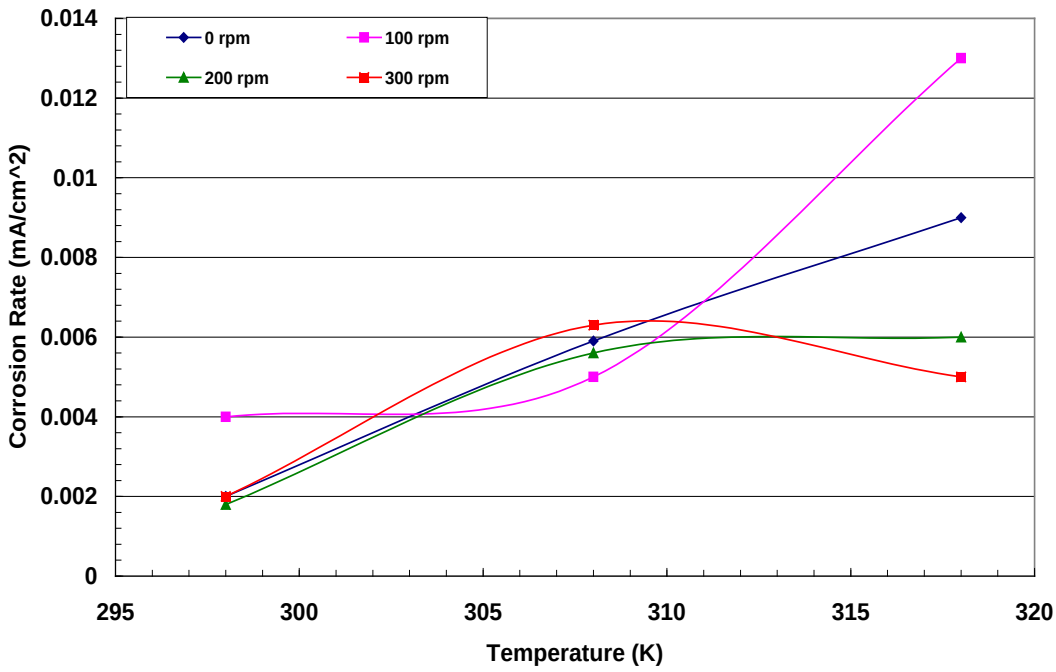

Fig. (5.45) Effect of temperature on the corrosion rate of 202 SS at different speeds of rotation in 3.5wt% of NaCl solution

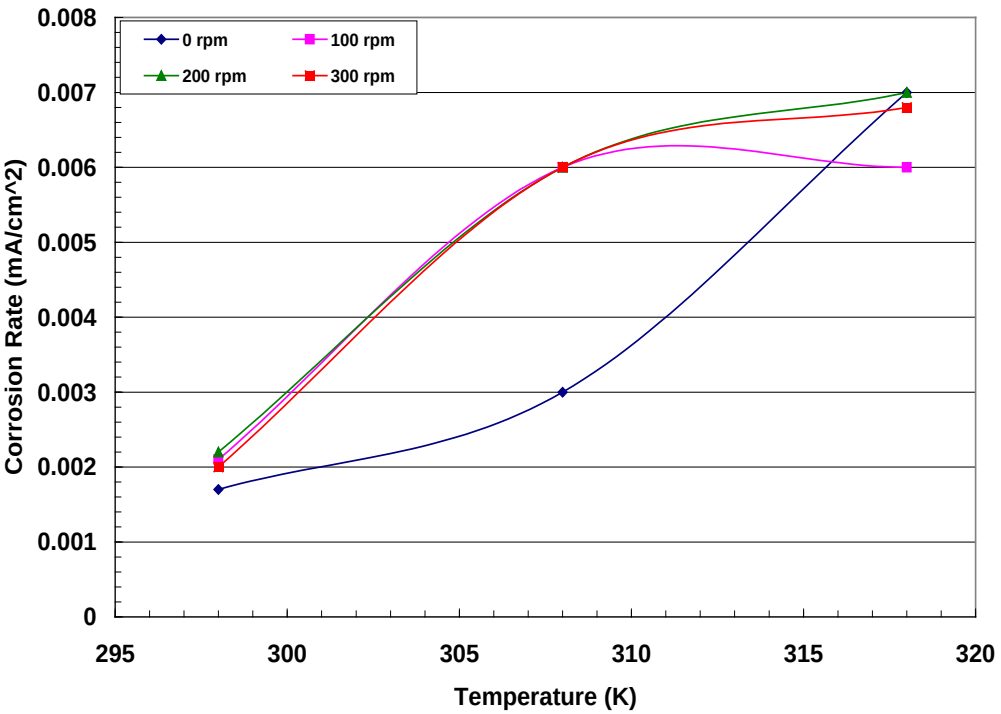

Fig. (5.46) Effect of temperature on the corrosion rate of 202 SS at different speeds of rotation in 2.5wt% of NaCl solution

5.3.2.2 Effect of NaCl concentration

Tables (5.34-5.36), show the effect of NaCl concentration on the corrosion rate of 202 SS at (298,308 and 318)K with various rotation speeds (0,100,200 and 300)r.p.m. These tables show that at constant speed the corrosion current density almost increases with increasing the concentration of NaCl . This is in agreement with those of many workers [2,85] as discussed before in section (5.2.2.2).

Table (5.34) Effect of NaCl % solution on the corrosion rate of 202 SS at 298K at different rotation speeds

NaCl wt%	0 r.p.m	100 r.p.m	200 r.p.m	300 r.p.m
	$i_{corr.}$ (mA/cm^2)	$i_{corr.}$ (mA/cm^2)	$i_{corr.}$ (mA/cm^2)	$i_{corr.}$ (mA/cm^2)
2.5	0.0017	0.0021	0.0022	0.002
3.5	0.002	0.004	0.0018	0.002

Table (5.35) Effect of NaCl % solution on the corrosion rate of 202 SS at 308K at different rotation speeds

NaCl wt%	0 r.p.m	100 r.p.m	200 r.p.m	300 r.p.m
	$i_{corr.}$ (mA/cm^2)	$i_{corr.}$ (mA/cm^2)	$i_{corr.}$ (mA/cm^2)	$i_{corr.}$ (mA/cm^2)
2.5	0.003	0.006	0.006	0.006
3.5	0.0059	0.005	0.0056	0.0063

Table (5.36) Effect of NaCl % solution on the corrosion rate of 202 SS at 318K at different rotation speeds

NaCl wt%	0 r.p.m	100 r.p.m	200 r.p.m	300 r.p.m
	$i_{corr.}$ (mA/cm^2)	$i_{corr.}$ (mA/cm^2)	$i_{corr.}$ (mA/cm^2)	$i_{corr.}$ (mA/cm^2)
2.5	0.007	0.006	0.007	0.0068
3.5	0.009	0.013	0.006	0.005

5.3.2.3 Effect of velocity

Figs.(5.47 and 5.48), show the effect of velocity on the corrosion rate of 202 SS at different temperatures (298,308 and 318)K in (3.5 & 2.5)wt% of NaCl solutions respectively. It can be seen that at 2.5wt% of NaCl the variation in the corrosion current density is small as the velocity increases (see Tables 5.34-5.36 and Fig. 5.48). At 3.5wt% of NaCl the corrosion current density decreases as the velocity increases at (298 and 318)K while at 308K the variation in corrosion current density is low .So these types of steel are concerned as not velocity limited (see section 2.5.5).

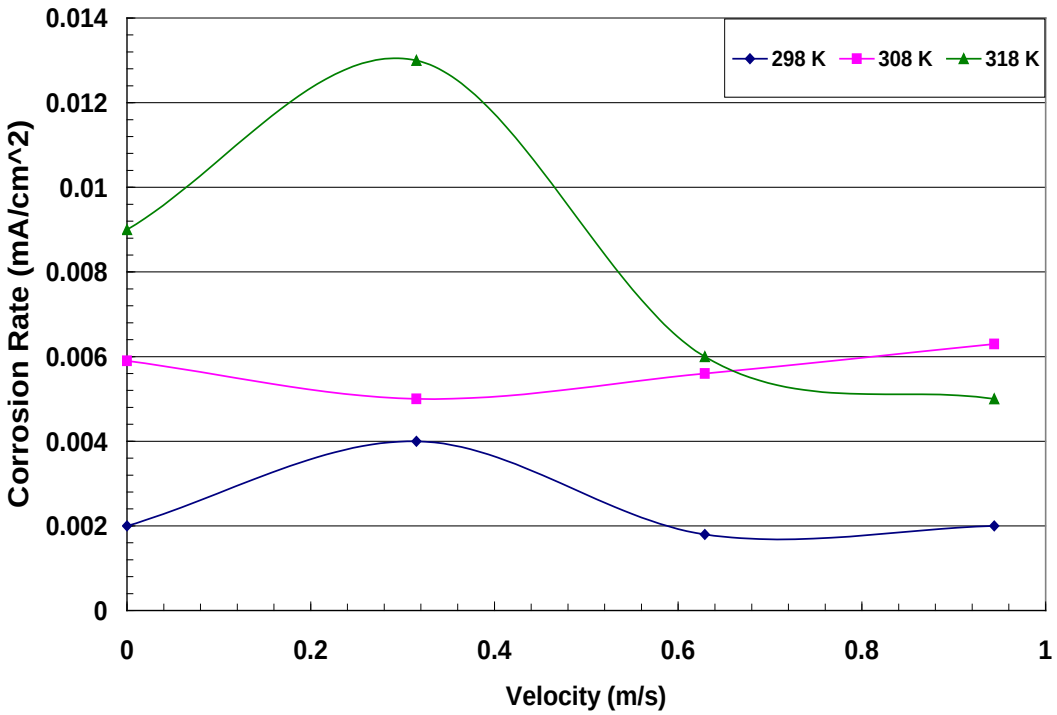

Fig. (5.47) Effect of velocity on the corrosion rate of 202 SS at different temperatures in 3.5 wt% of NaCl solution

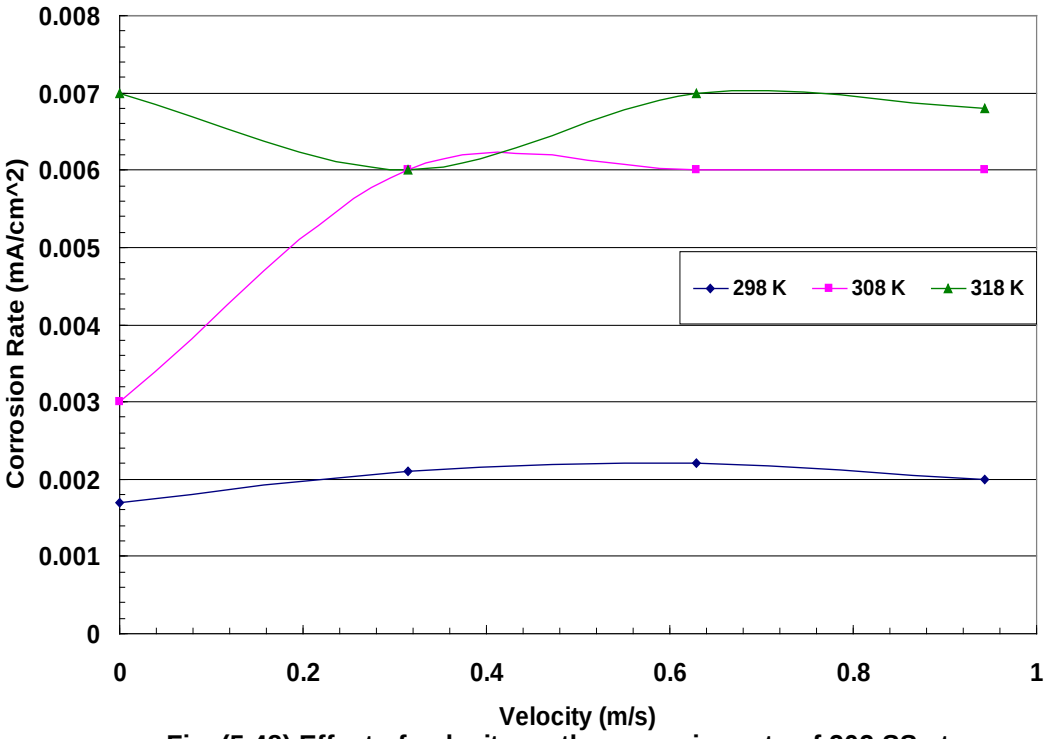

Fig. (5.48) Effect of velocity on the corrosion rate of 202 SS at different temperatures in 2.5wt% of NaCl solutions

Fig.(5.49-5.54),show the surface after potentiostatic polarization of 202 SS in the solution containing (3.5 & 2.5)%NaCl at different temperatures (298,308 and 318)K with various rotational speeds (0,100,200 and 300) r.p.m respectively.

Fig.(5.55), shows the surface after potentiostatic polarization of 202 SS in the solution containing (1.5) %NaCl at static condition with different temperatures (298,308 and 318)K .

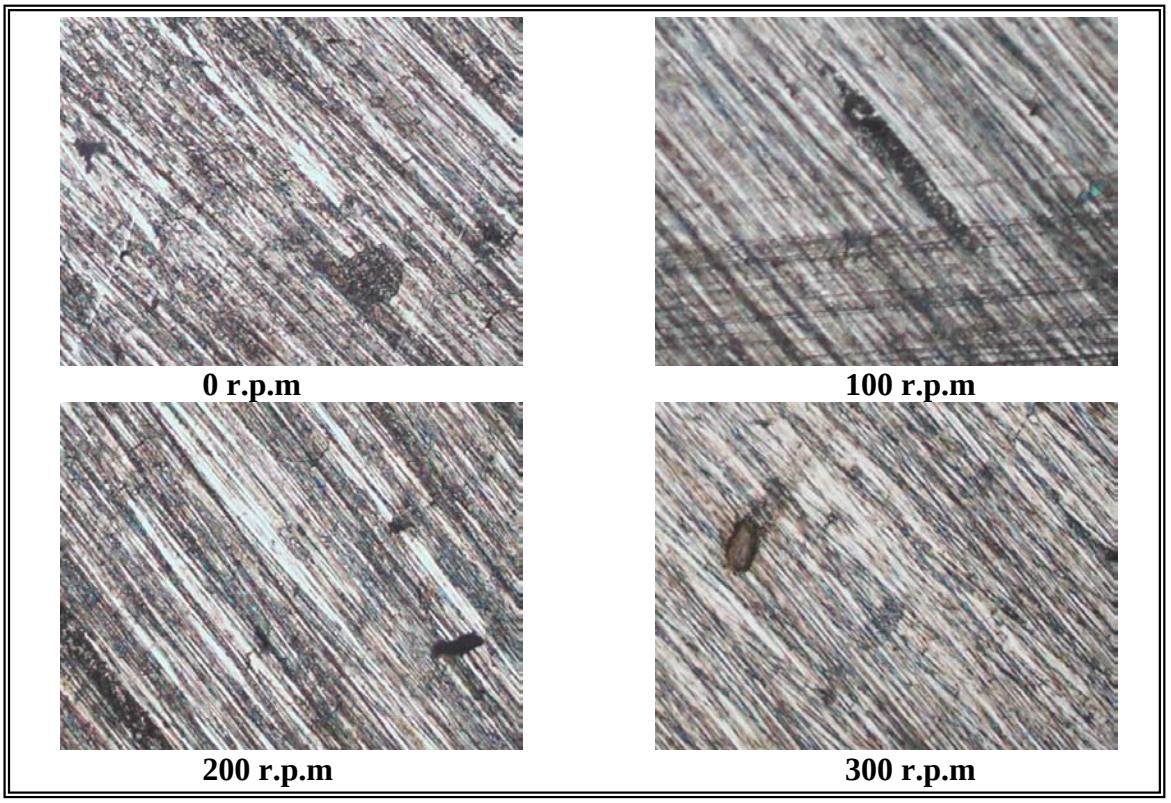

Fig. (5.49) 202 SS after potentiostatic polarization in 3.5% NaCl solutions at 298K, (270 X)

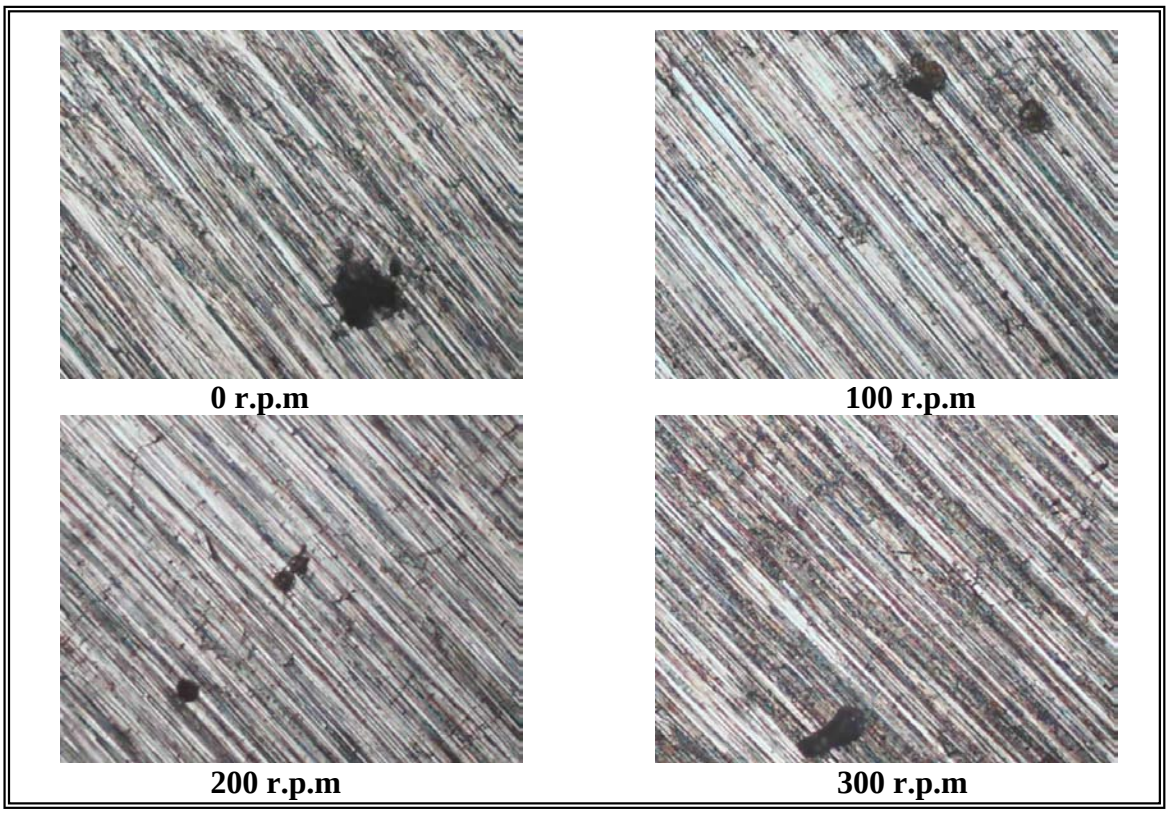

Fig. (5.50) 202 SS after potentiostatic polarization in 3.5% NaCl solutions at308K, (270 X)

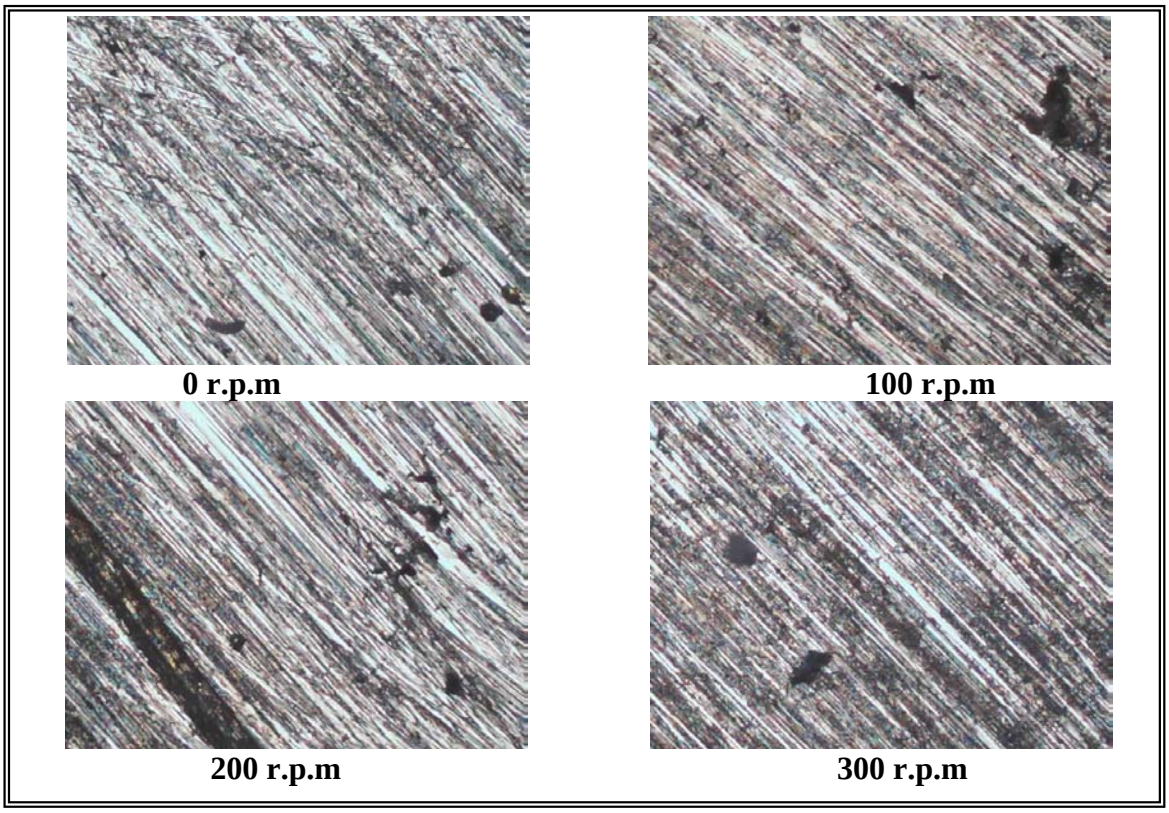

Fig. (5.51) 202 SS after potentiostatic polarization in 3.5% NaCl solutions at 318K, (270 X)

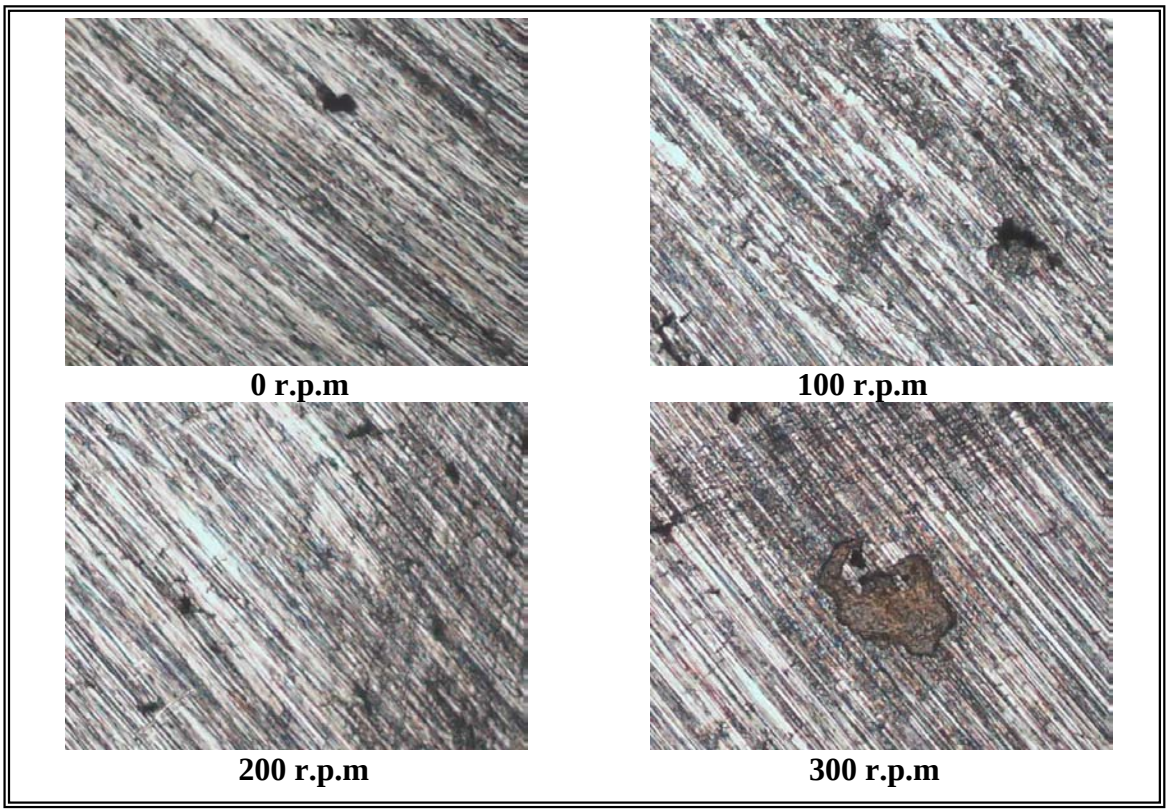

Fig. (5.52) 202 SS after potentiostatic polarization in 2.5% NaCl solutions at 298K, (270 X)

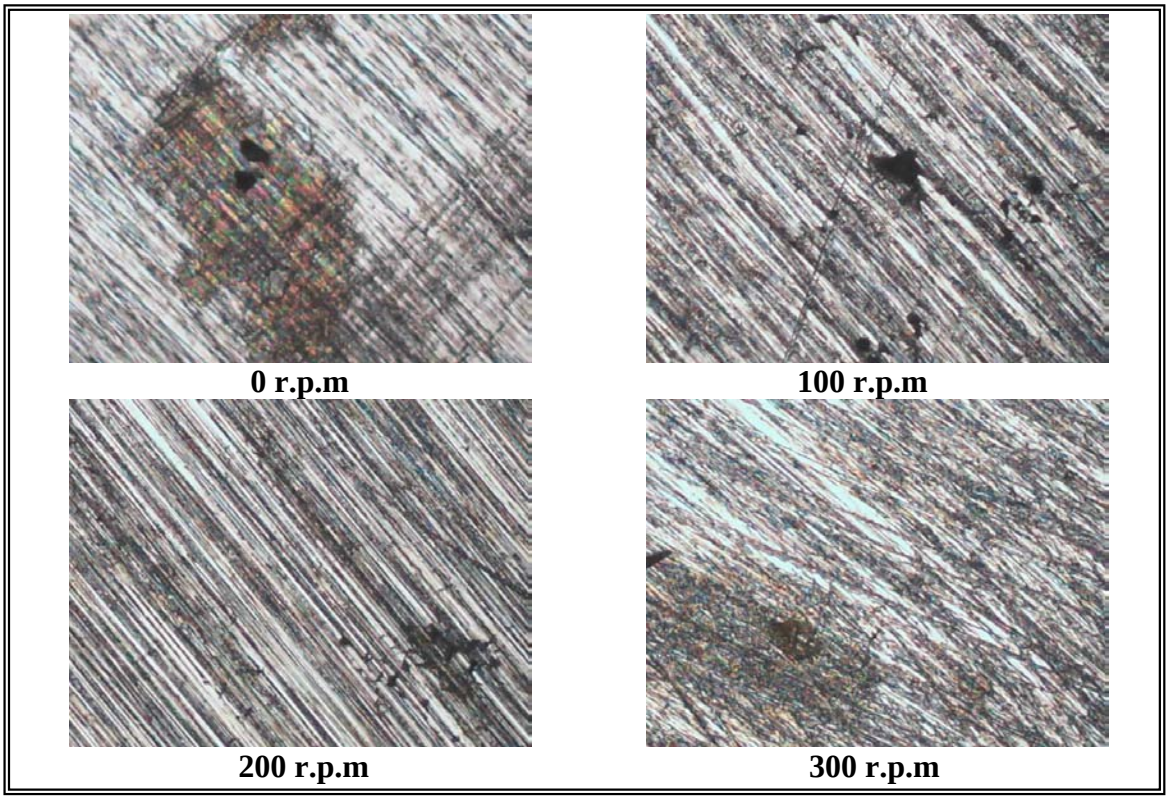

Fig. (5.53) 202 SS after potentiostatic polarization in 2.5% NaCl solutions at 308K, (270 X)

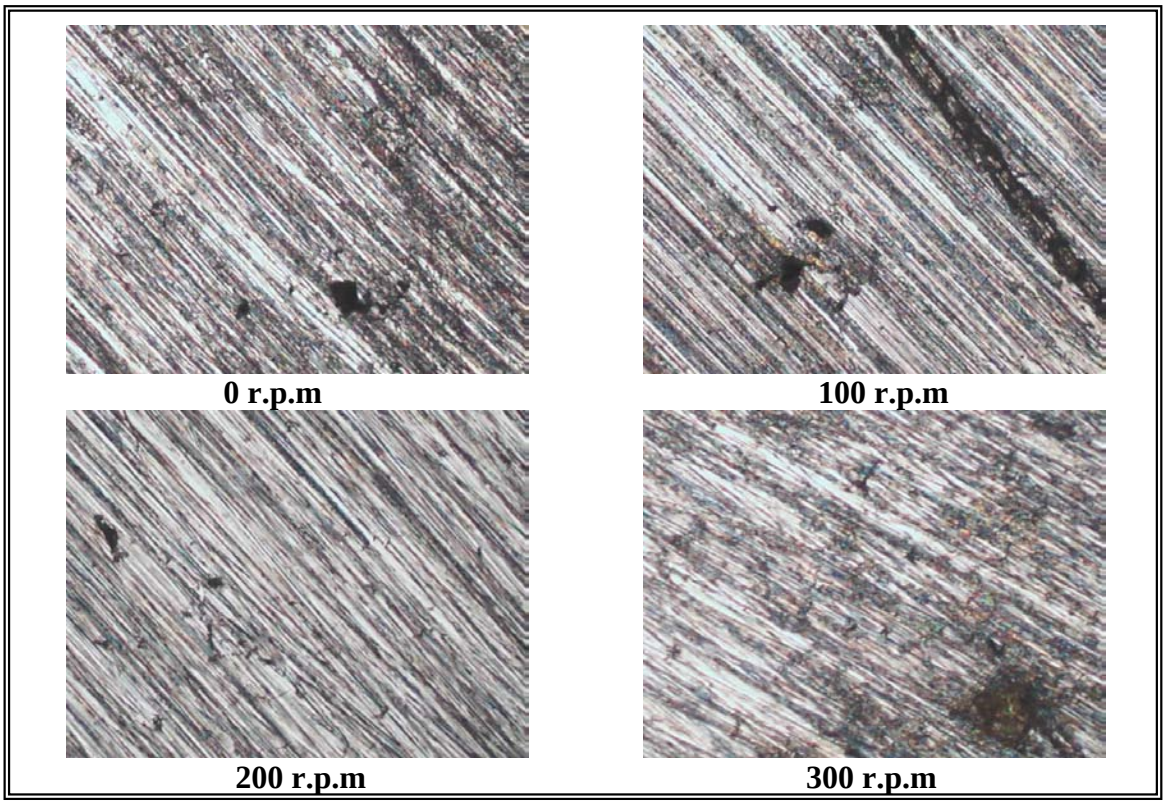

Fig. (5.54) 202 SS after potentiostatic polarization in 2.5% NaCl solutions at 318K, (270 X)

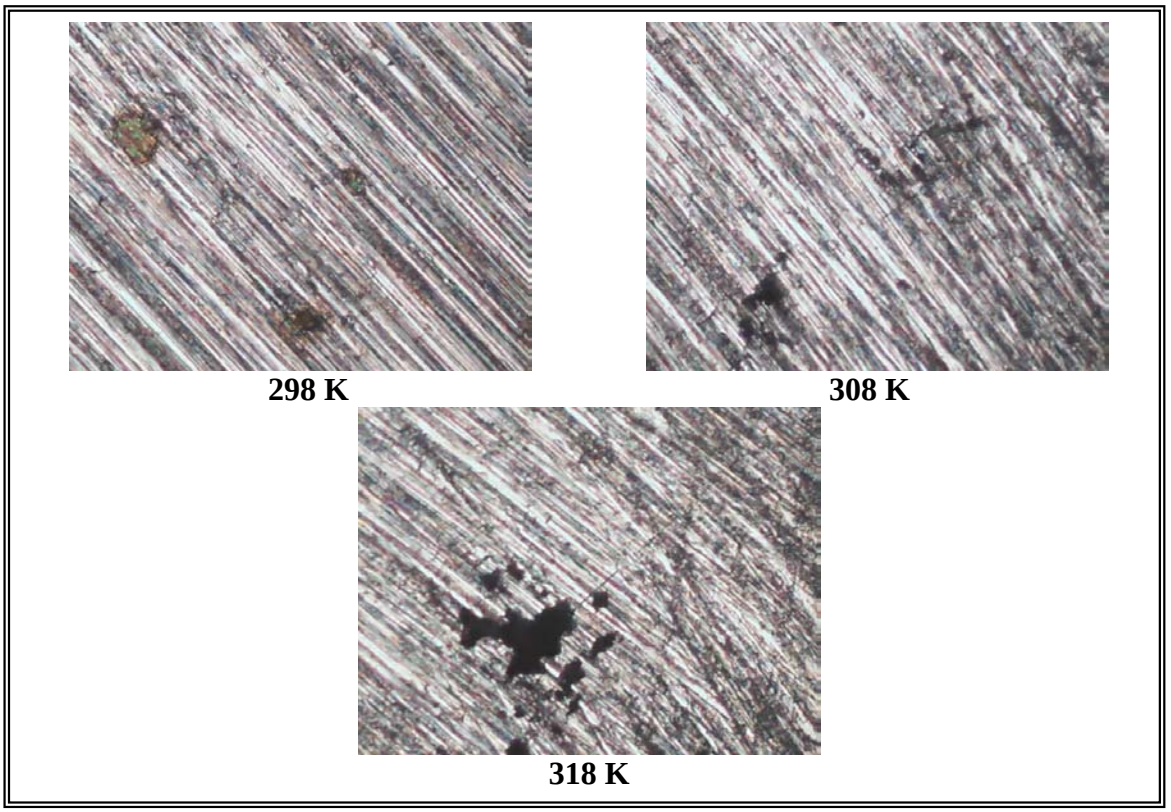

Fig. (5.55) 202 SS after potentiostatic polarization in 1.5% NaCl solutions at static condition, (270 X)

5.4 Comparison between 316L SS and 202 SS

From Figs. (B1-B27) Appendix B, and the results, it can be seen that the pitting corrosion resistance of 316L SS is higher than that of the 202 SS for all conditions in this study and the (E_{corr}.) of 316L SS is higher than that of 202 SS. Also the corrosion current density of 202 SS is higher than that of 316L SS, that means the latest metal (316L SS) has higher resistance to corrosion than 202 SS. The results for two metals can be attributed due to the difference in chemical compositions and the metallurgical structures between two alloys. These differences are according to the existence of (Cr, Ni, Mo) contents because they are the most alloying elements which have been found to affect pitting corrosion of SS.

The ratio of Cr for two types (316L and 202) of SS is approximately equal (16.7,17.3)wt% respectively (see Table 4.1). Stainless Steels basically derive their passive characteristics from alloying with Cr **(53).** Alloying iron with (Cr) shifts the primary passivation potential in the active direction. From Fig. (5.56), it could be noticed that as the Cr content increases, the pitting potential shifts to more noble value, since the Cr content of the two types of SS is in the range of (16.7-17.3) which has no great effect on the E_b.

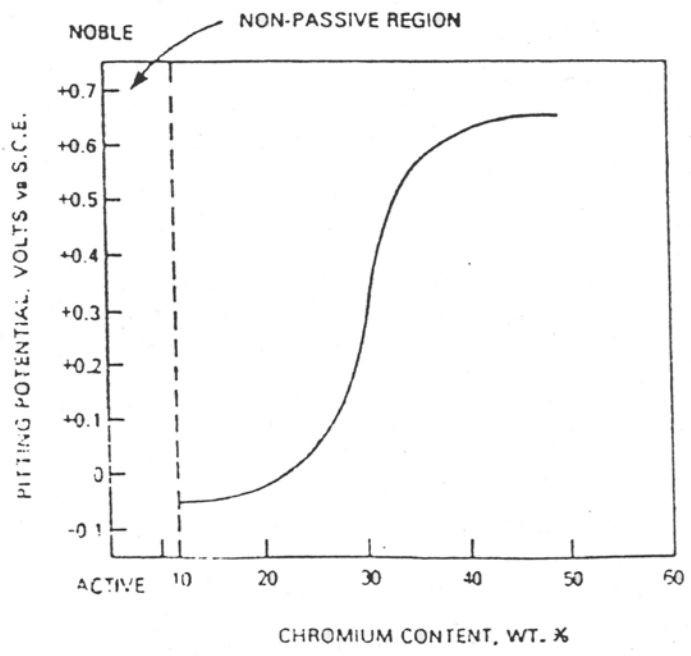

Fig,(5.56) Effect of Cr on pitting potential in Fe-Cr alloy in deareated 0.1N NaCl solution at 25 C. (73)

The composition of Ni for two types (316L & 202)of SS is equal to (10.2,4.1)wt% respectively (see Table 4.1).

It could be seen that the wt% of Ni in 316L SS is more than that of 202 SS, and that leads to increasing of the pitting potential i.e the addition of Ni increases the pitting resistance as shown in Fig (5.57).

However the breakdown potential of 202 SS is much lower than that of 316L SS because of the large difference in Ni content.

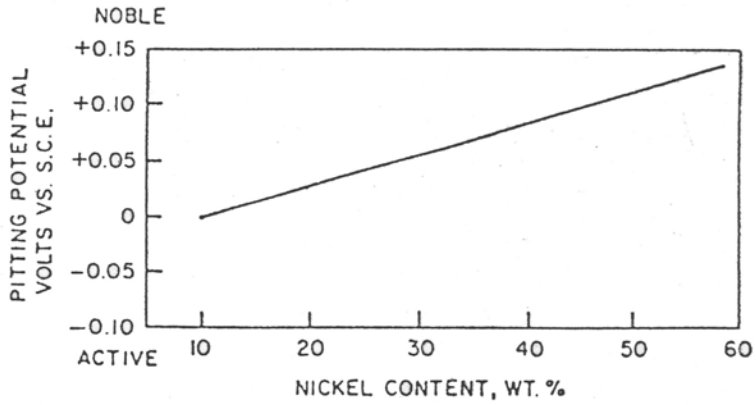

Fig.(5.57) Ni effect in Fe-15% Cr in 0.1N NaCl solution at 25 C.[73]

The addition of Mo to (Cr-Fe) alloys have strong beneficial influence on the passivity. Mo moves the pitting in the noble direction thus extending the passive region [53] as shown in fig. (5.58) .From Table (4.1) , it can be noticed that the wt% of Mo in 316L SS is more than that of 202 SS (2.0, 0.131) respectively. So that the breakdown potential of 316L SS is higher than that of 202 SS, moreover the range of passivity of 316L SS is higher than that of 202 SS as shown in the figures in(Appendix B).

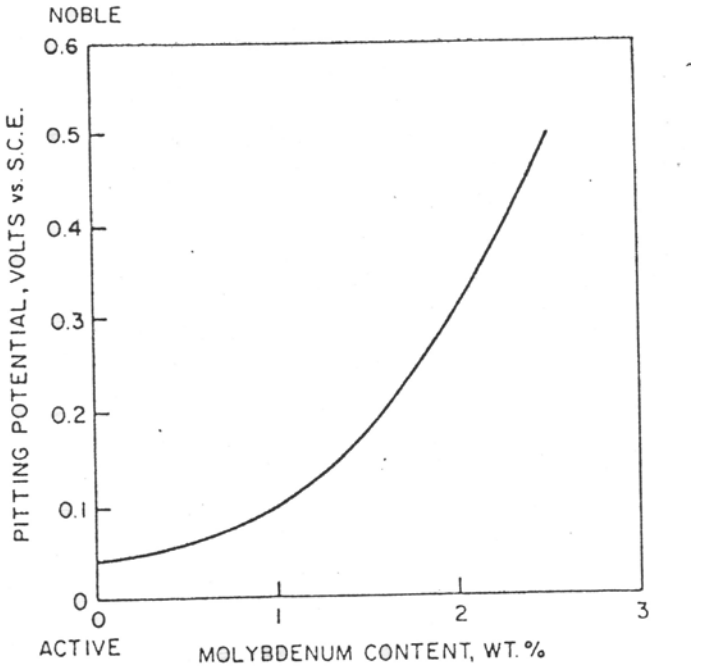

Fig.(5.58) Mo effect in Fe-13%Cr-15%Ni alloy in deareated 0.1N NaCl solution at 25C.[73]

Horvath and Uhlig [51] reported that the Mo existence is not always beneficial increasing the pitting resistance of SS, and they suggested that Mo effect depends on the type of SS, and the experimental conditions.

In summary the higher resistance of 316L SS than 202 SS is according to the alloying elements (Cr,Ni,Mo) which leads to high corrosion potential, long the passive region and higher pitting potential.

Chapter Six

Conclusions and Suggestions for Future Work

6.1 Conclusions

From the present study the following points can be concluded:

1. Pitting resistance of two types of SS (316L and 202) had a complex effect with different velocities of the solution (100,200and 300)r.p.m., the values of E_b at (0,100)r.p.m. goes to more noble direction. Above (200)r.p.m. E_b becomes independent on the velocity of the solution. The velocities are small effects on the corrosion current density($i_{corr.}$) at low concentration of NaCl solution. At 2.5%NaCl, the value of ($i_{corr.}$) is equal to (0.0014)mA/cm^2, while at 3.5%NaCl the ($i_{corr.}$) is equal to (0.0027)mA/cm^2.
2. For 316L SS, at room temperature and dynamic condition, the concentration of NaCl solution had effected on the E_b at different velocities of the solution. When the concentration of NaCl solution increases, E_b go to the noble direction. E_b=(-120,-160)mV at (2.5&3.5)%NaCl respectively in 298K.
3. For 316L SS, at room temperature (298)K and in static condition, E_b had independent on the concentration of NaCl solution(i.e E_b=-80mV) at (1.5,2.5and3.5)%NaCl, while at high temperatures E_b go to the active potential as the concentration of NaCl increases{i.e. E_b=(-80,-200,-220) at(1.5,2.5and3.5)%NaCl respectively.

4. For 316L, there is no clear effect of velocity on the E_b in different concentration of the solution at (2.5&3.5)%NaCl, whearse at constant velocity it had been a clear effect. At 100 r.p.m., the E_b go to the noble direction with increasing the concentration of NaCl solution.(E_b=-120, -60mV) respectively.

   The same effect have been obtained for 202 SS, i.e, as the velocity of the solution increase, E_b go to more noble. At different velocities the E_b go to more active as the concentration of NaCl solution increases. At 200 r.p.m.(E_b =-180,-220)mV at (2.5&3.5)%Nacl respectively while at 300 r.p.m. (E_b = -120,-220)mV at (2.5&3.5)%NaCl respectively.

5. The E_b has independent on the low values of scanning rates (10,15,20and30)mV/min., while at high scanning rate (40)mV/min. the passivation region clearly.

6.2 Suggestions for future work

The following suggestions are recommended for future work to study:

1. Similar work under dynamic conditions, using higher rotation speed (500-1000) r.p.m..
2. The effect of higher temperatures (50-100)ºC on the pitting corrosion under static conditions.
3. The effect of alloy elements in the pitting corrosion resistance, for example (304&304L) SS.
4. The influence of pH on the pitting corrosion under dynamic conditions may also been studied.

Appendix A

Potentiostatic Polarization Measured of (316L&L202)SS in NaCl solution

Table (A-1) Potentiostatic Polarization
Measured of (316L&202)SS at 298K & 0 r.p.m
in 3.5% NaCl solution

Time (min.)	Potential (mV)	316 L SS	202 SS
		Current Density (mA/cm^2)	Current Density (mA/cm^2)
1	-500	0.047	0.0329
2	-480	0.034	0.0127
3	-460	0.033	0.0095
4	-440	0.026	0.0059
5	-420	0.023	0.004
6	-400	0.015	0.0009
7	-380	0.01	0.002
8	-360	0.006	0.0044
9	-340	0.003	0.0057
10	-320	0.003	0.0079
11	-300	0.002	0.0102
12	-280	0.001	0.0111
13	-260	0.0003	0.012
14	-240	0.001	0.016
15	-220	0.002	0.03
16	-200	0.003	0.068
17	-180	0.003	0.322
18	-160	0.003	1.837
19	-140	0.003	5.273
20	-120	0.003	8.928
21	-100	0.003	12.11
22	-80	0.003	14.91
23	-60	0.005	17.4
24	-40	0.004	19.44
25	-20	0.005	21.01
26	0	0.007	22.34
27	20	0.011	24.56
28	40	0.016	27.35
29	60	0.019	28.93
30	80	0.027	30.15
31	100	0.033	31.32
32	120	0.043	32.35
33	140	0.055	34.56
34	160	0.07	36.78
35	180	0.1	38.67
36	200	0.13	40.35
37	220	0.175	42.77
38	240	0.229	44.18
39	260	0.305	47.55
40	280	0.412	
41	300	0.57	
42	320	0.785	
43	340	1.2104	
44	360	2.497	
45	380	5.105	
46	400	10.724	
47	420	18.118	
48	440	24.96	
49	460	31.05	
50	480	37.36	
51	500	42.4	

Table (A-2) Potentiostatic Polarizatic
of (316L&202)SS at 298K & 100 r.p
NaCl solution

Time (min.)	Potential (mV)	316 L SS
		Current Density (mA/cm^2)
1	-500	0.076
2	-480	0.052
3	-460	0.037
4	-440	0.024
5	-420	0.021
6	-400	0.016
7	-380	0.014
8	-360	0.009
9	-340	0.008
10	-320	0.0055
11	-300	0.004
12	-280	0.003
13	-260	0.0007
14	-240	0.0004
15	-220	0.0005
16	-200	0.0016
17	-180	0.003
18	-160	0.0031
19	-140	0.0035
20	-120	0.004
21	-100	0.0055
22	-80	0.0057
23	-60	0.0064
24	-40	0.0086
25	-20	0.012
26	0	0.017
27	20	0.024
28	40	0.033
29	60	0.043
30	80	0.06
31	100	0.076
32	120	0.095
33	140	0.115
34	160	0.146
35	180	0.186
36	200	0.262
37	220	0.371
38	240	0.51
39	260	0.682
40	280	0.863
41	300	1.102
42	320	1.41
43	340	1.72
44	360	2.08
45	380	2.485
46	400	2.87
47	420	3.42
48	440	4.04
49	460	4.81
50	480	5.53
51	500	6.3

ɔn Measured
ɔ.m in 3.5%

202 SS
Current Density (mA/cm^2)
0.0504
0.0308
0.0212
0.015
0.0102
0.008
0.0023
0.001
0.002
0.0039
0.0046
0.0053
0.0069
0.0092
0.015
0.032
0.089
0.289
1.439
4.695
9.987
11.375
11.859
18.218
20.642
24.829
28.53
28.82
30.08
30.85
35.64
36.14
36.93
40.31
42.22
42.55
48.24

Table (A-11) Potentiostatic Polarization Measured of (316L&202)SS at 318K & 200 r.p.m in 3.5% NaCl solution

Time (min.)	Potential (mV)	316 L SS Current Density (mA/cm^2)	202 SS Current Density (mA/cm^2)
1	-500	0.0995	0.096
2	-480	0.0829	0.077
3	-460	0.0566	0.049
4	-440	0.0371	0.03
5	-420	0.0266	0.019
6	-400	0.0256	0.0086
7	-380	0.01	0.00016
8	-360	0.0061	0.0053
9	-340	0.0045	0.0109
10	-320	0.0022	0.016
11	-300	0.00092	0.0215
12	-280	0.00054	0.0258
13	-260	0.00092	0.0313
14	-240	0.0034	0.0367
15	-220	0.0024	0.0451
16	-200	0.0036	0.0531
17	-180	0.004	0.0685
18	-160	0.0038	0.0893
19	-140	0.0046	0.13
20	-120	0.005	0.25
21	-100	0.0056	0.95
22	-80	0.0057	2.36
23	-60	0.0067	4.04
24	-40	0.011	6.44
25	-20	0.014	8.23
26	0	0.0195	10.5
27	20	0.036	11.35
28	40	0.0385	13.17
29	60	0.055	15.75
30	80	0.072	17.88
31	100	0.106	18.09
32	120	0.128	21.24
33	140	0.187	21.63
34	160	0.238	24.52
35	180	0.324	24.73
36	200	0.455	27.07
37	220	0.706	28.13
38	240	1.058	29.14
39	260	1.586	30.93
40	280	2.192	31.29
41	300	2.78	33.72
42	320	4.275	33.73
43	340	5.729	30.77
44	360	7.172	33.98
45	380	7.522	34.71
46	400	12.561	35.03
47	420	14.613	35.17
48	440	15.663	36.29
49	460	20.58	38.03
50	480	23.68	41.07
51	500	27.09	42

Table (A-12) Potentiostatic Pola Measured of (316L&202)SS at 318K in 3.5% NaCl solution

Time (min.)	Potential (mV)	316 L SS Current Density (mA/cm^2)
1	-500	0.123
2	-480	0.085
3	-460	0.058
4	-440	0.041
5	-420	0.03
6	-400	0.023
7	-380	0.018
8	-360	0.013
9	-340	0.009
10	-320	0.006
11	-300	0.004
12	-280	0.0023
13	-260	0.0005
14	-240	0.0009
15	-220	0.0017
16	-200	0.0034
17	-180	0.0042
18	-160	0.0057
19	-140	0.0091
20	-120	0.0129
21	-100	0.0179
22	-80	0.0214
23	-60	0.0256
24	-40	0.0289
25	-20	0.0332
26	0	0.0369
27	20	0.0432
28	40	0.0515
29	60	0.0601
30	80	0.0701
31	100	0.081
32	120	0.095
33	140	0.121
34	160	0.151
35	180	0.196
36	200	0.289
37	220	0.456
38	240	0.697
39	260	1.002
40	280	1.358
41	300	1.805
42	320	2.258
43	340	2.818
44	360	3.389
45	380	3.999
46	400	4.87
47	420	5.892
48	440	6.946
49	460	8.317
50	480	9.705
51	500	11.207

arization
. & 300 r.p.m

202 SS
Current Density (mA/cm^2)
0.158
0.102
0.0683
0.0409
0.024
0.0104
0.0027
0.0026
0.0073
0.0118
0.0165
0.0209
0.0266
0.033
0.042
0.0577
0.0789
0.135
0.278
0.795
2.488
4.925
7.61
10.293
12.37
13.98
16.04
17.46
19.29
21.36
22.48
24.19
25.71
26.24
26.37
26.36
27.58
28.44
30.07
30.99
31.85
33.7
35.25
37.32
39.33
41.63
43.75
45.94
47.24
49.91
51.2

Table (A-13) Potentiostatic Polarization Measured of (316L&202)SS at 298K & 0 r.p.m in 2.5% NaCl solution

Time (min.)	Potential (mV)	316 L SS	202 SS
		Current Density (mA/cm^2)	Current Density (mA/cm^2)
1	-500	0.054	0.024
2	-480	0.0422	0.017
3	-460	0.0313	0.013
4	-440	0.027	0.0092
5	-420	0.019	0.0063
6	-400	0.013	0.0036
7	-380	0.01	0.0012
8	-360	0.009	0.0006
9	-340	0.006	0.0026
10	-320	0.0042	0.0046
11	-300	0.0034	0.0061
12	-280	0.003	0.0085
13	-260	0.0012	0.0108
14	-240	0.0005	0.0123
15	-220	0.0007	0.0162
16	-200	0.0014	0.0216
17	-180	0.003	0.0429
18	-160	0.004	0.15
19	-140	0.005	0.825
20	-120	0.008	3.328
21	-100	0.0102	6.384
22	-80	0.0105	9.021
23	-60	0.0127	11.53
24	-40	0.0154	14.63
25	-20	0.02	17.11
26	0	0.0315	19.52
27	20	0.044	22
28	40	0.054	25.68
29	60	0.07	28.24
30	80	0.083	30.37
31	100	0.103	33.04
32	120	0.127	36.12
33	140	0.152	39.83
34	160	0.181	44.72
35	180	0.212	47.28
36	200	0.242	50.65
37	220	0.279	
38	240	0.329	
39	260	0.384	
40	280	0.472	
41	300	0.6	
42	320	0.865	
43	340	1.419	
44	360	2.725	
45	380	4.83	
46	400	8.85	
47	420	13.24	
48	440	17.79	
49	460	22.99	
50	480	28.99	
51	500	35.36	

Table (A-14) Potentiostatic Pola Measured of (316L&202)SS at 298K in 2.5% NaCl solution

Time (min.)	Potential (mV)	316 L SS
		Current Density (mA/cm^2)
1	-500	0.053
2	-480	0.039
3	-460	0.029
4	-440	0.0215
5	-420	0.017
6	-400	0.011
7	-380	0.0106
8	-360	0.0082
9	-340	0.0054
10	-320	0.0038
11	-300	0.0026
12	-280	0.0014
13	-260	0.0007
14	-240	0.0001
15	-220	0.0003
16	-200	0.0005
17	-180	0.0007
18	-160	0.0007
19	-140	0.0008
20	-120	0.0009
21	-100	0.0014
22	-80	0.0022
23	-60	0.0027
24	-40	0.0028
25	-20	0.0044
26	0	0.0047
27	20	0.0055
28	40	0.0078
29	60	0.0093
30	80	0.0129
31	100	0.0164
32	120	0.0207
33	140	0.0247
34	160	0.0309
35	180	0.037
36	200	0.0405
37	220	0.049
38	240	0.06
39	260	0.073
40	280	0.094
41	300	0.125
42	320	0.159
43	340	0.215
44	360	0.323
45	380	0.532
46	400	0.781
47	420	1.098
48	440	1.59
49	460	2.26
50	480	2.483
51	500	2.573

arization
. & 100 r.p.m

202 SS
Current Density (mA/cm^2)
0.05
0.0345
0.0258
0.0146
0.0109
0.0057
0.0025
0.00026
0.0031
0.0053
0.0064
0.009
0.011
0.0175
0.0204
0.0311
0.0535
0.1035
0.2522
0.737
3.1
5.398
8.585
11.108
13.897
17.789
20.337
20.54
24.895
25.85
29.963
30.54
32.624
33.913
34.836
37.342
37.953
38.813
40.594
43.46
46.25
48.8
52

Table (A-15) Potentiostatic Polarization Measured of (316L&202)SS at 298K & 200 r.p.m in 2.5% NaCl solution

Time (min.)	Potential (mV)	316 L SS	202 SS
		Current Density (mA/cm^2)	Current Density (mA/cm^2)
1	-500	0.0601	0.0618
2	-480	0.0418	0.0462
3	-460	0.032	0.0342
4	-440	0.0285	0.0235
5	-420	0.0196	0.0153
6	-400	0.0131	0.0091
7	-380	0.011	0.0039
8	-360	0.0079	0.0004
9	-340	0.0047	0.0035
10	-320	0.003	0.0055
11	-300	0.0012	0.0099
12	-280	0.0006	0.012
13	-260	0.0019	0.0145
14	-240	0.0022	0.0185
15	-220	0.0022	0.022
16	-200	0.0033	0.0288
17	-180	0.004	0.0346
18	-160	0.0042	0.0491
19	-140	0.0048	0.087
20	-120	0.005	0.209
21	-100	0.0053	0.505
22	-80	0.0054	1.29
23	-60	0.0056	3.23
24	-40	0.0058	5.8
25	-20	0.0076	8.39
26	0	0.0091	9.76
27	20	0.011	11.69
28	40	0.014	15.51
29	60	0.0176	17.64
30	80	0.021	18.7
31	100	0.025	20.59
32	120	0.03	23.95
33	140	0.037	25.78
34	160	0.042	27.48
35	180	0.047	29.07
36	200	0.053	30.26
37	220	0.058	30.46
38	240	0.063	30.79
39	260	0.073	32.43
40	280	0.083	33.09
41	300	0.099	34.14
42	320	0.118	36.46
43	340	0.16	38.12
44	360	0.25	39.64
45	380	0.4	44.23
46	400	0.65	48.14
47	420	1.1	49.33
48	440	1.65	52.24
49	460	2.34	
50	480	3.93	
51	500	6.21	

Table (A-16) Potentiostatic Pola Measured of (316L&202)SS at 298K in 2.5% NaCl solution

Time (min.)	Potential (mV)	316 L SS
		Current Density (mA/cm^2)
1	-500	0.053
2	-480	0.035
3	-460	0.0176
4	-440	0.011
5	-420	0.009
6	-400	0.0064
7	-380	0.0046
8	-360	0.0031
9	-340	0.002
10	-320	0.0006
11	-300	0.00005
12	-280	0.0002
13	-260	0.00037
14	-240	0.00042
15	-220	0.0009
16	-200	0.0013
17	-180	0.0015
18	-160	0.0018
19	-140	0.0023
20	-120	0.0029
21	-100	0.0029
22	-80	0.0029
23	-60	0.0033
24	-40	0.0035
25	-20	0.0043
26	0	0.005
27	20	0.006
28	40	0.0085
29	60	0.012
30	80	0.017
31	100	0.022
32	120	0.026
33	140	0.035
34	160	0.038
35	180	0.042
36	200	0.05
37	220	0.06
38	240	0.075
39	260	0.09
40	280	0.125
41	300	0.178
42	320	0.284
43	340	0.47
44	360	0.76
45	380	1.32
46	400	2.21
47	420	3.58
48	440	5.83
49	460	8.41
50	480	11.1
51	500	13.92

arization
. & 300 r.p.m

202 SS
Current Density (mA/cm^2)
0.0668
0.0429
0.036
0.021
0.013
0.0072
0.0028
0.00037
0.0018
0.0036
0.0055
0.0076
0.01
0.0114
0.0142
0.0169
0.0207
0.0255
0.0321
0.045
0.086
0.333
1.495
4.36
7.739
10.91
13.44
15.639
16.458
18.375
20.928
22.409
25.024
25.723
27.46
29.26
31.373
34.376
34.901
36.26
37.861
40.106
41.15
44.438
46.612
46.634
48.197
48.767
50.795

Table (A-17) Potentiostatic Polarization Measured of (316L&202)SS at 308K & 0 r.p.m in 2.5% NaCl solution

Time (min.)	Potential (mV)	316 L SS	202 SS
		Current Density (mA/cm^2)	Current Density (mA/cm^2)
1	-500	0.081	0.037
2	-480	0.053	0.028
3	-460	0.042	0.021
4	-440	0.033	0.0147
5	-420	0.026	0.0104
6	-400	0.02	0.0063
7	-380	0.013	0.0039
8	-360	0.0093	0.00099
9	-340	0.008	0.0012
10	-320	0.0043	0.0045
11	-300	0.0034	0.0071
12	-280	0.0016	0.0109
13	-260	0.0008	0.0153
14	-240	0.0004	0.0207
15	-220	0.001	0.0313
16	-200	0.0013	0.0408
17	-180	0.0021	0.0737
18	-160	0.004	0.338
19	-140	0.0057	3.15
20	-120	0.0108	10.74
21	-100	0.0157	18.16
22	-80	0.027	26.16
23	-60	0.038	33.19
24	-40	0.049	39.46
25	-20	0.062	45.68
26	0	0.073	51.87
27	20	0.095	
28	40	0.106	
29	60	0.132	
30	80	0.161	
31	100	0.187	
32	120	0.224	
33	140	0.275	
34	160	0.345	
35	180	0.468	
36	200	0.532	
37	220	0.748	
38	240	1.097	
39	260	1.44	
40	280	1.843	
41	300	2.33	
42	320	2.823	
43	340	3.364	
44	360	3.96	
45	380	4.65	
46	400	5.49	
47	420	6.29	
48	440	7.34	
49	460	8.71	
50	480	9.77	
51	500	11.63	

Table (A-18) Potentiostatic Pola Measured of (316L&202)SS at 308K in 2.5% NaCl solution

Time (min.)	Potential (mV)	316 L SS
		Current Density (mA/cm^2)
1	-500	0.086
2	-480	0.054
3	-460	0.041
4	-440	0.032
5	-420	0.026
6	-400	0.019
7	-380	0.013
8	-360	0.0098
9	-340	0.0073
10	-320	0.0046
11	-300	0.0034
12	-280	0.0014
13	-260	0.0007
14	-240	0.0004
15	-220	0.001
16	-200	0.0012
17	-180	0.0025
18	-160	0.0042
19	-140	0.0061
20	-120	0.011
21	-100	0.016
22	-80	0.027
23	-60	0.038
24	-40	0.049
25	-20	0.067
26	0	0.078
27	20	0.095
28	40	0.109
29	60	0.131
30	80	0.161
31	100	0.19
32	120	0.228
33	140	0.273
34	160	0.339
35	180	0.452
36	200	0.592
37	220	0.805
38	240	1.097
39	260	1.484
40	280	1.845
41	300	2.316
42	320	2.81
43	340	3.348
44	360	3.911
45	380	4.562
46	400	5.349
47	420	6.358
48	440	7.508
49	460	8.929
50	480	9.971
51	500	11.473

arization
. & 100 r.p.m

202 SS
Current Density (mA/cm^2)
0.077
0.0487
0.038
0.0256
0.0165
0.0084
0.0005
0.0056
0.0111
0.0168
0.0252
0.0319
0.0426
0.0546
0.0672
0.089
0.13
0.296
1.225
3.858
6.669
9.05
11.394
13.365
15.231
17.29
18.61
20.6
23.98
25.96
28.93
31.86
33.88
35.76
37.135
40.43
43.53
46.21
48.21
48.6
51.49
52.8

Table (A-19) Potentiostatic Polarization
Measured of (316L&202)SS at308K & 200 r.p.m
in 2.5% NaCl solution

Time (min.)	Potential (mV)	316 L SS	202 SS
		Current Density (mA/cm^2)	Current Density (mA/cm^2)
1	-500	0.064	0.102
2	-480	0.038	0.072
3	-460	0.02	0.045
4	-440	0.018	0.032
5	-420	0.015	0.017
6	-400	0.01	0.0092
7	-380	0.007	0.0011
8	-360	0.004	0.0029
9	-340	0.0025	0.0053
10	-320	0.0007	0.0077
11	-300	0.0009	0.0109
12	-280	0.0021	0.0127
13	-260	0.0026	0.015
14	-240	0.0037	0.018
15	-220	0.0048	0.0236
16	-200	0.005	0.034
17	-180	0.0051	0.0544
18	-160	0.0053	0.127
19	-140	0.0068	0.543
20	-120	0.0069	2.384
21	-100	0.007	4.504
22	-80	0.0076	7.087
23	-60	0.0083	9.16
24	-40	0.0088	11.96
25	-20	0.0099	13.39
26	0	0.0107	14.98
27	20	0.012	16.77
28	40	0.013	18.07
29	60	0.015	19.58
30	80	0.0152	20.95
31	100	0.017	23.05
32	120	0.02	24.59
33	140	0.024	27.88
34	160	0.031	30.88
35	180	0.042	33.89
36	200	0.059	35.85
37	220	0.094	37.33
38	240	0.15	39.35
39	260	0.225	40.29
40	280	0.45	42.26
41	300	1.04	42.92
42	320	2.275	45.25
43	340	4.45	46.4
44	360	7.3	47.34
45	380	10.46	49.61
46	400	13.7	
47	420	16.51	
48	440	19.5	
49	460	22.69	
50	480	24.71	
51	500	27.3	

Table (A-20) Potentiostatic Pola
Measured of (316L&202)SS at 308K
in 2.5% NaCl solution

Time (min.)	Potential (mV)	316 L SS
		Current Density (mA/cm^2)
1	-500	0.108
2	-480	0.057
3	-460	0.038
4	-440	0.03
5	-420	0.018
6	-400	0.013
7	-380	0.0046
8	-360	0.0033
9	-340	0.0032
10	-320	0.0031
11	-300	0.0026
12	-280	0.0009
13	-260	0.0007
14	-240	0.0003
15	-220	0.0004
16	-200	0.0006
17	-180	0.0012
18	-160	0.0013
19	-140	0.0024
20	-120	0.0026
21	-100	0.003
22	-80	0.0033
23	-60	0.004
24	-40	0.0047
25	-20	0.0056
26	0	0.0063
27	20	0.0076
28	40	0.0092
29	60	0.012
30	80	0.015
31	100	0.02
32	120	0.027
33	140	0.035
34	160	0.042
35	180	0.056
36	200	0.073
37	220	0.097
38	240	0.12
39	260	0.14
40	280	0.18
41	300	0.28
42	320	0.49
43	340	0.9
44	360	1.88
45	380	3.79
46	400	6.46
47	420	9.63
48	440	12.28
49	460	15.55
50	480	17.7
51	500	20.62

arization
. & 300 r.p.m

202 SS
Current Density (mA/cm^2)
0.137
0.102
0.063
0.04
0.025
0.015
0.0108
0.0023
0.0029
0.006
0.0104
0.016
0.024
0.0266
0.0425
0.0718
0.117
0.223
0.504
1.198
2.776
4.848
7.095
8.93
10.53
13.47
16.09
17.51
19.64
21.34
22.94
25.12
28.41
32.57
33.59
35.06
35.77
37.8
39.28
40.46
43.49
44.04
45.39
49.55
51.79

Table (A-21) Potentiostatic Polarization Measured of (316L&202)SS at318K & 0 r.p.m in 2.5% NaCl solution

Time (min.)	Potential (mV)	316 L SS	202 SS
		Current Density (mA/cm^2)	Current Density (mA/cm^2)
1	-500	0.0841	0.053
2	-480	0.0528	0.042
3	-460	0.04	0.034
4	-440	0.03	0.03
5	-420	0.024	0.021
6	-400	0.021	0.017
7	-380	0.014	0.011
8	-360	0.0107	0.005
9	-340	0.0074	0.0006
10	-320	0.0043	0.002
11	-300	0.0029	0.006
12	-280	0.0008	0.0085
13	-260	0.0002	0.013
14	-240	0.0013	0.019
15	-220	0.0016	0.028
16	-200	0.0017	0.063
17	-180	0.0028	0.3
18	-160	0.0034	2.09
19	-140	0.0046	5.67
20	-120	0.0053	8.11
21	-100	0.0074	10.44
22	-80	0.0091	12.41
23	-60	0.0107	14.58
24	-40	0.012	16.44
25	-20	0.015	18.47
26	0	0.017	21.22
27	20	0.019	25.47
28	40	0.021	27.88
29	60	0.025	30.32
30	80	0.031	32.84
31	100	0.038	36.08
32	120	0.049	37.9
33	140	0.073	42.96
34	160	0.163	49.68
35	180	0.368	
36	200	0.766	
37	220	1.28	
38	240	2.544	
39	260	4.55	
40	280	6.73	
41	300	9.3	
42	320	13.13	
43	340	16.81	
44	360	20.19	
45	380	25.97	
46	400	28.78	
47	420	33.85	
48	440	37.81	
49	460	42.56	
50	480		
51	500		

Table (A-22) Potentiostatic Pola Measured of (316L&202)SS at318K in 2.5% NaCl solution

Time (min.)	Potential (mV)	316 L SS
		Current Density (mA/cm^2)
1	-500	0.119
2	-480	0.083
3	-460	0.063
4	-440	0.043
5	-420	0.03
6	-400	0.021
7	-380	0.016
8	-360	0.0098
9	-340	0.005
10	-320	0.0034
11	-300	0.002
12	-280	0.0002
13	-260	0.0001
14	-240	0.0013
15	-220	0.0014
16	-200	0.0025
17	-180	0.003
18	-160	0.0035
19	-140	0.0037
20	-120	0.0042
21	-100	0.0043
22	-80	0.0049
23	-60	0.005
24	-40	0.0058
25	-20	0.0063
26	0	0.0074
27	20	0.0108
28	40	0.012
29	60	0.017
30	80	0.025
31	100	0.038
32	120	0.051
33	140	0.086
34	160	0.096
35	180	0.149
36	200	0.256
37	220	0.425
38	240	0.761
39	260	1.35
40	280	2.61
41	300	4.54
42	320	6.91
43	340	9.92
44	360	12.77
45	380	15.06
46	400	17.44
47	420	20.16
48	440	22.4
49	460	24.85
50	480	28.72
51	500	29.14

ɪrization
& 100 r.p.m

202 SS
Current Density (mA/cm^2)
0.0775
0.051
0.036
0.0225
0.0173
0.009
0.0046
0.0002
0.0037
0.0078
0.015
0.018
0.025
0.032
0.046
0.072
0.118
0.271
0.741
2.85
5.21
8.04
11.42
11.77
13.42
17.09
17.58
19.39
22
23.44
25.03
28.06
30.7
32.27
33.77
35.94
37.8
39.73
43.3
44.54
45.95
47.06
51.3
51.79

Table (A-23) Potentiostatic Polarization Measured of (316L&202)SS at 318K & 200 r.p.m in 2.5% NaCl solution

Time (min.)	Potential (mV)	316 L SS	202 SS
		Current Density (mA/cm^2)	Current Density (mA/cm^2)
1	-500	0.115	0.0928
2	-480	0.078	0.063
3	-460	0.068	0.034
4	-440	0.047	0.031
5	-420	0.034	0.021
6	-400	0.0165	0.011
7	-380	0.0109	0.0036
8	-360	0.0064	0.0046
9	-340	0.0021	0.013
10	-320	0.0012	0.0169
11	-300	0.0004	0.0197
12	-280	0.0012	0.023
13	-260	0.0032	0.0315
14	-240	0.0056	0.038
15	-220	0.0069	0.053
16	-200	0.0084	0.093
17	-180	0.0099	0.133
18	-160	0.012	0.377
19	-140	0.015	2.339
20	-120	0.018	5.997
21	-100	0.022	9.39
22	-80	0.025	12.03
23	-60	0.032	14.92
24	-40	0.037	16.99
25	-20	0.045	18.89
26	0	0.057	21.56
27	20	0.069	23.45
28	40	0.092	24.42
29	60	0.11	26.99
30	80	0.13	27.86
31	100	0.163	31.63
32	120	0.188	34.66
33	140	0.214	36.37
34	160	0.241	37.18
35	180	0.299	39.95
36	200	0.377	39.99
37	220	0.558	40.38
38	240	0.885	42.68
39	260	1.633	43.89
40	280	2.87	45.36
41	300	5.25	46.98
42	320	8.11	48.59
43	340	10.95	52.38
44	360	13.6	
45	380	16.76	
46	400	18.55	
47	420	20.65	
48	440	23.5	
49	460	25.89	
50	480	27.25	
51	500	30.19	

Table (A-24) Potentiostatic Pola Measured of (316L&202)SS at 318K in 2.5% NaCl solution

Time (min.)	Potential (mV)	316 L SS
		Current Density (mA/cm^2)
1	-500	0.11
2	-480	0.072
3	-460	0.051
4	-440	0.034
5	-420	0.025
6	-400	0.017
7	-380	0.015
8	-360	0.008
9	-340	0.0047
10	-320	0.0032
11	-300	0.0005
12	-280	0.00021
13	-260	0.0006
14	-240	0.0014
15	-220	0.0022
16	-200	0.0025
17	-180	0.0025
18	-160	0.0037
19	-140	0.0038
20	-120	0.004
21	-100	0.0047
22	-80	0.0049
23	-60	0.0055
24	-40	0.0056
25	-20	0.0069
26	0	0.0085
27	20	0.01
28	40	0.012
29	60	0.014
30	80	0.017
31	100	0.021
32	120	0.031
33	140	0.046
34	160	0.072
35	180	0.126
36	200	0.227
37	220	0.435
38	240	0.772
39	260	1.216
40	280	2.14
41	300	3.48
42	320	5.22
43	340	7.76
44	360	10.14
45	380	12.42
46	400	14.88
47	420	16.89
48	440	19.07
49	460	20.92
50	480	22.63
51	500	24.89

arization
. & 300 r.p.m

202 SS
Current Density (mA/cm^2)
0.145
0.099
0.067
0.045
0.029
0.016
0.0061
0.0007
0.007
0.013
0.0186
0.0246
0.032
0.04
0.048
0.0606
0.085
0.155
0.497
2.383
5.72
8.95
11.03
13.48
16.05
18.01
19.93
21.62
23.47
25.01
27.38
30.57
32.54
34.17
36.46
38.16
40.14
42.26
44.21
46.2
46.28
50.15
50.84
51.53
52.85

Table (A-25) Potentiostatic Polarization
Measured of (316L&202)SS at 298K & 0 r.p.m
in 1.5% NaCl solution

Time (min.)	Potential (mV)	316 L SS	202 SS
		Current Density (mA/cm^2)	Current Density (mA/cm^2)
1	-500	0.046	0.0301
2	-480	0.027	0.0211
3	-460	0.02	0.0135
4	-440	0.01	0.0115
5	-420	0.0095	0.0096
6	-400	0.0092	0.0076
7	-380	0.0072	0.0035
8	-360	0.0053	0.0023
9	-340	0.0036	0.00048
10	-320	0.001	0.0029
11	-300	0.00021	0.0055
12	-280	0.0011	0.0095
13	-260	0.0019	0.013
14	-240	0.0038	0.0183
15	-220	0.0045	0.024
16	-200	0.0056	0.0333
17	-180	0.0053	0.0425
18	-160	0.0057	0.073
19	-140	0.006	0.138
20	-120	0.0061	0.283
21	-100	0.0062	0.856
22	-80	0.0063	2.287
23	-60	0.0073	4.88
24	-40	0.009	8.86
25	-20	0.015	12.85
26	0	0.016	16.35
27	20	0.018	19.89
28	40	0.019	23.61
29	60	0.026	27.38
30	80	0.035	30.67
31	100	0.046	33.1
32	120	0.06	35.24
33	140	0.078	37.01
34	160	0.099	37.98
35	180	0.125	32.25
36	200	0.151	28.27
37	220	0.187	32.73
38	240	0.228	39.13
39	260	0.273	43.94
40	280	0.385	50.93
41	300	0.745	
42	320	1.435	
43	340	2.46	
44	360	4.11	
45	380	6.31	
46	400	8.82	
47	420	10.92	
48	440	14.87	
49	460	17.84	
50	480	19.37	
51	500	20.54	

Table (A-26) Potentiostatic Pola
Measured of (316L&202)SS at 308K
1.5% NaCl solution

Time (min.)	Potential (mV)	316 L SS
		Current Density (mA/cm^2)
1	-500	0.051
2	-480	0.039
3	-460	0.032
4	-440	0.03
5	-420	0.021
6	-400	0.017
7	-380	0.014
8	-360	0.011
9	-340	0.006
10	-320	0.004
11	-300	0.0006
12	-280	0.0007
13	-260	0.0009
14	-240	0.001
15	-220	0.0011
16	-200	0.0012
17	-180	0.0032
18	-160	0.0032
19	-140	0.0034
20	-120	0.0035
21	-100	0.0037
22	-80	0.0054
23	-60	0.0063
24	-40	0.0103
25	-20	0.013
26	0	0.016
27	20	0.02
28	40	0.024
29	60	0.029
30	80	0.034
31	100	0.039
32	120	0.044
33	140	0.052
34	160	0.06
35	180	0.07
36	200	0.085
37	220	0.105
38	240	0.138
39	260	0.222
40	280	0.368
41	300	0.683
42	320	1.296
43	340	2.29
44	360	4.02
45	380	6.24
46	400	8.7
47	420	10.66
48	440	14.53
49	460	17.6
50	480	19.32
51	500	20.33

arization
& 0 r.p.m in

202 SS
Current Density (mA/cm^2)
0.062
0.0417
0.0385
0.032
0.023
0.0184
0.0128
0.0075
0.004
0.0007
0.0036
0.0055
0.0093
0.0125
0.0151
0.0188
0.0215
0.025
0.031
0.038
0.067
0.195
1.29
4.01
7.3
10.3
12.97
15.32
20.37
22.18
24.86
27.52
28.6
29.83
30.85
34.43
37.81
43.31
39.11
45.26

Table (A-27) Potentiostatic Polarization
Measured of (316L&202)SS at 318K & 0 r.p.m
in 1.5% NaCl solution

Time (min.)	Potential (mV)	316 L SS	202 SS
		Current Density (mA/cm^2)	Current Density (mA/cm^2)
1	-500	0.104	0.0512
2	-480	0.064	0.0484
3	-460	0.058	0.0364
4	-440	0.041	0.0329
5	-420	0.033	0.0228
6	-400	0.021	0.011
7	-380	0.015	0.01
8	-360	0.009	0.005
9	-340	0.0009	0.0006
10	-320	0.008	0.0005
11	-300	0.019	0.004
12	-280	0.029	0.0056
13	-260	0.041	0.0066
14	-240	0.048	0.0094
15	-220	0.051	0.011
16	-200	0.052	0.0125
17	-180	0.05	0.015
18	-160	0.052	0.018
19	-140	0.056	0.023
20	-120	0.055	0.0417
21	-100	0.056	0.116
22	-80	0.059	0.429
23	-60	0.063	1.092
24	-40	0.073	2.44
25	-20	0.08	4.22
26	0	0.1	6.32
27	20	0.13	8.61
28	40	0.166	11.61
29	60	0.212	12.63
30	80	0.265	19.15
31	100	0.338	25.46
32	120	0.411	30.68
33	140	0.495	36.16
34	160	0.603	41.08
35	180	0.714	43.48
36	200	0.86	45.31
37	220	1.015	44.91
38	240	1.23	36.08
39	260	1.48	47.57
40	280	1.784	
41	300	2.178	
42	320	2.622	
43	340	3.127	
44	360	3.65	
45	380	4.21	
46	400	4.72	
47	420	5.16	
48	440	7.95	
49	460	9.46	
50	480	11.09	
51	500	14.01	

Table (A-3) Potentiostatic Polarization Measured of (316L&202)SS at 298K &200 r.p.m in 3.5% NaCl solution

Time (min.)	Potential (mV)	316 L SS Current Density (mA/cm^2)	202 SS Current Density (mA/cm^2)
1	-500	0.07	0.0352
2	-480	0.052	0.0208
3	-460	0.039	0.0114
4	-440	0.025	0.0079
5	-420	0.019	0.0037
6	-400	0.014	0.0021
7	-380	0.007	0.0001
8	-360	0.0046	0.001
9	-340	0.0033	0.0016
10	-320	0.0025	0.0026
11	-300	0.0015	0.0027
12	-280	0.0007	0.0033
13	-260	0.0004	0.0046
14	-240	0.0011	0.0052
15	-220	0.0021	0.006
16	-200	0.0031	0.0105
17	-180	0.0044	0.0205
18	-160	0.0057	0.0644
19	-140	0.0066	0.484
20	-120	0.0098	2.428
21	-100	0.012	8.45
22	-80	0.0141	11.216
23	-60	0.0145	13.103
24	-40	0.0147	14.636
25	-20	0.015	20
26	0	0.0159	20.53
27	20	0.0207	24.59
28	40	0.0289	24.78
29	60	0.0345	30.4
30	80	0.0372	30.69
31	100	0.0428	34.64
32	120	0.0508	36.78
33	140	0.0529	37.57
34	160	0.07	37.79
35	180	0.091	39.04
36	200	0.124	40.28
37	220	0.147	42.27
38	240	0.163	45.22
39	260	0.209	
40	280	0.285	
41	300	0.407	
42	320	0.585	
43	340	0.776	
44	360	0.972	
45	380	1.18	
46	400	1.367	
47	420	1.569	
48	440	1.886	
49	460	2.128	
50	480	3.27	
51	500	4.03	

Table (A-4) Potentiostatic Polarization Measured of (316L&202)SS at 298K & 300 r.p.m in 3.5% NaCl solution

Time (min.)	Potential (mV)	316 L SS Current Density (mA/cm^2)	202 SS Current Density (mA/cm^2)
1	-500	0.066	0.046
2	-480	0.041	0.0301
3	-460	0.024	0.0193
4	-440	0.017	0.0111
5	-420	0.014	0.0062
6	-400	0.0092	0.0034
7	-380	0.0073	0.0009
8	-360	0.0041	0.0014
9	-340	0.0027	0.0021
10	-320	0.0025	0.0027
11	-300	0.0005	0.0036
12	-280	0.0003	0.0051
13	-260	0.0004	0.0057
14	-240	0.0014	0.0076
15	-220	0.0023	0.0102
16	-200	0.0034	0.0172
17	-180	0.0051	0.0328
18	-160	0.0068	0.0827
19	-140	0.01	0.345
20	-120	0.011	1.71
21	-100	0.0136	6.01
22	-80	0.0136	9.53
23	-60	0.0137	14.48
24	-40	0.0144	16.71
25	-20	0.0147	19.81
26	0	0.0155	21.42
27	20	0.0187	24.42
28	40	0.0205	26.22
29	60	0.0253	29.66
30	80	0.03	32.387
31	100	0.0326	34.92
32	120	0.0405	35.04
33	140	0.049	36.13
34	160	0.05	41.04
35	180	0.06	42.5
36	200	0.079	42.79
37	220	0.095	44.22
38	240	0.128	48.39
39	260	0.208	51.28
40	280	0.306	
41	300	0.443	
42	320	0.609	
43	340	0.793	
44	360	1.02	
45	380	1.26	
46	400	1.53	
47	420	1.795	
48	440	2.06	
49	460	2.328	
50	480	2.903	
51	500	3.383	

Table (A-5) Potentiostatic Polarization Measured of (316L&202)SS at 308K & 0 r.p.m in 3.5% NaCl solution

Time (min.)	Potential (mV)	316 L SS Current Density (mA/cm^2)	202 SS Current Density (mA/cm^2)
1	-500	0.053	0.0612
2	-480	0.0365	0.0417
3	-460	0.027	0.0344
4	-440	0.019	0.0233
5	-420	0.016	0.0189
6	-400	0.012	0.0117
7	-380	0.0102	0.0087
8	-360	0.008	0.002
9	-340	0.0053	0.0027
10	-320	0.0043	0.0064
11	-300	0.0028	0.01
12	-280	0.002	0.0178
13	-260	0.001	0.0263
14	-240	0.0006	0.0362
15	-220	0.00047	0.0457
16	-200	0.00042	0.063
17	-180	0.00057	0.0937
18	-160	0.00073	0.1787
19	-140	0.00078	0.572
20	-120	0.00083	2.184
21	-100	0.002	4.541
22	-80	0.0027	6.86
23	-60	0.0045	8.769
24	-40	0.006	10.604
25	-20	0.0087	12.128
26	0	0.0109	13.716
27	20	0.0146	15.182
28	40	0.0193	16.753
29	60	0.0272	19.133
30	80	0.034	23.54
31	100	0.047	26.33
32	120	0.0727	29.34
33	140	0.0807	32.28
34	160	0.0926	38.08
35	180	0.1199	41.68
36	200	0.149	46.52
37	220	0.223	49.7
38	240	0.361	
39	260	0.5922	
40	280	1.3	
41	300	3.408	
42	320	7.331	
43	340	12.84	
44	360	18.734	
45	380	25.93	
46	400	31.43	
47	420	37.615	
48	440	42.614	
49	460	48.07	
50	480		
51	500		

Table (A-6) Potentiostatic Polarization Measured of (316L&202)SS at 308K & 100 r.p.m in 3.5% NaCl solution

Time (min.)	Potential (mV)	316 L SS Current Density (mA/cm^2)	202 SS Current Density (mA/cm^2)
1	-500	0.086	0.0762
2	-480	0.0581	0.0589
3	-460	0.0558	0.0428
4	-440	0.0472	0.0319
5	-420	0.0408	0.0217
6	-400	0.0227	0.0137
7	-380	0.0161	0.0082
8	-360	0.0127	0.003
9	-340	0.0097	0.001
10	-320	0.0054	0.0049
11	-300	0.003	0.0076
12	-280	0.0026	0.0112
13	-260	0.00052	0.0153
14	-240	0.0001	0.0207
15	-220	0.0009	0.0282
16	-200	0.0012	0.0424
17	-180	0.0025	0.082
18	-160	0.0028	0.189
19	-140	0.005	0.777
20	-120	0.0057	2.49
21	-100	0.0084	5.25
22	-80	0.011	6.5
23	-60	0.012	7.55
24	-40	0.0123	9
25	-20	0.017	11.01
26	0	0.0196	12.37
27	20	0.024	14.07
28	40	0.0283	15.4
29	60	0.0365	16.62
30	80	0.0437	18.65
31	100	0.0472	19.22
32	120	0.059	20.76
33	140	0.08	22.29
34	160	0.1116	24.98
35	180	0.16	25.25
36	200	0.219	26.77
37	220	0.3687	29.52
38	240	0.502	32.07
39	260	0.687	34.87
40	280	0.941	36.75
41	300	1.01	41.45
42	320	1.672	42.49
43	340	2.139	43.78
44	360	2.543	48.33
45	380	2.602	
46	400	3.133	
47	420	3.834	
48	440	4.391	
49	460	5.152	
50	480	5.941	
51	500	7.26	

Table (A-7) Potentiostatic Polarization Measured of (316L&202)SS at 308K &200 r.p.m in 3.5% NaCl solution

Time (min.)	Potential (mV)	316 L SS Current Density (mA/cm^2)	202 SS Current Density (mA/cm^2)
1	-500	0.102	0.106
2	-480	0.07	0.083
3	-460	0.048	0.06
4	-440	0.037	0.044
5	-420	0.03	0.029
6	-400	0.027	0.015
7	-380	0.016	0.0056
8	-360	0.0094	0.0002
9	-340	0.01	0.0053
10	-320	0.004	0.0095
11	-300	0.0022	0.013
12	-280	0.0013	0.0159
13	-260	0.0018	0.0196
14	-240	0.0018	0.024
15	-220	0.0027	0.028
16	-200	0.0045	0.032
17	-180	0.0056	0.039
18	-160	0.0055	0.046
19	-140	0.0055	0.063
20	-120	0.007	0.119
21	-100	0.0072	0.425
22	-80	0.0089	1.709
23	-60	0.009	3.41
24	-40	0.0104	6.17
25	-20	0.0109	8.39
26	0	0.014	10.05
27	20	0.0162	12.29
28	40	0.021	14.09
29	60	0.025	16.6
30	80	0.03	18.05
31	100	0.035	19.61
32	120	0.043	21.29
33	140	0.053	23.09
34	160	0.0635	23.8
35	180	0.08	24.89
36	200	0.107	26.6
37	220	0.1606	27.42
38	240	0.287	28.54
39	260	0.49	29.59
40	280	0.94	31.27
41	300	1.92	31.33
42	320	3.16	32.91
43	340	4.826	34.34
44	360	7.86	34.47
45	380	11.5	36.03
46	400	14.14	39.25
47	420	16.36	40.05
48	440	21.85	41.18
49	460	22.83	42.22
50	480	25.87	45.4
51	500	27.66	46.55

Table (A-8) Potentiostatic Polarization Measured of (316L&202)SS at 308K & 300 r.p.m in 3.5% NaCl solution

Time (min.)	Potential (mV)	316 L SS Current Density (mA/cm^2)	202 SS Current Density (mA/cm^2)
1	-500	0.0896	0.104
2	-480	0.065	0.0818
3	-460	0.0462	0.0573
4	-440	0.0355	0.0437
5	-420	0.0225	0.0262
6	-400	0.0171	0.0164
7	-380	0.015	0.0085
8	-360	0.006	0.0004
9	-340	0.0028	0.0057
10	-320	0.0007	0.0133
11	-300	0.0002	0.0202
12	-280	0.0016	0.0266
13	-260	0.0023	0.0343
14	-240	0.0034	0.0423
15	-220	0.0043	0.0521
16	-200	0.0055	0.065
17	-180	0.0054	0.098
18	-160	0.0054	0.172
19	-140	0.0063	0.506
20	-120	0.0067	1.433
21	-100	0.0072	3.25
22	-80	0.0093	4.85
23	-60	0.0104	6.143
24	-40	0.0107	7.194
25	-20	0.0126	8.807
26	0	0.0153	10.311
27	20	0.0175	10.962
28	40	0.0213	11.23
29	60	0.025	11.89
30	80	0.029	12.45
31	100	0.034	12.88
32	120	0.0395	13.53
33	140	0.0481	14.67
34	160	0.058	14.98
35	180	0.0736	15.33
36	200	0.1	16.79
37	220	0.14	18.43
38	240	0.237	21.56
39	260	0.434	25.14
40	280	1.184	33.69
41	300	2.92	36.23
42	320	5.926	36.65
43	340	10.16	37.8
44	360	13.587	39.2
45	380	17.326	44.11
46	400	20.71	44.65
47	420	24.41	45.8
48	440	27.53	50.73
49	460	30.16	
50	480	33.8	
51	500	36.15	

Table (A-9) Potentiostatic Polarization
Measured of (316L&202)SS at 318K & 0 r.p.m
in 3.5% NaCl solution

Time (min.)	Potential (mV)	316 L SS	202 SS
		Current Density (mA/cm^2)	Current Density (mA/cm^2)
1	-500	0.0744	0.0538
2	-480	0.059	0.0439
3	-460	0.048	0.0326
4	-440	0.039	0.0251
5	-420	0.0301	0.0207
6	-400	0.0203	0.0203
7	-380	0.0136	0.0045
8	-360	0.0097	0.0009
9	-340	0.0093	0.005
10	-320	0.007	0.011
11	-300	0.0056	0.0177
12	-280	0.004	0.0233
13	-260	0.00042	0.0315
14	-240	0.00052	0.0446
15	-220	0.00063	0.0686
16	-200	0.00341	0.179
17	-180	0.0058	0.853
18	-160	0.0073	2.755
19	-140	0.0113	5.468
20	-120	0.0169	9.05
21	-100	0.0217	12.79
22	-80	0.0298	16.56
23	-60	0.033	19.2
24	-40	0.0408	22.24
25	-20	0.052	25.03
26	0	0.069	27.61
27	20	0.089	30.9
28	40	0.1178	33.14
29	60	0.1634	35.5
30	80	0.2363	37.6
31	100	0.3915	39.54
32	120	0.633	33.52
33	140	1.073	34.55
34	160	1.481	38.48
35	180	2.3373	45.36
36	200	4.46	
37	220	7.4	
38	240	11.86	
39	260	16	
40	280	20.21	
41	300	25.068	
42	320	29.81	
43	340	34.268	
44	360	38.836	
45	380	43.63	
46	400	48.69	
47	420		
48	440		
49	460		
50	480		
51	500		

Table (A-10) Potentiostatic Pola
Measured of (316L&202)SS at 318K
in 3.5% NaCl solution

Time (min.)	Potential (mV)	316 L SS
		Current Density (mA/cm^2)
1	-500	0.081
2	-480	0.075
3	-460	0.063
4	-440	0.06
5	-420	0.038
6	-400	0.028
7	-380	0.018
8	-360	0.0101
9	-340	0.0045
10	-320	0.0025
11	-300	0.0016
12	-280	0.0007
13	-260	0.0014
14	-240	0.0027
15	-220	0.0046
16	-200	0.0056
17	-180	0.0084
18	-160	0.0126
19	-140	0.0155
20	-120	0.02
21	-100	0.022
22	-80	0.023
23	-60	0.034
24	-40	0.036
25	-20	0.041
26	0	0.042
27	20	0.048
28	40	0.057
29	60	0.063
30	80	0.08
31	100	0.096
32	120	0.126
33	140	0.158
34	160	0.222
35	180	0.289
36	200	0.4
37	220	0.59
38	240	1.05
39	260	1.46
40	280	2.2
41	300	2.73
42	320	4.01
43	340	4.23
44	360	5.53
45	380	5.86
46	400	6.22
47	420	6.92
48	440	7.57
49	460	7.635
50	480	8.32
51	500	9.31

arization
. & 100 r.p.m

202 SS
Current Density (mA/cm^2)
0.129
0.0926
0.0693
0.0517
0.0375
0.0246
0.0108
0.0011
0.005
0.0106
0.016
0.023
0.0305
0.043
0.0688
0.111
0.246
0.853
2.68
5.875
10.677
11.43
14.57
17.62
19.687
22.115
23.148
26.5
27.59
29.91
30.28
33.1
35.8
36.17
38.49
39.63
38.74
34.6
36.22
39.28
41.66
43.07
45.38
46.79
47.37
49.98

Appendix B

Potentiostatic Curves of Two Types of Stainless Steels (316L & 202)

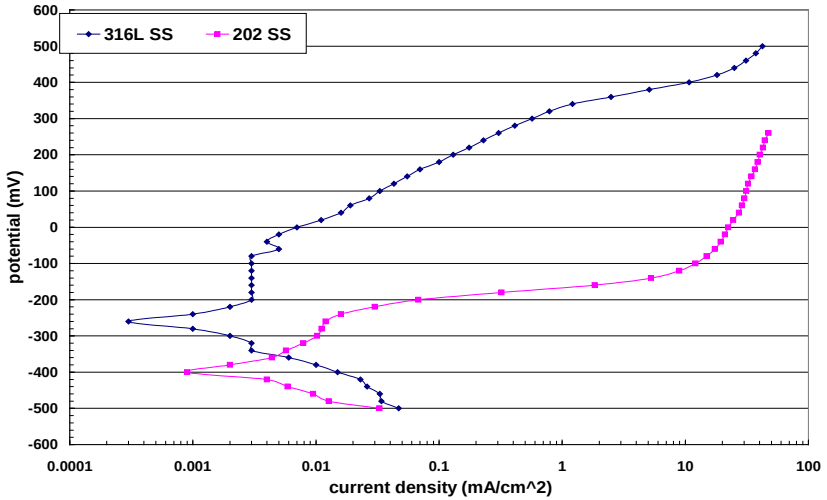

Fig.(B.1)polarization curves of two types of SS at 298k & 0 r.p.m. in 3.5%NaCl solution

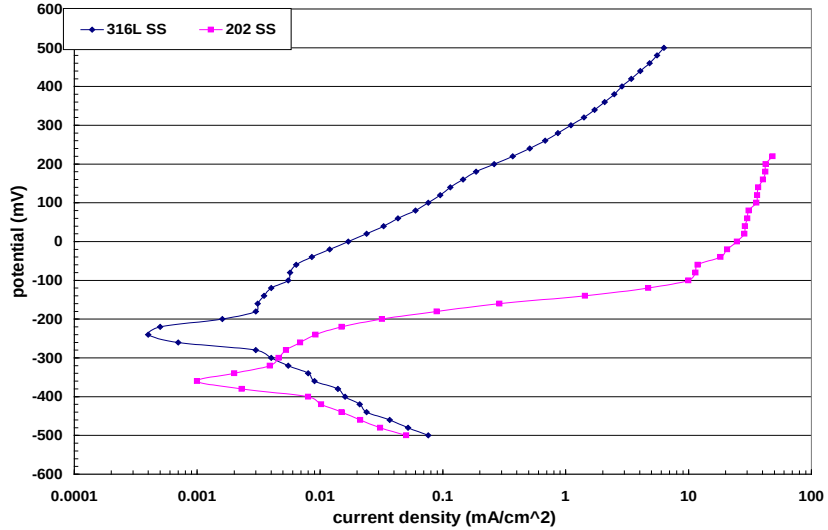

Fig.(B.2)polarization curves of two types of SS at 298k & 100 r.p.m. in 3.5%NaCl solution

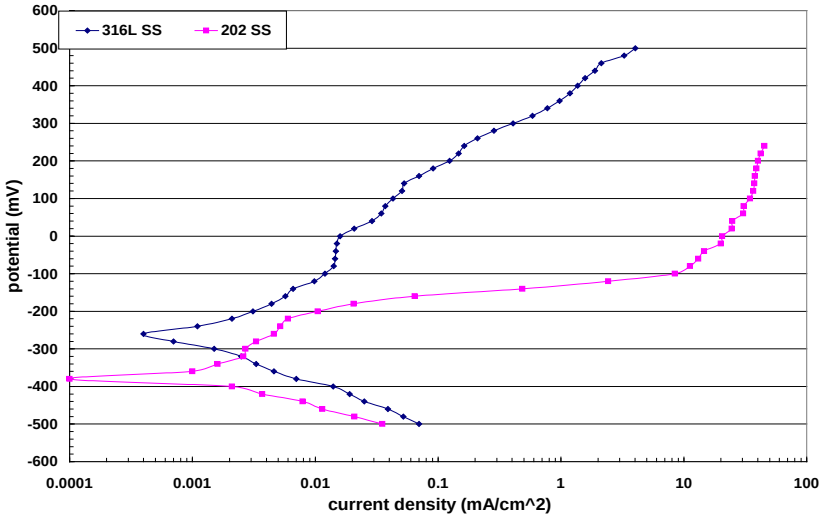

Fig.(B.3)polarization curves of two types of SS at 298k & 200 r.p.m. in 3.5%NaCl solution

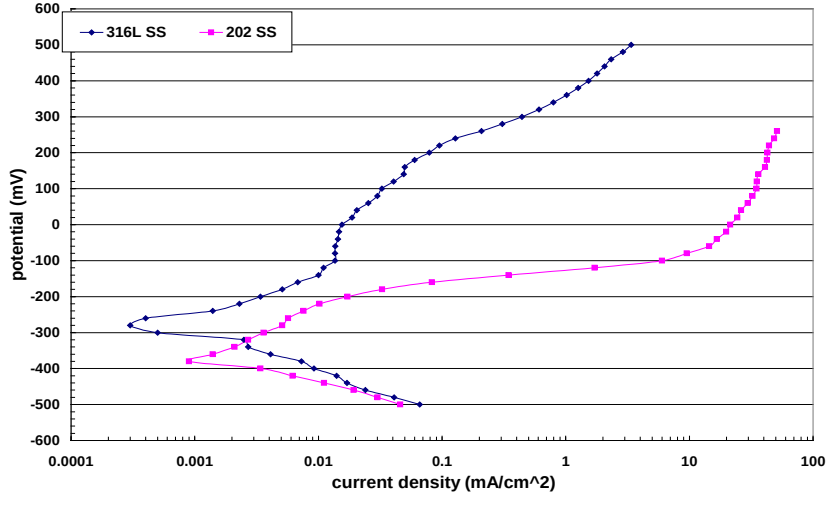

Fig.(B.4)polarization curves of two types of SS at 298k & 300 r.p.m. in 3.5%NaCl solution

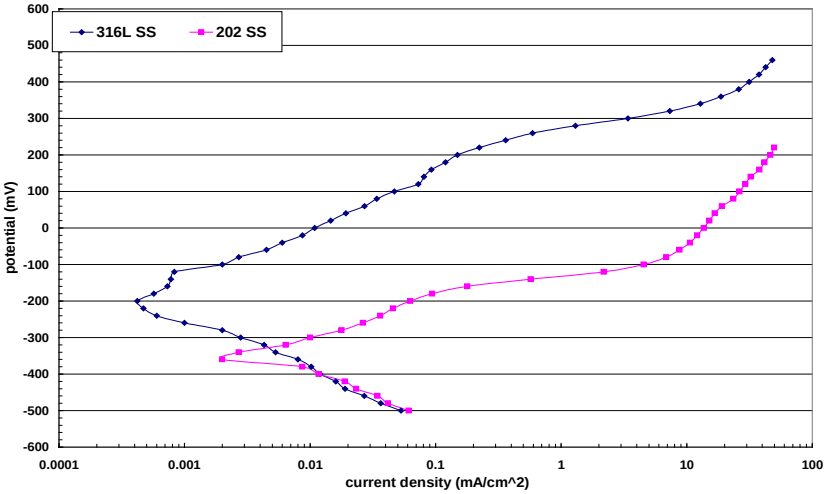

Fig.(B.5)polarization curves of two types of SS at 308k & 0 r.p.m. in 3.5%Nacl solution

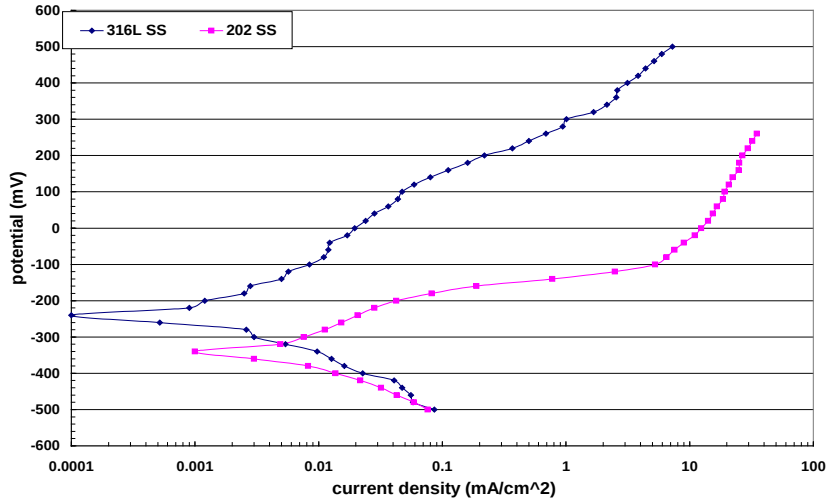

Fig.(B.6)polarization curves of two types of SS at 308k & 100 r.p.m. in 3.5%NaCl solution

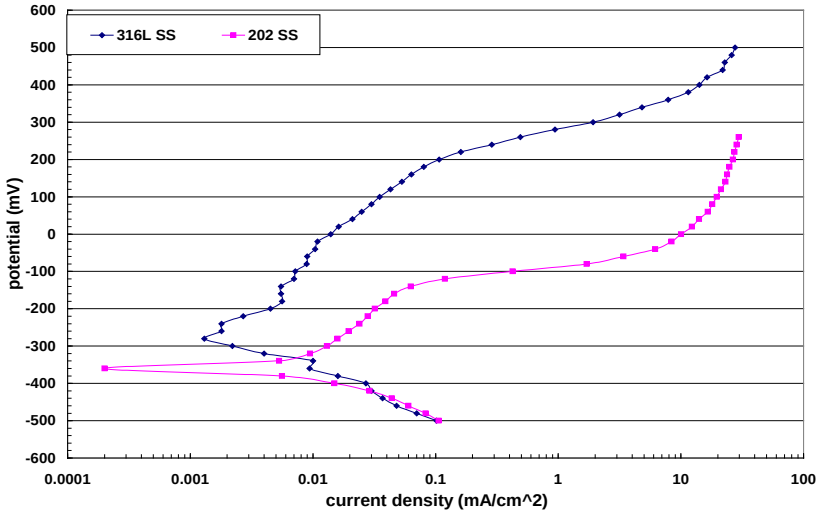

Fig.(B.7)polarization curves of two types of SS at 308k & 200 r.p.m. in 3.5%NaCl solution

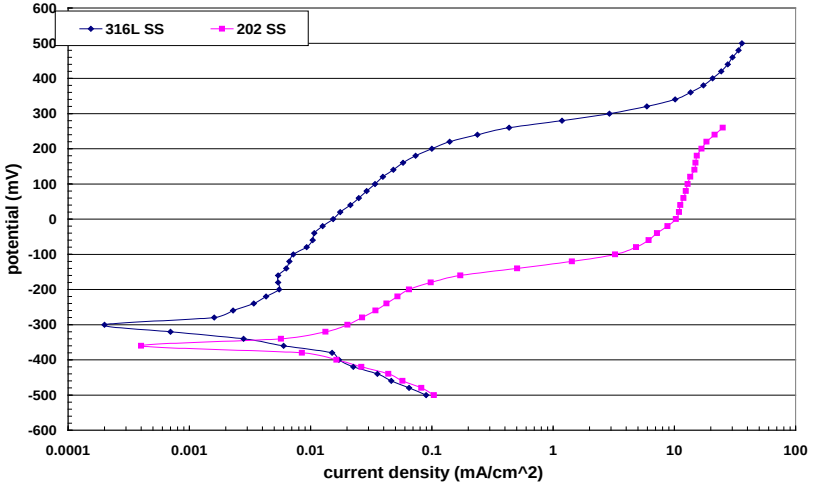

Fig.(B.8)polarization curves of two types of SS at 308k & 300 r.p.m. in 3.5%NaCl solution

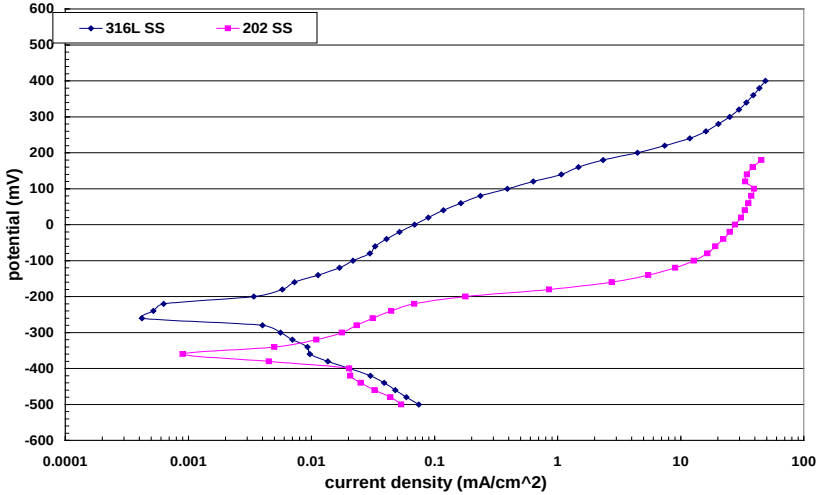

Fig.(B.9)polarization curves of two types of SS at 318k & 0 r.p.m. in 3.5%NaCl solution

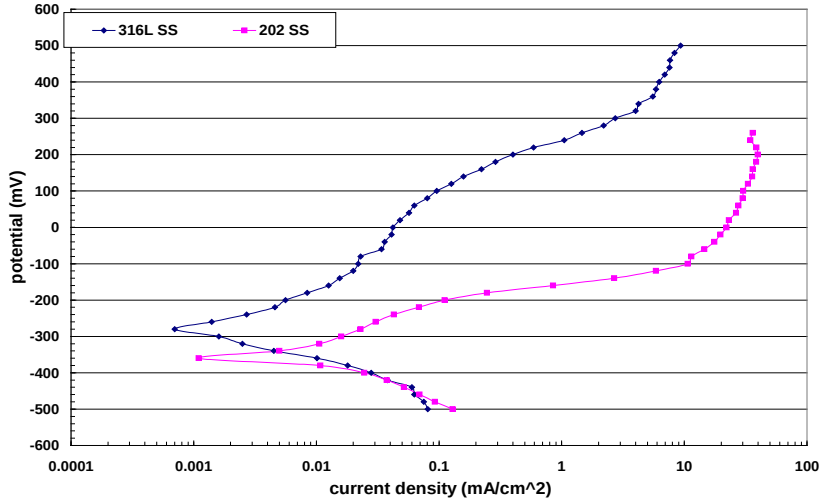

Fig.(B.10)polarization curves of two types of SS at 318k & 100 r.p.m. in 3.5%NaCl solution

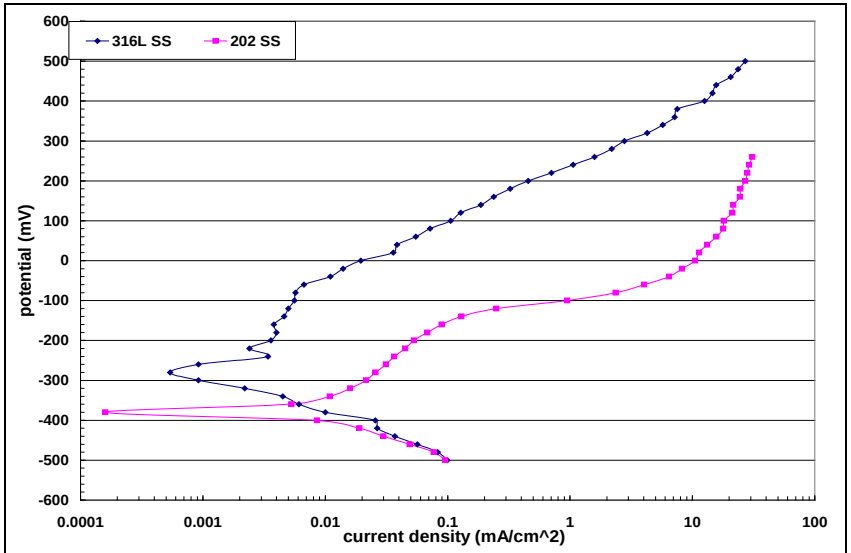

Fig.(B.11)polarization curves of two types of SS at 318k & 200 r.p.m. in 3.5%NaCl solution

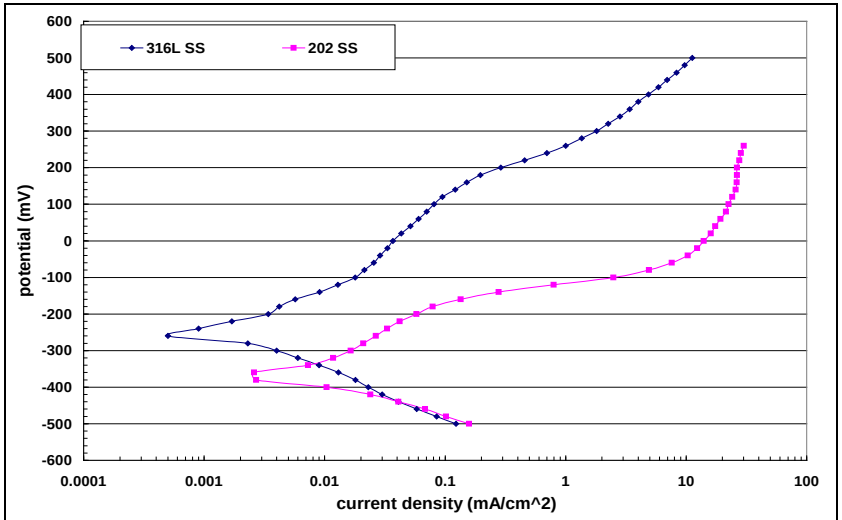

Fig.(B.12)polarization curves of two types of SS at 318k & 300 r.p.m. in 3.5%NaCl solution

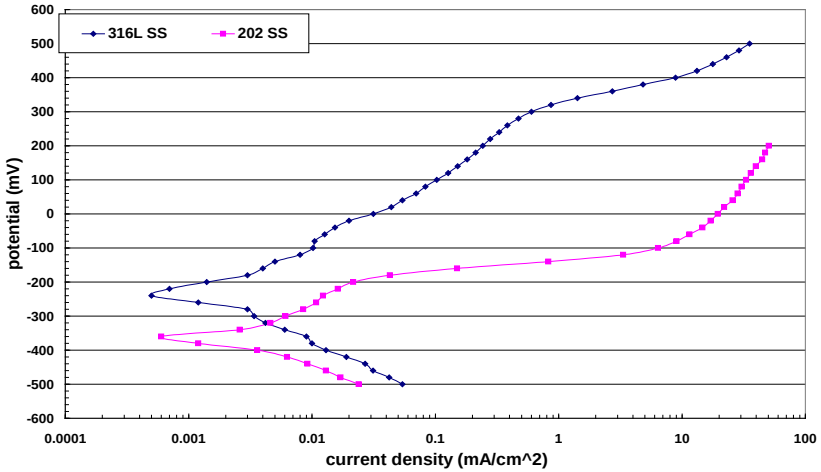

Fig.(B.13)polarization curves of two types of SS at 298k & 0 r.p.m. in 2.5%NaCl solution

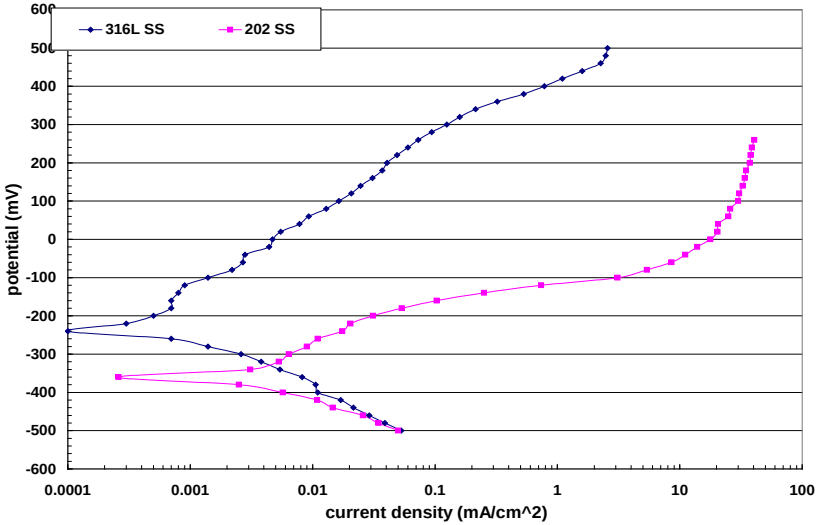

Fig.(B.14)polarization curves of two types of SS at 298k & 100 r.p.m. in 2.5%NaCl solution

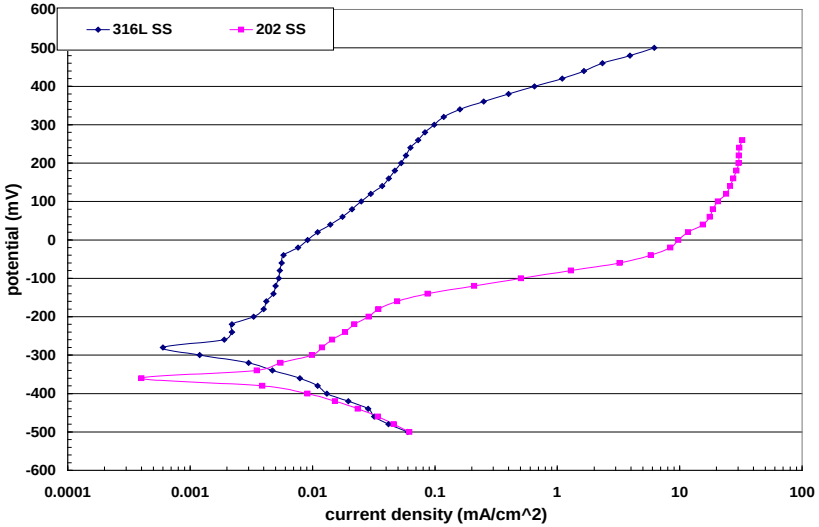

Fig.(B.15)polarization curves of two types of SS at 298k & 200 r.p.m. in 2.5%NaCl solution

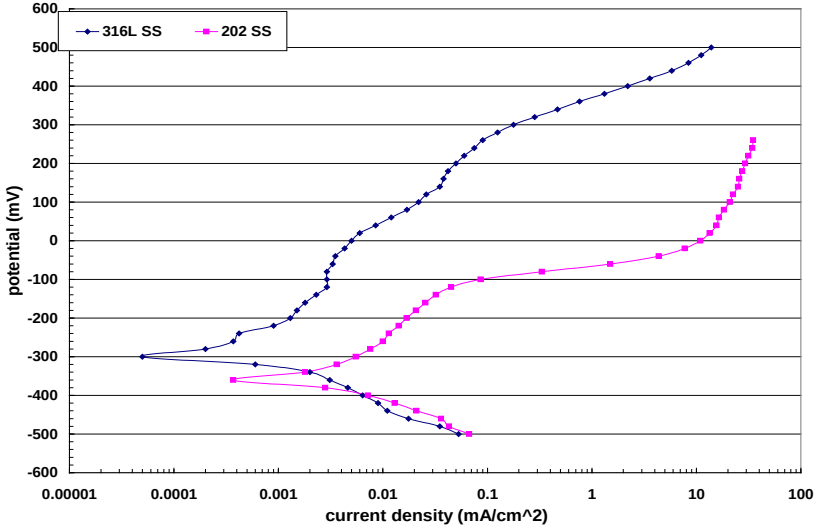

Fig.(B.16) polarization curves of two types of SS at 298k & 300 r.p.m. in 2.5%NaCl solution

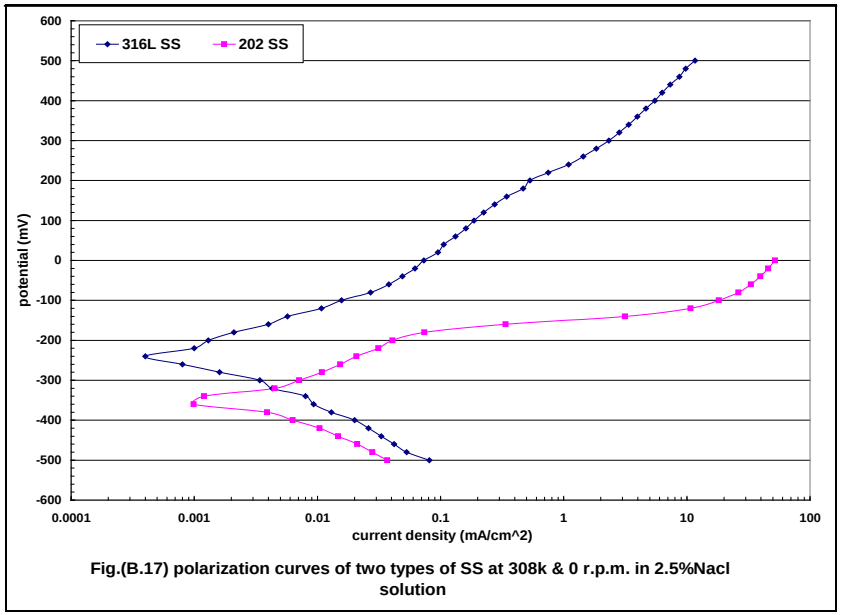

Fig.(B.17) polarization curves of two types of SS at 308k & 0 r.p.m. in 2.5%Nacl solution

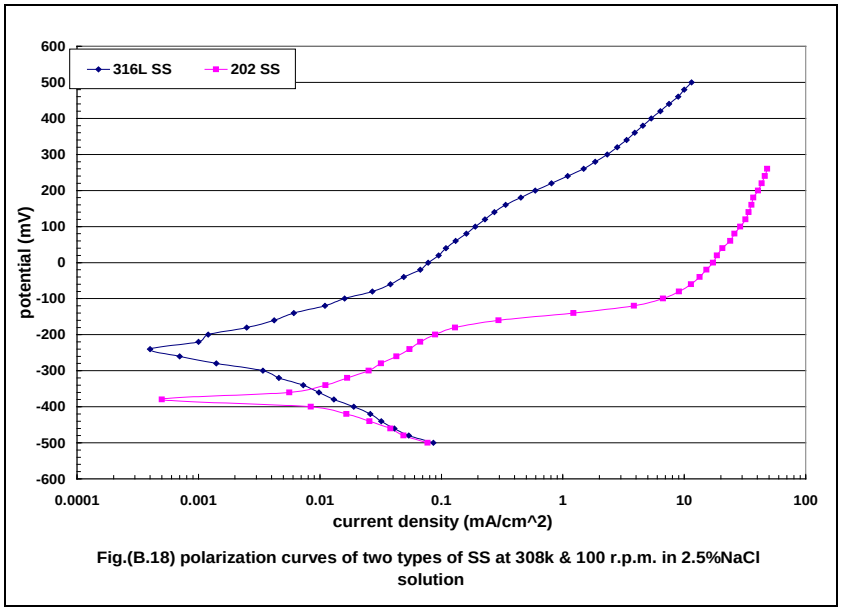

Fig.(B.18) polarization curves of two types of SS at 308k & 100 r.p.m. in 2.5%NaCl solution

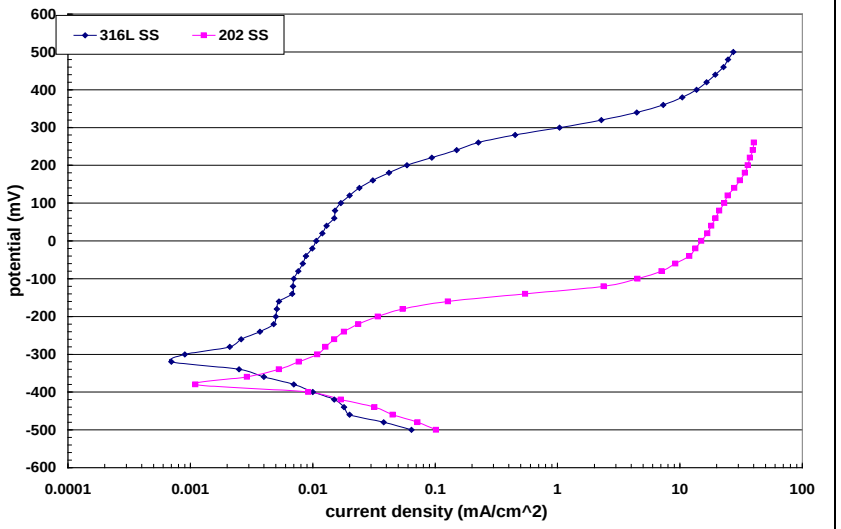

Fig.(B.19) polarization curves of two types of SS at 308k & 200 r.p.m. in 2.5%NaCl solution

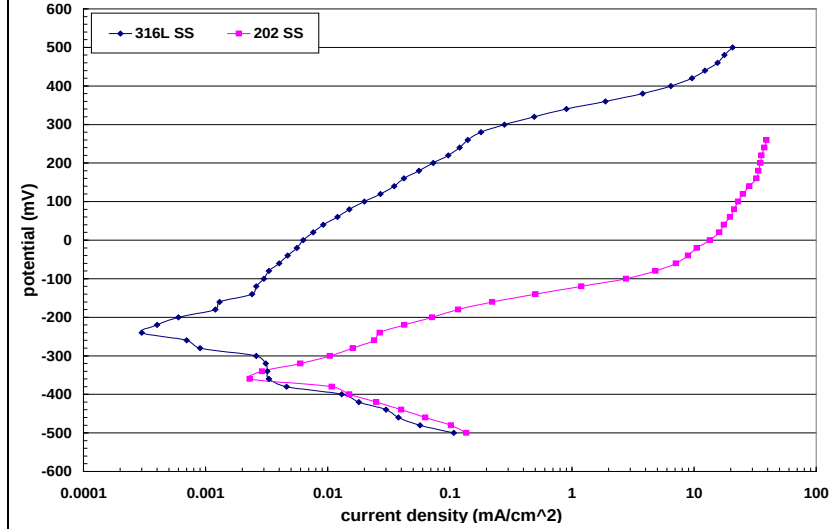

Fig.(B.20) polarization curves of two types of SS at 308k & 300 r.p.m. in 2.5%NaCl solution

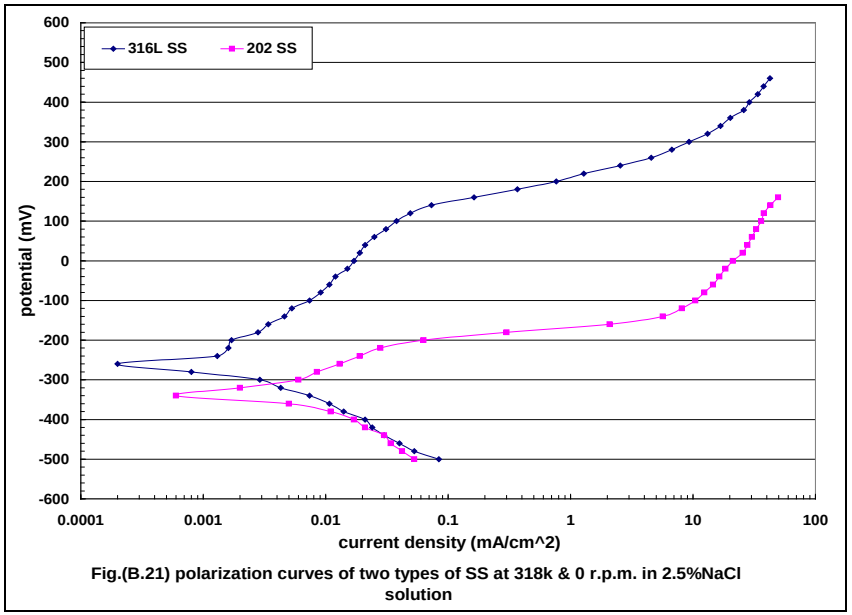

Fig.(B.21) polarization curves of two types of SS at 318k & 0 r.p.m. in 2.5%NaCl solution

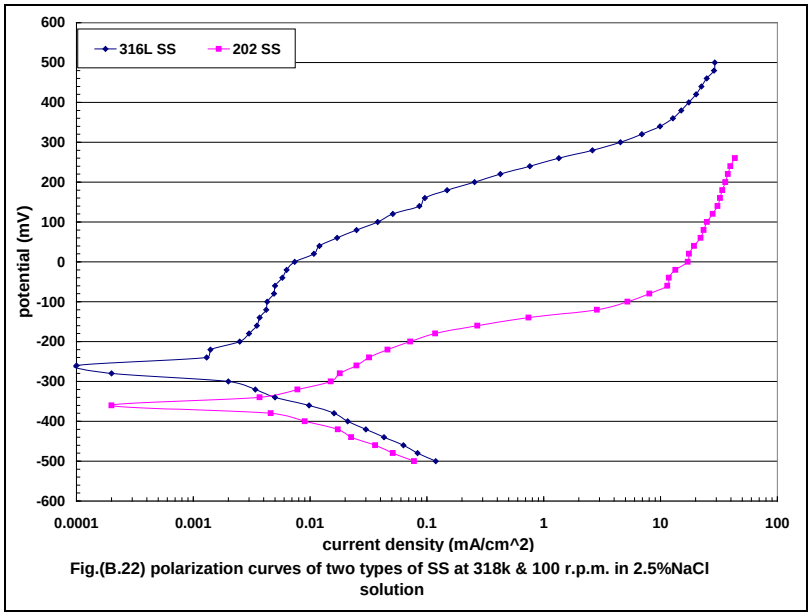

Fig.(B.22) polarization curves of two types of SS at 318k & 100 r.p.m. in 2.5%NaCl solution

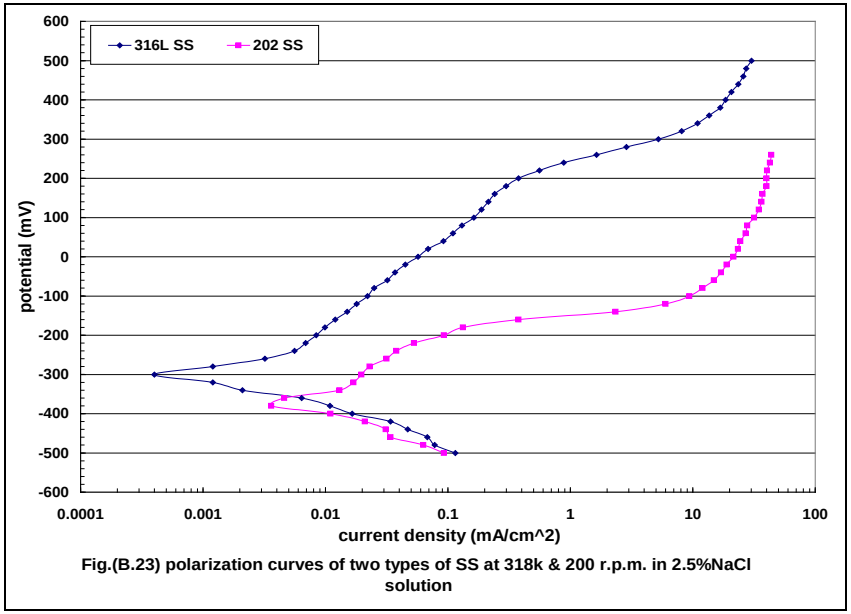

Fig.(B.23) polarization curves of two types of SS at 318k & 200 r.p.m. in 2.5%NaCl solution

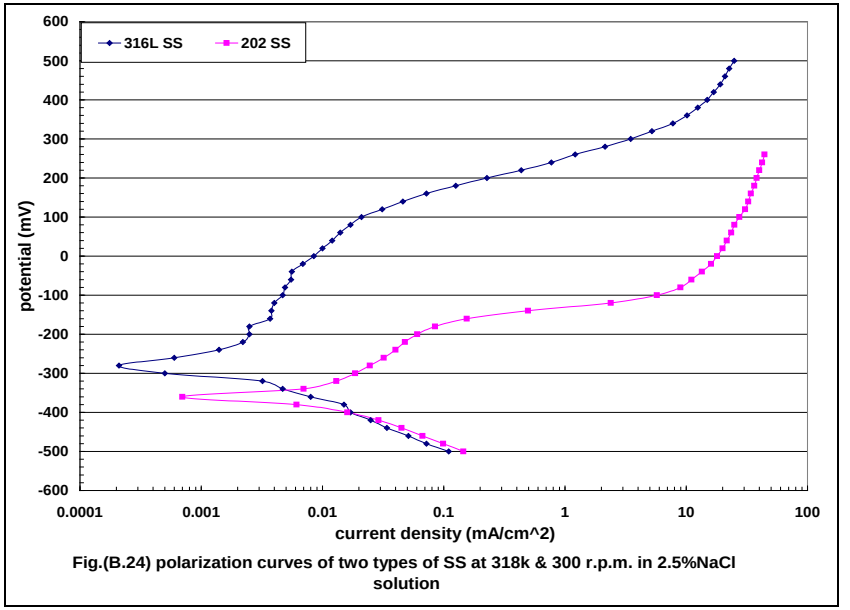

Fig.(B.24) polarization curves of two types of SS at 318k & 300 r.p.m. in 2.5%NaCl solution

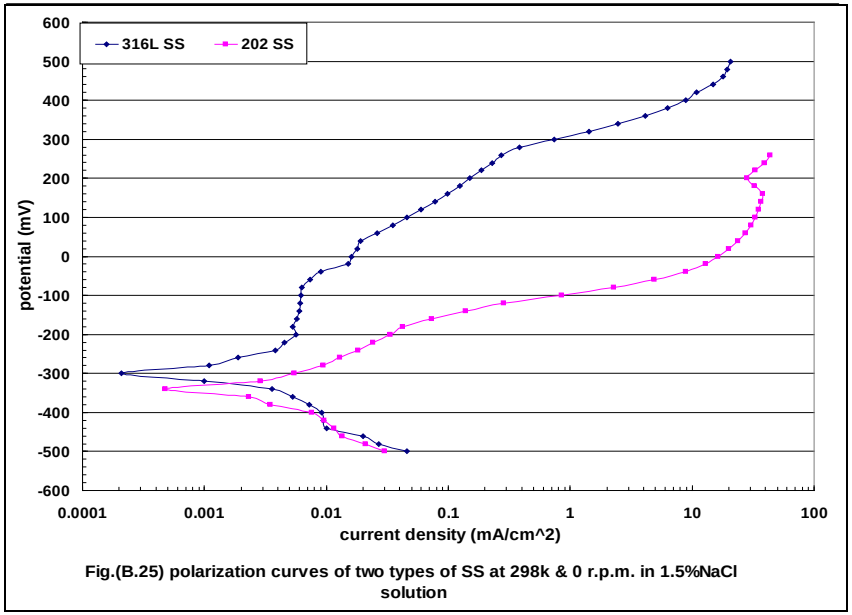

Fig.(B.25) polarization curves of two types of SS at 298k & 0 r.p.m. in 1.5%NaCl solution

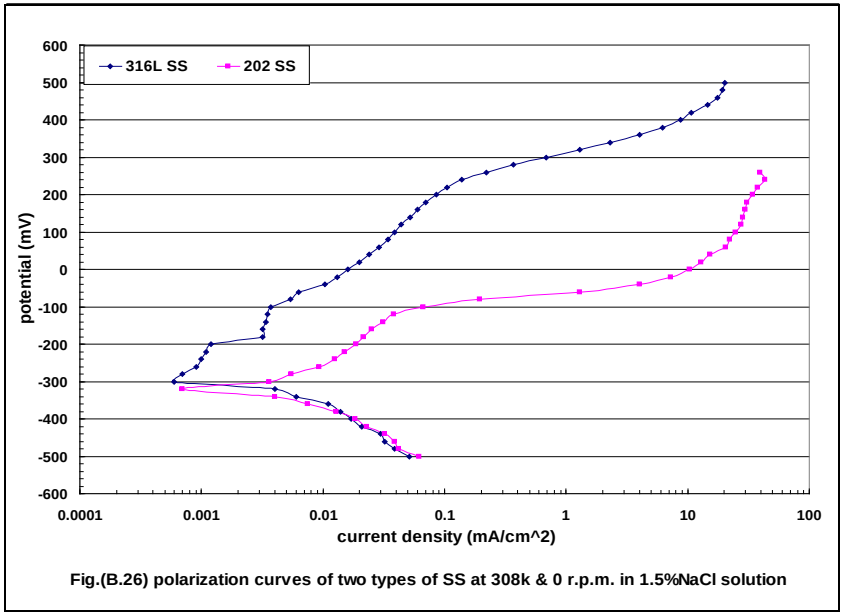

Fig.(B.26) polarization curves of two types of SS at 308k & 0 r.p.m. in 1.5%NaCl solution

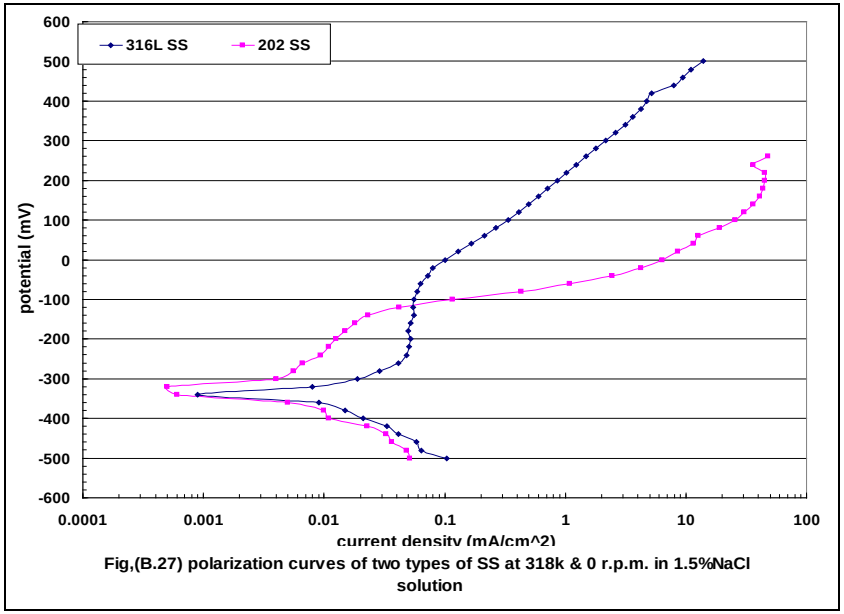

Fig,(B.27) polarization curves of two types of SS at 318k & 0 r.p.m. in 1.5%NaCl solution

References:

1. Fontana, M.G. and Green, N.D., "Corrosion Engineering", 3rd ed., McGraw-Hill, New York (1987).
2. Uhlig, H.H. and Revie, R.W., "Corrosion and Corrosion control", 3rd ed. John Wiley, New York, (1984).
3. Shreir, L.L., Jarman, R.A. & Burstein, G.T., "Corrosion" Vol.1, Metal/ Environment Reactions, 3rd ed.,(1994).
4. West, J.M., "Basic Corrosion and Oxidation", Ellis Horwood Ltd., West Sussex (1980).
5. Roberge, P.R., “Handbook of Corrosion Engineering” McGraw- Hill, U.S.A., (2000).
6. Stansbury, E.E. and Buchanan, R.A., “Fundamentals of Electrochemical Corrosion”, ASM International, (2000).
7. Tretheway, K. R. and Chamberlain," J. Corrosion Science and Engineering", 2nd Edition. , Longman, London, (1996).
8. Shreir,L.L.,"Corrosion", Metal/Environment Reactions, Newnes Butten worths, 2nd ed., vol.1, (1976).
9. West, J. M., "Electrode position and Corrosion Processes", Van Nostrand Reinhold Company, 2nd ed.,(1971).
10. Steigerwald, R. F.," Corrosion", No.24,p. 1, (1968).
11. From internet on, Technical Hand book of Stainless, Atlas steels, Corrosion resistance at the http://www.corrosion.ksc.nasa.gov, (2001).
12. Hoar T.P.," Corrosion Science" ,7 , 341 , (1967)
13. Uhlig H.H,"History of passivity, Experiments and Theories" , Passivity of the 4th Sysmposium on Passivity , edited by Frankenthal and J. Kruger, Electrochemical. Soc. Princton, N.J (1978).
14. Wagner C.," Corrosion Science" ,(1965)

15. Kabanove B., Burstein R., and Frumkin A., "Discussions Faraday Society, 1, 259,(1947)(as quoted in 2).
16. Frankenthal,R., "Journal of the Electrochemical Society",114,542, (1967).
17. Mc Adam, D. J. and Gell, G.W., "Pitting and its Effect on the Fatigue Limit of Steels Corroded Under Various Conditions" Journal of the Proceedings of the American Society for Testing Materials, Vol.41,(1928).
18. Nguyen, T.H. and Foley, R.T." On the Mechanism of Pitting of Aluminum," Journal of the Electrochemical Society, Vol.126, No.11,1979.
19. Frankel G.S., "Pitting Corrosion of Metal"; A Review of the Critical Factors, J. Electrochemical Society, Vol. 145, 1998.
20. From internet on “Pitting Corrosion” ch.9, KAIST, at http://corrosion.kaist.ac.kr.
21. Baroux B., Further Insights on the Pitting Corrosion of Stainless Steels, "Corrosion Mechanisms in Theory and Practice", 2nd ed. ,P. Marcus, Ed,. Marcel Dekker,(2002).
22. Smialowska- Szklarska Z., "Pitting Corrosion of Metals", NACE,(1986).
23. Leckie H.P. and Uhlig H.H.,"J. Electrochemical Society", Vol.113,(1966) (cited in 19).
24. Galvele J.R.," Corrosion Science", Vol.21, (1981)(cited in 19).
25. Galvele J.R.," J. Electrochemical Society", Vol. 123, (1976) (cited in 19).
26. Burstein G.T. and Mattin S.P., The Nucleation and Early Stages of Growth of Corrosion Pits, "Critical Factors in Localized Corrosion II", Vol.PV 95-15 (1995) (cited in 19).
27. Beck T.R. and Alkire R.C.,"J. Electrochemical Society", Vol.126, (1979) (cited in 19).
28. Beck T.R. and Alkire R.C.,"J. Electrochemical Society", Vol.129, (1982) (cited in 19).

29. Alkire R.C. and Wong K.P., "Corrosion Science", Vol.28.(1988) (cited in 19).
30. Alkire R.C. and Feldman M.,"J. Electrochemical Society", Vol. 135,(1988) (cited in 19).
31. Wong K.P. and Alkire R.C.," J. Electrochemical Society", Vol. 137, (1990) (cited in 19).
32. Strehblow H.H., "Werkst. Korros.", Vol. 27,(1976) (cited in 19).
33. Strehblow H.H.," Mechanisms of Pitting Corrosion", Corrosion Mechanisms in Theory and Practice, P. Marcus and J. Ouder, Ed., Marcel Dekker,(1995) (cited in 19).
34. Frankel G.S., Stockert L., Hunkeler F., and Boehmi H., " Corrosion", Vol.43, (1987) (cited in 19).
35. Pessall N.and Liu C.," Electrochemical Acta", Vol.16,(1971)(cited in 19).
36. Hisamatsu Y. Yoshii T., and Matsumura Y.," Electrochemical and Microscopical Study of Pitting Corrosion of Austenitic Stainless Steel", Localized Corrosion, Vol.NACE-3,R.W. Staeble ,B,F. Brown, J. Kruger and A. Agrawal, Ed.,NACE,(1974)(cited in 19).
37. Williams D.E., Stewar J., and Balkwill P.H., Corrosion Science, Vol.36,(1994) (cited in 19).
38. Ezuber H. and Newman R.C., Growth-Rate Distribution of Metastable Pits. Critical Factors in Localized Corrosion, Vol. PV 92-9,(1992) (cited in 19).
39. Pistorius P.C. and Burstein G.T.," Corrosion Science", Vol. 33 (1992) (cited in 19).
40. Pistorius P.C. and Burstein G.T.," Corrosion Science", Vol. 36 (1994) (cited in 19).
41. Wood G.C., Sutton W.H., Richardson J.A, Riley T.N.K., and Malherb A.G.," The Mechanism of Pitting of Aluminum and Its Alloys", Localized

Corrosion, R.W. Staehle, B.F. Brown, J. Kruger, and A.Agrawal, Ed.,NACE,(1974) (cited in 19).

42. Pride S.T., Scully J.R, and Hudson J.L.," J. Electrochemical society", Vol.141,(1994) (cited in 19).
43. Baroux B., Further Insights on the Pitting Corrosion of Stainless Steels, "Corrosion Mechanisms in Theory and Practice", Marcus P. and Oudar J., Ed., Marcel Dekker,(1995) (cited in 19).
44. Isaacs H., Bertocci U., Kruger J., and Smialowska S., Ed., "Advances in Localized Corrosion", Vol. NACE-9,NACE,(1990) (cited in 19).
45. "Conducting Cyclic Potentiodynamic Polarization Measurments for Localized Corrosion Susceptibility of Iron-, Nickel-, or Cobalt-Based Alloys," Annual Book of ASTM Standards, ASTM(cited in 19).
46. Wild B.E. and Williams E.," J. Electrochemical Society", Vol.117,(1970) (cited in 19).
47. Wild B.E., "On Pitting and Protection Potentials": Their Use and Possible Misuses for Predicting Localized Corrosion Resistance of Stainless Alloys in Halide Media, Localized Corrosion, Vol. NACE-3,R.W. Staehle, B.F. Brown, J.Kruger, and A. Agrawal,Ed., NACE,(1974) (cited in 19).
48. Yasuda M., Weinberg F., and Tromans D.," J. Electrochemical Society", Vol. 137 (1990) (cited in 19).
49. Sridhar N. and Cragnolino G.A.," Corrosion", Vol. 49 (1993) (cited in 19).
50. Dunn D.S., Pan Y.M., and Cragnolino G.A.," Stress Corrosion Cracking, Passive and Localized Corrosion of Alloy22 High Level Radioactive Waste Containers" , NACE,(2000).
51. Horvath J. and Uhlig H.H.," J. Electrochemical Society", Vol.115.(1968).
52. Sedriks A.J.," Effects of Alloy Composition and Microstructure on the Localized Corrosion of Stainless Steels", Advances in Localized

Corrosion, Vol. NACE-9, Isaacs H.. Bertocci U., Kruger J., and Smialowska S.,Ed., NACE (1990) (cited in 19).

53. Sedriks A. J.," Corrosion of Stainless Steels", Wiley-Inter science , (1996) (cited in 19).
54. Eklund G.S.," J. Electrochemical Society", Vol.121,(1974) (cited in 19).
55. Wranglen G.," Corrosion Science" , Vol. 14,(1973) (cited in 19).
56. Sedricks, A. J.," Corrosion", Vol.42(1986) (cited in 19).
57. Arnvig P.E. and Biogard A.D., Paper 437," Corrosion 96", NACE,(1996) (cited in 19).
58. Arnvig P.E. and Davision R.M., Paper 209," Process 12th International Corrosion Congress",(Houston, TX),(1993) (cited in 19).
59. Brigham R.J. and Tozer E.W.," Corrosion", Vol.29,(1973) (cited in 19).
60. Brigham R.J. and Tozer E.W., Corrosion, Vol.30,(1974) (cited in 19).
61. Qvarfort R.," Corrosion Science", Vol.28,(1988) (cited in 19).
62. Qvarfort R.," Corrosion Science", Vol.29,(1989) (cited in 19).
63. Laycock N.J., Moayed M.H., and Newman R.C.," Prediction of Pitting Potentials and Critical Pitting Temperatures", Critical Factors in Localized Corrosion II,Vol.PV95-15(1995) (cited in 19).
64. Pourbaix M., et al.," Corrosion science",Vol.3,(1963).
65. Kolotyrkin J.M., Golovina G.V., and Florianovich G.M., SSSR D.A.N., Vol.148,(1963).
66. Fokin M.N., Kurtepov M.M., and Bachkareva V.J., Sbornik Pokorrozji, Moskov(1965).
67. Pourbaix, M.," Corrosion Science". 30,963, (1990).
68. Smialowska- Szklarska Z., "Corrosion Industrial Problems" , Treatment and Control Techniques.,Vol. 2,(1987).
69. Wang H.J. and Smialowska-Z.Szklrska,"Corrosion",Vol.44,(1988).
70. deWexler S.B. and Galvele J.R.," J. Electrochemical Society", Vol. 121,(1974) (cited in 19).

71. Sandwith Colin and Randy K. Kent, University of Washington, MDE Engineers, Inc."Corrosion – Related Failures".
72. Tuthill A.H. and Schillmoler C.M.," Guidelines for Selection of Marine Materials", Ocean Science and Engineering Conference, Marine Technology Society, Washington, (1965)(cited in 71).
73. Stein A.A., MIC in the Power Industry," Microbiologically Influenced Corrosion", Korbin G., Ed., NACE International, (1993)(cited in 6).
74. Little B., Wagner P., and Mansfeld F.," Microbiological influenced Corrosion of Metals and Alloys", Int. Mater. Rev., Vol.36,(1991)(cited in 6).
75. Laycock N. J. and Newman R.C.,"Corrosion Science",Vol. 39,(1997) (cited in 19).
76. Shibata T.and Takeyama T.," Corrosion" , Vol.33,(1977) (cited in 19).
77. Rockel, M. B.,"Use of Highly Alloyed Stainless Steels and Nickel Alloys in the Chemical Industry", ACHEMA Conference ,June (1978).
78. Tverbrg, J. C." Stainless Steel Primer", Flow Control Magazine.(2000).
79. Uhlig, Herbert H.," The Corrosion Handbook", john Wiley& Sons, New York,(1951).
80. Tverbrg, J. C." Conditioning of Stainless Steel Surfaces for Better Performance", Stainless Steel World, April (1999).
81. Zapffe, Carl,"Stainless Steels", The American Society for Metals, Cleveland, Ohio, (1949).
82. Parr, j. Gordon and Hanson, Albert," Introduction to Stainless steel", The American Society for Metals",(1965).
83. Kovach, C.W. and Redmond, J. D." Correlations Between the Critical Crevice Temperature, PRE-Number, and Long- Term Crevice Corrosion Date for Stainless Steels" Paper 267, Corrosion 95, National Association of Corrosion Engineers.

84. Salh SH. M. "Pitting Corrosion of Carbon Steel in Sodium Molybdate Solutions", M.Sc. Thesis, U.O.T. (1990).
85. Malik Anees U and Al-Fozan Saleh A.," Pitting Behavior of Type 316L SS in Arabian Gulf Sea Water" Technical Report No.SWCC (RDC)-22 october ,(1992).
86. Moreno D.A., Ibars J.R., Ranninger C., and Videla H.A." Use of Potentiodynamic Polarization to Assess Pitting of Stainless Steels by Sulfate- Reducing Bacteria" National Association of Corrosion Engineers,(1992).
87. Smialoska- Szklarska Z.," Effect of Alloying Elements and Breakdown of Passivity of Fe- and Ni- Based Alloys", The Ohio State U., June (1992).
88. Dawood L. M.," Pitting Corrosion of Duplex Stainless Steel", M.Sc. Thesis , U.O.T.(1993).
89. Park J.J., Pyun S.I., Lee W.J., and Kim H.P.," Effect of Bicarbonate Ion Additives on Pitting Corrosion of Type 316L SS in Aqueous 0.5M Sodium Chloride Solution", NACE International (1999).
90. Kolman D.G., Ford D.K., Butt D.P., and Nelson T.O.," Corrosion of 304 SS Exposed To Nitric Acid-Chloride Environments", Los Alamos, NM87545(1999).
91. Newman R.C.,"Understanding the Corrosion of Stainless Steel", Whitney W.R., Award Lecture, NACE (2001).
92. Yashiro H., Hirayasu D.,and Kumagai N.," Effect of Nitrogen Alloying on the Pitting of Type 310 SS",Vol.42 ,(2002).
93. Neusa A.F., and Steshan W.,"Correlation between Corrosion Potential and Pitting Potential for AISI 304L Austenitic SS IN 3.5% NaCl Aqueous Solution", Mat.Res. Vol.5, No.1 ,(2002).
94. Martin A.R., Ricardo M.C., and Raul B.R.," Effect of Fluoride Ions on the Anodic Behavior of Mill Annealed and Aged Alloy 22",(2003).

95. Jacek G.C.,Jozef G., and Jan M." The effect of sequence of sol-gel multilayer coatings deposition on corrosion behavior of 316L SS", Material Science, Vol.21, No.4.(2003).
96. Kear G., Barker B.D., and Walsh F.C." Electrochemical Study of UNS S32550 Super Duplex Stainless Steel Corrosion in Turbulent Seawater Using the Rotating Cylinder Electrode", Vol.60, No.6,NACE,(2004).
97. Zhenqiang W.,Paul D.,and Ponisseril S.," Surfactants as Green Inhibitors for Pitting Corrosion of Stainless Steels", Paper N0.04539,NACE,(2004).
98. Gaben F., Vuillemin B., and, Oltra R.," Influence of the Chemical Composition and Electronic Structure of Passive Films Grown on 316L SS on Their Transient Electrochemical Behavior", J. Electrochemical Society,151,(2004).
99. Guo M., Li D., Rao S.X.,and Guo B.L.,"Effect of Environmental Factors on the Corrosion of 2024T3 Aluminum Alloy", Vol.28,(2004).
100. Carranza R.M., Giordano C.M., Rodriguez M.A.,and Rebak R.B."Corrosion Behavior of Alloy 22 in Chloride Solutions Containing Organic Acids",(2005).
101. Refaey A.M., Taha F., and Abd El-Malak A.M."Corrosion and Inhibition of 316 L SS in neutral medium by 2-Mercaptobenzimidazole", J. Electrochemical science,(2006).
102. James H., B.S.M.E.," Stainless Steel Process Equipment and Chloride-Induced Failyre",(2006).
103. Lameche S., Nedjar R., Rebbah H., Adjeb A." Effect of Temperature on the Pitting of three Stainless Steels in Chloride Containing Solutions",Vol.7 JCSE (2006).
104. Yahia L., Khireddine M.H.," Influence of Cold Work by Traction on the Resistance of 304L SS to Pitting Corrosion", Vol.10,JCSE,(2007).

105. Troels M., Jan E.F." Unusual Corrosion Failures of Stainless Steel in Low Chloride Waters", Force Technology ,NACE corrosion ,Paper 08174,(2008).
106. Mok, W.Y., Jenkins, A.E. and Gamble, C.G., JCSE, Vol.6, Paper C072, (2003).
107. Annual Book of ASTM Standards, part 10, G59, (1980).
108. Annual Book of ASTM Standards, part 10, G31, (1980).
109. Efird,D.K. & Moller, E.G., MP, Vol. 18, No.9 (1979).
110. Man, C.H.&Gabe, R.D., Corrosion, Vol.(21),No.9(1981)(cited in 88).
111. Speller, Corrosion Causes and Preventation, P.42, McGraw-Hill Book Co., New York,(1951).
112. James, K., Rice, P.E. Consulting Engineer ,"Drew Principles of Industrial Water Treatment", Olney, Maryland,(1977).
113. Mahato, B.K., Voora, S.K.,&Shemilt, L.W., Corrosion science, Vol.8,p.(173-193),(1968).
114. Mansfeld F. and Kenkel J.V., Corrosion,35,43,(1979)(cited in 84).
115. Ross,T.K. and Hitchen,B.P.L., Corrosion Science,1,15, (1961).
116. Birbilis, N, Padgett, B.N., Buchheit, R.G.," Electrochemical Acta",50(2005).
117. Birbilis, N, phD Thesis, Monash University, Australia, (2004) (cited in 116).
118. Schwenk,W., Corrosion, Vol.20,No.4,(1964)(cited in 88).
119. Broli A. and Holtan H., Corrosion Science,(1973)13,237.
120. Broli A., Holtan H.,and Midjo M., British Corrosion J.(1973),8,173.

الخلاصة

يتناول البحث دراسة تأثير بعض المتغيرات على التآكل النقري لنوعين من الفولاذ المقاوم للصدأ (202&316L) وكذلك دراسة سلوكهما الكهروكيميائي في المحلول الملحي كلوريد الصوديوم(NaCl) بأستخدام تقنية الاستقطاب .

تم استعمال منظومة قطب الاسطوانة الدوارة (RCE) من أجل توفير الظروف المطلوبة.

أجريت تجارب الاستقطاب بدراسة تأثير درجات الحرارة (318,308,298) كلفن عند ظروف السكون و ظروف تغير تركيز المحلول الملحي كلوريد الصوديوم (NaCl)بمعدل (1.5,2.5,3.5)%كنسبه وزنيه .

دراسة تأثير تغير سرعه الدوران (300,200,100) دورة بالدقيقه ولتراكيزمختلفه للمحلول الملحي (2.5&3.5)%من كلوريد الصوديوم NaCl ولدرجات حراريه (318,308,298) كلفن على السلوك الكهروكيميائي .

وكذلك دراسة تأثير معدل المسح (Scan Rate) بمعدل (40,30,15,10) ملي فولت بالدقيقه على السلوك الكهروكيميائي للمعدن نوع (316L) المقاوم للصدأ وبدرجة حرارة (308)كلفن وبتركيز (3.5)% من محلول كلوريد الصوديوم(NaCl).

ومن نتائج هذا البحث انه في حالة زيادة درجات الحراره وتركيز كلوريد الصوديوم في المحلول يؤدي الى تقليل جهد الانكسار (E_b).للفولاذ من نوع 316L فان النقصان يكون من(80-الى 220-)ملي فولت بينما للفولاذ من نوع 202 يكون من(120-الى 260-)ملي فولت وكذلك تبين بانه التآكل النقري لكلا نوعي الفولاذ يكون اكثر عند ظروف السكون.

ومن الممكن التأكيد عند معدل المسح 40 ملي فولت بالدقيقه فان من الممكن ملاحظة منطقة الخموليه بوضوح بينما من الصعب ملاحظة هذه المنطقه عند معدلات المسح الاخرى(30,20,15,10)ملي فولت بالدقيقه. وهذا يعطي كدليل جيد على ان منطقة الخموليه تعتمد على معدل المسح الحرج لذلك فان معدل المسح يجب ان يختار بعنايه للحصول على

استجابة حالة الاستقرار لمنطقة الخموليه معتمد ا على نوع السبيكه والمحلول الاليكتروليتي.

ان معدل التآكل (i_{corr}.) يتغير تغيرا بسيطا عند تغير سرعة الدوران للقطب (RCE)(100-300)دورة بالدقيقه . بالنسبه للفولاذ نوع SS 316L (-0.0019 0.0018,0.0015-0.0014)ملي امبير / السنتمتر المربع عند (3.5&2.5)% NaCl و298 كلفن ,(0.0023-0.0018,0.0018-0.0016) ملي امبير /السنتمتر المربع عند (3.5&2.5)NaCl% و 308 كلفن , (0.0028-0.0028,0.0028-0.0025) ملي امبير / السنتمتر المربع عند (3.5&2.5) NaCl% و 318 كلفن بينما للفولاذ نوع 202SS (0.002-0.004,0.002-0.0021) ملي امبير / السنتمتر المربع عند (3.5&2.5)% NaCl و298 كلفن , (0.0063-0.005,0.006-0.006)ملي امبير /السنتمتر المربع عند (3.5&2.5)% NaCl و308 كلفن , (-0.005-0.0013,0.0068 0.006)ملي امبير / السنتمتر المربع عند (3.5&2.5)% NaCl و318 كلفن.

ومن نتائج البحث ايضا انه بزيادة تركيز كلوريد الصوديوم في المحلول يؤدي الى زيادة معدل التآكل ولكلا ال نوعين من الفولاذ . للفولاذ نوع SS 316L فأن الزياده من(0.0027-0.0012)ملي امبير / السنتمتر المربع بينما للفولاذ نوع SS 202 (-0.009 0.0016)ملي امبير/ السنتمتر المربع.

واخيرا نستنتج من هذا البحث ان الفولاذ المقاوم للصدأ نوع 316Lهو اكثر مقاومه للتآكل النقري بالمقارنه مع الفولاذ نوع 202وتحت نفس الظروف(E_b للفولاذ نوع 316L SS اعلى من E_b للفولاذ نوع 202 SS).

وزارة
التعليم العالي والبحث العلمي
الجامعة التكنولوجية
قسم الهندسة الكيمياوية

تأثير عوامل مختلفه على التآكل النقري للفولاذ المقاوم للصدأنوع (202&316L)

رسالة مقدمة إلى قسم الهندسة الكيمياوية – الجامعة التكنولوجية كجزء من متطلبات الدراسة لنيل درجة ماجستير علوم في الهندسة الكيمياوية

إعداد
طه حسن عبود

إشراف
د. شذى أحمد سامح

تشرين الثاني 2008